

PLASTIC DEFORMATION OF LAMINATED METALS

by

Verguts, Hugo, b.e.w.ir.

A Thesis

Submitted to the School of Graduate Studies
in Partial Fulfillment of the Requirements
for the Degree
Master of Engineering

December, 1972

MASTER OF ENGINEERING (1972)
(Mechanical Engineering)

McMaster University
Hamilton, Ontario.

TITLE: Plastic Deformation of Laminated Metals

AUTHOR: Hugo L. G. M. Verguts, b.e.w.ir.
(Katholieke Universiteit Leuven).

SUPERVISOR: Dr. R. Sowerby

NUMBER OF PAGES: PART A, TEXT, viii, 130, A90. PART B, FIGURES AND
PROGRAMS.

SCOPE AND CONTENTS:

Gaining insight into the pressworking properties of laminated sheet metal is the aim of this work. One of the deformation processes in which the difference in behaviour between single and laminated sheet metal is most distinct and possibly the easiest to analyze is that of pure plastic bending. A bending theory, initially proposed by Crafoord, is further developed to analyze the pure bending of laminated metals. The bending behaviour of single and laminated nonstrain hardening and strain hardening sheets, with and without Bauschinger effect, is treated extensively from a theoretical point of view.

Stretch forming, bending and deep drawing tests on laminated sheets are also performed experimentally. It is found that the orientation of the laminated sheet during the deformation process has a significant influence on the bending behaviour and the deep drawability of laminated sheet. The change in deep drawability can be qualitatively predicted from the bending behaviour.

ACKNOWLEDGEMENTS

The author is pleased to record his sincere gratitude to his supervisor, Dr. R. Sowerby for suggesting the problem for investigation and for his guidance and encouragement throughout this work. The valuable discussions the author had with Dr. R. Sowerby made it a rewarding experience.

The author is also grateful to Professor J. Peters and Professor Dr. M. C. deMalherbe for their suggestion to spend a year at McMaster University.

The author is indebted to the Department of Mechanical Engineering for the scholarship award and the teaching assistantship.

The grant, given by Vlaamse Leergangen, Leuven, Belgium and the study leave granted by the Nationaal Fonds voor Wetenschappelijk Onderzoek, Brussel, Belgium are gratefully acknowledged.

Thanks are due to Mrs. A. Neil and Miss B. Bedell for their expert typing of the manuscript.

The materials used in the experiments were supplied free of charge, by Texas Instruments Inc., (Attleboro, Mass., U.S.A.).

The investigation was supported in part by the National Research Council of Canada Grant No. A8120.

TABLE OF CONTENTS

PART A: TEXT

<u>CHAPTER</u>		<u>PAGE</u>
1	INTRODUCTION	
	1.1. Laminated Composites; Definition, Use and Manufacture.	1
	1.1.1. Why Composite Materials are Used.	1
	1.1.2. Laminated Composites.	4
	1.1.2.1. Non-Metallic Laminates.	5
	1.1.2.2. Non-Metallic, Metallic Laminates.	6
	1.1.2.3. Metallic Laminates.	8
	1.1.3. Manufacture of Metallic Laminates.	12
	1.2. State of the Art of the Plastic Deformation of Laminated Metals	16
	1.3. Scope of this Work.	20
2	EXPERIMENTAL STRETCHING OF LAMINATED SHEET BY THE BULGE TEST	22
	2.1. Materials Used in the Experiments.	22
	2.2. Biaxial Stretching of Laminated Sheet.	29
	2.2.1. Balanced Biaxial Stretching.	30
	2.2.2. Forming Limit Diagram.	32
	2.2.3. Conclusion.	35
3	GENERAL THEORY OF PLASTIC SHEET BENDING	36
	3.1. Basic Assumptions	36
	3.1.1. Homogeneous Material	36

<u>CHAPTER</u>		<u>PAGE</u>
	3.1.2. Isotropic Material.	36
	3.1.3. Pure Bending Assumption.	37
	3.1.4. Plane Strain Assumption.	38
	3.1.5. Radial Sections in the Bend Remain Plane.	38
	3.1.6. Incompressible Material.	38
	3.1.7. Rigid-Plastic Material.	39
	3.2. Essential Features of the Pure Plane Strain Plastic Bending Theory.	40
	3.2.1. Equilibrium Equation.	40
	3.2.2. Yield Condition for Plane Strain	40
	3.2.3. Tangential Strain and Unelongated Layer.	42
	3.2.4. The Neutral Layer.	44
	3.2.5. The Movement of Individual Layers.	47
	3.2.6. Introduction of Dimensionless Parameters.	48
	3.2.7. Change in Sheet Thickness.	50
	3.2.8. General Method of Solution.	53
	3.2.9. Radial and Tangential Stresses and Bending Moment.	57
	3.3. Conclusion.	57
4	PLASTIC PLANE STRAIN BENDING OF NONSTRAIN- HARDENING LAMINATED SHEET	59
	4.1. Plastic Bending of a Nonstrain- hardening Monometal.	59

<u>CHAPTER</u>		<u>PAGE</u>
4.2.	Plastic Bending of Nonstrain-hardening Bimetal Sheet.	62
4.2.1.	Introduction.	62
4.2.2.	Example 1.	64
4.2.3.	Example 2.	67
4.2.4.	Influence of the Relative Thickness of the Two Laminates.	69
4.2.5.	Influence of the Yield Strength Ratio.	72
4.2.6.	Conclusion.	73
4.3.	Plastic Bending of Nonstrain-hardening Trimetal Sheet.	73
4.3.1.	Introduction	73
4.3.2.	Examples of Soft Core Trimetal.	74
4.3.3.	Influence of Relative Laminate Thicknesses on the Bending of 2-1-2 Trimetal	75
4.3.4.	Examples of Strong Core Trimetal	79
4.3.5.	Influence of Relative Laminate Thickness on the Bending of 1-2-1 Trimetal.	81
4.3.6.	Concluding Remarks.	82
4.4.	Conclusions for the Bending of Nonstrainhardening Sheets.	83
5	PLASTIC BENDING OF STRAINHARDENING SHEET	86
5.1.	Bending of Strainhardening Monometal Sheet without Bauschinger Effect.	86
5.1.1.	Introduction.	86
5.1.2.	Example.	88
5.1.3.	Influence of the Stress Strain Curve Parameters.	91

CHAPTERPAGE

5.2.	Bending of Strainhardening Monometal Sheet with Simplified Bauschinger Effect according to Crafoord.	94
5.2.1.	Introduction.	94
5.2.2.	Example.	96
5.2.3.	Influence of Stress Strain Parameters.	97
5.3.	Bending of Strainsoftening Monometal Sheet.	98
5.4.	Bending of Laminated Strainhardening Sheet in the Absence of Bauschinger Effect.	100
5.5.	Conclusions.	103
6	BENDING AND DEEP DRAWING EXPERIMENTS ON LAMINATED SHEET.	105
6.1.	Bending of Laminated Sheet Metal.	105
6.1.1.	Experimental Procedure.	105
6.1.2.	Bending of Sheet D: Theoretical and Experimental.	107
6.1.3.	Conclusions.	112
6.2.	Deep Drawing Experiments on Laminated Sheet.	113
6.2.1.	Experimental Procedure.	114
6.2.2.	Results of Deep Drawing Experiments.	115
6.2.3.	Qualitative Description of the Deep Drawing Behaviour of Laminated Bimetal Sheet.	118
6.2.4.	Comparison of our Deep Drawing Results with Experiments Performed by Other Authors.	123

<u>CHAPTER</u>		<u>PAGE</u>
	6.2.5. Conclusions on Deep Drawing Experiments.	124
7	CONCLUSIONS AND SUGGESTIONS FOR FURTHER WORK	127
	BIBLIOGRAPHY	131
APPENDIX I	A Set of Relations between Dimensionless Parameters and the Geometry of the Bend.	A1
APPENDIX 2	Derivation of Change in Sheet-Thickness Formulas.	A4
APPENDIX 3	Bending of a Rigid-Plastic, Nonstrain-hardening Monometal Sheet.	A7
APPENDIX 4	Bending of a Rigid-Plastic, Nonstrain-hardening Bimetal Sheet.	A11
APPENDIX 5	Bending of a Rigid-Plastic, Nonstrain-hardening Laminated Sheet.	A26
APPENDIX 6	Influence of the Original Neutral Layer Position on the Change in Relative Sheet Thickness at the Commencement of the Bending Process.	A39
APPENDIX 7	Bending of Laminated Sheet, Composed of Rigid-Plastic, Strainhardening Materials without Bauschinger Effect.	A42
APPENDIX 8	Bending of a Rigid-Plastic Strainhardening Sheet, with Bauschinger Effect as suggested by Crafoord.	A63
APPENDIX 9	Accuracy of Computer Programs.	A80

CHAPTER 1

INTRODUCTION

The reasons for the use of laminated materials, a description in some detail of the most important laminates used today and their mode of manufacture, will be given first in this introduction. A brief survey of the state of the art of plastically deforming laminated materials follows. Finally, the scope of this thesis will be explained.

1.1. Laminated Composites; Definition, Use and Manufacture

1.1.1. Why Composite Materials are Used

The demands on materials imposed by engineering applications can be very diverse. Some sought after properties of materials are listed below.

1. Mechanical Properties

- high strength to weight ratio
- high ductility
- good formability
- weldability
- fracture toughness
- fatigue behaviour
- creep behaviour

2. Thermal Properties

- thermal insulation
- excellent heat transfer characteristics

- high or low coefficient of thermal expansion
 - effects of temperature on mechanical properties (e.g., high temperature creep)
 - melting point
3. Electrical Properties
- electrical insulation
 - excellent electrical conductivity
 - magnetic properties (e.g., permeability)
4. Chemical Properties
- corrosion resistance
5. Nuclear Properties
- effects of radiation on the material
 - nuclear cross section for specific nuclear reactions
6. Tribological Properties
- wear resistance
 - abrasion resistance
 - surface hardness
 - surface roughness
7. Aesthetic Properties
- color
 - surface appearance (e.g., for decorative purposes)
8. Cost
- availability (scarce or abundant)
 - production cost

It is virtually impossible to meet all the above needs simultaneously (if this is ever required). In some applications, the material needs only a few of the above properties, and requirements can be easily met by a wide variety of traditional materials. In other applications, the demands are more severe and/or more diverse, and can be met by improving materials. A great deal of research has gone into these methods of improvement. In metals, for instance, change in properties can be obtained by mechanical working, heat treatment and the use of alloy elements. Plastics can be improved by developments in organic chemistry.

However, demands for some applications can not be met by simple single-component materials acting alone. It becomes necessary to combine several materials into a composite to which each constituent not only contributes its share, but whose combined action transcends the sum of the individual properties, and provides new performance unattainable by the constituents alone. This combination of materials can be done in different ways. One way is to distribute the properties of both materials evenly over the composite. This can be done with powder metallurgy, the dispersion of particles in a matrix (fillers in plastics), or the use of reinforcing fibres (whiskers in metals, glass-fibres in plastics). But this even distribution of material properties over the whole composite is not always necessary or desirable. For some applications, the best solution is to have non-uniform material properties. The juxtaposition of materials,

taking full advantage of the properties of the composing single materials and of the properties of the whole composite, is realized in laminated materials. Examples include structural sandwiches and thermostat metals. Section 1.1.2. will treat the laminated materials in detail.

The above shows that materials can be classified as follows.

1. Single Component Materials
 - A. Traditional materials (wood, metal)
 - B. Improved traditional materials
2. Composite Materials
 - A. Laminates of single component materials
 - B. Totally integrated composites (e.g., whiskers in a softer matrix)

1.1.2. Laminated Composites

The use of laminated materials is very old. The Egyptians used laminated wood, the Romans used plywood for furniture, and swordmakers made arms from laminated steel. Present-day applications of laminated composites are far ranging.

The remainder of this section is intended to show the reader who is not familiar with this field what types of laminates do exist, where they are used and how they are manufactured. Most of the material presented in this section will be found in the work by Dietz [1].

Since laminate types are very numerous, classifying them is not straightforward. An attempt has been made to classify

them as laminates composed of non-metallic elements, laminates that exist, or can exist, of metals and non-metals, and metallic laminates. It is stressed however, that this classification is not rigid, and deviation from it occurs.

1.1.2.1. Non-Metallic Laminates

- A. Plywood is a panel consisting of an odd number of plies of wood veneer with the grain of alternate plates at right angles. These plies are bonded together under hydraulic pressure with water resistant or water-proof adhesives. Plywood is used in furniture, but its main use is in residential construction.
- B. Structural glued laminated timber consists of assemblies of suitably selected and prepared wood laminations securely bonded with adhesives. The grain of all laminations is approximately parallel longitudinally. Glued laminated members can be fabricated in almost any length, size, or structural shape. They are used for beams, columns, arches and domes.
- C. High pressure plastic laminates are made from a layup of sheets of paper, cloth, asbestos, synthetic fiber or glass in sandwich construction, each bonded with a suitable resin. They are pressed between metal pressure plates at required temperature and pressure till polymerization is finished. Originally, they replaced mica as an insulator, and their main use is still as a quality electrical insulator. Some are also used for decorative purposes.

D. Glass composites or laminates consist of two or more layers of glass bonded to one or more layers of plastic material to produce a composite structure. They are used to improve the safety characteristics of glass, as in automobile windshields; to produce resistance to penetration by missiles, as in bullet-resisting glass; or to achieve special optical properties, as in light filters. Another form of glass 'laminates' are insulating-glass windows, consisting of multiple layers of glass separated by air cells to provide thermal insulation.

1.1.2.2. Non-Metallic, Metallic Laminates

A. Structural sandwiches are constructions comprising a combination of alternating dissimilar simple or composite materials, assembled and intimately fixed in relation to each other so as to use the properties of each to specific structural advantage for the whole assembly. They are a special form of laminated composite in which thin, strong, stiff, hard and relatively heavy facings are combined with thick, relatively soft, light and weaker cores to provide a light-weight composite much stronger and stiffer in most respects than the sum of the individual stiffness and strengths. Thin strips of metal are easily bent and a block of plastic foam is easily broken, but when the metal strips are bonded to opposite faces of the plastic foam the resulting

sandwich structure resists bending and requires a heavy load to break it.

Applications of sandwich construction include aircraft wings, helicopter rotor blades, aircraft fuselage primary structure. Less exotic applications involve the use of structural building panels in industrial building construction.

- B. Glassed steel is a family of laminates, each member of which consists of a glass structure (which may vary in formulation and number of layers) applied and then fused by high-temperature firing to a base metal, usually mild steel. Unlike most other laminates, glassed steel is formed into its desired size and shape before the laminate, in this case glass, is applied to the base metal. This type of laminate can be tailored to its use by the selection of glass formulation and base metal.

Coatings of amorphous glass, inert and smooth, are used in making corrosion-resistant process equipment for chemical, petrochemical, pharmaceutical, plastic, brewery and biochemical process industries.

Coatings of crystallised glass are also used for corrosion resistance, but provide in addition abrasion resistance, impact resistance, thermal shock, and even electrical insulation.

1.1.2.3 Metallic Laminates

- A. Laminates in which the surface is essentially only a protective coating, like plated, galvanised and similarly thinly coated metals.
- B. A type of lamination is the provision of a hard, wear resistant layer on metal parts by fusion welding. The surface overlay deposited may be required for wear resistance, corrosion resistance, heat resistance. This hard facing of metal parts is widespread where the above specifications must be met. (e.g., rolling mill guides, engine valves, forming dies, plowshares, etc.).
- C. A similar type of laminate is the one formed by flame or plasma spraying of metal or ceramic to a substrate. These laminates are used for wear and abrasion resistance (carbide spraying), corrosion protection (anodic or cathodic coatings), electrical conduction (copper spraying) or electrical insulation (aluminum oxide spray), high temperature applications (spray of refractory materials).
- D. Another important class of laminates are the thermostat metals. A thermostat metal is a composite material, usually in the form of sheet or strip, comprising two or more materials of any appropriate nature, metallic or otherwise, which, by virtue of the different coefficients of thermal expansion of the components, tends to alter its curvature when its temperature is

changed. Thermostat metals can be used in a variety of ways when a change in temperature can be used to control, regulate, compensate, indicate and the like.

Four main processes are used to create a bond between components.

1. Casting the lower-melting alloy on the solid higher melting one.
 2. Joining the components directly by heat and static pressure in a press.
 3. Joining the components directly by heat and the dynamic pressure of a hot-rolling mill.
 4. Joining the components directly by dynamic pressure alone at room temperature (cold rolling).
- E. Aluminum alloy laminates are laminates of two or more aluminum alloys of different compositions metallurgically bonded (mostly sheet products). The core alloy is chosen to have the required mechanical characteristics, such as high strength, or formability or ductility.
1. When the coating alloy is chosen for the anodic protection it gives to the core alloy, the laminate is known as Alclad. Alclad is extensively used in aircraft design, tube sheets for condensers and heat exchangers, van containers for shipboard and highway transport, high quality industrial siding and roofing panels.

2. When the coating alloy has a melting point appreciably lower than that of the core, and good fluidity in the liquid state, the sheet is known as brazing sheet. This can be used for construction of extremely lightweight, high-strength sandwich panels (same type as the ones in section 1.1.2.2.A)
 3. In specific applications, when resistance per se against chemical solutions is required, a corrosion resistant coating is selected as cladding. This laminate is used in the chemical industry.
 4. Finally, there is a group of clad sheet products having a pleasing uniform appearance after etching and finished anodic coatings. This sheet type is known as clad reflector sheet, and is used in reflectors and sidings of buildings.
- F. Stainless-steel-clad metals include stainless-clad steel, stainless-clad aluminum and stainless-clad copper.
1. Stainless-clad steels are used for the corrosion resistance of the stainless steel cladding and the good heat transfer characteristics of the core. Stainless-clad steel is used in processing industries and for pressure vessels. In double clad, it is extensively used for cooking utensils.
 2. In stainless-clad aluminum, the cleanability, stain-resistance, strength and toughness of stainless steel is combined with the lightness and excellent heat-transfer

characteristics of aluminum. This indicates why this material is very widely used in the manufacture of cooking utensils, the more since it has good drawability. The electrical properties of aluminum, combined with the properties of stainless steel, make it a candidate for use in the electrical field.

3. Stainless-clad copper shows similar characteristics to stainless-clad aluminum, and is also used for cooking utensils and in the electrical field.
- G. Nonferrous-clad steels include a wide variety, such as nickel-clad steel, Monel-clad steel, Inconel-clad steel, copper-clad steel, cupro-nickel-clad steel, aluminum-clad steel. Nickel clad steel is used for equipment handling hot concentrated caustic in alkali, rayon, soap and process industries. It is also used for pressure vessels and chemical tanks. Monel-clad steel is used for heat-transfer equipment that has to be resistant to sodium chloride. Inconel-clad steel has uses similar to the previous clads, with the advantage that it can be used in oxidizing and reducing environments. In copper-clad steels, the strength imparted by the backing steel allows the corrosion resistant properties of copper to be utilized at temperatures and pressures far exceeding those where solid copper can be used. In addition to this, advantage can be taken of the excellent heat transfer properties of the copper. Hence, its use in heat exchangers,

kettles and the like is not surprising. Aluminum clad high carbon steel is used in the manufacture of heavy current conductors. The steel provides the strength, and the aluminum the good electrical conductivity.

- H. Laminates for the nuclear industry , in which uranium fuel is clad with aluminum, stainless steel, Zircaloy.

1.1.3. Manufacture of Metallic Laminates

Metallic laminates can be produced in a lot of different ways. Where the manufacturing method will be described in detail, bonding of stainless steel to carbon steel will be used as example.

- A. Fusion welding
- B. Flame or plasma spraying
- C. Casting the lower-melting alloy on the solid higher melting one. One can weld two stainless steel plates together at the edges, after inserting a parting compound, such as chromium oxide, between the two to prevent bonding between the stainless steel plates, and place the plates in an ingot mold. Molten steel is then cast around these plates. The ingot is then hot rolled to convenient thickness, the welded areas of the stainless steel plates are cut away, and the result is two simple clad plates. Double clad, that is stainless clad on either side of the carbon steel core, can be produced by placing stainless steel properly in the mold and pouring molten steel between them.

- D. Another way to produce stainless clad carbon steel is one in which a mixture for producing stainless steel, consisting of ferroalloys and other metals, is placed on the carbon steel slab, and the mixture as well as the steel slab are melted by electric arcs. A mold is used around the upright carbon steel slab to retain molten metal until solidification occurs. After that, the stainless steel-carbon slab can be further processed.
- E. The most commonly used method is the pack assembly. Carbon steel slabs and stainless steel plates are suitably packed together, and the edges of the pack are welded together. Welding tends to minimize the oxidation of the surfaces to be bonded and keeps the various components in proper register during further processing. After welding, the assembly is heated and hot rolled sufficiently to achieve a bond. The welded edges can then be removed, and the clad plates can be further processed.
- Because of the high chromium content of stainless steel, there is a strong tendency for chromium oxide to form on the surface. This oxide is a severe deterrent to bonding. In an attempt to prevent this chromium oxide formation, several techniques have been developed and described in patents. One of them is to plate or coat the stainless steel surface to be bonded with iron or nickel. Another solution is to evacuate the pack to a low residual pressure after welding to remove essenti-

- ally all oxidizing atmosphere. To achieve optimum bonding, all surfaces to be bonded have to be as clean and as oxide-free as possible. The assembly must also be at the proper temperature for hot rolling.
- The rolling step has to give a sufficient reduction to bring the surfaces to be bonded in intimate contact, and to break up any oxide film that eventually may have formed. Similar pack assembly hot or cold rolling is also applied for a lot of other types of laminated metal sheet. Table 1.1 gives the amount of reduction required for successful bonding for different laminates.
- F. The vacuum brazing technique can be used to bond stainless steel to carbon steel. Brazing alloy is placed on the surfaces to be bonded. The assembly is welded all around the edges, evacuated and heated under vacuum to achieve bonding. No reduction is required to achieve bonding, and the plates used can already have their final thicknesses.
- G. Explosive welding can also be used to achieve bonding. The clad metal is held at a controlled distance from the base metal and the explosive charge is detonated. This brings the surfaces to be bonded into intimate contact and bonding is achieved.
- H. All the above methods provide metallurgical bonding. Nonmetallurgical bonding can be achieved by using adhesives to bond the materials.

TABLE 1.1

Minimum Reduction Required to
Produce a Bond in Roll Bonding

METALS USED	% REDUCTION	COMMENTS	REFERENCE
Copper	45	-	Agers (2)
Aluminium	40	-	"
Copper and Aluminium	65	-	Donelan (3)
-	40	Minimum to pro- duce any bond- ing	Rollason (4)
-	70	To give 100% bonding	"
-	2	Small work rolls in vacuum	"
Niobium to Steel	30-40	10-15% per pass	Krivososov et al (5)
Refractory or Reactive metal Combinations	5-40	Rolled in inert atmosphere	Bianchi (6)

I. Laminated bar or tube type products can also be produced by other processes, such as extrusion.

There may be other processes used to produce laminates of which the author is not aware. It is hoped that this description has helped the reader to realize the importance of laminated materials.

1.2. State of the Art of the Plastic Deformation of Laminated Metals

It was outlined in section 1.1.3. that several methods of plastic deformation, such as rolling and extrusion, are used to provide a metallurgical bond by pressure welding between dissimilar metals to manufacture laminates. A lot of research has therefore gone into this laminate producing process.

Laminated rods, tubes and cans can be formed by the extrusion of dissimilar metals. This type of process has successfully been developed for the production of nuclear fuel elements, see Internal Atomic Energy Authority [7]. In recent years, the extrusion of dissimilar metals has been extended into more general fields of application. The interested reader is referred to work done at Batelle Memorial Institute [8], Nuclear Metals Inc. [9], and Cleveland Crane and Engineering [10], and to Whitfield [11]. A summary of the mechanical and metallurgical factors involved in co-extrusion of dissimilar metals is given by Loewenstein and Tuffin [12]. It is interesting to note that it was even suggested to extrude simultaneously through a single die two billets of different materials held in separate

containers, to form bimetallic strip. See Darling [13], and Alexander and Whitlock [14].

Rolling of dissimilar metals is used to produce a laminated sheet by pressure welding. But the interest in rolling dissimilar metals was also generated by the fact that a high strength material, while rolled in a loose pack, i.e., the high strength metal is simply put between sheets or slabs of softer metal, can be more easily deformed than when rolled as a single sheet. This loose pack rolling is used in the rolling of stainless steel and titanium. Hence, work has been carried out on rolling dissimilar metals, both for non-bonded and bonded packs. More information on the rolling of laminates can be found in Arkulis [15], Arnold and Whitton [16], Pomp and Lueg [17]. It may be useful to point out that rolling is the process for which the most work describing the plastic deformation of laminated materials has been done.

In most cases, the laminated material is not produced in its final shape in the bonding process. Hence, mechanical working to change the geometry is necessary. The same processes as used for single materials can be used. The fact that the material is laminated can have an effect on how well these processes can be carried out. It was mentioned before that loose pack rolling of soft clad high strength materials is easier than the rolling of the single strong material. This is an example in which the cladding makes the deformation process easier to perform. This however is not always the case. An

example is the drawing of copper coated steel wires. Failure of the wire can occur, although an unclad steel wire of the same size can be drawn without difficulty. These two examples make it clear that it is necessary to analyze the mechanics of the plastic deformation of laminated materials to gain insight into the deformation patterns, and to understand why certain processes are easier to perform with laminated materials, while others are more difficult.

One of the techniques applied to analyze laminate plastic deformation is to assume that the different laminates undergo equal straining. An equivalent flow stress, determined by the traditional law of mixtures, can then be determined as a function of the separate yield stresses and the volume fraction of the layers in the composite. The composite is then treated as a single metal with a flow stress the equivalent flow stress. The plastic behaviour of laminates in tension, compression, rolling, drawing and extrusion has been described using this equivalent flow stress. See Weinstein and Pawelski [18], Atkins and Weinstein [19], Arkulis [15]. The equal strain hypothesis for all layers requires, since all the material deforms plastically, that the stresses in the different materials are different (since they have different yield stresses). The different behaviour of laminated and single materials in the two examples above, rolling of loose pack and wiredrawing of copper coated steel, can be accounted for by this difference in stresses in the different laminates.

Hawkins and Wright [20], [21] mention a different hypothesis, namely that the stress in the different components is equal. Since the different materials have different yield strength, the strains in the different components will generally be different, so that the different materials must be free to deform independently from each other. They indicate that in practice, the behaviour of a laminated composite will always lie between the behaviour found by using the equal strain hypothesis, and the one found by using equal stress. For fully bonded laminated materials, no relative movement at the laminate interface will be allowed, and the equal strain hypothesis seems therefore more appropriate than the equal stress hypothesis.

More involved analysis of plastic deformation of laminated composites has been made by slip line analysis for plane strain processes. See Brovman and Yudin [22], who indicate how plane strain compression, rolling, drawing and extrusion of laminated materials can be analyzed, and Arcisz [23], who analyses the cutting of bimetallic strip by smooth rigid punches.

Not much information is available with regard to the pressforming properties of clad materials. Substantial improvement in drawability, over conventional steel sheet, have been reported for tin, - see Duckett et al [24] - and zinc, - see Nelson [25], coated steel. The improvement in drawability seems to be attributed to the coating metal acting as a solid-state lubricant or as an aid in retaining the lubricating oil film.

Rathbone [26] did stretch forming on mild steel-stainless steel laminates, and found deeper penetrations when the thick component (mild steel) was the outer one. But he did not indicate if the deeper penetrations were obtained because the outer component was the thicker one, or because it was mild steel rather than stainless steel.

Some more information became available with the work of Hawkins and Wright [20], [21], who investigated the press-formability of copper-mild steel laminated sheets. They found that the stretch formability of a copper-steel bimetal is dependent on the ductility of the outer component, and not on the ductility of the composite as a whole, see Fig. 1.1. They also found that the thickness strains over the punch nose in deep drawn cups of copper-steel bimetal was greater when the outer component was copper, see Fig. 1.2, and that the degree of thinning increased with percent copper, see Fig. 1.3. Hawkins and Wright also calculated the punch loads for deep drawing and stretch forming using the equal strain hypothesis, and their calculated values were in close agreement with their experimental values.

1.3. Scope of this Work

This work will investigate the behaviour of laminated metal sheets in metalworking operations. The pressworking of sheet consists basically of two operations, stretch forming and deep drawing. Stretch forming of laminated sheet will be

investigated with the use of the hydrostatic bulge test. Deep drawing is a more complex operation than stretching, as shown by the stress system on a segment of a deep drawn cup shown in Fig. 1.4. Deep drawing tests in bimetals will be done to compare the results with those obtained by Hawkins and Wright. When deep drawing a cup, bending and unbending of the material takes place. The author felt that whichever laminate is on the outside of the deep drawn cup could be of importance in this bending and unbending. A big portion of this work will therefore be devoted to an analysis of the bending of laminated sheet.

CHAPTER 2

EXPERIMENTAL STRETCHING OF LAMINATED SHEET BY THE BULGE TEST

2.1. Materials Used in the Experiments

Four different laminates were used. They are described in Table 2. All laminates were delivered in coils. One of the coils, laminate D, was probably the endzone of a sheet and was not perfectly bonded. Thus it was possible to separate the stainless steel from the aluminum for part of the coil. These sheets will be called D-SS and D-AL. A replacement coil for D was ordered, and this coil was labeled DD. The relative thickness of each laminate in the sheets was determined by preparing metallographic specimens of cross-sections of the sheet, and measuring the relative thickness under a measuring microscope. The metallographic specimens were etched with Keller's etch in an attempt to identify the different aluminum laminates. Photo micrographs are shown in Fig. 2.1. The distinction between the two aluminum laminates was clear for material B only. In materials C, D and DD no clear boundary or change in structure is visible.

Tensile tests on the different sheets were performed using the tensile test specimen of Fig. 2.2. Specimens were cut out under 0° , 45° and 90° to the rolling direction, and tested in an Instron Tensile Testing Instrument using a .5 in/min crosshead speed and an extensometer with .5 in. gauge length and

Table 2.1
COMPOSITION OF THE LAMINATED SHEETS

Sheet	Composition	Percentage of Laminate %	Nominal Sheet Thickness 10^{-3} in	Real Sheet Thickness 10^{-3} in
B	434 SS	40.4	22.5	23.3
	C22 AL*	core 4.2		
	5052 AL	55.4		
C	201 SS	39.7	22.5	23.0
	C22 AL	core } 60.3		
	5052 AL			
D	304 SS	18.0	51	54.0
	C22 AL	core } 82.0		
	3003 AL			
D-SS	304 SS	100	-	9.85
D-AL	C22 AL	100	-	45.9
	3003 AL			
DD	304 SS	17.7	51	53.3
	C22 AL	core } 82.3		
	3003 AL			
E	430 SS	29.7	50	51.0
	C22 AL	core 67.5		
	Zinc	2.8		

* C22 AL is 1100 AL with 1.5% to 1% Si.

50 percent maximum elongation for determination of the load-elongation curve. For every test, values of the .2 percent yield strength, the ultimate tensile strength and the uniform elongation were determined. A set of about ten points in the plastic region of every stress-strain curve were taken to determine the parameters A , ϵ_0 and n in the stress-strain relation

$$\bar{\sigma} = A (\epsilon_0 + \bar{\epsilon})^n$$

Between two and six tests were performed for every sheet in the different directions. The averages of these tests were used to calculate the values given in Table 2.2, and to determine the stress-strain curves given in Fig. 2.3 to Fig. 2.9. The above given stress-strain relation fits very well the experimental stress-strain curves for sheets B, C and D-SS. However, the suggested stress-strain curve does not provide a good fit for the test data of materials D-AL, E, D and DD. Fig. 2.7 and 2.9 give the suggested stress-strain curve and some experimental curves for sheets D-AL, and E. It is clear that the suggested stress-strain curve is not suited to describe the experimental data. The strain values obtained in the tensile tests of materials D-AL and E are very low, as can be verified in Table 2.2. For such small elongations, the elastic and plastic strains are of the same order of magnitude. Since the suggested stress-strain curve has no terms to account for elastic behaviour, the fit of that curve is poor for materials

Table 2.2. Tensile Properties of
the Laminated Sheets

Sheet Composition given in Table 2.1)	Angle of Tensile Axis with Rolling Direction.	Yield Stress 10 ³ psi	Ultimate Tensile Strength *		Percentage Uniform Elongation **		Stress-Strain Curve Parameters $\bar{\sigma} = A (\epsilon_0 + \bar{\epsilon})^n$		
			10 ³ psi	10 ³ psi	%		A 10 ³ psi	ϵ_0	n
-	0								
B	0	46.0	54.0		10		76.6	.0083	.111
	45	46.2	54.2		8.6		72.5	.0017	.083
	90	47.0	55.9		10		76.6	.0035	.095
	average	46.4	54.7		9.5		75.2	.0045	.096
C	0	-	70.7		39		141	.0946	.426
	45	-	68.7		40		136	.0875	.410
	90	-	67.9		37		137	.149	.503
	average	-	69.1		39		138	.111	.447
D ***	0	28.6	39.9	39.7	1.2	20	57.7	.581	.766
	45	28.6	37.9	37.7	1.5	15	46.4	.777	.869
	90	28.6	39.0	38.5	1.4	15	44.7	.846	.961
	average	28.6	38.9	36.6	1.37	17	49.6	.735	.865
D-SS	0	77.1	109		34		224	.0953	.447
	45	73.6	104		38		196	.0533	.341
	90	73.3	104		35		215	.126	.503
	average	74.7	106		36		212	.0916	.430
D-AL ****	0	24.8	28.7		1.10		224	0.	.419
	45	25.1	28.0		1.03		203	0.	.418
	90	25.8	28.6		.96		219	0.	.409
	average	25.3	28.4		1.03		215	0.	.415

continued

Table 2.2. Continued

Sheet Composition given in Table 2.1)	Angle of Tensile Axis with Rolling Direction	Yield Stress 10 ³ psi	Ultimate Tensile Strength		Percentage Uniform Elongation		Stress-Strain Curve Parameters $\bar{\sigma} = A (\epsilon_0 + \bar{\epsilon})^n$		
			*	*	**	**	A 10 ³ psi	ϵ_0 -	n -
DD ***	0	32.7	36.4	38.0	.7	30	69.3	.223	.475
	45	31.2	34.7	35.7	.8	30	66.1	.239	.476
	90	33.3	34.7	35.7	.6	30	64.6	.209	.449
	average	32.4	35.4	36.4	.7	30	66.7	.224	.467
E ****	0	56.8	60.5		1.26		173	0.	.218
	45	52.9	58.2		1.36		248	0.	.301
	90	60.1	63.5		.71		1616	0.	.639
	average	56.6	60.8		1.11		-	-	-

*: The first value given in this column for sheet D or DD is the stress, i.e., load divided by original area, corresponding to the first maximum in the load-elongation curve. The second value gives the stress corresponding to the second maximum.

**: The first value given in this column for sheet D or DD is the percentage elongation corresponding to the first maximum in the load-elongation curve. The second value gives the elongation corresponding to the second maximum.

***: The stress-strain parameters for sheets D and DD given in this table relate to zone 3 of the stress-strain curve, as explained in the text and in Fig. 2.5 and 2.8.

****: The fit of the power-law with the stress-strain curve for sheets D-AL and E is poor. Since the strain attainable in the tensile tests was very low, the elastic and plastic strain are of the same order of magnitude. This explains the poor fit.

D-AL and E. The suggested stress-strain curve does not provide a perfect fit for the experimental curves of materials D and DD for a different reason. Sheets D and DD have a load-elongation curve with two maximums. The load goes through a first maximum at a small strain, the load then decreases, starts to increase again, and reaches the second maximum at a high strain. Final necking and fracture follow. The first maximum load is the biggest one for sheet D, and hence, this first maximum determines the ultimate tensile strength for this material. For sheet DD, the second maximum is the larger one. An example of the load-elongation curve of a specimen of sheet D is given in Fig. 2.10. Note that the first maximum in the load of tensile specimen D occurs between 1. and 1.25 percent elongation. The maximum elongation of the aluminum part of sheets D, D-AL, for a specimen in the rolling direction has an average value of 1.1 percent, as indicated in Table 2.2. It is therefore thought that the first maximum in the tensile tests on materials D and DD is related to the fact that the aluminum has reached its maximum load carrying ability. Since the aluminum is supported by the stainless steel, any increase in load must be absorbed by the stainless steel. It is possible that, when the aluminum is maximally loaded, the decrease in cross sectional area due to further elongation has a greater effect on the total load than the effect of the strainhardening of the stainless steel. Hence, the load goes through a maximum. However, real localized necking does not occur. For further elongation, the strainhardening of the stainless steel becomes the more important

influence, and the load starts to increase. The new maximum the load will reach, and at which necking starts, is dependent on the stainless steel properties. The stress-strain curve of the specimen of sheet D, whose load-elongation curve is featured in Fig. 2.10, is given in Fig. 2.5. Its stress-strain curve consists of three zones. In zone 1, the stress-strain curve is very steep. This is the elastic zone. For zone 2, the curve decreases in slope and becomes horizontal. The beginning of this horizontal part coincides with the first maximum in the load-elongation curve, and the horizontal part itself with the decrease in load after this first maximum. In zone 3, the stress-strain curve increases almost linearly with increasing strain. The stress-strain curve in zone 3 can be represented by

$$\bar{\sigma} = A (\epsilon_0 + \bar{\epsilon})^n$$

The values for A , ϵ_0 and n given in Table 2.2 for materials D and DD determine the stress-strain curve in zone 3 for these materials.

It may be pointed out that in all the tensile tests of laminated sheets, curling of the testpieces along the longitudinal tensile axis (thus in transverse direction of the testpiece) was observed during the tests. An example is shown in Fig. 2.11. This has also been reported by Hawkins and Wright [20], and they attribute this curling to different R-values

for the different laminates. Since the R-value is the ratio between width and thickness strain, a difference in R-values between the laminates will cause a different width strain for the same elongations. This causes stresses in the width direction of the tested specimen, which can be relieved by curling of the testpiece. When the laminated testspecimens fracture, the laminated layers unload elastically. The difference in their modulus of elasticity causes the testpiece to bend along the transverse direction during this unloading. Although no investigation in this curling and elastic bending was carried out, it is important to know that the same effect applies when pressforming laminated sheets. Warping of the formed sheets can occur, especially for asymmetric shapes.

It was indicated that part of sheet D was defectively bonded. A tensile test specimen of that defective material is shown in Fig. 2.12. At fracture, the bond between the different laminates becomes loose, and the laminates necked under different angles to the longitudinal axis.

2.2. Biaxial Stretching of Laminated Sheet

It was pointed out in Chapter 1, section 1.2, that Hawkins and Wright [20], [21] have found that the stretch-formability of a copper-steel bimetal is bigger when the copper is on the outside than when the steel is, see Fig. 1.1. It is interesting to check if their claim, that the stretch-formability is only dependent on the ductility of the outer component, is valid for the laminates that we have available. They performed

stretching by the Erichsen-test. The stretching tests carried out on our laminates were performed by the hydrostatic bulging of circular and elliptical diaphragms. All sheets contain a stainless steel laminate on one side. Tests were done with the stainless steel either on the outside or on the inside of the bulge, to see if this made a difference in stretch-formability. Balanced biaxial stressing by bulging circular diaphragms was carried out for all sheets available, and will be treated in section 2.2.1. A forming limit diagram for the sheet DD was determined by bulging elliptical diaphragms, and this is discussed in section 2.2.2.

2.2.1. Balanced Biaxial Stretching

During the hydrostatic bulging of a circular diaphragm of an isotropic material, the material in the pole is subject to an equal biaxial stress system. The bulge test allows to determine a stress-strain curve of the material for strains that are bigger than the ones that can be obtained in a tensile test, since the point of instability, i.e., the onset of necking, occurs at a higher strain. Analysis of the deformation process in the circular bulge test has been performed by Hill [27] and Mellor [28].

The biaxial test equipment used is shown in Fig. 2.13, and is described by Albertin [29]. The deformation history during a circular bulge test is determined by recording the hydrostatic pressure, the radius of curvature at the pole and the strain at the pole. The two latter ones are measured by

a combined spherometer and extensometer, originally described in Johnson et al [30]. During the tests of circular diaphragms of laminated sheet with the stainless steel to the outside of the bulge, it was noted that the sharp points of the extensometer, which normally should follow the deformation of the bulge, slipped on the very smooth stainless steel surface. To be able to measure the strains without the extensometer, square grids of .098 in spacing were printed on the specimens using a photoresist technique. The grid spacing at the pole after deformation determines the maximum strain the sheet has undergone. It was tried to use a replica technique, as described by Van Minh et al [31], since it is easier and more accurate to measure the deformed grid spacing on a replica than on the bulged specimens. Attempts to produce good replicas were unsuccessful and hence, the strain measurements were done by placing the bulged specimens under a measuring microscope.

Circular bulge tests were performed on sheets B, C, D and DD. Figs. 2.14, 2.15, 2.16 and 2.17 show the representative strain at the pole, the radius of curvature at the pole and the pressure for the failure of the specimens of sheets B, C, D, and DD respectively. The first three specimens in these figures are diaphragms tested with the stainless steel to the outside of the bulge and the last three specimens are tested with the stainless steel to the inside. For some specimens, the strain at the pole at fracture could not be determined accurately. This accounts for the

missing points on the graphs. A comparison, for every sheet, of the results of the specimens with stainless steel to the outside, or to the inside, shows that, if there is a difference in the maximum stretching deformation between the two cases, then that difference is of the same order of magnitude as the differences between the different specimens for the same case. The results in Figs. 2.14, 2.15, 2.16 and 2.17 do not allow to conclude that there is a difference between tests with one laminate to the inside or to the outside, and as such, cannot be used to confirm the results of Hawkins and Wright. To determine if there is a difference in stretch forming behaviour with one laminate to the outside or the inside of the sheet, should require an extensive series of tests for materials B, C, D and DD. Since the bulge tests themselves require a large amount of work, since the amount of laminated material available was limited, and since the results thus far obtained show no significant difference in behaviour, no further tests on the stretch forming of the sheets B, C and D were performed.

Attempts were made to bulge circular specimens of sheet E, but the material always fractured at the edge of the specimens near or in the clamping ring. The material could not sustain the bending that occurs near the rim when the specimen starts to bulge.

2.2.2. Forming Limit Diagram

The circular bulge test allows a sheet to be stressed at the pole in balanced biaxial tension. When elliptical instead

of circular diaphragms are used, the stress at the pole is still biaxial tension, but the principal stresses are not equal. By changing the ratio between the major and minor axis of the elliptical diaphragms, different stress ratios and hence different strain ratios, can be obtained at the pole of the bulge. The forming limit, i.e., the maximum allowable strain in rolling and transverse direction of the sheet, can be determined for different strain ratios. The data so collected form the forming limit curve for that sheet material. Fig. 2.18 shows a typical forming limit curve, and different laboratory tests to determine different points on the curve.

A part of the forming limit curve for sheet DD was determined using the elliptical dies, shown in Fig. 2.19, having aspect ratios 4:3, 2:1 and 4:1, and the circular die, Fig. 2.13. A detailed description can be found in Yousif et al. [32] and Albertin [29]. The strains in rolling and transverse direction were determined by using the method described in section 2.2.1. For every die, tests were done with the major axis in both rolling and transverse directions. All tests were performed twice with stainless steel to the inside of the bulge, and twice to the outside. The results of these tests are featured in Fig. 2.20. For the specimens in region 1 the major axis of the elliptical dies was parallel to the rolling direction, and in region 2 the major axis was parallel to the transverse direction of the sheet. The specimens tested in the 4:1, and one in the 2:1 aspect ratio die, failed prematurely at the rim of the

diaphragm. These points are represented on the graph, but do not really belong to the forming limit curve.

The tests in region 1 seem to indicate that the stainless steel to the inside of the bulge gives higher strains. In region 2, it is however less certain if there is a difference between stainless steel on the inside or outside. Hence, another variable is introduced, since the rolling direction has been reversed with respect to maximum strain axis.

It is clear in Fig. 2.20 that higher strains can be obtained when the rolling direction is parallel to the major strain axis (region 2, i.e., rolling direction along minor axis of elliptical dies). In a sheet with planar isotropy (or fully isotropic) the behaviour in region 1 or 2 should be the same. Since the maximum strain attainable at the pole is different for regions 1 and 2, the sheet must be planar anisotropic. This is not surprising, since during the rolling of even monometal sheet some form of anisotropy is produced.

Although higher strains seem to be obtained when the aluminum is on the outside of the bulge when the rolling direction is parallel to the minor strain axis (region 1), it is less certain if there is a difference in region 2. The number of tests performed, two for every configuration, is not sufficient to draw valid conclusions from this graph. No more of material DD could be used for determination of the forming limit curve, since the remaining material was needed for other experiments.

2.2.3. Conclusion

The results found in sections 2.2.1. and 2.2.2. on the stretching forming of laminated sheet do not allow to draw any firm conclusions regarding the influence of the outside laminate on the stretch forming operation. More tests than were performed for this thesis are necessary to see how big the influence of the outside laminate on the stretch forming of laminated sheet really is.

In bending, however, where the outside surface is loaded in tension and the inside one in compression, it can be expected that, if the sheet is laminated, the relative position of the laminates in the sheet will have an influence on the bending of the sheet. Since bending and unbending occurs in deep drawing operations, an understanding of the bending of laminated sheet could help to understand the deep drawing behaviour of laminates. Hence, the next chapters will deal with plastic bending. Experiments on the deep drawing of laminated sheet will be treated after an insight into the plastic bending of laminates has been obtained.

CHAPTER 3

GENERAL THEORY OF PLASTIC SHEET BENDING

This chapter provides a general theory of plastic sheet bending following the earlier work of Crafoord [33]. The essential features of the theory are given, along with the basic assumptions used in developing the theory.

3.1. Basic Assumptions

3.1.1. Homogeneous Material

This means that the material is considered to be free from defects, such as inclusions, cavities, and the material properties must be uniform from point to point.

When considering laminated sheet, we allow for different properties of the different laminates, but every laminate must be homogeneous.

This also implies that the bonding between different laminates is such that it can sustain the deformations without failure of the bond. No voids between the different laminates are allowed, since we will suppose that points in different laminates that are infinitesimally close, will undergo exactly the same deformation.

3.1.2. Isotropic Material

This assumption is quite common in the analysis of plastic deformation of materials. It is expected, however,

that clad sheet metal, produced by cold roll-bonding, will have a certain degree of planar anisotropy. It could be worthwhile to analyze the plastic plane strain bending of anisotropic sheet, and compare it with the bending of an isotropic material, but this is not included in the present study.

In the bending of laminated sheet, the different laminates will have a different plastic stress-strain behaviour, but each laminate is considered to be isotropic. Thus orthotropic laminates, like fibres embedded in a metal matrix, are excluded.

3.1.3. Pure Bending Assumption

Pure bending signifies that there are no resultant normal or radial forces on the radial cross sections of the bend, and that there are no external forces, neither tangential nor radial, acting on the inner or outer surfaces of the bent sheet. This type of bend can be carried out by the four point bend test. See Fig. 3.1, and Crafoord [33], Horrocks and Johnson [34].

Crafoord [35] has pointed out that the industrial bending carried out in vee-formed tools can justifiably be assumed to be pure bending, since the shear stresses are only a small fraction of the other stresses in the bent material. That industrial bending methods can be readily approximated by pure bending was also pointed out by other authors, see for example Onat and Shield [36], Drucker [37], Hodge [38].

3.1.4 Plane Strain Assumption

Bending a strip with a width of the same order of magnitude as the thickness, results in plane stress bending since there is no significant stress in the width direction. In this case the bent strip shows anticlastic curvature. See Horrocks and Johnson [34].

For a sheet whose width is many times its thickness, the central sections of the sheet are prevented to deform in the width direction, the anticlastic deformation is restrained in the central sections, and a state of plane strain exists in these sections. Strictly speaking, a state of plane strain does not exist at the edge of the sheet.

However, when the ratio of sheet width to thickness is big enough, this different deformation pattern at the edge of the sheet can be neglected, and the entire sheet is considered to deform in plane strain.

3.1.5. Radial Sections in the Bend Remain Plane

This is the traditional Bernoulli hypothesis, and applies since the shearing stresses are neglected. However, this assumption is only valid in the zone of pure bending. In the four point bend test, for example, Figs. 3.1 and 3.2, the zones between the outside points are not subjected to pure bending, and the hypothesis does not apply there.

3.1.6. Incompressible Material

This assumption is frequently used in the study of metalworking processes, and sufficient data exists to support

the assumption.

3.1.7. Rigid-Plastic Material

The elastic behaviour of the material is neglected in the pure plastic bending model to hold the theory as simple as possible.

This implies that the theory cannot describe the bending in its early stages, where the material is mainly elastic. It also means that the theory cannot give any information on spring-back, since this phenomenon is caused by the elasticity of the material.

It is thought, however, that in the case of severe bending the influence of the elastic properties of the material is small compared to the large plastic deformations.

The analysis for the pure bending of an elastic-perfectly plastic material (mono-metal) has been made by Shaffer and House [39], [40]. The elastic-perfectly plastic behaviour of bimetal thermostats has been published by Mahrenholtz and Johnson [41].

The purely elastic behaviour of laminated sheets has been given by Ashton, Halpin and Petit [42], Ashton and Whitney [43], Calcote [44], Astm-Stp 450 [45]. The interested reader is also referred to the Journal of Composite Materials where the purely elastic behaviour of laminates is featured.

3.2. Essential Features of the Pure Plane Strain Plastic Bending Theory

3.2.1. Equilibrium Equation

Fig. 3.3 represents an infinitesimal element in the bending zone. Due to the symmetry of the deformed element, the principal stresses act in the radial, tangential and width directions. The sections of the element are therefore shear stress-free. The symmetry of the element requires that the tangential stress σ_ϕ be independent of the angular position ϕ of the section.

The equilibrium equation is therefore

$$\sigma_\phi - \sigma_r = r \frac{d\sigma_r}{dr} \quad (3.2.1)$$

3.2.2. Yield Condition for Plane Strain

It is assumed that the material follows the Von Mises yield criterion and the Levi-Mises flow rule. Since there are no shear stresses, the principal directions of stress and strain coincide, and will be indicated by the indices 1, 2 and 3, so that $\sigma_1 \geq \sigma_2 \geq \sigma_3$. The effective stress is given by

$$\bar{\sigma} = \frac{1}{\sqrt{2}} \sqrt{(\sigma_1 - \sigma_2)^2 + (\sigma_2 - \sigma_3)^2 + (\sigma_3 - \sigma_1)^2}$$

Since the material is rigid-plastic, the strain and strain increments are the plastic strain and plastic strain increments. The effective strain increment is therefore

$$d \bar{\epsilon} = \sqrt{\frac{2}{3} (d \epsilon_1^2 + d \epsilon_2^2 + d \epsilon_3^2)}$$

For plane strain conditions, with straining prevented in the 2 direction,

$$d \epsilon_2 = 0$$

With the Levi-Mises flow rule, with σ_m being the hydrostatic pressure, this yields

$$\sigma_m = \sigma_2 = (\sigma_1 + \sigma_3)/2$$

Since the constancy of volume requires

$$d \epsilon_1 + d \epsilon_2 + d \epsilon_3 = 0$$

Then

$$d \epsilon_1 = - d \epsilon_3$$

And hence,

$$d \bar{\epsilon} = \frac{2}{\sqrt{3}} |d \epsilon_1| \quad (3.2.2.)$$

It is assumed that the yield condition can be described by a relationship between the equivalent stress and the integral of the equivalent strain increments.

$$\bar{\sigma} = H \left(\int d \bar{\epsilon} \right)$$

Under plane strain conditions, the Von Mises yield criterion can be reduced to

$$\bar{\sigma} = \frac{\sqrt{3}}{2} (\sigma_1 - \sigma_3)$$

Where

$$\sigma_1 \geq \sigma_2 \geq \sigma_3$$

And

$$\sigma_2 = (\sigma_1 + \sigma_3)/2$$

Hence,

$$\sigma_1 - \sigma_3 = \frac{2}{\sqrt{3}} H \left(\int d\bar{\epsilon} \right) \quad (3.2.3.)$$

which is the yield criterion for plane strain.

3.2.3. Tangential Strain and Unelongated Layer

Assume that l_0 is the distance between two parallel crosssections of the sheet when it is flat. After bending, these two sections remain plane and are radial sections with included angle ϕ . A flat layer in the original sheet assumes the form of a cylinder. The tangential strain of this layer is

$$\epsilon_\phi = \ln \frac{l}{l_0} = \ln \frac{r\phi}{l_0} \quad (3.2.4)$$

During the bending of the sheet there will be a particular layer whose length, for a given angle of ϕ , is unchanged and measures l_0 . This layer is known as the unelongated

layer and specifying its radius as r_o it follows that

$$r_o \phi = l_o \quad (3.2.5)$$

The tensile strain for an arbitrary layer is therefore

$$\epsilon_\phi = \ln \frac{r}{r_o} \quad (3.2.6)$$

Defining r_m as the radius of the central layer, r_i the radius of the inside layer and r_y the radius of the outside layer, then

$$r_m = (r_i + r_y)/2 \quad (3.2.7)$$

Therefore

$$\epsilon_\phi = \ln r/r_m + \ln r_m/r_o \quad (3.2.8)$$

Since plastic bending occurs under constant volume,

$$l_o t_o = \frac{\phi}{2} (r_y^2 - r_i^2) = \frac{\phi}{2} (r_y - r_i) (r_y + r_i)$$

$$l_o t_o = \phi t r_m$$

With (3.2.5), this becomes

$$\frac{t}{t_o} = \frac{r_o}{r_m} \quad (3.2.9)$$

Hence

$$\epsilon_\phi = \ln \frac{r}{r_m} + \ln \frac{t_o}{t} \quad (3.2.10)$$

3.2.4. The Neutral Layer

The neutral layer in plane strain bending is usually defined as the layer in which the tangential stress σ_ϕ changes from compressive to tensile when we cross that layer from the inside of the bend to the outside. See Fig. 3.4. However, Crafoord [33] has indicated that σ_ϕ can be compressive to the outside of the neutral layer, which makes the previous definition invalid. The present investigation also shows that, in the bending of laminated sheet, we can have different radii in one bend where σ_ϕ changes sign. This can be illustrated with Fig. 3.5, in which the radial and tangential stress distribution across the sheet thickness is given for a sheet consisting of three laminates bent to a relative curvature $\kappa = 1$. The two cladding laminates have four times the yield strength of the core laminates. The percentages of the different laminates in the sheet is twenty percent for the cladding on the inside of the bend, forty percent for the soft core, and forty percent for the clad on the outside of the bent sheet. The stress distributions of Fig. 3.5 were determined using the techniques described in Chapter 4 and Appendix V. Fig. 3.5 shows that σ_ϕ changes three times in sign across the sheet thickness. Once in the inside clad laminate, at the neutral radius, once at the laminate boundary radius inside clad-core, and once for a radius in the core laminate.

It seems therefore appropriate to review the definition of the neutral layer.

For plane strain conditions,

$$\sigma_m = \sigma_z = (\sigma_\phi + \sigma_r)/2$$

where σ_m is the hydrostatic pressure. The deviatoric stresses are then

$$\sigma_\phi' = \frac{1}{2} (\sigma_\phi - \sigma_r)$$

$$\sigma_r' = \frac{1}{2} (\sigma_r - \sigma_\phi)$$

$$\sigma_z' = 0$$

so that

$$\sigma_\phi' = -\sigma_r'$$

when $\sigma_\phi > \sigma_r$, thus σ_ϕ' positive, then the yield criterion (3.2.3) becomes

$$\sigma_\phi - \sigma_r = \frac{2}{\sqrt{3}} H \left(\int d\bar{\epsilon} \right) \quad (3.2.3A)$$

when $\sigma_\phi < \sigma_r$, thus σ_ϕ' negative, then

$$\sigma_\phi - \sigma_r = -\frac{2}{\sqrt{3}} H \left(\int d\bar{\epsilon} \right) \quad (3.2.3B)$$

This leads to the following definition of the neutral layer in plastic bending.

'The layer (surface), for which the deviatoric tangential stress changes sign in pure plastic plain strain bending, is called the neutral layer (surface). Its radius is the neutral

radius." This implies that the material on the outside of the neutral surface is subject to a stress system with a tensile deviatoric tangential stress and a compressive deviatoric radial stress. The material on the inside of the neutral surface undergoes a compressive deviatoric tangential stress, and a tensile deviatoric radial stress.

Since plastic behaviour is independent of hydrostatic pressure, and the principal directions of stress and strain coincide, $d \epsilon_{\phi}$ has the same sign as σ'_{ϕ} . In addition to this, $d \epsilon_{\phi}$ has to vary continuously across the sheet thickness, (compatibility of deformations), so that $d \epsilon_{\phi} = 0$ when σ'_{ϕ} changes sign. Hence, the last definition of the neutral surface is completely equivalent to the following one :

"The layer (surface), for which the tangential strain increment $d \epsilon_{\phi}$ is zero, is called the neutral layer (surface)".

It is obvious that, when the yield condition (3.2.3A) or (3.2.3B) is substituted in equilibrium equation (3.2.1), the equilibrium equation is different, depending on which side of the neutral layer the material for which the equation is valid is situated. For materials to the outside of the neutral surface in the bend, the equilibrium condition becomes

$$r \frac{d \sigma_r}{dr} = \frac{2}{\sqrt{3}} H \left(\int d \bar{\epsilon} \right) \quad \text{for } r \geq r_n \quad (3.2.1A)$$

whereas, for materials to the inside, the equilibrium requires that

$$r \frac{d \sigma_r}{dr} = - \frac{2}{\sqrt{3}} H \left(\int d \bar{\epsilon} \right) \quad \text{for } r \leq r_h \quad (3.2.1B)$$

3.2.5. The Movement of Individual Layers

During the plastic bending of a sheet the unelongated layer moves through the thickness of the sheet. Thus there is a region in the sheet which has first undergone compressive straining followed by tensile straining. Consequently for strain hardening materials (with or without Bauschinger effect), it is necessary to follow the straining path of the individual layers. Essentially this means that the strains for each layer have to be compounded and that the current tangential strain, i.e., $\epsilon_\phi = \ln r/r_0$, is not sufficient in itself to determine the stress state. The analysis becomes even more involved when dealing with laminated materials but the method still involves following the straining path of individual layers through the thickness of the sheet.

When bending a mono-metal, it is convenient to characterize every material layer by a scalar λ , where $0 \leq \lambda \leq 1$. λ being the volume fraction of material embraced by a particular layer and the inside surface of the strip. Thus during the bending of a strip, defining $\lambda = 0$ implies that the layer coinciding with the inside surface of the bend is being considered, and similarly $\lambda = 1$ fixes the layer at the outside surface. This volume fraction λ does not change during bending, and therefore defines the material layer completely.

Considering a layer with volume fraction λ which assumes a radius r after bending, it can be found, using the definition of λ , that

$$\lambda = (r^2 - r_i^2) / (r_y^2 - r_i^2) \quad (3.2.11)$$

Hence,

$$r = \sqrt{r_i^2 + \lambda (r_y^2 - r_i^2)} \quad (3.2.12A)$$

Considering the bending of laminates, a material boundary can also be characterised by a scalar μ indicating the volume fraction of material contained by this boundary and the inside surface of the bent sheet. These μ -values remain constant during bending, and behave exactly in the same way as the λ -values for material layers. For instance, the radius r_b of the material boundary characterized by volume fraction μ , is

$$r_b = \sqrt{r_i^2 + \mu (r_y^2 - r_i^2)} \quad (3.2.12B)$$

3.2.6. Introduction of Dimensionless Parameters

(1.) Proksa [46] introduced the ratio between the actual sheet thickness and the central layer radius ^{r_m} as a dimensionless quantity to measure the 'amount of bending'. This quantity is called the relative curvature,

$$\kappa = \frac{t}{r_m} \quad (3.2.13)$$

Its value can vary between 0 and 2. The value 0 applies when the sheet is flat, i.e., $r_m = \infty$. The value 2 applies when $r_i = 0$, since then $r_m = r_y = \frac{t}{2}$. Its value is 1 when $r_i = t/2$, since then $r_m = t$.

(2.) Proksa [46] also introduced the ratio between the current sheet thickness and the original sheet thickness. This ratio is called the relative sheet thickness.

$$\eta = t/t_0 \quad (3.2.14)$$

Introduction of η gives for the tangential strain

$$\epsilon_\phi = \ln r/r_n - \ln \eta \quad (3.2.15)$$

(3.) It is important to know the position of the neutral layer during the bending process. Crafoord [33] introduces the ratio between the neutral layer radius and the unelongated layer radius to get a dimensionless indication of the neutral layer position.

$$\rho = r_n/r_0 \quad (3.2.16)$$

It will be shown in section 3.2.8 that the values of κ , η , and ρ are sufficient to describe the bending process. The reader who wishes to know how the bent geometry is expressed in function of dimensionless parameters, is referred to Appendix I.

In some cases it is easier to use, not ρ , but another

dimensionless parameter instead to indicate the neutral layer position. The introduction of the volume fraction λ to identify individual material layers, can also be used to define the current position of the neutral layer in the material. When the λ -value of the material layer which is currently the neutral layer is used to define the neutral layer by putting

$$\lambda_n = \lambda$$

Then the values of κ , η and λ_n are also sufficient to describe the bending process. In fact, there are two ways to define the dimensionless position of the neutral layer, using ρ or λ_n . The use of λ_n gives us a very good insight into what is happening to the materials in the neighbourhood of the neutral layer. When λ_n decreases during bending, it means that material, previously in compression ($\sigma_\phi < \sigma_r$), becomes loaded in tension ($\sigma_\phi > \sigma_r$). When λ_n increases during the bending process (possible for laminated sheet), material previously loaded in tension becomes loaded in compression.

3.2.7. Change in Sheet Thickness

In Section 3.2.4. it is shown that the neutral layer is the layer in the bend for which the tangential strain increment $d \epsilon_\phi$ equals zero.

Since

$$(\epsilon_\phi)_{r=r_n} = \ln r_n / r_0 = \ln \rho$$

Then

$$(d \varepsilon_{\phi})_{r=r_n} = \frac{d\rho}{\rho} = 0 \quad (3.2.17)$$

The neutral layer does not change its length, and consists of the same material for an infinitesimal increase in bending. Therefore, the value of λ_n , the volume fraction of material contained by the neutral layer on the inside of the bend, remains unchanged for that infinitesimal increase in bending.

Therefore,

$$d \lambda_n = 0$$

When (3.2.17) and (3.2.18) is expressed as a function of κ , η , ρ , they give the sheet thickness relation

$$\frac{d\eta}{d\kappa} = \frac{1}{2} - \left(\frac{1 - \frac{\kappa^2}{4}}{\eta^2 \rho^2} - 1 \right) \quad (3.2.19)$$

The detailed derivation of this results is given in Appendix II, If (3.2.17) and (3.2.18) are expressed in function of κ , η , λ_n , (3.2.19) becomes

$$\frac{d\eta}{d\kappa} = - \frac{1}{2} \frac{\eta}{\kappa} \left[\frac{1 - 2 \lambda_n^{-\kappa/2}}{(1 - \frac{\kappa}{2})^2 + 2 \lambda_n \kappa} \right] \quad (3.2.20)$$

In Appendix II is also shown that this can be expressed as

$$\frac{dn}{d\kappa} = - \frac{1}{2} \left(\frac{r_i r_y}{r_n^2} - 1 \right) \frac{n}{\kappa} \quad (3.2.21)$$

when this relation is expressed in terms of the current sheet thickness, t , and the bend angle ϕ between two radial cross-sections, it gives

$$\frac{dt}{t} = - \frac{1}{2} \left(1 - \frac{r_n^2}{r_i r_y} \right) \frac{d\phi}{\phi} \quad (3.2.22)$$

3.2.8. General Method of Solution

The pure bending problem theory gives us really two differential equations

(1) Equilibrium equation

$$\sigma_{\phi} - \sigma_r = r \frac{d \sigma_r}{d r} \quad (3.2.1)$$

(2) Sheet thickness equation

$$\frac{d \eta}{d \kappa} = - \frac{1}{2} \frac{\eta}{\kappa} \left(\frac{1 - \frac{\kappa^2}{4}}{\eta^2 \rho^2} - 1 \right) \quad (3.2.19)$$

or

$$\frac{d \eta}{d \kappa} = - \frac{1}{2} \frac{\eta}{\kappa} \left[\frac{1 - 2 \lambda_n - \kappa/2}{(1 - \frac{\kappa}{2})^2 + 2 \lambda_n \kappa} \right] \quad (3.2.20)$$

and the yield condition

$$\sigma_{\phi} - \sigma_r = \frac{2}{\sqrt{3}} H \left(\int d \bar{\epsilon} \right) \quad \text{for } r \geq r_n \quad (3.2.3A)$$

$$\sigma_{\phi} - \sigma_r = - \frac{2}{\sqrt{3}} H \left(\int d \bar{\epsilon} \right) \quad \text{for } r \leq r_n \quad (3.2.3B)$$

Substitution of (3.2.3A) and (3.2.3B) in (3.2.1) gives

$$r \frac{d \sigma_r}{d r} = \frac{2}{\sqrt{3}} H \left(\int d \bar{\epsilon} \right) \quad \text{for } r \geq r_n \quad (3.2.1A)$$

$$r \frac{d \sigma_r}{d r} = - \frac{2}{\sqrt{3}} H \left(\int d \bar{\epsilon} \right) \quad \text{for } r \leq r_n \quad (3.2.18)$$

When we know the behaviour of η and ρ or η and λ_n as a function of κ , we are able to calculate all the strains, stresses and moments for a complete solution. This is clear when it is realized that by knowing κ , η , ρ or κ , η , λ_n we can calculate all the radii (see Appendix I), therefore all the strains, etc.

The problem is thus to solve the sheet thickness equation (3.2.19) or (3.2.20). We know the starting condition for this differential equation. It is the unbent condition, for which

$$\kappa = 0$$

$$\eta = 1$$

and the starting values for ρ or λ_n are determined by the equilibrium (no resultant normal stress on a radial section) when the yield stress for zero strain works on the section (radial stresses are zero). The problem is then to integrate a function with one independent and two dependent variables, and this is one dependent variable too much for immediate solution. The independent variable is κ , and the dependent variables are η and ρ or λ_n . The second dependent variable, ρ or λ_n , can be determined by using the equilibrium equation, and really defines the position of the neutral layer. This equilibrium equation is itself a differential equation, which can be integrated along the sheet thickness. Integration can be carried out to r , or, with transformation from r to λ , to λ .

This equilibrium equation is subject to the following boundary conditions.

1. Since the inside surface of the bend is a free surface, the radial stress there is zero.

$$\sigma_r = 0 \quad \text{for } r = r_i \quad \text{or } \lambda = 0$$

2. This applies also at the outer surface of the bend.

$$\sigma_r = 0 \quad \text{for } r = r_y \quad \text{or } \lambda = 1$$

3. Equilibrium can only be satisfied when the radial stress is continuous. This means that

3A. on every material boundary (for laminated sheet), the radial stress in one material must be the same as in the other material.

3B. in the neutral layer, there is only one value for the radial stress.

We can now integrate the equilibrium equation (3.2.1A) from the inside surface of the bend, with known boundary conditions, for increasing values of r or λ . (Condition 1). If, during this integration, we move from one laminate to the adjoining one by crossing the material boundary, we use condition 3A: the radial stress at the outside of one laminate must be the same as the radial stress at the inside of the adjoining laminate. The equilibrium equation can also be integrated starting from the

outside surface of the bend, equation (3.2.1B), using starting condition 2, and when a material boundary is crossed, (condition 3A), the radial stress at the inside of one laminate is the same as the one at the outside of the adjoining one. Condition 3B makes it now possible to find the position of the neutral layer. The radial stress, found by integrating the equilibrium equation from the inside of the bent sheet, has to be identical with the one found by integrating from the outer surface, when the layer considered is the neutral layer (or the radius is the neutral radius).

In the easiest cases, the integration of the equilibrium equation can be done analytically, and the neutral layer position can be found by solving an equation, derived from condition 3B by an iterative procedure, for ρ . In such a case, ρ is known in function of κ and η , and the sheet thickness equation can be integrated to κ without any difficulty.

In more difficult cases, like a strainhardening material without Bauschinger effect, when the effective stress is dependent on the current strain and the previous material history (due to reversals of stress system when the neutral layer passes through the material), the integration of the equilibrium equation must be done numerically, and the position of the neutral layer λ_n is found iteratively by finding the value for λ for which the radial stresses, by integrating from the inside or the outside of the bend, are the same. Once λ_n is

known in function of κ and η , we just integrate the sheet thickness relation to κ .

3.2.9. Radial and Tangential Stresses and Bending Moment

The radial stresses follow out of the integration of the equilibrium equation with the boundary conditions given in section 3.2.6. The tangential stresses follow out of

$$\sigma_{\phi} = \sigma_r + \frac{2}{\sqrt{3}} H \left(\int \frac{2}{\sqrt{3}} |d \epsilon_{\phi}| \right) \quad (3.2.23A)$$

with

$$r \geq r_n$$

and

$$\sigma_{\phi} = \sigma_r - \frac{2}{\sqrt{3}} H \left(\int \frac{2}{\sqrt{3}} |d \epsilon_{\phi}| \right) \quad (3.2.23B)$$

with

$$r \leq r_n$$

The bending moment can be found by calculating

$$M = \int_{r_i}^{r_y} \sigma_{\phi} r dr = \frac{r_y^2 - r_i^2}{2} \int_0^1 \sigma_{\phi} d \lambda \quad (3.2.24)$$

3.3. Conclusion of this Chapter

This chapter has provided an outline to the method of solution for the plane strain bending of rigid-plastic materials. The numerical technique developed is capable of

evaluating the change in sheet thickness and the magnitude of the required bending moment during continuous bending of the sheet.

The simplest case to which the theory can be applied is that of bending a non-hardening mono-metal and this is treated in Chapter 4, section 4.1. The method is then extended for non-strainhardening bi-metals (section 4.2) and tri-metals (section 4.3.). The bending of strainhardening sheet is more involved, and is treated in Chapter 5. A comparison is made between the bending of a strainhardening material without Bauschinger effect, and a material with a Bauschinger effect in a simplified form, as suggested by Crafoord [33]. An attempt to explain the instability in bending of materials with an upper yield point (such as mild steel) is given, followed by the behaviour of strainhardening laminated sheet in bending.

Although the general method of approach, outlined in section 3.2.6., is valid for all the above mentioned cases, each case has some distinct features which can simplify or complicate the solution method. Computer programs for all the cases have been developed. The programs for complicated cases involve a different approach than the ones for simpler cases, however, they are general in the sense that they can be used to solve for the less complicated cases. This way, the validity and accuracy of the numerical methods can be checked. Of course, this is done at the expense of central processing unit time and memory requirements. The results are presented in the following chapters, and the programs in Appendices.

CHAPTER 4

PLASTIC PLAIN STRAIN BENDING OF NONSTRAIN- HARDENING LAMINATED SHEET

The bending of a single nonstrainhardening strip occurs under constant bending moment without change in strip thickness.

However, when bending a sheet, composed of nonstrainhardening laminates of different yield strength, neither the bending moment nor the thickness remain constant. It is interesting to note that a thickening of the sheet can occur, and that a decrease in bending moment results in instability of the bending, causing localised bending.

The bending of a nonstrainhardening single sheet, hereafter referred to as monometal, will be treated first to show the different features of plastic plain strain bending, followed by a treatment of the bending of sheets composed of two and three nonstrainhardening laminates. These will be referred to as bi- and trimetals respectively.

4.1. Plastic Bending of a Nonstrainhardening Monometal

Hill [47] has pointed out that the plane strain bending of an ideally plastic material occurs without change in sheet thickness and under constant bending moment. This result can be analytically arrived at by using the bending theory expounded in Chapter 3, and is featured in Appendix III.

The distribution of radial and tangential stress across the thickness of the bent sheet is shown in Fig. 4.1 for different values of the relative curvature κ . The radial stress is zero at the inside and outside radius, as required by the boundary conditions. The radial stress reaches its maximum compressive value at the neutral layer radius. It is also seen that the radial stress is very small compared to the tangential stress in the early stages of the bending process (small values of κ). This shows clearly why in a lot of simplified bending theories the radial stress is assumed to be zero. The jump of the tangential stress at the neutral radius is caused by the non-elastic material. An elastic-plastic material should have a continuous tangential stress. The reader is referred to Shaffer and House [39], [40], for the treatment of the plane strain bending of an elastic-perfectly plastic monometal.

Fig. 4.2 shows how ten originally equidistant fibres in the sheet move across the thickness of the bent sheet during bending. It is clear that a layer of material, of finite thickness, towards the outside of the bend becomes thinner during bending, while the reverse happens for a layer towards the inside of the bend. The unelongated fiber always coincides with the central fibre but the neutral layer moves towards the inside of the bend. This inside movement of the neutral layer has for result that some fibres will become shorter during the initial stages of the process, - when they are situated to the inside of the bend with regard to the current neutral fibre,

but will start to elongate as soon as the neutral fibre crosses them. However, the global effect of these thickening and thinning layers on the sheet thickness is nil. The sheet retains its original thickness.

It is shown in Appendix III that the ratio of the volume of material contained between the neutral surface and the inside surface of the bend to the total sheet volume, given by λ_n , is a linear function of the relative curvature κ . The same applies for λ_o , the volume fraction of material contained to the inside of the unelongated surface. See Fig. 4.2BIS.

Fig. 4.3 shows the tangential strain to which ten originally equidistant fibres are subjected during the bending. All fibres with $\lambda > 0.5$ are only subjected to an ever increasing tensile tangential strain ϵ_ϕ . But fibres with $\lambda < 0.5$ are first subjected to a compressive ϵ_ϕ causing the fibre to shorten. When they coincide with the neutral layer, as shown in section 3.2.4., ϵ_ϕ reaches a minimum. When the sheet is bent further ϵ_ϕ starts to increase. $d\epsilon_\phi$ is now positive, and the fibre elongates. The tangential strain of the neutral layer $\epsilon_{\phi n}$ is a function of the relative curvature κ and is a curve going through the minima of the ϵ_ϕ - κ curves for different fibres. $\epsilon_{\phi n}$ is therefore the minimum value ϵ_ϕ has ever reached for a fibre through which the neutral layer has passed. $\epsilon_{\phi n}$ indicates thus the maximum compressive tangential strain such a fibre has undergone.

These results can be analytically derived by using the results of Appendix III and the formulas of Appendix I. The results in this section, although known for many years, have been repeated to remove any doubts as to what is happening during the bending of a rigid nonstrainhardening monometal, and to compare them with the bending of laminated sheet. The known analytic solution for this case is also used to check the accuracy of numerical methods developed to solve the bending of more complicated sheets.

4.2. Plastic Bending of Nonstrainhardening Bimetal Sheet

4.2.1. Introduction

The general theory of sheet bending can be applied to calculate the bending of nonstrainhardening bimetal sheet. How this is done is featured in detail in Appendix IV. Since no full analytic solution was found, a FORTRAN program for use on a digital computer is provided as well.

The essence of the treatment in Appendix IV is that the dependent variable ρ in the sheet thickness relation can

$$\frac{dn}{d\kappa} = -\frac{1}{2} \frac{\eta}{\kappa} \left[\frac{1 - \frac{\kappa^2}{4}}{\eta^2 \rho^2} - 1 \right] \quad (3.2.19)$$

be expressed as a function of κ and η , so that (3.3.19) reduces to the form

$$\frac{dn}{d\kappa} = f(\kappa, \eta)$$

which can be numerically integrated. However, the function $f(\kappa, n)$ depends upon which side of the laminate boundary the neutral layer is currently located. When the original neutral layer is situated in the outside laminate, then it is possible that the neutral surface moves across the material surface during the bending. A different expression for the sheet thickness relation applies before and after the neutral layer crosses the laminate boundary.

Sections 4.2.2. and 4.2.3. will feature two examples of the bending of laminated sheet. Both examples consider a laminated sheet with two laminates having the same thickness before bending, and with one laminate having twice the yield strength of the other one. The examples differ in that in section 4.2.2. the strongest laminate will be situated at the outside surface of the bend, whereas in section 4.2.3. the strongest laminate will be at the inside. After insight into the bending of a nonstrainhardening bimetal has been gained by these two examples, the influence of the relative thickness of the two laminates will be discussed in section 4.2.4 and the influence of the yield strength ratio in section 4.2.5.

The laminate at the inside of the bend will be called laminate 1, and has a yield strength A_1 . The outside laminate is laminate 2 with yield strength A_2 . Furthermore, as defined in Appendix IV

$$\alpha_1 = \frac{2}{\sqrt{3}} A_1$$

$$\alpha_2 = \frac{2}{\sqrt{3}} A_2$$

The position of the laminate boundary is defined by μ , which is the ratio between the original thickness of the inside laminate to the total original sheet thickness.

4.2.2. Example 1

$$\underline{A_1 = 1, A_2 = 2, \mu = 0.50}$$

In this example, the two laminates have the same original thickness and the yield strength of the outside laminate is twice the one for the inside laminate.

Fig. 4.4. illustrates that the thickness of the sheet increases during the bending (η increases for increasing κ), and that the bending moment is rising. This is completely different from the bending of a nonstrainhardening monometal, which occurs under constant thickness and constant bending moment. The fact, that an increase in thickness during the bending occurs is very significant.

The relative sheet thickness η and the bending moment M have a flexure point for $\kappa = 0.70$. This is the value of κ for which the neutral layer coincides with the laminate boundary. This happens when the volume fraction embraced by the neutral surface and the inside surface of the bent sheet is the same as the volume fraction embraced by the laminate boundary surface

and the inside surface of the bent sheet.

Hence,

$$\lambda_n = \mu = 0.50$$

The neutral layer crosses the material boundary at that stage in the bending, and the sheet thickness differential equation for $\kappa < 0.70$ and $\kappa > 0.70$ is different. This explains the change in second derivative of the relative sheet thickness η and the bending moment M at this point. This change in sheet thickness relation is caused by the change in analytical expression for the ratio between the neutral layer radius and the unelongated layer radius, ρ . That ρ and λ_n show a change in slope at that point, is not surprising. The unelongated layer position given by λ_0 in Fig. 4.4. shows no change in slope at that point. This can be explained by the fact that λ_0 is only dependent on κ and η - see equation (I.13), and η has no change in slope.

λ_n and λ_0 seem to be linear functions of κ . This is similar to their linearity in the case of a nonstrainhardening monometal (see Fig. 4.2BIS). Examining this result, an analytical solution to the problem might appear tenable and investigation of this might be worthwhile. The author attempted a numerical solution by choice feeling an analytical solution would be tedious.

Note also in Fig. 4.2BIS that λ_n is bigger for all κ values in this case than in the bending of a nonstrainhardening monometal.

How ten originally equidistant fibres move during the bending is shown in Fig. 4.5. The outside laminate thins, and the inside laminate thickens during the bending. Hence, in the bent sheet, the inside weak laminate is thicker than the outside strong laminate. Thus, since the whole sheet thickens the thickening of the inside laminate is greater than the thinning of the outside laminate.

The tangential strain ϵ_{ϕ} for these equidistant fibres as a function of κ is shown in Fig. 4.6. As for the monometal, the line $\epsilon_{\phi n}^{-\kappa}$ connects the minima of the $\epsilon_{\phi}^{-\kappa}$ curves for different λ values. Note that the $\epsilon_{\phi n}^{-\kappa}$ curve has a change in slope when the neutral layer crosses the laminate boundary. When Fig. 4.6 is compared with Fig. 4.3, it is very clear that all the fibres, for all κ values, undergo less (in the algebraic sense) tensile tangential straining for this bimetal than for the monometal. This means that the outside layers will thin less than for a monometal, and that the inside layers will thicken more. This can also clearly be seen by comparing Fig. 4.5 with Fig. 4.2. This is consistent with the thickening up of the sheet during bending, and is, in fact, directly related to the thickening up of the sheet. Since

$$\epsilon_{\phi} = \frac{1}{2} \ln \left[\left(1 - \frac{\kappa}{2}\right)^2 + 2 \lambda \kappa \right] - \ln \eta \quad (I.9)$$

the tangential strain of the fibre λ is composed of two components. First, the strain which the fibre would undergo when

the sheet should not change its thickness, which is ϵ_ϕ of (1.9) with $\eta=1$ and which is the same as for the bending of a non-strainhardening monometal, pictured in Fig. 4.3. The second part of ϵ_ϕ is

$$- \ln \eta$$

and is fully composed of the change in relative thickness of the sheet. The $\epsilon_\phi - \kappa$ curve can therefore be derived from Fig. 4.3 if the $\eta - \kappa$ curve for the bending of the sheet is known. Equation (1.9) can be interpreted as saying that, when the sheet thickness is bigger than the original one, all the fibres have undergone less (in the algebraic sense) tensile tangential straining than in the case of a nonstrainhardening monometal. Also, that, when $\eta < 1$, all the fibres have undergone more (in the algebraic sense) tensile tangential straining than in the nonstrainhardening monometal case. This observation is completely general and completely independent of the type of sheet. This will apply to all the cases which are further dealt with in the present work.

4.2.3. Example 2

$$\underline{A_1=2, A_2=1, \mu=.5}$$

This bimetal sheet is the same one as in example 1 (section 4.2.2), the only difference is that the sheet is bent with the strong laminate at the inside surface of the bend. The behaviour during bending in this case is completely different from example 1. The figures illustrating this are Figs. 4.8, 4.9

4.10 and 4.11. The most important feature is that during the bending the bending moment decreases. ($M/t_0^2 - \kappa$ -curve in Fig. 4.8). This is caused by the fact that the thickness decreases (η decreases). Comparing Fig. 4.10 with Fig. 4.3 for a nonstrainhardening monometal shows that all the layers for all κ values undergo more (in the algebraic sense) tensile tangential straining than in the monometal. All the layers thin therefore more than in the monometal bending, which results in a decrease in sheet thickness. Although a solution for the plain strain bending has been established, this solution will not be observed should we bend such a sheet. Since the bending moment monotonically decreases for increasing values of the relative curvature, the pure uniform bending is an unstable process.

A general treatment of instability phenomena is outside the scope of this thesis. The point that is being made here is a relatively simple one, namely that the bending moment decreases from the onset of the process, and in this sense the process is unstable. This is the same concept as defining the point of instability in a tensile test as the point of maximum load.

What would happen in practice in the plane strain bending of a laminate unstable in the above sense is that pure bending would not take place as predicted, but a localized kink in the sheet would occur. This has been observed in some experiments performed as part of this thesis and reported in Chapter 6. This localised kinking has also been reported in private communication

with Mr. John Hiam (Dofasco) who attempted to bend a low carbon steel which exhibited a pronounced upper and lower yield point. The same phenomenon was observed by Horrocks and Johnson [34]. This type of instability is discussed at greater length in Chapter 5.

4.2.4. Influence of the Relative Thickness of the Two Laminates

The value for μ , the ratio between the original inside laminate thickness to the original thickness of the whole sheet, will be changed between 0 and 1. The values for the yield stresses will be $A_1 = 2$, $A_2 = 1$ or the reverse, $A_1 = 1$, $A_2 = 2$.

In Fig. 4.12, the μ -values on the right side represent the sheet with the strong layer on the outside, whereas the μ -values on the left represent laminated sheet with the strong layer on the inside of the bent sheet. The two ways a single laminated sheet can be bent are represented by μ -values whose sum is one, and who are symmetrical around the vertical centre line of the graph. The graph shows the relative sheet thickness η and the neutral layer position λ_n as a function of μ for different κ -values. The sheets with the strong laminate on the outside thicken up during bending. The same sheets bent when the strong laminate is on the inside, i.e., the sheet is simply reversed, always thin. Laminated sheets with μ -values near 0 or 1 show a smaller change in thickness than sheets with intermediate μ . This could be expected, since for $\mu = 0$ or 1, the sheet is a nonstrainhardening monometal, which bends without

change in thickness. Consider the laminates represented on the right side in Fig. 4.12. It is not possible to indicate which sheet composition is going to thicken most, since the maximum of the η - μ curve is different for different values of the relative curvature κ , and shifts to decreasing μ for increasing κ .

Fig. 4.13 features the bending moment (reduced to the original sheet thickness) M/t_0^2 as a function of μ for different values of κ . The bending moment increases for increasing κ for the sheets with the strong laminate on the outside. When the strong material is on the inside of the bend, the moment decreases and uniform bending is unstable. When the left side of Fig. 4.13 is turned to the right along the central axis, this results in Fig. 4.14, which shows the continuity between the bending to one side or to the other. The M - μ curves for constant κ have a flexure point when the neutral layer coincides with the laminate boundary. The reason for this is again that the sheet thickness relation changes when the neutral layer crosses the laminate boundary.

The bending moment as a function of κ for different μ values is plotted in Fig. 4.15. This graph affirms that all the bimetal sheets with the strong laminate at the outside are stable, but, when reversed, are unstable. It is also possible to reduce the bending moment to the current sheet thickness, that is M/t^2 . This value is not proportional to the real bending moment for the sheet, since

$$t = t_0 \eta$$

changes as a function of κ . But the plot of M/t^2 as a function of κ for different μ in Fig. 4.15 shows very clearly the influence of the neutral layer crossing the material boundary. It is seen that M/t^2 can decrease for increasing κ when the strong laminate is on the outside. This means, since M/t_0^2 is monotonically increasing, that this increase in real bending moment is caused by the increase in sheet thickness. Analogously for the sheet bent the other way, M/t^2 can increase for increasing κ , but since M/t_0^2 decreases this must be caused by decreasing sheet thickness. However, the M/t^2 graph indicates that the change in total sheet thickness is not solely responsible for the behaviour of M . Different influences on M are at work, namely the change in sheet thickness, the thickening of the inside laminate and the thinning of the outside laminate, and the shift of the neutral layer during the bending.

The bending of the laminated sheet changes the relative thicknesses of the two composing laminates. This is featured in Fig. 4.17. The outside laminate always thins, and the inside one always increases in thickness. The relative change in thickness is dependent on μ and κ . This effect can be important. Say that a strong, but thin cladding is applied on a weak inside material (thus μ close to 1). Fig. 4.17 shows that the strong, thin cladding can undergo a considerable thinning when on the outside of the bent sheet. This can be important

when the clad layer is provided for corrosion resistance. The effect on the load carrying capacity of the bent sheet can also be serious although the thinning of the strong clad is compensated by the thickening of the thick inside laminate. Nevertheless, it will be shown in Chapter 6 that this thinning and thickening of laminates changes the load carrying capacity of the sheet and has a serious influence on the deep drawing behaviour of laminated sheet.

It is possible to plot bending moment and thickness change in function of κ and μ in a single graph, Fig. 4.18. This graph illustrates again the continuity between the bending of a sheet one way or the other. It is repeated that the bending with the strong laminate on the inside is unstable, and that the given solution is only valid for uniform bending. This solution gives therefore only an indication of how the bending will proceed in such a case.

4.2.5. Influence of the Yield Strength Ratio

When $A_1/A_2 = 1$, the two laminates are identical. The sheet is in fact a monometal, and bends under constant thickness and constant bending moment. Section 4.2.4. has shown that for $A_1/A_2 = 2$, the sheet thickens up and the bending moment increases. If the sheet is bent the other way around, $A_1/A_2 = 1/2$, the sheet thins and the bending is unstable. It may be anticipated that, for $A_1/A_2 > 1$, the bigger A_1/A_2 , the more the sheet will thicken and the bending moment increase. Also, that,

for $A_1/A_2 < 1$, the smaller A_1/A_2 , the more thinning will occur and the more the bending moment will decrease. Some preliminary trial runs for $A_1/A_2 = 1/4, 3/4, 4, 4/3$ and $\mu = .5$ confirmed this.

4.2.6 Conclusion

Uniform bending of a nonstrainhardening bimetal sheet with the strong laminate on the outside of the bend occurs with an increase in sheet thickness. However, the strong outside laminate thins during the process.

The uniform bending of a nonstrainhardening bimetal sheet with the weak laminate on the outside is not possible due to decrease in bending moment and thickness. Instead, localised bending takes place.

4.3. Plastic Bending of Nonstrainhardening Trimetal Sheet

4.3.1. Introduction

The same solution method as for bimetal sheet can be used for multilaminated sheet. In that case, the sheet thickness relation changes every time the neutral layer crosses a laminate boundary. This is due to the fact that the analytical expression for ρ is different. However, if the sheet thickness relation (3.2.20) is used

$$\frac{d\eta}{d\kappa} = - \frac{1}{2} \frac{\eta}{\kappa} \left[\frac{1 - 2 \lambda_n - \kappa/2}{2\kappa \lambda_n + (1 - \frac{\kappa}{2})^2} \right] \quad (3.2.20)$$

and the value of λ_n as a function of κ and η is determined in a numerical way, the change in sheet thickness relation is not explicitly present in the solution method. This different approach to solve the bending of laminated nonstrainhardening sheet is featured in Appendix V.

Although the technique that is developed has the capability of solving all multilaminated nonstrainhardening bending problems, an analysis has only been made for two types of trimetals. Both types are similar in the sense that the inside and the outside clad of a sheet are the same material. In the first type, the cladding has a yield strength twice as big as the one for the core laminate. For the second type, the core has a yield strength of twice the cladding yield strength. For both types, the influence of the percentage inside clad, the percentage core and the percentage outside clad on the bending will be studied. Two examples of the type with the soft core will be featured in section 4.3.2, and the influence of the relative composition of the sheet will be explained in section 4.3.3. Section 4.3.4. will feature two examples of the sheet with the strong core, and section 4.3.5 explains the influence of the relative percentages of the different laminates. Finally, section 4.3.5. will give some conclusive remarks on the trimetal bending.

4.3.2. Examples of Soft Core Trimetal

The composition of the nonstrainhardening trimetals used

as examples in this section are given in Table 4.1.

1. Example 1 Sheet 2-1-2 (40-40-20)

Fig. 4.19 shows that the material will thin during bending, and that the bending moment decreases for increasing relative curvature. It can therefore be concluded that uniform bending of this sheet will be unstable.

2. Example 2 Sheet 2-1-2 (20-40-40)

Fig. 4.20 indicates that the sheet will thicken up for values of the relative curvature less than .48, and that the sheet will start to thin if the bending is carried further. The bending moment increases for increasing κ -values up to $\kappa = .48$, reaches a maximum at that value, and decreases when κ increases above .48. This indicates that the uniform bending can be carried out up to a relative curvature .48. If the sheet must be bent further, uniform bending is unstable, and localised bending occurs. Fig. 4.21 gives the radial and tangential stress distribution across the sheet thickness for different κ -values.

In these two examples, bending of the sheet to one side is always unstable, whereas bending the same sheet to other side is only stable up to a certain value of the relative curvature. Section 4.3.3. will show if this behaviour is general for this type of trimetal.

4.3.3. Influence of Relative Laminate Thicknesses on the Bending of 2-1-2 Trimetal

The different sheet compositions have been plotted

Table 4.1. Sheet Compositions of Examples
in Section 4.3.2.

Example	Sheet	Laminate Position in Bend	Laminate Number i	Yield Strength of Lamin- ate i	Volume Percentage of Laminate i	μ -Values	
						μ_{i1}	μ_{i2}
1	2-1-2 (40-40-20)	inside clad	1	2	40	0.	0.4
		core	2	1	40	0.4	0.8
		outside clad	3	2	20	0.8	1.0
2	2-1-2	inside clad	1	2	20	0.	0.2
		core	2	1	40	0.2	0.6
		outside clad	3	2	40	0.6	1.0

Table 4.2. Sheet Compositions of Examples
in Section 4.3.4.

Example	Sheet	Laminate Position in Bend	Laminate Number i	Yield Strength of Lamin- ate i	Volume Percentage of Laminate i	μ -Values	
						μ_{i1}	μ_{i2}
1	1-2-1 (40-40-20)	inside clad	1	1	40	0.	0.4
		core	2	2	40	0.4	0.8
		outside clad	3	1	20	0.8	1.0
2	1-2-1 (20-40-40)	inside clad	1	1	20	0.	0.2
		core	2	2	40	0.2	0.6
		outside clad	3	1	40	0.6	1.0

in a triangular co-ordinate system, see Fig. 4.22. Every point in the triangle represents a sheet composition. The percentages of inside, core and outside laminate will be measured by the distance of the point to the three sides of the triangle. Of course, the sum of all percentages is equal to hundred.

All compositions with the same percentage core lie on a horizontal line. All composites with the same ratio of percentage inside clad to percentage outside clad lie on a straight line going through the top of the triangle. Symmetrical trimetals, i.e., with same percentage inside and outside clad, are situated on a vertical going through the top of the triangle. If point E represents a certain composition, then point F, the point symmetrical to E with regard to the symmetrical trimetal line, represents the same sheet but bent to the other side. The three corners of the triangle represent monometals while each side of this triangle represents a bimetal.

Fig. 4.23 gives the influence of the sheet composition on the stability of the uniform bending of 2-1-2 sheet. The base line of the triangle represents a nonstrainhardening monometal. Since these bends under constant bending moment, these laminates are really on the limit of stability. The right side of the triangle represents a 2-1 bimetal, the strong laminate on the inside of the bend. Section 4.2.4 has shown us that these sheets are always unstable in uniform bending. The left side of the triangle represents the 1-2 bimetals, strong laminate is the outside one. These sheets bend always stable, as indicated in

section 4.2.4. The three corners of the composition triangle represent monometals, and are therefore on the limit of stability. The bending behaviour for a whole array of compositions inside the triangle has been calculated with the computer program given in Appendix V, and this gives the following results.

1. The bending of symmetrical 2-1-2 trimetals is always unstable.
2. The bending of 2-1-2 trimetals with more inside clad than outside clad is always unstable (right half of the triangle in Fig. 4.23).
3. 2-1-2 trimetals with more outside clad than inside clad can be uniformly bent up to a certain value for the relative curvature. This value is dependent on the sheet composition. Once the bending is carried out further, a kink in the sheet will develop since uniform bending is unstable. Points in the triangle whose maximum bending moment occurs for the same values of relative curvature, can be connected with a line which can be called 'line of limit of stability for that κ -value'. All points to the centre of the triangle with regard to a line of limit of stability cannot be uniformly bent up to that κ -value. All points to the outside of the triangle (thus to the left of that line of limit of stability) undergo stable bending when bent to that κ -value. These lines of limit of stability

can also be plotted in function of the ratio between percentage inside clad to percentage outside clad, see Fig. 4.24. It is obvious that the point of instability for different material compositions is mostly dependent on that ratio, and only to a slight extent dependent on the percentage core. This means, see Fig. 4.24, that the degree of uniform stable bending is mainly determined by the ratio of inside to outside percentage cladding. When the ratio is small, the bend can be carried out in a stable manner up to high values of the relative curvature. When that ratio increases, but stays smaller than one, the bend is still stable, but only up to a value of the relative curvature that decreases with increasing ratio. When the ratio reaches zero, - the sheet is now a symmetrical 2-1-2 trimetal-, that value of κ for maximum bending moment reaches zero, and uniform bending is unstable from the beginning on. All compositions for which that ratio equals or is bigger than one, are essentially unstable.

Figs. 4.25, 4.26 and 4.27 give the change in sheet thickness for different 2-1-2 sheets for $\kappa = .25, .50,$ and 1.00 respectively. As expected, the monometals do not show any change in sheet thickness. Composites with only a few percentage core material thicken or thin less than sheets with a sizeable amount of core. The sheets represented on the left triangle side, 2-1 bimetals, become thicker during the bending,

and the composition with maximum increase in thickness is different for different relative curvature, as was pointed out in section 4.2.4. The lines of limit of stability are also indicated in Fig. 4.25, 4.26 and 4.27. For sheets in the left half of the triangle, the sheet compositions lying on the limit of stability line reached their maximum thickness and will become unstable when bent further.

4.3.4. Examples of Strong Core Trimetal

The composition of the nonstrainhardening trimetals used as examples in this section are given in Table 4.2.

1. Example 1 Sheet 1-2-1 (40-40-20)

Fig. 4.28 indicates that the bending is stable (increasing bending moment) and that the sheet increases in thickness during the process. Note the flexure point in the moment and the relative sheet thickness when the neutral layer crosses a laminate boundary.

2. Example 2 Sheet 1-2-1 (20-40-40)

Fig. 4.29 gives the solution for the bending of this sheet. We see that the bending moment first decreases, goes through a minimum and then increases above the original moment. The same applies for the relative sheet thickness. How can this be physically interpreted? If we make the assumption that local bending could be described by the theory for uniform bending, then the following is plausible. When we try to bend the sheet, a local bend appears on a material inhomogeneity. The sheet bends

locally till the κ -value for minimum bending moment is reached. Further bending in that place requires an increase in bending moment, so that the local bend can both spread through the rest of the sheet, and further increase its relative curvature at the same time. This process goes on, till the sheet has reached a uniform curvature given by the κ -value where the bending moment reaches its original value. If the bending is carried further, it will proceed uniform in a stable fashion. Of course, this explanation is based on very speculative assumption, namely that local bending can be described as uniform bending. For the moment, it is the best assumption that can be made, and the above gives at least an indication of what could happen in reality. The same phenomenon exists in the elastic bending of rectangular plates with cambered cross sections as reported by Bellow and Semeniuk [48]. However, the "kink-through", i.e., the sudden increase in bending angle, occurs in their plates when the material is completely elastic, and since the elastic deformations are small, uniform and localised bending can be described the same way. In plasticity, the difference between local and uniform bending is important since the deformations are large.

These two examples show how the same sheet of a 1-2-1 trimetal is fully stable when bent to one side, while bent to the other side there is an original unstable "snap-through", followed by stable bending. Section 4.3.5 will show if this is general for 1-2-1 nonstrainhardening trimetal sheet.

4.3.5. Influence of Relative Laminate Thickness on the Bending of 1-2-1 Trimetal

Fig. 4.30 shows all the different compositions of the 1-2-1 trimetal. The base of the triangle and the top represent monometals, and bend therefore on the limit of stability (constant bending moment). The left side of the triangle represents 2-1 bimetals, and section 4.2.4 has shown that these can be bent uniformly. The right side of the triangle represents 1-2 bimetals, and these are fully unstable, i.e., bending moment is monotonically decreasing for increasing relative curvature. Investigation of an array of different trimetal sheet compositions has revealed that.

1. The bending of symmetrical 1-2-1 trimetals is always stable.
2. The bending of 1-2-1 trimetals in the right half of the composition triangle is always stable. In other words, 1-2-1 trimetals with more inside cladding than outside cladding bend uniformly.
3. 1-2-1 trimetals with more outside clad than inside clad, hence in the left half of the triangle, show a decreasing bending moment, that reaches a minimum, and then starts to increase.

If our assumed explanation is correct, this should indicate that a local bend appears in the sheet, that this localised bend spreads through the entire sheet, and that from then on the bending goes on in a stable, uniform way.

In the left side of the triangle, the sheet compositions for which the bending moment reaches its minimum for the same value of κ are connected by a "line of limit of instability". It is remarkable that these lines are the same as the "lines for limit of stability" in Fig. 4.23 for the 2-1-2 sheet. Fig. 4.23 could be used for the 1-2-1 sheet if we change everywhere the words stable by unstable and unstable by stable. Stable bending in the right half in Fig. 4.30 for the 1-2-1 sheet, corresponds to unstable bending in the right half in Fig. 4.23 for 2-1-2 sheet. Minimum in bending moment at a certain κ -value for a certain sheet composition in 1-2-1 sheet corresponds to maximum in bending moment for the same composition at the same κ -value for the 2-1-2 sheet.

The change in sheet thickness in function of the material composition for different κ -values is featured in Fig. 4.31, 4.32 and 4.33. Interpretation is left to the reader, and is similar to the interpretation of Figs. 4.25, 4.26 and 4.27.

4.3.6. Concluding Remarks

The bending of the 1-2-1 and 2-1-2 trimetals has introduced two new types of bending behaviour, namely stable bending followed by unstable bending - this bending type shows a maximum in the bending moment, and unstable bending followed by stable bending - this type shows a minimum in bending moment. The most interesting feature really is that this complicated phenomena already occurs for bending of nonstrainhardening laminated sheet.

4.4. Conclusions for the Bending of Nonstrainhardening Sheets

The application of the general theory of sheet bending, featured in Chapter 3, on the bending of laminated nonstrainhardening sheet, has given new insights into the bending process. The results of this investigation are

1. Nonstrainhardening monometal bends under constant thickness and constant bending moment.
2. Nonstrainhardening bimetal with strong laminate on the outside of the bend sheet deforms under an increasing bending moment and thickens up.
3. Nonstrainhardening bimetal with weak laminate at the outside of the bend thins and shows localised bending due to a decreasing bending moment.
4. Nonstrainhardening trimetals can deform under four different modes, namely
 - A. Fully stable
 - B. Fully unstable
 - C. Stable followed by unstable
 - D. Unstable followed by stable

It was known that strainhardening sheets can bend under mode 4.C., and that bending of a material with upper yield point is unstable. But it has not been shown before that these behaviour patterns in bending can be found in nonstrainhardening laminated sheets. The different bending modes are caused by the introduction of a nonuniform yield strength across the sheet. A careful analysis of all the examples treated in this

chapter shows that, at the start of the bending process, the sheet thickens up when the original neutral layer is situated to the outside of the central layer, remains at constant thickness when the neutral layer and central layers coincide, and thins when the neutral layer lies to the inside of the central layer. In other words, this means that $\frac{dn}{dk}$ is positive, zero or negative when $\kappa = 0$ for λ_n greater than, equal to or less than 0.50 respectively. It is shown in Appendix VI that this is general in sheet bending. Hence, by determining the neutral layer position of the flat sheet, one knows, without further analysis, how the sheet thickness will change in the beginning of the bending. The influence of this original neutral layer position on the original change in sheet thickness explains why the same nonstrainhardening laminate, when bent to one side, is stable and is unstable when bent to the other side. If in one case $\lambda_n > .50$, the sheet originally thickens, and since, for an infinitesimal small bend, the neutral layer position doesn't change, the radial stress is still negligible and the material is nonstrainhardening, the bending moment increases and the bending is originally stable. However, when the same sheet is bent the other way, $\lambda_n < .50$, the sheet thins originally, the bending moment decreases due to the decrease in sheet thickness, and the bend is unstable.

This chapter shows that the different bending modes can be caused by the introduction of a nonuniform yield strength across the sheet. The same will happen when a strainhardening material is bent. The inside and outside layers will strainharden

more than the centre layers due to bigger deformations on the inside and outside radii. This makes the sheet similar to a 2-1-2 trimetal. Since the neutral layer moves to the inside of the bend, the outer "2" layer will be thicker than the inside "2" layer, and the bending will be of the type stable-unstable. This is just an example of the type of extrapolation that could be made from the results on nonstrainhardening laminated sheet, and will be justified in Chapter 5.

CHAPTER 5

PLASTIC BENDING OF STRAINHARDENING SHEET

The previous chapter has given an extensive survey of the behaviour in plane strain bending of rigid-plastic, nonstrainhardening single and laminated sheets. Real metals however have no yield stress that is independent of strain. It is therefore useful to investigate how the strainhardening of a material will influence its bending behaviour. The bending of a monometal sheet, consisting of a strainhardening material without any Bauschinger effect, will be treated in section 5.1. Real materials can show a Bauschinger effect, and the influence of a simplified Bauschinger effect as suggested by Crafoord [33] on the bending of strainhardening monometal sheet will be investigated in section 5.2. Some materials, like mild steel, show an upper and lower yield point. The bending of these materials will be simulated by calculating the behaviour of a strain-softening material in bending in section 5.3. Since the ultimate aim of this work is to give insight into the forming properties of laminated materials, the bending of laminated strainhardening sheets will be treated in section 5.4.

5.1. Bending of Strainhardening Monometal Sheet without Bauschinger effect

5.1.1. Introduction

The bending of such a sheet can still be described by the theory presented in Chapter 3. Since the material has no

Bauschinger effect, the effective yield stress of a layer in the bent sheet is dependent on the effective strain only, and not dependent on the strain path to which the layer has been subjected during the bending.

It was shown before that for nonstrainhardening materials the neutral layer moves to the inside of the sheet during bending. This will also be shown to be the case for the bending of a strainhardening monometal. This inside movement of the neutral layer, plus the movement of the layers to the outside of the bent sheet due to constant volume considerations, have for result that some layers in the sheet will first be loaded in compressive straining - when they are situated on the inside of the neutral layer - and later on in tensile straining. For these layers, the effective strain $\bar{\epsilon}$, needed to calculate the effective stress, cannot be determined by the value of the tangential strain alone. Determination of $\bar{\epsilon}$ involves the use of the layer strain for which the strain direction reversal occurred. How this is done exactly, is shown in detail in Appendix VII. Since the calculation of $\bar{\epsilon}$ involves the knowledge of the straining path of individual layers, which are defined by their λ -value, i.e., the ratio of the material volume embraced by the layer and the inside surface of the bent sheet to the total sheet volume, it is quite permissible to describe the bending in terms of κ , η and λ_n , so that sheet thickness equation (3.2.20) will be integrated.

$$\frac{d\eta}{d\kappa} = - \frac{1}{2} \frac{\eta}{\kappa} \left[\frac{1 - 2\lambda_n - \kappa/2}{2\kappa\lambda_n + (1 - \frac{\kappa}{2})^2} \right] \quad (3.2.20)$$

The second dependent variable, λ_n , is found by integrating the equilibrium equation over the sheet thickness. This involves the knowledge of $\bar{\sigma}$, hence of $\bar{\epsilon}$, and since the value of $\bar{\epsilon}$ is not analytically known for layers that have undergone strain direction reversal, but must be determined separately, and numerically, for every layer, the equilibrium equation for these layers must be integrated numerically. This makes the solution method far more "computer time" consuming than the solutions for nonstrainhardening materials. The method of solution is described in detail in Appendix VII. The program presented there can use two different types of stress-strain curves, and can calculate the behaviour of laminated strainhardening sheet. Calculations for a single sheet of strainhardening material can be done by supposing the sheet is composed of two identical laminates. The stress-strain curves that the program can use are

$$\text{type 1} \quad \bar{\sigma} = A + B \bar{\epsilon}^n$$

$$\text{type 2} \quad \bar{\sigma} = A (B + \bar{\epsilon})^n$$

5.1.2. Example

To illustrate the bending of a strainhardening mono-metal without Bauschinger effect, the solution for a sheet with stress-strain curve

$$\bar{\sigma} = A (B + \bar{\epsilon})^n$$

$$A = 1$$

$$B = .01$$

$$n = .5$$

will be given in some detail.

Fig. 5.1 shows the relative sheet thickness η , the neutral layer position λ_n and the bending moment M/t_0^2 in function of the relative curvature κ for the bending of this material. The same figure also gives in dotted line the same variables for the bending of a nonstrainhardening monometal, with $\bar{\sigma} = \text{constant} = AB^n$. This gives the same yield stress for zero strain for both materials. It is clear from Fig. 5.1 that:

1. The relative sheet thickness η decreases when the strainhardening material is bent. For a nonstrainhardening material the thickness remains constant.
2. The neutral layer λ_n is always more to the inside of the sheet for a strainhardening material than for a nonstrainhardening one.
3. The bending moment for the strainhardening material increases first, reaches a maximum, and then decreases further on. This means that the pure bending of the strainhardening material becomes unstable once the κ -value for which the maximum bending moment occurs is reached. By comparison, the bending moment for the nonstrainhardening material is constant. This maximum in bending moment for strainhardening materials can be explained as follows. Two effects influence the bending moment at the same time. One is the increase in tangential stresses, caused by strainhardening, and the other one is the thinning of the sheet. In the

early stages of the bending process, the strainhardening influence is most important, and the bending is stable. When the thinning of the sheet becomes as important as the strainhardening, a maximum in the bending moment occurs, and the bend becomes unstable.

Fig. 5.2 shows, on the right side, how two originally equidistant layers are situated in the sheet after bending to a relative curvature $\kappa = 1$. The left side of the figure shows the tangential strain ϵ_ϕ and the value $\frac{\sqrt{3}}{2} \bar{\epsilon}$, proportional to the equivalent strain, across the sheet thickness. The cross-hatched zone between $|\epsilon_\phi|$ and $\frac{\sqrt{3}}{2} \bar{\epsilon}$ lines shows the equivalent in tangential strain of the strain that cannot be calculated by the tangential strain. It is evident that, whereas at the unelongated layer the tangential strain is zero, the equivalent strain is different from zero, since that layer has undergone a compressive-tensile cycle with zero final tangential strain. Fig. 5.2 shows also the equivalent yield stress across the sheet thickness. It is clear that $\bar{\epsilon}$ is greater on the inside surface of the sheet than on the outside, and the same applies for the effective yield stress $\bar{\sigma}$. Fig. 5.3 shows the radial and tangential stress distribution across the sheet thickness. This can be compared with the stress distributions for a non-strainhardening monometal, Fig. 4.1. The minimum of σ_ϕ in Fig. 5.3 in the neighborhood of the unelongated layer is of course caused by the minimum of $\bar{\sigma}$ at the unelongated layer (Fig. 5.2).

5.1.3. Influence of the Stress Strain Curve Parameters

Calculations on the bending of sheets have been performed using the following stress-strain curve

$$\bar{\sigma} = A (B + \bar{\epsilon})^n$$

with parameters

A	B	n
1	.1	.5
1	.01	.5
1	.001	.5
1	.1	.2
1	.01	.2
1	.001	.2

The value of A was not changed because this value is only a scaling factor determining the absolute magnitude of the stresses and the bending moment. Values of η , λ_n , M/t_o^2 in function of κ for the materials with $n = .5$ are given in Fig. 5.4 and 5.5, and for the material with $n = .2$ in Figs. 5.6 and 5.7. The dotted line in the $\lambda_n - \kappa$ graphs of Figs. 5.4 and 5.6 represent the neutral layer position for a nonstrainhardening monometal. It is seen that in all cases the neutral layer moves more to the inside than for the nonstrainhardening case. However, it can be seen that λ_n moves more to the inside for a higher value of the strainhardening index n or for a lower value of the material prestrain B. This is logical, since the

lower n , or the bigger B , the closer the stress-strain curve comes to a straight horizontal line $\bar{\sigma} = \text{constant}$. The graph also indicate that the relative sheet thickness decreases more for higher n or lower B . The same result applies here. The more the stress-strain curve deviates from the nonstrainhardening horizontal line $\bar{\sigma} = \text{constant}$, the more the sheet thins for the same value of κ .

Comparison of the bending moments shows that the bending moment is bigger for low n values or high values of B . This could be expected, since the stress-strain curve for $n = .2$ lies above the one for $n = .5$, and the stress strain curve moves to the left, and therefore up for the same $\bar{\epsilon}$, for increasing B .

The κ -value for maximum bending moment, and therefore the limit of stability, becomes smaller for decreasing values of the strainhardening index n . The influence of B on $\kappa_{M_{\max}}$ could not be established, due to the limited accuracy of the moment calculation (see Appendix IX).

It was explained that the bending moment is influenced by the strainhardening and the sheet thickness. Lower values for n cause less sheet thinning, and less strainhardening. But the results seem to indicate that the effect of less strainhardening is the more important one, so that instability occurs earlier in the bending process.

Table 5.1 gives the maximum compressive radial stress (this one occurs at the neutral layer radius) for the bending of different sheets for different κ -values. It is seen that the

TABLE 5.1

MAXIMUM COMPRESSIVE RADIAL STRESS

Stress-Strain Curve $\bar{\sigma} = A (B + \bar{\epsilon})^n$ Parameters			$ \sigma_r _{\max} = \sigma_r _{r = r_n}$			
A	B	n	$\kappa = .1$	$\kappa = .2$	$\kappa = .5$	$\kappa = 1.0$
1.	.1	.5	.0204	.0455	.1443	.4062
1.	.01	.5	.0109	.0291	.1126	.3570
1.	.001	.5	.0094	.0267	.1087	.3565
1.	.1	.2	.0377	.0790	.2178	.5224
1.	.01	.2	.0293	.0652	.1951	.4941
1.	.001	.2	.0273	.0631	.1925	.4915

maximum value of the radial stress increases with increasing κ -values, with increasing B and with decreasing n. This could be expected, since the stress-strain curve gives, for the same $\bar{\epsilon}$, higher $\bar{\sigma}$ values for increase in B or decrease in n.

5.2. Bending of Strainhardening Monometal Sheet with Simplified Bauschinger effect according to Crafoord

5.2.1. Introduction

As pointed out in the previous section, the layers in a bent sheet between the original neutral layer and the current neutral layer undergo a reversal in straining. They were originally subjected to compressive tangential straining, and are subsequently loaded in tension. Bauschinger [50], [51] reported in 1881 that the yield point in tension or compression is lowered after plastic deformation in the opposite direction. A plausible, but qualitative, explanation for the Bauschinger effect is that the deformation within the material is not homogeneous. This could be due to the variously oriented crystals in the material or internal stresses between dislocations. In a process like bending, nonhomogeneous deformation is also caused by the nature of the process itself, causing stress differences between various points of a piece of material. Whatever the cause of this nonhomogeneous deformation, when the material after deformation in one straining direction is unloaded, internal stresses will remain present. When the material is then loaded in the same straining direction, the material will yield at the same stress level as before the loading was applied. But, if the material is loaded in the opposite

direction, the presence of the residual stresses will cause high stresses in certain parts of the material, and yielding will occur at an apparently reduced stress. This decrease in yield strength after reversal of straining direction is called the Bauschinger effect.

Fig. 5.8 shows the relationship between stress and final strain for brass sheet which has been subjected to varying pre-compression, and is the result of experiments performed by Crafoord [33]. The same figure also shows the same relationship if it was assumed the material doesn't have any Bauschinger effect. The same stresses can be plotted against the effective strain for various pre-strain, as in Fig. 5.9. It can be seen that the Bauschinger curves are of the form given in Fig. 5.10. Be_1 is a constant decrease in yield stress, function of the compressive prestrain, while the decrease Be_2 decreases very rapidly with increasing strains. Of course, the stress strain curve is quite complicated. Crafoord suggested to approximate the Bauschinger curves by the following stress strain curve. After strain reversal, the yield stress is assumed to be constant and equal to the yield stress for zero effective strain until the final strain is zero. After that, the yield stress increases at the same rate as in the original stress-strain curve for zero prestrain. This curve suggested by Crafoord is plotted in function of final strain in Fig. 5.11, and the difference with the ones for no Bauschinger effect and real Bauschinger effect is very clear.

The value of the Crafoord way of accounting for the Bauschinger effect is that it is simple to analyze the bending of sheet with such a stress-strain curve. How this is done is explained in Appendix VIII.

5.2.2. Example

To illustrate the bending of a strainhardening material with Bauschinger effect according to Crafoord's model, the solution for a sheet with stress-strain curve

$$\bar{\sigma} = A (B + \bar{\epsilon})^n$$

$$A = 1$$

$$B = .01$$

$$n = .5$$

will be given.

Fig. 5.12 gives the solution for a sheet with these stress-strain curve parameters with Bauschinger effect, and also without Bauschinger effect. It is clear that the sheet with Bauschinger effect thins more, has a lower bending moment, and has a neutral layer position closer to the inside of the bent sheet than for a sheet without Bauschinger effect. The sheet with Bauschinger effect becomes unstable earlier in the bending process than the one without. This could be attributed to the fact that the first one thins more.

Fig. 5.13 shows the positions of ten originally equidistant layers in the sheet bend to $\kappa = 1$. It also shows the distribution of ϵ_ϕ , $\frac{\sqrt{3}}{2} \bar{\epsilon}$ and $\bar{\sigma}$ across the sheet thickness. The zone between the neutral layer and the unelongated layer has a

constant yield stress value, as required by the stress-strain curve used here. This low value of $\bar{\sigma}$ in that region is responsible for the faster thinning of the sheet than with a no Bauschinger strainhardening material. Fig. 5.14 shows the radial and tangential stress distribution across the sheet thickness. The parameters σ_r and σ_ϕ both show a discontinuity in derivative at the unelongated layer. This is due to the discontinuity of the stress-strain curve for the layer with strain reversal which has currently a zero tangential strain. Fig. 5.14 also shows that the tangential stress can be negative for layers to the outside of the neutral layer. In the case shown here, σ_ϕ even doesn't change sign at the neutral layer. This shows very clearly why a new definition of neutral layer was introduced in Chapter 3, section 3.2.4.

5.2.3. Influence of Stress Strain Parameters

The same stress strain curves as used for section 5.1.3, with the only difference of the introduction of the Bauschinger effect, will be used here. The results are presented in Figs. 5.15 to 5.18.

It is seen that the influence of B and n on $\eta-\kappa$, $\lambda_n - \kappa$ and M- κ curves is the same. It can be noted, however, that a change in B brings a bigger change for the material with Bauschinger effect than for the one without. This can be explained by the fact that the flat portion of the stress strain curve, used in the case of strain reversal, is given by $\bar{\sigma}_0 = A B^n$. A decrease in B here brings not only the strain-

hardening part of the curve down but also the flat portion. This increases the effect of low values due to reversal of stress, and hence causes relatively more thinning than in the case of a material without Bauschinger effect.

These results are based on the Crafoord model for the Bauschinger effect. It is virtually impossible to check these results out in practice. First, the real Bauschinger effect does not follow the simplified Crafoord model, and second, how can one get materials with same stress strain curve, but one with, and one without Bauschinger effect?

5.3. Bending of Strainsoftening Monometal Sheet

Horrocks and Johnson [34] found during their experiments on mild steel (a material with a pronounced upper yield point) that pure bending could not be carried out. A kink in the mild steel plates developed, and bending occurred locally. It was also reported by John Hiam, Dominion Foundries and Steel, in private communication, that they had problems with kinking in uncoiling mild steel sheet. This problem can be overcome by performing the uncoiling process by feeding the sheet through a series of unbending rolls. Since programs for calculating bending behaviour in sheets were developed in this thesis, it was interesting to know if this kinking, i.e., instability in bending, could be predicted by this bending theory.

The behaviour in bending of a sheet with stress strain curve

$$\bar{\sigma} = A + B \bar{\epsilon}^n$$

with $A = 2$
 $B = -1$
 $n = .5$

was determined with the program developed in Appendix VII. The stress strain curve was chosen to give an approximation for a material with upper yield point. The results simulate only the early bending behaviour of mild steel since mild steel also shows strainhardening, which was not included in the model stress strain curve used. The bending behaviour of the simulated material is given in Fig. 5.19. It is seen that the bending moment decreases for increasing values of relative curvature κ . This explains the instability in pure bending of such a sheet. Note also that the sheet thickness increases and that the neutral layer is more to the outside surface of the sheet than in the case of a nonstrainhardening material. It can be concluded that the effect of strainsoftening on the bending behaviour is the reverse of the influence of strainhardening.

Fig. 5.20 shows the stress distribution across the sheet thickness for the bending of a strainsoftening sheet. It is seen that $|\sigma_\phi - \sigma_r| = \bar{\sigma}$ decreases to the in-or outside surface of the sheet, This is as expected, since $\bar{\sigma}$ decreases for increasing strain $\bar{\epsilon}$. The "bump" in σ_ϕ near the unelongated layer is caused by the strain reversal of layers in the centre zone of the sheet, and the fact that it was assumed there is no Bauschinger effect. This "bump" is in the opposite direction as the one for strainhardening sheet, shown in Fig. 5.3.

It was shown in this section that the effect of an upper yield point in a material, which was approximated by a strainsoftening stress-strain curve, on the bending of a sheet is to make the bending unstable.

5.4. Bending of Laminated Strainhardening Sheet in the Absence of Bauschinger Effect

The bending behaviour of such sheets can be calculated using the computer program presented in Appendix VII. To illustrate some features present in the bending of these materials, that were not present in the bending of nonstrain-hardening laminates presented in Chapter 4, or in the bending of strainhardening monometals, presented previously in this chapter, the bending behaviour of a laminated sheet consisting of two laminates of equal original thickness will be reported. One laminate will be nonstrainhardening and will be further referred to as NSH. Using the strain stress curve

$$\bar{\sigma} = A (B + \bar{\epsilon})^n$$

this can be very successfully approximated with

$$A = 1$$

$$B = 1$$

$$n = 10^{-10}$$

The original yield stress of this laminate is then $\bar{\sigma} (\bar{\epsilon}=0) = 1$. The other laminate is strainhardening and will be referred to as SH. The same stress strain curve type is used, this time with

$$A = 5$$

$$B = .01$$

$$n = .5$$

The original yield stress of the strainhardening laminate is then $\bar{\sigma} (\bar{\epsilon}=0) = 5(.01)^{.5} = .5$. The stress strain curves of both laminates are shown in Fig. 5.21. It is clear that for low strains, the nonstrainhardening laminate is the strongest. For high strains, the strainhardening laminate is the strongest.

Fig. 5.22 shows the η - κ and λ_n - κ curves for the bending of the same sheet, once with the strainhardening laminate on the outside (NSH-SH sheet), and once with the strainhardening laminate on the inside of the sheet (SH-NSH sheet). It is seen that, for the SH-NSH sheet, the neutral layer at the beginning of the bending process is situated to the outside of the central layer ($\lambda_n > .5$). It is shown in Appendix VI that this means that, originally, the sheet thickness will increase. That this occurs indeed, is shown in the η - κ graph. Further on in the bending, the inside strainhardening laminate becomes stronger than the NSH laminate. As seen in Chapter 4, this will cause the sheet to thin. This is seen to occur, and the neutral layer will now be closer to the inside of the bend as in a NSH monometal. The strainhardening of inside laminate and the thinning of the whole sheet have both their influence on the bending moment, Fig. 5.23, which shows a maximum. Originally, the strainhardening has the biggest influence, and, later on, the thinning of the sheet will be the dominant factor. The

same sheet bend the other way (the NSH-SH sheet) has its original neutral layer position to the inside of the central layer at the commencement of bending. Hence, $\lambda_n < .5$ and Appendix VI shows that the sheet will originally thin, as indeed it does, see Fig. 5.22. The strainhardening of the SH laminate will cause the neutral layer to move more to the outside surface of the sheet. The neutral layer in nonstrain-hardening laminates and strainhardening monometals moves always to the inside surface of the bent sheet. The possibility of the neutral layer moving to the outside surface of the bent sheet is a feature that is peculiar to the bending of laminated strainhardening sheets. Where the bending progresses, the neutral layer will have a maximum in its movement to the outside, and will, from then on, move to the inside surface of the sheet. The sheet soon has its strongest laminate on the outside, and the sheet will thicken up. Since the sheet strainhardens and thickens, the bending moment will monotonically increase, as shown in Fig. 5.23.

The fact that the neutral layer can move to the outside of the sheet during part of the bending process is significant in another respect. Layers, originally subjected to tensile straining, can be overtaken by the neutral layer and be loaded in compression. Later on, when the neutral layer moves back to the inside of the sheet, the same layer undergoes a second strain direction reversal. Fig. 5.24 shows the tangential stress for different layers in the NSH-SH sheet. Layer $\lambda = .5$, for example, has first increasing ϵ_ϕ , then decreasing ϵ_ϕ , and then

increasing ϵ_ϕ again. This means that the layer goes subsequently through tension, compression, tension. Since for this sheet, Fig. 5.22, the original neutral layer is situated at $\lambda = .375$, and the maximum position of λ_n occurs for $\lambda = .525$, all the layers with $.375 < \lambda < .525$ have two stress reversals (if the sheet is bent further than $\kappa = 1.07$). Of course, the classical compression-tension loading is still present for other layers. The possibility of this double stress reversal is typical for the bending of strainhardening laminated sheets.

An example of the bending of a sheet consisting of two strainhardening laminates will be presented in Chapter 6. It is thought that a more general presentation on the bending of laminated strainhardening sheet is only of limited value, since the important bending phenomena have been covered, and since the number of free choice parameters is too big.

5.5. Conclusions

The application of the general bending theory to materials with a strain dependent yield stress has shown the following.

1. The bending of a strainhardening monometal sheet without Bauschinger effect occurs under decreasing sheet thickness. The bending moment increases in the beginning and reaches a maximum. Further bending is unstable.
2. The bending of a strainhardening monometal with Bauschinger effect is similar to that without. The sheet will thin more for the same relative curvature, and the point

of instability in bending will be reached earlier.

3. A material with upper yield point, such as mild steel, can be simulated by a strainsoftening material. The bending of a strainsoftening material is unstable from the beginning of the process. This explains the bending instability of mild steel.
4. It was shown that during bending some layers are subjected to a compressive-tensile stress cycle. In laminated strainhardening sheets, however, tensile compressive and tensile-compressive-tensile stress cycles are possible, since the neutral layer can move to the outside surface of the sheet during the bending of these sheets.

The treatment of Chapters 3, 4 and 5 has given an insight into the plastic bending of single and laminated materials. This insight will be used to explain the actual behaviour of laminated sheets in bending and deep drawing experiments, which will be presented in the following chapter.

CHAPTER 6

BENDING AND DEEP DRAWING EXPERIMENTS ON LAMINATED SHEET

6.1. Bending of Laminated Sheet Metal

6.1.1. Experimental Procedure

It was indicated in Chapter 3, Figs. 3.1 and 3.2, how pure bending could be carried out using the four point bend test. This test set-up ensures that the bending moment in the test section between the two middle points' or rollers is constant, and that no transverse forces act on the test section. Theoretically, this test method should be excellent. The laminated sheet metal available for testing is rather thin. Hence, in order to get a high relative curvature ($\kappa = \frac{t}{r_m}$), the radius of the bend must be small, and since the sheet is thin, the test section will be small. Hence, the distance between the rollers of a four point bending rig must be small. Development of a rig of such a small size was expected to cause some problems, and it was thought not to be worthwhile, since only a few tests would be carried out. Bending methods used in industry could not be used either, since they do not result in pure bending. A method used by Crafoord [33] comes close to realizing pure bending, and is simpler than the four-point bend test. The testing principle is shown in Fig. 6.1. The sheet strip is clamped between a fixed and a movable jaw fitted with a long lever. When a transverse load is applied at the

end of the lever, a constant transverse force acts along the strip to be tested, while the bending moment varies linearly along the strip. When the lever is long enough, the transverse force is small and the bending moment practically constant along the test strip. A testing rig, consisting of two jaws, which can clamp strips 2 in wide for a depth of 3/4 in, and a lever of 40 in length, fitted to one of the jaws, were used in the experiments. The sheet to be tested is thin ($t_0 \approx .050$ in), and the jaws are heavy. When the sheet is tested as shown in Fig. 6.1, with the width directions of the sheet horizontal, then the movable jaw itself forms a big load on the test specimen, due to gravitational forces. The transverse load is not situated at the end of the lever, but at the edge of the sheet to be tested, so that this load causes a nonuniform bending moment and a significant transverse force along the test strip. The test set up was hence rotated over 90° along its longitudinal axis, so that the width direction of the sheet is vertical. The weight of the movable jaw loads the sheet now in the width direction. This load can be removed by supporting the movable clamp.

It was determined that the maximum relative curvature of sheets with original thickness $t_0 = .050$ in, when bent in the fixture described above could be obtained when the original length of the test section was $l_0 = .36$ in. Specimens of sheets D, D-SS and D-AL with this test section length and a width of 1 in were tested in the rig. After bending, the specimens were cut in half in their longitudinal direction, the

sections polished, and the change in thickness of the whole sheet and of the different laminates determined under a travelling microscope. The specimens were cut in half since the end aspects of the bent strip cannot be used for thickness measurements, since deformation therein is not plain strain (the end aspects show anticlastic curvature). The inside and outside bending surfaces were plotted on graph paper, and the average radius determined graphically. Since the sheet thickness is already known, the value of the relative curvature $\kappa = \frac{t}{r_m}$ can be determined.

Only a limited number of tests were performed, due to the lengthy procedure and the small accuracy attainable in the measurements. The difficulties encountered with the above bending rig, e.g., the weight of the jaws, and the clamping of the sheet in the jaws, suggest that it might be worthwhile to develop a four point bending rig for testing thin sheets.

6.1.2. Bending of Sheet D: Theoretical and Experimental

The pure bending of laminated sheet D could be computed since the stress-strain curves for the aluminum and stainless steel laminates are known. Using the program BENDING described in Appendix VII, and the stress-strain curve

$$\bar{\sigma} = A (B + \bar{\epsilon})^n$$

with the values of A, B and n for the laminates D-SS and D-AL given in Table 2.2, and width $\mu = .18$ when the stainless steel

is on the inside of the test sheet, while $\mu = .82$ when the steel is on the outside, gives the bending behaviour for sheet D shown in Fig. 6.2. The stress-strain curve parameters for D-SS and D-AL are approximately the same, except that parameter B for D-AL is zero. Hence, the sheet bends almost like a strain hardening monometal except in the beginning, when the aluminum is supposed to have no strength ($B = 0$). It is seen in Fig. 6.2, that sheet D would bend stable, since the bending moment increases for increasing κ , irrespective of the laminate that is on the outside of the bend.

It was explained in Chapter 2 with Fig. 2.7 that the stress-strain curve parameters for D-AL in Table 6.2 give a poor fit to the experimental stress-strain curve. Fig. 2.7 shows that the stress values become nearly constant in the last phases of the tensile tests as D-AL. However, the 'best fit' stress-strain curve of type $\bar{\sigma} = A (B + \bar{\epsilon})^n$ does not level off for higher strains, and extrapolation of the yield stress in the aluminum, using this stress-strain curve, for higher strain values gives erroneous results. Hence, the bending behaviour for sheet D given in Fig. 6.2 will not be true, except for small values of κ .

The stress-strain curve for sheet D-AL was then replaced by a nonstrain hardening curve $\bar{\sigma} = 29000$ psi. (This was realised in the program BENDING by using the curve $\bar{\sigma} = A (B + \bar{\epsilon})^n$ with $A = 29000$, $B = 1$ and $n = 10^{-10}$).

The bending behaviour of sheet D, with the aluminum laminate nonstrainhardening and the stainless steel laminate unchanged, is given in Fig. 6.3 and 6.4. When the stainless steel is on the outside of the bent sheet, the sheet thickens, and the bend is stable. When the aluminum is on the outside, the sheet thins, and the bend is unstable. Note however that, in the last case, the bending moment decreases only slightly for small κ -values. Note also that the $\lambda_n - \kappa$ curve in this curve shows a discontinuity in slope when $\lambda_n = .18$, i.e., when the second layer crosses the laminate boundary. Similar behaviour was found in nonstrainhardening laminated sheets (Chapter 4). Fig. 6.5 shows the relative laminate thickness as a function of κ . As for nonstrainhardening bimetals, the outside laminate thins, and the inside laminate thickens. Note however that the increase in stainless steel laminate thickness, when it is on the inside of the bend, reaches a maximum. Once $\kappa > 1.5$, the decrease in total sheet thickness causes even the inside stainless steel laminate to decrease in thickness. Such behaviour was not encountered for nonstrain hardening bimetals (Fig. 4.17):

When Figs 6.2 and 6.5 are compared, it can be seen that the choice of stress-strain curve for the aluminum laminate has a big influence on the bending behaviour of sheet D. It follows from Fig. 2.7 that the aluminum can be considered strain hardening for very small strains, and must be considered nonstrain hardening for larger strains. It is therefore thought that Fig. 6.2 describes the bending of sheet D in the very beginning, and that Fig. 6.3, 6.4 and 6.5 apply when the bending is more advanced.

The limit of applicability of Fig. 6.2 should be reached when the strain in the most strained aluminum layer reaches approximately .01, the value of $\bar{\epsilon}$ for which the strains in the aluminum levels off. Assuming constant sheet thickness, it can be derived from Fig. 4.3 that this occurs when $\kappa \approx .025$. Further bending of the sheet will deviate from the solutions given by Fig. 6.2, and will come close to the solution suggested by Fig. 6.3, 6.4. For large values of κ , it is suggested that solution Fig. 6.1, 6.4 will hold.

Experimental bending of sheet D yielded the following results. It was found that, when the sheet was bent with the stainless steel as the outside laminate, the bending was stable and uniform, the sheet thickness increased, and the stainless steel laminate became thinner while the aluminum one became thicker. The results of a few tests are shown in Fig. 6.6, and the graph shows that, in general, the experimental behaviour agrees with the bending solution given derived for nonstrain hardening aluminum.

When the sheet D was bent with the aluminum on the outside of the bend, bending was uniform (and stable) at the beginning and the sheet became thinner. This agrees with the behaviour of sheet D when the aluminum is considered strain-hardening (see Fig. 6.6). However, once a uniform relative curvature of $\kappa = .08$ was reached, kinking occurred, and the bending proceeded locally. This can be explained as follows. In the beginning of the bend, the aluminum strainhardens, so

that, even with decreasing sheet thickness, the bending moment rises (see Fig. 6.2). However, once $\kappa \approx .025$ is reached, the most severely strained aluminum layers do not harden any more, and have a constant yield stress. Then bending proceeds, the zone of nonstrainhardening aluminum increases, and hence the increase in bending moment becomes smaller than suggested by Fig. 6.2. Since the solution for the bending of sheet D with nonstrainhardening aluminum indicates only a slight decreasing bending moment for low κ -values, the transition between the two solutions is not abrupt. However, around $\kappa \approx .08$, the moment reaches a maximum, and decreases thereafter, as suggested by Fig. 6.4. The strain in the aluminum outside layer reaches then .04, or four times the value for which the zone of constant stress in the aluminum starts. That the bending is now unstable is logical, since the inside stainless steel is the strongest laminate (and can even strainharden), while the outside weak aluminum has reached its maximum stress.

A few bending experiments on sheets D-SS and D-AL were performed. The bending of the strainhardening stainless steel occurred uniform and stable, with decrease in sheet thickness. This behaviour agrees with what is known of the bending of strainhardening monometals, as featured in Chapter 5. Instability did not occur, since the bending rig did not allow testing up to the high κ -values for which a maximum in bending moment exists. The bending of the aluminum was peculiar. The aluminum sheet could be bent uniformly up to a small value of κ , after which a kink in the sheet developed and the bending proceeded

locally. A possible explanation is that initially the aluminum strainhardens with small strains, but can be considered as non-strainhardening for values above .01. It can then be approximated by a 2-1-2 trimetal (Chapter 4), with the inside "2" laminate thicker than the outside "2" laminate, since the strains are higher at the inside surface of the bend, as indicated in Fig. 4.3. Such a trimetal always bends unstable, as seen in Fig. 4.23. Hence, in the beginning of the process, the aluminum is strainhardening, and bending is therefore stable. But when the outside layers reach the strain for which they become non-strainhardening, the sheet starts to resemble a 2-1-2 trimetal with more inside clad than outside clad, and the bending will become unstable.

6.1.3 Conclusions

It was shown that the bending theory developed is able to describe the bending of laminated sheet, and that the results of theory and experiment agree in general. However, it was made clear that one must be careful when using stress-strain curves to describe laminate behaviour, since the choice of the wrong curve will give a wrong solution to the bending of laminated sheet. It was also found that the stress-strain curves used, the power laws

$$\bar{\sigma} = A (B + \bar{\epsilon})^n$$

or

$$\bar{\sigma} = A + B \bar{\epsilon}^n$$

or the nonstrainhardening case,

$$\bar{\sigma} = \text{constant},$$

are not sufficient to describe the stress-strain behaviour of the aluminum. A stress-strain curve with marked hardening for small strains, but practically no hardening at higher strains should be used to describe the aluminum. This can be realised by using a Voce stress-strain curve

$$\bar{\sigma} = \sigma_{\infty} - (\sigma_{\infty} - \sigma_s) e^{-\bar{\epsilon}/\epsilon_c}$$

where σ_{∞} indicates a constant stress which would be obtained with large strains, σ_s corresponds to the tensile stress of the material, and ϵ_c is a constant expressed as a characteristic strain. It is suggested that the program BENDING (that calculates the bending of laminated strainhardening sheet) will be adapted to be able to solve the bending of laminates with the Voce stress-strain curve.

6.2 Deep Drawing Experiments on Laminated Sheet

It was shown in Section 6.1 that whichever laminate is on the outside of the bend has an influence on the pure bending behaviour of non symmetrical laminated sheet. Bending also occurs in deep drawing, and although this bending is not pure plain strain bending, the insight gained in the pure bending of laminated sheet will be of help in understanding the

deep drawing behaviour.

6.2.1. Experimental Procedure

Deep drawing experiments were performed on a Hille 20/40 Universal Sheet Metal Testing Machine. A schematic test set up is shown in Fig. 6.7. Circular specimens of 2.5, 3, 3.5 and 4 in. diameter were machined out of material E, D and DD. Four specimens of each size for the different materials were tested, two with the stainless steel on the outside of the deep drawn cup, and two with the stainless steel on the inside. The blanks were lubricated on both sides with Molyslip, the clamping load used was 22000 lbs, and the punch speed approximately 15 ins/min. A circular grid of lines with a pitch of 0.05 in. was photographically printed on the side of the specimens which became the outside of the drawn cups. The deep drawing load versus punch travel was recorded for all specimens. The calibration curves for the load were not available, hence the load values will be indicated in millivolt. The load values will only be used for comparative purposes, thus the calibration is not of prime importance. Thickness measurements were performed before and after deep drawing. The thickness of the drawn cups was measured on the intersection of two perpendicular radial lines with circular grid lines with radii 0.5 to 1.25 in. in the undeformed grid system. These measurements gave the cup thickness over the punch nose and the punch radius. Cups of sheet DD were sectioned in half, the cross sections polished, and the thickness of the aluminum and stainless steel laminates

measured under a travelling microscope.

6.2.2. Results of Deep Drawing Experiments

1. Tests on Sheet E

No specimens of sheet E with the stainless steel on the outside of the cup could be successfully drawn without fracture. Fracture occurred in the rolling direction of the sheet, on both sides of the punch nose. However measurements were taken on the cups drawn from blanks 2.5 in diameter, even though fracture occurred, and this allowed some assessment to be made of the thickness variation over the punch nose and radius.

Specimens of sheet E with the stainless steel on the inside of the cup could be drawn from blanks with 2.5 or 3 in diameter. Larger blanks failed, again with fracture in the rolling direction. The maximum drawing loads of the tested specimens are given in Table 6.1. A comparison between them is not possible, since all specimens with stainless steel on the outside of the cup fractured. Thickness measurements on the drawn cups from blank size 2.5 in diameter are reported in Fig. 6.8. It is clear that the specimens with stainless steel on the inside of the cup show a thinning where they are bent over the punch radius, whereas the ones with stainless steel on the outside become thicker. However, these last ones failed.

Material E does not seem to be suitable to study the deep drawing behaviour of laminated sheet, since its formability is limited. The maximum elongation in the tensile test was very

low, stretching with the bulge test could not be performed, and cup drawing was not very successful either.

2. Tests on Sheets D and DD

Deep drawn cups with stainless steel on the inside of the cup will further be designated as SS IN, while cups with stainless steel on the outside will be indicated as SS OUT. For example, a specimen from a blank of 3.5 in diameter with stainless steel on the inside of the cup, will be indicated as ϕ 3.5 SS IN.

The maximum deep drawing loads for cups of materials D and DD are given in Table 6.1 and Fig. 6.9. The maximum deep drawing load for the ϕ 2.5 SS IN case seems to be higher than for the ϕ 2.5 SS OUT case, while the reverse is true for ϕ 3.5 blanks, i.e., the maximum load is higher for ϕ 3.5 SS OUT than for ϕ 3.5 SS IN. The difference in maximum loads for the ϕ 3 blanks seem to be inclusive, while the comparison for the ϕ 4 blanks cannot be made, since all ϕ 4 SS OUT specimens failed, while the ϕ 4 SS IN specimens could be successfully drawn. Punch load versus punch travel for two cups of material DD from ϕ 2.5 in blanks is featured in Fig. 6.10 while curves for ϕ 3.5 in blanks of material D are given in Fig. 6.11. Figs. 6.10 and 6.11 show that the total punch travel to draw a cup is longer for the SS IN case than for the SS OUT. This means that the SS IN cups have a greater cup height. These figures also illustrate the point that for small blanks, bigger loads were

required for SS IN than for SS OUT, while the reverse is true for bigger blanks.

Thickness measurements on the ϕ 2.5 in blanks of sheets D and DD are featured in Figs. 6.12 and 6.13. For both materials, the cups with SS IN thin around the punch radius, while the cups with SS OUT thicken. Thinning of the sheet in the cup wall occurs for both cases. Thickness measurements taken with a ball-ended micrometer around the punch radius of cups of material DD are shown in Fig. 6.14. As was indicated before, the sheet around the punch radius thins in the ϕ 2.5 SS IN case, while it thickens in the ϕ 2.5 SS OUT case. This local thinning of the sheet in the ϕ 2.5 SS IN case explains why the cup height is greater, as can be seen in Fig. 6.10 (the bigger the punch travel the deeper the draw). Fig. 6.14 indicates that, with increasing blank size, the sheet around the punch radius becomes progressively thinner. This holds for both SS IN and SS OUT. However, the influence of increasing blank size is far greater for the SS OUT case than for the SS IN case. Note however, that even for the ϕ 3.5 SS OUT blank the decrease in sheet thickness around the radius is less than for ϕ 3.5 SS IN. The result of this is that the ϕ 3.5 SS IN cup is deeper than the ϕ 3.5 SS OUT cup, as can be seen in Fig. 6.11. The influence of increasing blank size on the SS OUT cups will ultimately make the sheet thickness of these cups around the punch radius so thin that failure along these thinned zones will occur, as it does for the ϕ 4 SS OUT blanks.

Thickness measurements of sectioned cups of sheet DD under a measuring microscope are featured in Figs. 6.15 and 6.16. It is clear that the change in relative thickness of the aluminum laminate for both cases, SS IN or SS OUT, shows the same trends as the change in thickness of the whole sheet around the punch radius. This is not surprising, since the aluminum laminate makes up 82 percent of the sheet. Fig. 6.15 indicates that in the SS OUT case the stainless steel laminate becomes thinner for all blank sizes and that the thinning of the stainless steel is more severe than the thinning of the whole sheet. This means that, over the punch radius, regardless of the thinning or thickening of the whole sheet, the percentage stainless steel in the sheet at the place, expressed as stainless steel thickness to total sheet thickness, becomes lower than the original 18 percent. Fig. 6.16 indicates that in the SS IN case the stainless steel laminate thickens over the punch radius, although the whole sheet thins. Hence, the ratio of steel thickness to total sheet thickness at that place becomes bigger than 0.18.

The interpretation of these experimental deep drawing results will be given in Section 6.2.3. The insight into the bending process previously gained will allow a clearer picture of the deep drawing behaviour of laminated sheet to be drawn.

6.2.3. Qualitative Description of the Deep Drawing Behaviour of Laminated Bimetal Sheet

In what follows the author has attempted to provide an explanation of the experimental observations made when deep drawi

laminated sheet. While acknowledging that the arguments are not always rigorous some attempt has been made to provide a qualitative account of the deep drawing behaviour using some of the results from the pure bending work.

Consider the deep drawing of a blank with a diameter only slightly bigger than the punch diameter, so that the blank diameter is smaller than the inside diameter of the clamping ring. Different stages in the process are shown in Fig. 6.17. It is clear that the deformation of element A of the blank consists mainly of bending, whereas the deformation of element B is restricted to drawing in. To maintain constancy of volume, element B of the blank will thicken during this radial drawing.

As an example, a blank of sheet D will be used to illustrate the drawing of a bimetal sheet. First, consider the deep drawing of a cup with the stainless steel on the outside of the cup (SS OUT). When element B draws in radially, it also rotates. (This is not bending!). The final radius of the SS laminate will be bigger than for the AL laminate (since SS is on the outside). Hence, due to constancy of volume, the AL laminate will thicken up more than the SS laminate, so that the percentage of the SS laminate, expressed as thickness ratio, will be smaller in element B after deep drawing than before. Element A deforms in bending. Since the strong SS laminate is on the outside, element A will become thicker. But the SS laminate will thin and the AL laminate will thicken, as indicated by the bending of sheet D with SS OUT in Fig. 6.5.

When a cup is drawn with stainless steel on the inside (SS IN), element B will thicken. But this time, since the final radius of the stainless steel is smaller than the one for the aluminum, the SS will thicken more than the AL laminate. Element A is deformed in bending, and since the stainless steel is on the inside, the sheet at A will thin, the AL laminate will thin, but the SS laminate will thicken as follows out of Fig. 6.5. It can be verified that this behaviour is the same as the one found experimentally for the ϕ 2.5 in blanks. Furthermore, when the SS IN and SS OUT cases are compared, it can be concluded that the SS becomes thicker, everywhere when the sheet is deformed in the SS IN case, whereas the SS becomes thinner at the punch radius (element A) for SS OUT. This could account for the fact that the maximum punch load is slightly larger in the SS IN case than for SS OUT for the ϕ 2.5 in blanks since the SS is the strongest laminate and gives the most resistance to deformation.

Let us now consider the deep drawing of a blank with a diameter much bigger than the punch diameter, so that part of the blank will be clamped between clamping ring and die before and during the deep drawing process, see Fig. 6.17. When the drawing is only carried out as far as indicated by the last graph of Fig. 6.17, element D will be subjected to radial drawing in only. During this drawing in, element D will become thicker (constancy of volume), and both SS and AL laminates will thicken in the same proportion, since it makes no difference

during drawing of element D which element is on the side of the die or on the side of the clamping ring. Element C will thicken, as described for element D, between stages I and II. Between stages II and III, element C will be simultaneously subjected to bending, radial drawing in and stretching.

Element B will undergo radial drawing in, bending and stretching between I and II, and drawing in, debending and stretching between II and III. Finally, element A will be subjected to bending and stretching.

When a cup is drawn with stainless steel on the outside (SS OUT) the different sheet elements will deform as follows. Element D is subjected to pure drawing in, as mentioned before. The same applies for element C between stages I and II. Between stages II and III, element C is subjected to bending. The SS laminate is on the inside of the bend for element C, so that element C would thin, the SS thickens and the AL thins, if bending was the only deformation undergone by element C. Radial drawing in will cause element C to thicken, so that the final change in thickness of element C is uncertain (two opposite effects). However, the bending of element C will increase the percentage SS (as thickness ratio in the sheet) above the original one in the sheet. Since SS is the strong laminate, this will cause the load for deep drawing to become bigger than when this relative thickening of SS should not happen. Element A is bent with SS in the outside of the bend, so that SS will thin, AL thicken, and total element A will thicken. However, due to

the drawing in of the blank, element A is also stretched. Since the SS percentage in element C has increased, the drawing load is higher, and element A will be stretched more. Our experiments indicated that the stretching was the more important factor, hence element A thins. It is the stainless steel in element A that has to take most of the drawing load. The SS at element A will thin for two reasons. Firstly, due to bending of element A, and secondly, due to stretching of element A, caused by an increasing drawing load for drawing in of the blank, itself caused by an increase in SS percentage at element C as a result of bending of element C.

When a blank is drawn with stainless steel on the inside (SS IN), deformation proceeds as follows. Element C will be drawn in more as in the previous case, but during bending of element C, the SS laminate is the outside one in the bend. Hence, the SS will thin, and the total sheet thickens due to bending. Hence, the SS percentage, as thickness ratio, will decrease in element C. This will cause a decrease in drawing load as compared to the case where this SS percentage should not decrease. The bending of element A results in the thickening of the SS, and the thinning of the whole sheet. Since the drawing load is less than usual, the stretching at element A will be less. Hence the sheet at element A will thin more than predicted by bending alone, but, since the SS laminate has thickened, the sheet at element A is really stronger than the original sheet.

When SS IN and SS OUT are compared, it is found that,

1. SS OUT: SS percentage in element C increases
increase in drawing load
SS percentage in element A decreases
SS in element A thins
2. SS IN: SS percentage in element C decreases
decrease in drawing load
SS percentage in element A increases
SS in element A thickens (or thins slightly)

Since the SS laminate in element A has to transmit the drawing load, it is clear that the SS OUT blanks will fail for smaller diameter blanks than the SS IN blanks. This is due to two effects. Firstly, for SS OUT, the drawing load is bigger than for SS IN, and secondly, for SS OUT, the SS laminate in element A is thinner than in the SS IN case. Hence, failure in SS OUT will occur first. This finding agrees with what was found experimentally.

6.2.4. Comparison of our Deep Drawing Results with Experiments Performed by other Authors

Hawkins and Wright [20], [21] have performed deep drawing tests on copper-mild steel laminated sheet. Some of their results have been briefly reported in Chapter 1, Section 1.2. They found, Figs. 1.2 and 1.3 that the amount of the thinning over the punch nose in their deep drawn cups was greater when the outer component was the softer one. This agrees with the present experiments on aluminum-stainless steel laminated sheet, see Fig. 6.14.

They also indicated that they found lower cup heights when the stronger steel component was the outer one. The same observation was made in this work, where the cup height is lower when the stainless steel is the outer component of the stainless steel-aluminum sheet, see Figs. 6.10 and 6.11 (greater punch travel means greater cup height).

Hawkins and Wright [20] also found experimentally that the limiting drawing ratios of laminated sheet was dependent on the tool geometry. They mentioned especially the ratio of punch profile radius to sheet thickness. It is shown in Section 6.2.3 that bending over the punch radius and bending over the die radius has an influence on the drawability of bimetal sheet. Since the 'severity' of these bends can be characterised by the relative curvature values of these bends, i.e., the ratio of sheet thickness to punch profile radius and the ratio of sheet thickness to die profile radius, it is easily understood that the bigger these ratios are, the bigger the difference in drawability between blanks of the same size but with a different laminate on the outside of the cup, will be.

6.2.5. Conclusions on Deep Drawing Experiments.

It is found that during the deep drawing of a bimetal sheet the deep drawing performance is dependent upon which material is to the outside of the drawn cup. The limiting drawing ratio is bigger when the soft laminate is on the outside

of the cup. Two effects seem to be important. Firstly, the bending over the punch radius can decrease or increase the thickness of the strong material, depending on which laminate is on the outside of the cup. Secondly, the bending over the die radius will influence the relative thickness of the strong laminate over the die radius, and this will increase or decrease the drawing load. The thinning of the strong layer at the punch radius occurs for the same draw as the increase in deep drawing load, and vice versa. Hence, both effects have the same influence on the limiting drawing ratio. The magnitude of both effects will depend on the relative curvature of the bend over the punch radius and die radius, so that tool geometry will have an influence on the drawability.

Table 6.1. Deep Drawing Loads

Blank Diameter in	Laminate Orientation		Sheet E			Sheet D			Sheet DD		
	SS OUT	SS IN	Speci- men	Load mV	Failure	Speci- men	Load mV	Failure	Speci- men	Load mV	Failure
2.5		✓	G	1.22		E	.84		D	.80	
		✓	H	1.24		F	.84		E	.80	
	✓		C	1.10	✓	A	.84		A	.78	
	✓		B	1.12	✓	B	.82		B	.78	
3.0		✓	K	3.60		I	2.55		I	2.44	
		✓	L	3.65		J	2.50		J	2.44	
	✓		-	-	✓	G	2.60		G	2.46	
	✓		-	-	✓	H	2.55		H	2.44	
3.5		✓	-	-	✓	M	4.40		M	4.35	
		✓	-	-	✓	N	4.35		N	4.30	
	✓		-	-		K	4.80		K	4.35	
	✓		-	-		L	4.85		L	4.45	
4.0		✓	-	-		Q	6.9		Q	6.6	
		✓	-	-		R	7.0		R	6.6	
	✓		-	-		O	7.1	✓	O	7.1	✓
	✓		-	-		P	7.0	✓	P	6.8	✓

CHAPTER 7

CONCLUSIONS AND SUGGESTIONS FOR FURTHER WORK

The preceding chapters have demonstrated, both theoretically and experimentally, that the behaviour of laminated materials under certain forming processes is strongly influenced by the respective strengths of the various laminates and the orientation of the laminated sheet in the forming process.

Of the deformation processes considered here the influence of the orientation of the laminated sheet is most marked in the deep drawing and pure bending process.

Although deformation processes consisting only of pure bending are rare it is felt that the work presented here will provide some insight into more complicated deformation processes involving laminated materials.

Further conclusions which are generally, but not entirely, restricted to the actual materials tested in this present investigation are listed below.

1. The load-elongation curve of laminated sheet tensile specimens can have more than one maximum, although the single composing materials have only one maximum in their load-elongation curve.
2. The investigations carried out on the stretch-forming of asymmetric laminated sheets seem to indicate that slightly higher strains are attainable when the weak laminate is on the outside surface. The amount

of testing performed is not sufficient to draw any firm conclusions.

3. The original neutral layer position λ_n at the commencement of bending determines if the sheet will thicken or thin at the start of the bending process.
4. The bending of laminated non strain hardening sheets can occur under increasing or decreasing sheet thickness and uniform bending can be unstable.
5. The sheet thickness decreases and the bending moment reaches a maximum during the bending of strainhardening single sheets without Bauschinger effect. The sheet thickness decreases more and the bending moment reaches its maximum later in the process when the strain hardening index increases.
6. The influence of the Bauschinger effect on the bending of single strain hardening sheet is to increase the amount of thinning and to make the bend unstable earlier in the deformation process.
7. During the bending of single sheets, the neutral layer moves to the inside surface of the bend, so that centre layers will be successively loaded in compression-tension. During the bending of laminated strain hardening sheets however, the neutral layer can move to the outside surface of the bend, so that centre layers can also be loaded in a tension-compression and tension-compression-tension cycle.

8. In the deep drawing tests on asymmetric laminated sheets, greater cup height and greater drawability were obtained when cups were formed so that the softer laminate was on the outer surface of the cups.

The present investigation provides a theoretical analysis of the pure bending deformation process. It is possible to extrapolate results obtained by pure bending theory to more complicated deformation processes to gain insight into the mechanics of these processes. But to predict, quantitatively, the deformation of laminated sheets in these processes, further development of the bending theory is necessary. Concurrently, more experimental work has to be done on deforming laminated materials. Topics that need further investigation are listed below.

1. The bending theory should be applied to analyze the repeated bending and debending of the same sheet.
2. The pure bending theory should be extended to solve the problem of plane strain bending under superimposed tensile stress.
3. Extension of the bending theory to bending under superimposed biaxial tensile stress should make it possible to predict the behaviour of laminated sheet in the hydrostatic bulge test.
4. More experiments on laminated sheet using the hydrostatic bulge test are necessary.
5. A detailed analysis of the simultaneous asymmetric drawing in and bending as occurs in the deep drawing of

of circular blanks over the die radius could give quantitative information on the deep drawing behaviour of laminated sheet.

6. Further experimental research into the deep drawing of laminated sheet is necessary. In particular, to investigate the effects of tool geometry, with more attention being paid to the ratio of punch profile to sheet thickness and the ratio of die profile radius to sheet thickness. It is also suggested that laminate thickness measurements to taken over the die radius of partially drawn cups.
7. The pure bending theory should be extended to cover the bending of elastic-plastic materials of arbitrary stress-strain curve, so that spring-back and residual stresses in deformed laminated materials can be evaluated.

REFERENCES

1. Dietz, G. H., editor,
Composite Engineering Laminates,
M.I.T. Press, Cambridge, Massachusetts (1969).
2. Agers, B. M.,
Mechanisms of Pressure Welding,
Ph.D. Thesis, Univ. of Wales (1962).
3. Donelan, J. A.,
Sheet Met. Ind., 40, p. 863 (1963).
4. Rollason, E. C.,
Ibid (Discussion).
5. Krivonosov, Y. I., et al.,
Tsvet Metall, (12), p. 8 (1966).
6. Bianchi, L. M.,
Met. Prog., 87 (3), p. 127 (1965).
7. International Atomic Energy Authority,
Fabrication of Fuel Elements with Special Emphasis on
Cladding Materials,
Mech. Eng., London, 5 (51), pp. 367-368 (1960).
8. Anon.,
Extrusion Cladding of Aluminum,
Light Metal Age, 24 (3/4), pp. 6-7 (1966).
9. Anon,
Co-Extrusion Includes more Materials for Industry's Demands,
Iron Age Metalwkg Int., 1 (3), pp. 30-31 (1962).
10. Anon,
Materials: Metals - Steel-Aluminum Marriage,
Prod. Eng., 37, (9), p. 70 (1966).
11. Whitfield, E.,
A Preliminary Study of the Co-extrusion of Dissimilar Metals,
N.E.L. Report No. 265, Ministry of Technology, National
Engineering Laboratory, Glasgow (1967).
12. Loewenstein, P. and Tuffin, W. B.,
Metallurgical Bonding of Dissimilar Metals by Co-extrusion,
West Concord, Massachusetts: Nuclear Metals Division,
Testron Incorporated.

13. Darling, A. S.,
Improvement in and Relating to the Production of Composite
Metallic Strip or Rod.
U.K. Pat. No. 882, 693, (1961).
14. Alexander, J. M. and Whitlock, B. C.,
Extrusion of a Bi-metallic Strip from Separate Containers.
Proc. Inst. Mech. Engrs., 180, (31) (1965/66).
15. Arkulis, G. E.,
Compound Plastic Deformation of Layers of Different Metals,
Israel Program for Scientific Translations, Jerusalem (1965).
(Translated from 'Sovmestnaya plasticheskaya deformatsiya
raznykh metallov', Isdatel'stvo Metallurgiya, Moskva,
(1964).)
16. Arnold, R. R., and Whitton, P. W.,
Proc. I. Mech. E., 173, (8), p. 241 (1959).
17. Pomp, A. and Leug, W.,
Kaiser Wilhelm Inst. Iron Res., 24, p. 123 (1942).
18. Weinstein, A. S., and Pawelski, O.,
Plane Strain Drawing of Sandwiched Metals,
Advances in Machine Tool Design and Research, 8th Int.
M.T.D.R. Conference, pp. 961-980 (1967).
19. Atkins, A. G., and Weinstein, A. S.,
The Deformation of Sandwich Metals,
Inst. J. Mech. Sci., Pergamon Press, 12, pp. 641-657 (1970).
20. Hawkins, R., and Wright, J. C.,
The Deformation Properties of Clad Sheet Metals,
(Copper/Mild Steel Sandwich Sheet),
External Report, Dept. of Metallurgy, Univ. of Aston,
Birmingham (1970).
21. Hawkins, R. and Wright, J. C.,
Mechanical Properties and Pressformability of Copper/Mild
Steel Sandwich Sheet Materials.
Journal of the Inst. of Metals, 99, pp. 357-371 (1971).
22. Brovman, M. Ya., and Yudin, Yu. S.,
Certain Problems of Pressworking Bimetal,
Kuznechno-Shtampovochnoye Proizvodstvo, 1, pp. 3-5 (1963).
23. Arcisz, M.,
Cutting of a Bimetallic Strip by Smooth Rigid Punches,
J. Mech. Phys. Solids, Pergamon Press, London, 17, pp. 437-
458 (1969).
24. Duckett, R., Barry, B. T. K. and Robins, D. A.,
Sheet Met. Ind., 45, p. 666 (1968).

25. Nelson, P. G.,
Met. Prog., 78, p. 93 (1960).
26. Rathbone, A. M.,
Iron Age, 200, p. 70 (Nov. 16th) (1967).
27. Hill, R.,
A Theory of the Plastic Bulging of a Metal Diaphragm
by Lateral Pressure,
Phil. Mag., (Ser. 7), 41, p. 1133 (1950).
28. Mellor, P. B.,
Stress Forming under Fluid Pressure, J. Mech. Phys.
Solids, 5, p. 41 (1956).
29. Albertin, P. M.,
Development of the Biaxial Stress Test for Sheet Material,
Masters Thesis, McMaster University (1972).
30. Johnson, W., Duncan, J. L., Kormi, K. Sowerby, R. and
Travis, F. W.,
A Rapid Method of Determining Stress-Strain Curves for
Sheet Metal Using the Bulge Test,
Proc. 4th Int. M.T.D.R. Conference, pp. 275-288 (1963).
31. Van Minh, M., Duncan, J. L., and Sowerby, R.,
Statistical Investigation of Limit Strains in Biaxial
Stretching of Sheet Steel: Interim Report,
McMaster University, ME/72/PROD/REP/2, (1972).
32. Yousif, M. I., Duncan, J. L. and Johnson, W., Plastic
Deformation and Failure of Thin Elliptical Diaphragms,
Int. J. Mech. Sci., 12, p. 959-972 (1970).
33. Crafoord, R.,
Plastic Sheet Bending,
Ph.D. Thesis, Chalmers Tekniska Högskola, Göteborg,
(1970).
34. Horrocks, D., and Johnson, W.,
On Anticlastic Curvature with Special Reference to Plastic
Bending: A Literature Survey and Some Experimental
Investigations,
Int. J. Mech. Sci., Pergamon Press, 9, pp. 835-861 (1967).
35. Crafoord, R.,
Kraft-^agförloppet vid Fribockning av Plåt,
Lic.diss. Mek. Tekn. Chalmers University of Technology,
Göteborg (1965).

36. Onat, E. and Shield, R.,
The Influence of Shearing Forces on the Plastic Bending
of Wide Beams,
Second U.S. National Congress of Applied Mechanics,
University of Michigan, Ann Arbor (1954).
37. Drucker, D.,
The Effect of Shear on the Plastic Bending of Beams,
J. Appl. Mech., 23, pp. 509-514 (1956).
38. Hodge, P.,
Interaction Curves for Shear and Bending of Plastic Beams,
J. Appl. Mech., 24, pp. 453-456 (1957).
39. Shaffer, B. W., and House, R. N. Jr., Displacements in a
Wide Curved Bar Subjected to Pure Elastic-Plastic Bending.
J. Appl. Mech., Trans. ASME, 79, pp. 447-452 (1957).
40. Shaffer, B. W., and House, R. N. Jr.,
The Elastic-Plastic Stress Distribution within a Wide
Curved Bar Subjected to Pure Bending,
J. Appl. Mech., Trans. ASME, 77, pp. 305-310 (1955).
41. Mahrenholtz, O., and Johnson, W.,
On Bimetal Thermostats,
Int. J. Mech. Sci., Pergamon Press, 4, pp. 35-52 (1962).
42. Ashton, J. E., Halpin, J. C. and Petit, P. H.,
Primer on Composite Materials: Analysis,
Progress in Materials Science Series, Volume III,
Technomic Publishing Co. Inc., Stanford, Conn., (1969).
43. Ashton, J. E. and Whitney, J. M.,
Theory of Laminated Plates,
Progress in Materials Science Series, Volume IV,
Technomic Publishing Co., Inc., Stanford, Conn (1970).
44. Calcote, L. R.,
The Analysis of Laminated Composite Structures,
Van Nostrand Reinhold Co., New York, (1969).
45. ASTM-STP 460,
Composite Materials: Testing and Design,
A Symposium of the ASTM at New Orleans, La., 11-13 Feb.,
1969.
ASTM Special Technical Publication 460,
Philadelphia, Pa. (1969).
46. Proksa, F.,
Zur Theorie des Plastisches Blechbiegens
Diss. TH Hannover(1958).

47. Hill, R.,
The Mathematical Theory of Plasticity,
Clarendon Press, Oxford, (1950).
48. Bellow, D. G., and Semeniuk, A.,
The Inherent Bending Instability of Rectangular Plates
with Cambered Transverse Cross-Sections,
Int. J. Mech. Sci., Pergamon Press, 10, pp. 201-209,
(1968).
49. Froberg, C. E.,
Introduction to Numerical Analysis,
Addison-Wesley Publ. Co., Reading, Massachusetts,
p. 22 (1969).
50. Bauschinger, J.,
Ziviling, 27, pp. 453-456 (1881).
51. Bauschinger, J.,
Mitt. Mech. Lab.,
T.H. München, (1886).

APPENDIX I

A SET OF RELATIONS BETWEEN DIMENSIONLESS PARAMETERS
AND THE GEOMETRY OF THE BENDDefinitions and Trivial Formulas

$$t = r_y - r_i \quad (I.1)$$

$$r_m = (r_y + r_i)/2 \quad (3.2.7)$$

$$\kappa = t/r_m \quad (3.2.13)$$

$$\eta = t/t_o \quad (3.2.14)$$

$$\rho = r_n/r_o \quad (3.2.16)$$

$$\lambda = (r^2 - r_i^2)/(r_y^2 - r_i^2) \quad (3.2.11)$$

$$\varepsilon_\phi = \ln r/r_o = \ln r/r_m - \ln \eta \quad (3.2.6)$$

$$(3.2.15)$$

Geometry of Bend in Function of κ , η , ρ

$$r_m = \frac{\eta t_o}{\kappa} \quad (I.2)$$

$$r_i = r_m \left(1 - \frac{\kappa}{2}\right) \quad (I.3)$$

$$r_y = r_m \left(1 + \frac{\kappa}{2}\right) \quad (I.4)$$

$$r_o = r_m \eta \quad (I.5)$$

$$r_n = r_m \eta \rho \quad (I.6)$$

$$t = \eta t_o \quad (I.7)$$

A layer with the volume function λ , has as current radius

$$r = \sqrt{r_i^2 + \lambda (r_y^2 - r_i^2)} \quad (3.2.12A)$$

$$\text{or} \quad r = r_m \sqrt{\left(1 - \frac{\kappa}{2}\right) + 2\lambda\kappa} \quad (I.8)$$

The tangential strain for that layer is

$$\epsilon_\phi = \frac{1}{2} \ln\left[\left(1 - \frac{\kappa}{2}\right)^2 + 2\lambda\kappa\right] - \ln \eta \quad (I.9)$$

These relations show that the dimensionless parameters κ , η , ρ are sufficient to describe the geometry and the strains in the current bend.

The current values of κ , η and ρ , together with yield conditions and equilibrium equation, contain sufficient information to describe fully the current bend.

Geometry of Bend in Function of κ , η , λ_n

Out of the definition for the volume fraction λ_n for the neutral layers, given in Section 3.2.6 and equation (3.2.11) follows that

$$\lambda_n = (r_n^2 - r_i^2) / (r_y^2 - r_i^2) \quad (I.10)$$

Using (I.2) to (I.6), this becomes

$$\lambda_n = \frac{\eta^2 \rho^2 - \left(1 - \frac{\kappa}{2}\right)^2}{2\kappa} \quad (I.11)$$

The same can be done for the unelongated layer. The volume fraction λ_o of the layer that is currently unelongated, is

$$\lambda_o = (r_o^2 - r_i^2)/(r_y^2 - r_i^2) \quad (I.12)$$

and hence

$$\lambda_o = \frac{\eta^2 - (1 - \frac{\kappa}{2})^2}{2\kappa} \quad (I.13)$$

(I.11) yields

$$\eta^2 \rho^2 = (1 - \frac{\kappa}{2})^2 + 2\lambda_n \kappa \quad (I.14)$$

Therefore,

$$r_n = r_m \sqrt{(1 - \frac{\kappa}{2})^2 + 2\lambda_n \kappa} \quad (I.6.BIS)$$

It is easily seen that, by replacing formula (I.6) by (I.6.BIS), the current bend can as well be fully described by κ, η, λ_n as by κ, η, ρ .

APPENDIX II

DERIVATION OF CHANGE IN SHEET-THICKNESS FORMULAS

It was explained in Section 3.2.7 that

$$d \rho = 0 \quad (3.2.17)$$

$$d \lambda_n = 0 \quad (3.2.18)$$

for an infinitesimally small increase in bending.

Using the differential of (I.14) yeilds

$$2\eta \rho^2 d\eta + 2\rho \eta^2 d\rho = -(1 - \frac{\kappa}{2}) d\kappa + 2\kappa d\lambda_n + 2\lambda_n d\kappa$$

Substituting λ_n with (I.11) and using (3.2.17) yields

$$2\eta^2 \rho^2 \frac{d\eta}{\eta} = \frac{d\kappa}{\kappa} [-\kappa(1 - \frac{\kappa}{2}) + \eta^2 \rho^2 -(1 - \frac{\kappa}{2})^2]$$

and hence

$$\frac{d\eta}{d\kappa} = -\frac{1}{2} \frac{\eta}{\kappa} \left[\frac{1 - \frac{\kappa^2}{4}}{\eta^2 \rho^2} - 1 \right] \quad (3.2.19)$$

which is the sheet thickness relation in functions of κ , η , ρ .

Using (I.14), $d\eta/d\kappa$ can be expressed in function of κ , η , λ_n .

$$\frac{d\eta}{d\kappa} = -\frac{1}{2} \frac{\eta}{\kappa} \left[\frac{1 - 2\lambda_n - \kappa/2}{2\kappa\lambda_n + (1 - \frac{\kappa}{2})^2} \right] \quad (3.2.20)$$

The use of (I.3), (I.4) and (I.6) transforms (3.2.19) into

$$\frac{d\eta}{d\kappa} = -\frac{1}{2} \frac{\eta}{\kappa} \left[\frac{r_i r_y}{r_n} - 1 \right] \quad (3.2.21)$$

It is also possible to express the sheet thickness relation in terms of the current sheet thickness t , the radii r_i , r_y , r_n , and the bend angle ϕ between two radial cross sections.

Differentiation of (3.2.14) and (3.2.13) results in

$$\frac{d\eta}{\eta} = \frac{dt}{t} \quad (II.1)$$

and

$$\frac{d\kappa}{\kappa} = \frac{dt}{t} - \frac{dr_m}{r_m} \quad (II.2)$$

When ℓ_n is the length of the neutral layer between radial cross sections including an angle ϕ , and ℓ_o the distance between these cross sections is the inlet condition, then

$$\varepsilon_\phi = \ell_n \ell_n / \ell_o$$

Since $(d\varepsilon_\phi)_{r=r_n} = \frac{d\rho}{\rho} = 0$ (3.2.17)

$$\frac{\ell_o}{\ell_n} d(\ell_n) = 0 \quad (II.3)$$

Using (I.6) and

$$l_n = r_n \phi$$

yields for (II.3)

$$d(\eta \rho r_m \phi) = 0$$

or

$$\frac{d\eta}{\eta} + \frac{d\rho}{\rho} + \frac{dr_m}{r_m} + \frac{d\phi}{\phi} = 0$$

Since (3.2.17) also implies that

$$d\rho = 0$$

and using (II.1), this results in

$$\frac{dt}{t} + \frac{dr_m}{r_m} + \frac{d\phi}{\phi} = 0 \quad (\text{II.4})$$

Substituting (II.1), (II.2) and (II.4) in (3.2.21) results finally in

$$\frac{dt}{t} = -\frac{1}{2} \frac{d\phi}{\phi} \left[1 - \frac{r_n^2}{r_i r_y} \right] \quad (3.2.22)$$

APPENDIX III

BENDING OF A RIGID-PLASTIC, NON STRAIN HARDENING MONOMETAL SHEET

The results of this derivation can be found in Hill [46]. The yield condition for such a material is

$$\bar{\sigma} = H(\int d\bar{\epsilon}) = Y = \text{constant}$$

where σ is the yield stress in uniaxial tension. Combination of yield condition for plane strain and equilibrium (formulas (3.2.1A) and (3.2.1B)) results for this material in

$$r \frac{d\sigma_r}{dr} = \frac{2}{\sqrt{3}} Y \quad \text{for } r_n \leq r \leq r_y \quad (\text{III.1})$$

$$r \frac{d\sigma_r}{dr} = -\frac{2}{\sqrt{3}} Y \quad \text{for } r_i \leq r_n \leq r_n \quad (\text{III.2})$$

Integration of (III.1) to r , with boundary condition

$$(\sigma_r)_{r=r_y} = 0$$

gives

$$\sigma_r = \frac{2}{\sqrt{3}} Y \ln \frac{r}{r_y} \quad \text{for } r_n \leq r \leq r_y$$

Integration of (III.2) to r , with boundary condition

$$(\sigma_r)_{r=r_i} = 0$$

gives

$$\sigma_r = -\frac{2}{\sqrt{3}} Y \ell_n \frac{r}{r_i} \quad \text{for } r_i \leq r \leq r_n$$

The radius of the neutral layer r_n is as yet unknown. The continuity of σ_r at $r = r_n$ requires however that

$$(\sigma_r)_{r=r_n} = \frac{2}{\sqrt{3}} Y \ell_n \frac{r_n}{r_y} = -\frac{2}{\sqrt{3}} Y \ell_n \frac{r_n}{r_i}$$

Hence,

$$r_n^2 = r_i r_y$$

Substituting this value for r_n in the sheet thickness relation (3.2.21) gives

$$\frac{d\eta}{d\kappa} = 0$$

Since $\eta = 1$ for $\kappa = 0$, $\eta = 1$ for all values of κ . Therefore, $t = t_0$ and the thickness is constant during the bending process. The dimensionless neutral layer position ρ can be found by substituting $\frac{d\eta}{d\kappa} = 0$ and $\eta = 1$ in sheet thickness relation (3.2.19), which yields

$$\rho^2 = 1 - \frac{\kappa^2}{4}$$

(III.3)

Using (3.2.23A) and (3.2.23B) yields for the hoop stresses

$$\sigma_{\phi} = \frac{2}{\sqrt{3}} Y \left(1 + \ell_n \frac{r}{r_y} \right) \quad \text{for } r_n \leq r \leq r_y$$

$$\sigma_{\phi} = - \frac{2}{\sqrt{3}} Y \left(1 + \ell_n \frac{r}{r_i} \right) \quad \text{for } r_i \leq r \leq r_n$$

Hence, the bending moment becomes

$$M = \int_{r_i}^{r_y} \sigma_{\phi} r dr = \frac{2}{\sqrt{3}} Y \frac{t^2}{4}$$

The bending moment is therefore constant during bending. If Tresca's yield condition instead of Von Mises's had been used, with k the maximum shear stress of the material, the bending moment would have been

$$M = 2k \frac{t^2}{4}$$

Using (I.5) shows that the unelongated layer is the same as the central layer

$$r_o = r_m$$

The tangential strain when a layer is the neutral layer ϵ_{ϕ_n} , is

$$\epsilon_{\phi_n} = \ell_n \frac{r_n}{r_o} = \ell_n \rho = \frac{1}{2} \ell_n \left(1 - \frac{k^2}{4} \right)$$

The volume fraction λ for the neutral layer is (use (I.11) and (III.3))

$$\lambda_n = \frac{1}{2} \left(1 - \frac{\kappa}{2}\right)$$

Hence, λ_n is a linear function of κ , with $\lambda_n = 1/2$ for $\kappa = 0$ and $\lambda_n = 0$ for $\kappa = 2$. The volume fraction λ for the unelongated layer is (use (I.13))

$$\lambda_o = \frac{1}{2} \left(1 - \frac{\kappa}{4}\right)$$

λ_o is also linear in κ , with $\lambda_o = 1/2$ for $\kappa = 0$ and $\lambda_o = 1/4$ for $\kappa = 2$.

APPENDIX IV

BENDING OF A RIGID-PLASTIC, NON STRAIN HARDENING BIMETAL SHEET

IV.1 Description of the Two Laminates

Laminate 1 will be on the inside of the bent sheet, and laminate 2 will be at the outside. A_1 and A_2 are the respective yield strengths in uniaxial tension for the laminates. Since both materials are non-strainhardening, the effective yield stress is

$$\bar{\sigma}_1 = A_1$$

$$\bar{\sigma}_2 = A_2$$

When we define

$$\alpha_1 = \frac{2}{\sqrt{3}} A_1$$

$$\alpha_2 = \frac{2}{\sqrt{3}} A_2$$

the yield criterion (3.2.3A) becomes, with r_b the radius of the laminate boundary,

$$\left. \begin{array}{l} \sigma_\phi^1 - \sigma_r^1 = \alpha_1 \text{ for } r \leq r_b \\ \sigma_\phi^2 - \sigma_r^2 = \alpha_2 \text{ for } r \geq r_b \end{array} \right\} \text{ and } r_n \leq r \leq r_y \quad (\text{IV.1.1A})$$

$$\left. \begin{array}{l} \sigma_\phi^1 - \sigma_r^1 = \alpha_1 \text{ for } r \leq r_b \\ \sigma_\phi^2 - \sigma_r^2 = \alpha_2 \text{ for } r \geq r_b \end{array} \right\} \text{ or } \lambda_n \leq \lambda \leq 1 \quad (\text{IV.1.2A})$$

and (3.2.3B) becomes

$$\left. \sigma_{\phi}^1 - \sigma_r^1 = -\alpha_1 \text{ for } r \leq r_b \right\} \text{ and } r_i \leq r \leq r_n \quad (\text{IV.1.1B})$$

$$\left. \sigma_{\phi}^2 - \sigma_r^2 = -\alpha_2 \text{ for } r \geq r_b \right\} \text{ or } 0 \leq \lambda \leq \lambda_n \quad (\text{IV.1.2B})$$

The equilibrium condition (3.2.1A) becomes

$$\left. r \frac{d\sigma_r^1}{dr} = \alpha_1 \text{ for } r \leq r_b \right\} \text{ and } r_n \leq r \leq r_y \quad (\text{IV.1.3A})$$

$$\left. r \frac{d\sigma_r^2}{dr} = \alpha_2 \text{ for } r \geq r_b \right\} \quad (\text{IV.1.4A})$$

while (3.2.1B) becomes

$$\left. r \frac{d\sigma_r^1}{dr} = -\alpha_1 \text{ for } r \leq r_b \right\} \text{ and } r_i \leq r \leq r_n \quad (\text{IV.1.3B})$$

$$\left. r \frac{d\sigma_r^2}{dr} = -\alpha_2 \text{ for } r \geq r_b \right\} \quad (\text{IV.1.4B})$$

Laminate 1 has an original thickness t_{10} , and laminate 2, t_{20} .

The original sheet thickness is therefore

$$t_0 = t_{10} + t_{20}$$

When we define

$$\nu = \frac{t_{10}}{t_{10} + t_{20}} = \frac{t_{10}}{t_0}$$

then μ indicates the volume fraction of material contained by the boundary surface between the two laminates and the inside surface of the bent sheet. These μ -value remains constant during the bending (see Section 3.2.5). Therefore, when we know the inside and the outside radius of the bend, we know also the radius of the laminate boundary r_b , since

$$r_b = \sqrt{r_i^2 + \mu(r_y^2 - r_i^2)} \quad (3.2.12B)$$

IV.2 Initial Conditions

The initial conditions for the integration of the sheet thickness equation are known, namely

$$\kappa = 0$$

$$\eta = 1$$

$$\rho = 1$$

Furthermore, the position of the neutral layer, given by λ_n , can be calculated at the start of the bending process. When the originally flat sheet is bent an infinitesimally small amount, the radial stress can be assumed to be zero. The tangential stress is then, according to (IV.1.1A) to (IV.1.2B),

$$\left. \begin{array}{l} \sigma_{\phi}^1 = \alpha_1 \quad \text{for } \lambda < \mu \\ \sigma_{\phi}^2 = \alpha_2 \quad \text{for } \lambda > \mu \end{array} \right\} \text{and } \lambda \geq \lambda_n$$

$$\left. \begin{array}{l} \sigma_{\phi}^1 = -\alpha_1 \quad \text{for } \lambda < \mu \\ \sigma_{\phi}^2 = -\alpha_2 \quad \text{for } \lambda > \mu \end{array} \right\} \text{and } \lambda \leq \lambda_n$$

The position of the neutral layer can be found by requiring that the resultant normal stress on a radial cross section be zero. Figure IV.1 shows that, if

$$\alpha_1 \mu = \alpha_2 (1 - \mu)$$

then

$$\lambda_n = \mu$$

When

$$\alpha_1 \mu > \alpha_2 (1 - \mu)$$

the neutral layer is in laminate 1, and Figure IV.2 shows that

$$\lambda_n = \frac{\alpha_2}{2\alpha_1} (1 - \mu) + \frac{\mu}{2}$$

Whereas, when

$$\alpha_1 \mu < \alpha_2 (1 - \mu)$$

the neutral layer is in laminate 2, and it can be calculated with Figure IV.3 that

$$\lambda_n = \frac{1}{2} + \frac{\mu}{2} - \frac{\alpha_1}{2\alpha_2} \mu$$

The values of λ_n for different combinations of μ and α_1/α_2 are plotted in Figure IV.4. It is interesting to note that an arbitrary bimetal sheet, for example point A in Fig. IV.4, with $\alpha_1/\alpha_2 = 2$ and $\mu = .2$, is point symmetrical to the centre point $\alpha_1/\alpha_2=1$ and $\mu = .5$ of the graph, with the same laminate bended to the other side, which is point B with $\alpha_1/\alpha_2 = 1/2$ and $\mu = .8$. Point A lies in the zone for which $\lambda_n^0 > \mu$, hence, for point B, $\lambda_n^0 < \mu$.

It is also very useful to know the original bending moment.

For the infinitesimally small bend,

$$M = \int_{r_i}^{r_y} \sigma_\phi r dr = t_0^2 \int_0^1 \sigma_\phi \lambda d\lambda$$

Hence, when $\lambda_n < \mu$, see Figure IV.2,

$$\frac{M}{t_0^2} = \int_0^{\lambda_n} -\alpha_1 \lambda d\lambda + \int_{\lambda_n}^{\mu} \alpha_1 \lambda d\lambda + \int_{\mu}^1 \alpha_2 \lambda d\lambda$$

$$\frac{M}{t_0^2} = -\lambda_n^2 \alpha_1 + \frac{\mu^2}{2} (\alpha_1 - \alpha_2) + \frac{\alpha_2}{2}$$

Analogously, when $\lambda_n > \mu$, it can be found with the help of Figure IV.3, that

$$\frac{M}{t_0^2} = -\lambda_n^2 \alpha_1 + \frac{\mu^2}{2} (\alpha_2 - \alpha_1) + \frac{\alpha_2}{2}$$

Since the original position of the neutral layer, λ_n , is known, the bending moment M is determined by the above formulas.

IV.3 Solution Method

The method of approach is explained in Section 3.2.8. The variables κ , η and ρ will be used to describe the bending behaviour. Hence, the sheet thickness equation

$$\frac{d\eta}{d\kappa} = -\frac{1}{2} \frac{\eta}{\kappa} \left(\frac{1 - \frac{\kappa^2}{4}}{\eta^2 \rho} - 1 \right) \quad (3.2.19)$$

will be integrated to κ . The initial conditions are given in the previous section. The second dependent variable ρ will be determined by integrating (IV.1.3A) to (IV.1.4B) along the sheet thickness. Since the neutral layer can occur either in laminate 1 or laminate 2, two cases have to be considered.

IV.3.1 The Neutral Layer Occurs in Laminate 1 ($r_n \leq r_b$)

The combined equilibrium and yield conditions that apply are these

$$r \frac{d\sigma_r^1}{dr} = -\alpha_1 \text{ for } r_i \leq r \leq r_n \quad (IV.1.3B)$$

$$r \frac{d\sigma_r^1}{dr} = \alpha_1 \text{ for } r_n \leq r \leq r_b \quad (IV.1.3A)$$

$$r \frac{d\sigma_r^2}{dr} = \alpha_2 \text{ for } r_b \leq r \leq r_y \quad (IV.1.4A)$$

Integration of (IV.1.3B), with boundary condition

$$(\sigma_r^1)_{r=r_i} = 0$$

yields

$$\sigma_r^1 = -\alpha_1 \ell_n \frac{r}{r_i} \quad r_i \leq r \leq r_n \quad (\text{IV.3.1})$$

The radial stress at the neutral layer is therefore

$$(\sigma_r^1)_{r=r_n} = -\alpha_1 \ell_n \frac{r_n}{r_i} \quad (\text{IV.3.2})$$

Integration of (IV.1.4A), with boundary condition

$$(\sigma_r^2)_{r=r_y} = 0$$

yields

$$\sigma_r^2 = \alpha_2 \ell_n \frac{r}{r_y} \quad r_b \leq r \leq r_y \quad (\text{IV.3.3})$$

The radial stress at the laminate boundary is

$$(\sigma_r^2)_{r=r_b} = \alpha_2 \ell_n \frac{r_b}{r_y}$$

Integration of (IV.1.3A), with boundary condition

$$(\sigma_r^1)_{r=r_b} = (\sigma_r^2)_{r=r_b}$$

gives

$$\sigma_r^1 = \alpha_1 \ell_n \frac{r}{r_b} + \alpha_2 \ell_n \frac{r_b}{r_y} \quad r_n \leq r \leq r_b \quad (\text{IV.3.4})$$

The radial stress at the neutral layer is then also

$$\left(\sigma_r^1\right)_{r=r_n} = \alpha_1 \ell_n \frac{r_n}{r_b} + \alpha_2 \ell_n \frac{r_b}{r_y} \quad (\text{IV.3.5})$$

Since the radial stress must be continuous, (IV.3.2) and (IV.3.5) must be identical. Hence,

$$\alpha_1 \ell_n \frac{r_n}{r_b} + \alpha_2 \ell_n \frac{r_b}{r_y} = -\alpha_1 \ell_n \frac{r_n}{r_i}$$

This relation defines the neutral layer radius, and can be expressed as a function of κ, η, ρ with the use of (I.3), (I.4), (I.6) and (3.2.12B).

$$\begin{aligned} 2\alpha_1 \ell_n (\eta \rho) - \alpha_2 \ell_n \left(1 + \frac{\kappa}{2}\right) - \alpha_1 \ell_n \left(1 - \frac{\kappa}{2}\right) \\ + (\alpha_2 - \alpha_1) \frac{1}{2} \ell_n \left[\left(1 - \frac{\kappa}{2}\right)^2 + 2\mu\kappa\right] = 0 \end{aligned} \quad (\text{IV.3.6})$$

Equation (IV.3.6) defines ρ in function of κ and η . It is this value for ρ which must be substituted in the sheet thickness relation (3.2.19) to solve η to κ . (IV.3.6) can also be written

$$\begin{aligned} X1 = \ell_n (\rho^2 \eta^2) = \ell_n \left(1 - \frac{\kappa}{2}\right) + \frac{\alpha_2}{\alpha_1} \ell_n \left(1 + \frac{\kappa}{2}\right) \\ + \frac{1}{2} \left(1 - \frac{\alpha_2}{\alpha_1}\right) \ell_n \left[\left(1 - \frac{\kappa}{2}\right)^2 + 2\mu\kappa\right] \end{aligned}$$

so that

$$\eta^2 \rho^2 = \exp(X1) \quad (\text{IV.3.7})$$

Substitution in (3.2.19) leads to

$$\frac{d\eta}{d\kappa} = -\frac{1}{2} \frac{\eta}{\kappa} \left(\frac{1 - \frac{\kappa^2}{4}}{\exp(X1)} - 1 \right) \quad (\text{IV.3.8})$$

where X1 is a function of κ only.

Equation (IV.3.8) can be successfully integrated to κ , with starting point $\kappa = 0$, $\eta = 1$. The position of the neutral layer, defined by ρ can always be found with equation (IV.3.7). The values of r_i , r_y , r_n , r_o , r_b can be expressed in function of κ , η , ρ using the formulas provided in Appendix I. The radial stress across the sheet thickness are given by (IV.3.1), (IV.3.3) and (IV.3.4). The tangential stresses are

$$\left. \begin{aligned} \sigma_{\phi}^1 &= -\alpha_1 \left(1 + \ell_n \frac{r}{r_i} \right) & r_i \leq r < r_n \\ \sigma_{\phi}^1 &= \alpha_1 \left(1 + \ell_n \frac{r}{r_b} \right) + \alpha_2 \ell_n \frac{r_b}{r_y} & r_n < r < r_b \\ \sigma_{\phi}^2 &= \alpha_2 \left(1 + \ell_n \frac{r}{r_y} \right) & r_b < r \leq r_y \end{aligned} \right\} \quad (\text{IV.3.9})$$

Using

$$M = \int_{r_i}^{r_y} \sigma_{\phi} r dr$$

yields

$$\begin{aligned}
M = & \alpha_1 \left(\frac{r_i^2}{4} + \frac{r_b^2}{4} \right) + \alpha_2 \left(\frac{r_y^2}{4} - \frac{r_b^2}{4} \right) \\
& - \alpha_1 \frac{r_n^2}{2} \left(1 + \ell_n \frac{r_n}{r_b} + \ell_n \frac{r_n}{r_i} \right) \\
& - \alpha_2 \frac{r_n^2}{2} \ell_n \frac{r_b}{r_y}
\end{aligned} \tag{IV.3.10}$$

IV.3.2 The Neutral Layer Occurs in Laminate 2 ($r_n \geq r_b$)

The combined equilibrium and yield conditions that apply in this case are

$$r \frac{d\sigma_r^1}{dr} = -\alpha_1 \quad r_i \leq r \leq r_b \tag{IV.1.3B}$$

$$r \frac{d\sigma_r^2}{dr} = -\alpha_1 \quad r_b \leq r \leq r_n \tag{IV.1.4B}$$

$$r \frac{d\sigma_r^2}{dr} = \alpha_2 \quad r_n \leq r \leq r_y \tag{IV.1.4A}$$

Integration of (IV.1.3B) with boundary condition

$$\left(\sigma_r^1 \right)_{r=r_i} = 0$$

yields

$$\sigma_r^1 = -\alpha_1 \ell_n \frac{r}{r_i} \quad r_i \leq r \leq r_b \tag{IV.3.11}$$

The radial stress at the laminate boundary is

$$\left(\sigma_r^1\right)_{r=r_b} = -\alpha_1 \ell_n \frac{r_b}{r_i}$$

Integration of (IV.1.4B) with boundary condition

$$\left(\sigma_r^2\right)_{r=r_b} = \left(\sigma_r^1\right)_{r=r_b}$$

gives

$$\sigma_r^2 = -\alpha_2 \ell_n \frac{r}{r_b} - \alpha_1 \ell_n \frac{r_b}{r_i} \quad r_b \leq r \leq r_n \quad (\text{IV.3.12})$$

The radial stress at the neutral radius is therefore

$$\left(\sigma_r^2\right)_{r=r_n} = -\alpha_2 \ell_n \frac{r_n}{r_b} - \alpha_1 \ell_n \frac{r_b}{r_i} \quad (\text{IV.3.13})$$

Integration of (IV.1.4A) with boundary condition

$$\left(\sigma_r^2\right)_{r=r_y} = 0$$

gives

$$\sigma_r^2 = \alpha_2 \ell_n \frac{r}{r_y} \quad r_n \leq r \leq r_y \quad (\text{IV.3.14})$$

Hence, the radial stress at the neutral layer is also

$$\left(\sigma_r^2\right)_{r=r_n} = \alpha_2 \ell_n \frac{r_n}{r_y} \quad (\text{IV.3.15})$$

Since (IV.3.13) and (IV.3.14) are identical,

$$\alpha_2 \ell_n \frac{r_n}{r_y} = -\alpha_2 \ell_n \frac{r_n}{r_b} - \alpha_1 \ell_n \frac{r_b}{r_i}$$

Substituting r_n , r_i , r_y and r_b in function of κ and η yields

$$2 \alpha_2 \ell_n (\eta \rho) - \alpha_2 \ell_n (1 + \frac{\kappa}{2}) - \alpha_1 \ell_n (1 - \frac{\kappa}{2})$$

$$+ \frac{1}{2} (\alpha_1 - \alpha_2) \ell_n [(1 - \frac{\kappa}{2})^2 + 2 \mu \kappa] = 0$$

or

$$X2 = \ell_n (\eta^2 \rho^2) = \ell_n (1 + \frac{\kappa}{2}) + \frac{\alpha_1}{\alpha_2} \ell_n (1 - \frac{\kappa}{2})$$

$$+ \frac{1}{2} (1 - \frac{\alpha_1}{\alpha_2}) \ell_n [(1 - \frac{\kappa}{2})^2 + 2 \mu \kappa]$$

Hence,

$$\eta^2 \rho^2 = \exp(X2) \quad (\text{IV.3.16})$$

The sheet thickness equation becomes then

$$\frac{d\eta}{d\kappa} = -\frac{1}{2} \frac{\eta}{\kappa} \left(\frac{1 - \frac{\kappa}{4}}{\exp(X2)} - 1 \right) \quad (\text{IV.3.17})$$

This can be solved by numerical integration. The radial stresses are given by (IV.3.11), (IV.3.12) and (IV.3.14). The tangential stresses are

$$\left. \begin{aligned}
 \sigma_{\phi}^1 &= -\alpha_1 \left(1 + \ell_n \frac{r}{r_i} \right) & r_i &< r < r_b \\
 \sigma_{\phi}^2 &= -\alpha_2 \left(1 + \ell_n \frac{r}{r_b} \right) - \alpha_1 \ell_n \frac{r_b}{r_i} & r_b &< r < r_n \\
 \sigma_{\phi}^2 &= \alpha_2 \left(1 + \ell_n \frac{r}{r_y} \right) & r_n &< r \leq r_y
 \end{aligned} \right\} \quad (\text{IV.3.18})$$

and the bending moment is

$$\begin{aligned}
 M &= \alpha_1 \left(\frac{r_b^2}{4} - \frac{r_i^2}{4} \right) + \alpha_2 \left(\frac{r_y^2}{4} - \frac{r_b^2}{4} \right) \\
 &\quad - \alpha_2 \frac{r_n^2}{2} \left(1 + \ell_n \frac{r_n}{r_y} + \ell_n \frac{r_n}{r_b} \right) \\
 &\quad - \alpha_1 \frac{r_n^2}{2} \ell_n \frac{r_b}{r_i}
 \end{aligned} \quad (\text{IV.3.19})$$

IV.4 Integration of Sheet Thickness Equation

It was indicated in Section IV.3 how the second dependent variable ρ in the sheet thickness equation (3.2.19) can be expressed in function of κ and η . According to where the original neutral layer is situated, equation (3.2.19) is reduced to equation (IV.3.8) or (IV.3.17). When the original neutral layer is situated in laminate 1 ($\lambda_n^0 < \mu$), we integrate (IV.3.8) for increasing values of κ . When the original neutral layer is situated in laminate 2 ($\lambda_n^0 > \mu$), the procedure to follow is a little more complicated. During the bending of nonstrain hardening bimetal, the neutral layer moves to the inside of the bent sheet for increasing κ -values, and can therefore cross the material boundary, when

it was originally situated in laminate 2. This crossing occurs when $\lambda_n = \nu$, which, according to (I.11), means that

$$\eta^2 \rho^2 = \left(1 - \frac{\kappa}{2}\right)^2 + 2 \nu \kappa$$

It can be verified that the respective equations of Sections IV.3.1 and IV.3.2 become identical for this value of $\eta \rho$ and $r_n = r_b$. The procedure to follow for integrating the sheet thickness equation when the original neutral layer is situated in laminate 2, is the following one. Integrate (IV.3.17), with initial conditions $\kappa = 0$ and $\eta = 1$, for increasing κ until $\lambda_n = \nu$, and integrate then further equation (IV.3.8) with as initial conditions the values for κ and η for which $\lambda_n = \nu$.

The integration of the sheet thickness equation is done numerically, and can be performed by a wide variety of numerical integration techniques. The Runge-Kutta method has been chosen because this method is easy to program (it is a single step method and does not involve any derivatives). The equation to integrate is

$$\frac{d\eta}{d\kappa} = f(\kappa, \eta)$$

The starting point is $\eta_0 = 1$, $\kappa_0 = 0$. Compute

$$k_1 = h f(\kappa_0, \eta_0)$$

$$k_2 = h f\left(\kappa_0 + \frac{1}{2}h, \eta_0 + \frac{1}{2}k_1\right)$$

$$k_3 = h f \left(\kappa_0 + \frac{1}{2}h, \eta_0 + \frac{1}{2} k_2 \right)$$

$$k_4 = h f \left(\kappa_0 + h, \eta_0 + \frac{1}{2} k_3 \right)$$

$$k = \frac{1}{6} (k_1 + 2k_2 + 2k_3 + k_4)$$

Then

$$\eta(\kappa_0 + h) = \eta_0 + k$$

Use now $\kappa_0 + h$ and $\eta_0 + k$ as new starting points for the next integration step. Etc.....

IV.5 Program BINSH

A FORTRAN program has been developed to perform all the necessary calculations to describe the plane strain bending of nonstrain hardening bimetal sheet. The accuracy of the program, with regard to the **step size** for the numerical integration, is covered in Appendix IX.

APPENDIX V

BENDING OF A RIGID-PLASTIC, NONSTRAINHARDENING LAMINATED SHEET

V.1 Introduction

The same approach as the one used for the nonstrainhardening bimetal sheet, as featured in Appendix IV, can be used for multi-laminated sheet. Instead of finding ρ and η as a function of κ as done in Appendix IV, the relation between λ_n , η and κ will here be used. This is partly done for the ease of the movement from one laminate to the next during the integration of the radial stress across the thickness of the sheet, and will also be used in the bending of strainhardening laminated sheet. This 'laminate-jumping' can here be explained and shown in its simplest form, without the complications that occur when the laminates are strainhardening. The fact that the λ_n -value will be determined in a numerical way by integrating the radial stress across the sheet thickness, and replaces the analytical calculations of ρ used in Appendix IV, removes the problem of the change in sheet thickness equation when the neutral layer crosses a laminate boundary, a problem that was encountered in Appendix IV when the original neutral layer did not occur in the inside laminate. The removal of this sheet thickness changeover is the main reason for the numerical determination of λ_n used here, and featured in the next sections.

V.2 Description of the Laminates

The sheet is composed of n laminates. The laminates are numbered from the inside to the outside of the bent sheet. Hence, laminate 1 is the one on the inner surface, and laminate n the one on the outer surface of the bend. The yield strength in uniaxial tension of

laminates i is A_i ,

$$\bar{\sigma}_i = A_i$$

so that

$$\alpha_i = \frac{2}{3} A_i$$

The yield condition for laminate i is, using (3.2.3A) and (3.2.3B),

$$\sigma_\phi^i - \sigma_r^i = \alpha_i \quad r_n < r \quad (V.2.1A)$$

$$\sigma_\phi^i - \sigma_r^i = -\alpha_i \quad r < r_n \quad (V.2.1B)$$

The equilibrium equation (3.2.1A) and (3.2.1B) for laminate i is then

$$r \frac{d\sigma_r^i}{dr} = \alpha_i \quad r_n \leq r \quad (V.2.2A)$$

$$r \frac{d\sigma_r^i}{dr} = -\alpha_i \quad r \leq r_n \quad (V.2.2B)$$

The boundary surface between laminate i and $j = i + 1$ will be identified by the volume fraction of material embraced by that surface and the inside surface of the bend. This volume fraction is a constant, and will be indicated as

$$V_{i2} = V_{j1}$$

The inside surface of the bent sheet is represented by

$$\psi_{i1} = 0$$

and the outside surface by

$$\psi_{n2} = 1$$

ψ_{i1} represents the surface of laminate i to the inside of the bend, and ψ_{i2} represents the one to the outside.

V.3 Initial Conditions

The initial conditions for the integration of the sheet thickness equation are

$$\kappa = 0$$

$$\eta = 1$$

and the exact position of the neutral layer, λ_n , at the commencement of bending. The same assumptions for finding the original λ_n are made as in Section IV.2, namely, that the flat sheet is bent an infinitesimally small amount, so that the radial stresses are negligible. The tangential stress in laminate i is then

$$\sigma_{\phi}^i = \alpha_i \quad \text{if } \lambda > \lambda_n$$

$$\sigma_{\phi}^i = -\alpha_i \quad \text{if } \lambda < \lambda_n$$

The resultant normal stress is first calculated in the hypothesis that the neutral layer should coincide with a material boundary. Define

$$p_1 = \sum_{i=1}^n \alpha_i (v_{i2} - v_{i1})$$

$$p_j = p_1 - 2 \sum_{i=1}^{j-1} \alpha_i (v_{i2} - v_{i1}) \text{ for } j = 2, \dots, n+1$$

where p_1 is the resultant normal force on the sheet should the neutral surface coincide with the inside surface of the sheet, and where p_j ($j = 2, \dots, n+1$) is the normal force when λ_n should coincide with laminate boundary v_{j1} . The true position of λ_n requires that the resultant normal force be zero.

If for a value of k ($k = 2, \dots, n$), $p_k = 0$, then $\lambda_n = v_{k1}$ is the original neutral layer position.

If all $p_k \neq 0$ ($k = 2, \dots, n$), it can be noted that $p_1 > 0$ and $p_{n+1} < 0$, and that p_k ($k = 1, \dots, n+1$) is monotonously increasing for increasing k . Hence, check for which value of k

$$p_k > 0$$

but $(k = 1, \dots, n)$

$$p_{k+1} < 0$$

The neutral layer occurs then in laminate k , and the exact position can be found by linear interpolation.

$$P_k (\nu_{k2} - \lambda_n) = P_{k+1} (\nu_{k1} - \lambda_n)$$

or

$$\lambda_n = \frac{(P_k \nu_{k2} - P_{k+1} \nu_{k1})}{P_k - P_{k+1}}$$

This procedure determines the original position of the neutral layer in the infinitesimally bent sheet.

The original bending moment can now easily be determined since the original tangential stresses and the neutral layer position are known. For the infinitesimally small bend,

$$M = \int_{r_i}^{r_y} \sigma_\phi r dr = t_0^2 \int_0^1 \sigma_\phi \lambda d\lambda$$

The neutral layer occurs in layer k , thus $\nu_{k1} < \lambda_n < \nu_{k2}$, and hence

$$\frac{M}{t_0^2} = \sum_{i=1}^k \int_{\nu_{i1}}^{\min(\nu_{i2}, \lambda_n)} (-\alpha_i) \lambda d\lambda + \sum_{i=k}^n \int_{\max(\nu_{i1}, \lambda_n)}^{\nu_{i2}} \alpha_i \lambda d\lambda$$

Therefore,

$$\frac{M}{t_o^2} = \sum_{i=1}^k \left(\frac{-\alpha_i}{2}\right) [(\min(r_{i2}, \lambda_n))^2 - r_{i1}^2] \\ + \sum_{i=k}^n \frac{\alpha_i}{2} [r_{i2}^2 - (\max(r_{i1}, \lambda_n))^2]$$

$$\min(x, y) = x \quad \text{if } x < y$$

$$= y \quad \text{if } x > y$$

$$\max(x, y) = x \quad \text{if } x > y$$

$$= y \quad \text{if } x < y$$

V.4 Solution Method

The general method of approach is explained in Section 3.2.8.

The variables κ , η and λ_n are used to describe the bending. The sheet thickness relation that will be integrated is

$$\frac{d\eta}{d\kappa} = -\frac{1}{2} \frac{\eta}{\kappa} \left[\frac{1 - 2\lambda_n - \kappa/2}{2\kappa\lambda_n + (1 - \frac{\kappa}{2})^2} \right] \quad (3.2.20)$$

The initial conditions are given in Section V.3. The second dependent variable λ_n will be determined by integrating the equilibrium--yield condition equations (V.2.2A) and (V.2.2B). In the further treatment, the symbol r_{i1} will stand for the radius of the inside boundary surface of

laminate i , and so will r_{i2} stand for its outside boundary surface radius. Hence, r_{11} indicates the inside surface of the whole sheet, and r_{n2} the outside sheet surface. Thus

$$r_{11} = r_i$$

$$r_{n2} = r_y$$

The radial stress in laminate i by integrating (V.2.2A) is found in the following way. The radial stress at the outside boundary surface of laminate i is

$$(\sigma_r^i)_{r = r_{i2}}$$

and is, for the moment, still unknown. The the radial stress σ_r^i for a radius r in laminate i is (integrate (V.2.2A) for decreasing r , starting at r_{i2}),

$$\sigma_r^i = \alpha_i \ell_n r - \alpha_i \ell_n r_{i2} + (\sigma_r^i)_{r = r_{i2}}$$

When $i = n$, $r_{n2} = r_y$ is the outside surface of the sheet, and since

$$(\sigma_r^n)_{r = r_{n2}} = 0, \sigma_r^i \text{ is known.}$$

When $i \neq n$, the continuity of radial stress requires that

$$(\sigma_r^{i+1})_{r=r_{i+1,1}} = (\sigma_r^i)_{r=r_{i2}}$$

Hence, if

$$(\sigma_r^{i+1})_{r=r_{i+1,1}}$$

can be calculated, σ_r^i is known.

$$(\sigma_r^{i+1})_{r=r_{i+1,1}}$$

is found by integration of (V.2.2A) in laminate (i + 1), with as boundary condition

$$(\sigma_r^{i+1})_{r=r_{i+1,2}}$$

If (i+ 1) is the outside laminate,

$$(\sigma_r^{i+1})_{r=r_{i+1,2}} = 0$$

and σ_r^i is known. If $i + 1 \neq n$, we proceed to the next laminate, $i + 2$, etc. . . . till we reach the outside laminate, for which

$$(\sigma_r^n)_{r=r_{n2}} = 0$$

Back substitution of the values

$$(\sigma_r^j)_{r=r_{j2}} \quad \text{for } j = i, \dots, n$$

determines the values of σ_r^i . This laminate-jumping to find the required boundary conditions for the integration of (V.2.2A) to find the radial stress at radius r in laminate i , can be shortly written as,

$$\sigma_r^i = \sum_{j=1}^n \alpha_j \ell_n \frac{\max(r, r_{j1})}{r_{j2}} \quad (V.4.1A)$$

$$r_{i1} \leq r \leq r_{i2} \text{ and } r \geq r_n$$

Laminate-jumping for the integration of (V.2.2B), with boundary condition

$$(\sigma_r^1)_{r=r_{11}} = 0 \text{ at inside of sheet, leads to}$$

$$\sigma_r^i = \sum_{j=1}^i (-\alpha_j) \ell_n \frac{\min(r, r_{j2})}{r_{j1}} \quad (V.4.1B)$$

$$r_{i1} \leq r \leq r_{i2} \text{ and } r \leq r_n$$

These formulas for the radial stress can be expressed in function of the μ -values, κ and η . This yields

$$\sigma_{r\lambda}^i = \sum_{j=1}^n \frac{\alpha_j}{2} \ell_n \left[\frac{\max \left(\left[\left(1 - \frac{\kappa}{2}\right)^2 + 2 \lambda \kappa \right], \left[\left(1 - \frac{\kappa}{2}\right)^2 + 2 \nu_{j1} \kappa \right] \right)}{\left(1 - \frac{\kappa}{2}\right)^2 + 2 \nu_{j2} \kappa} \right]$$

(V.4.2A)

for $\nu_{i1} \leq \lambda \leq \nu_{i2}$ and $\lambda \geq \lambda_n$

and

$$\sigma_{r\lambda}^i = \sum_{j=1}^i \left(\frac{-\alpha_j}{2}\right) \ell_n \left[\frac{\min \left(\left[\left(1 - \frac{\kappa}{2}\right)^2 + 2 \lambda \kappa \right], \left[\left(1 - \frac{\kappa}{2}\right)^2 + 2 \nu_{j2} \kappa \right] \right)}{\left(1 - \frac{\kappa}{2}\right)^2 + 2 \nu_{j2} \kappa} \right]$$

(V.4.2B)

for $\nu_{i1} \leq \lambda \leq \nu_{i2}$ and $\lambda \leq \lambda_n$

For clarity, the procedure followed above is in essence the one described in Section (3.2.8). The equilibrium equation is integrated from the outside surface of the bend to the first interlaminar boundary, and the value of the radial stress is determined. This way, we 'jumped' one laminate. Using this radial stress at that boundary as initial value, the equilibrium equation that applies for the laminate on the inside of that boundary is integrated to the next interlaminar boundary. This procedure is repeated until the laminate, in which the radius, for which the radial stress has to be calculated, is reached. For that laminate, the integration is carried out from the outside laminate radius to that radius. This explains the use of the maximum symbol in equations (V.4.1A) and (V.4.2A). In a similar way, integration can be carried out starting from the inside surface of the bend. This leads to formulas (V.4.1B) and (V.4.2B).

Using formulas (V.4.2A) and (V.4.2B), two values for the radial stress of a fibre, defined by the volume fraction λ , can be found. Of course, only one of these is the exact one. When λ is situated to the outside of the neutral fibre, (V.4.2A) will give the exact value. Otherwise, $\sigma_{r\lambda}^i$ will be determined by (V.4.2B). But for the neutral fibre, $\lambda = \lambda_n$, and the radial stress found by integrating the equilibrium equation for increasing or decreasing r must be the same. Hence, the fibre for which (V.4.2A) and (V.4.2B) give exactly the same radial stress, is the neutral fibre. The λ -value of that fibre is the sought after value of λ_n . The search for λ_n , the λ -value for which the difference between the two possible radial stresses is zero, is carried out with an iterative technique known as 'Regula Falsi', and this technique is described in FROBERG, [49], p 22.

Once λ_n is known, sheet thickness equation (3.2.20) can be numerically integrated using the 'Runge-Kutta' technique, described in Section IV.4. The switch in sheet thickness equation, which was required in the approach used in Appendix IV when the neutral layer crossed a material boundary, is automatically taken care of in the approach suggested in this section, since the λ_n value in function of κ and η is really determined in a numerical way, instead of an analytical one. The removal of this sheet thickness relation switch, which should become frequent in the case of multilaminated materials, is one of the reasons for the development of the solution method described in this Appendix.

V.5 Stress Distribution and Bending Moment

The radial stress in function of κ , η and λ is provided by (V.4.2A) when $\lambda \geq \lambda_n$ and by (V.4.2B) when $\lambda \leq \lambda_n$. The tangential stress is given by

$$\sigma_{\phi \lambda}^i = \alpha_i + \sigma_r^i \lambda \quad \lambda > \lambda_n$$

$$\text{and } \nu_{i1} < \lambda < \nu_{i2}$$

$$\sigma_{\phi \lambda}^i = -\alpha_i + \sigma_r^i \lambda \quad \lambda < \lambda_n$$

The bending moment at the commencement of bending ($\kappa = 0$) is given in Section V.3. Using

$$M = \int_{r_i}^{r_y} \sigma_{\phi} r dr$$

gives, when k is the laminate in which the neutral layer is situated,

$$M = \sum_{i=1}^k \int_{r_{i1}}^{\min(r_{i2}, r_n)} (-\alpha_i + \sigma_r^i \lambda) r dr$$

$$+ \sum_{i=k}^n \int_{\max(r_{i1}, r_n)}^{r_{i2}} (\alpha_i + \sigma_r^i \lambda) r dr$$

Since $\sigma_r^i \lambda$ is given by (V.4.2A) or (V.4.2B), the bending moment M is determined.

V.6 Program TRINSH

A FORTRAN program using the techniques described in this Appendix has been developed to calculate the plain strain bending of nonstrainhardening

multilaminated sheet. The accuracy of the program is discussed in Appendix IX.

APPENDIX VI

INFLUENCE OF THE ORIGINAL NEUTRAL LAYER POSITION ON THE
CHANGE IN RELATIVE SHEET THICKNESS AT THE
COMMENCEMENT OF THE BENDING PROCESS

For a flat sheet, $\kappa = 0$, $\eta = 1$, $\rho = 1$ and λ_n has a value which can be determined by the method described in Appendix IV, Section IV.2 or Appendix V, Section V.3. All the boundary conditions for the sheet thickness differential equation

$$\frac{d\eta}{d\kappa} = -\frac{1}{2} \eta \left[\frac{1 - 2\lambda_n - \kappa/2}{(1 - \frac{\kappa}{2})^2 + 2\lambda_n \kappa} \right] \quad (3.2.20)$$

are therefore known. The change in relative sheet thickness at the beginning of the bending process is given by

$$\left(\frac{d\eta}{d\kappa} \right)_{\kappa = 0} = -\frac{1}{2} (1 - 2\lambda_n) = -\frac{1}{2} + \lambda_n$$

This value gives the slope of the $\eta - \kappa$ curve for $\kappa = 0$. It is clear that, when $\lambda_n > .50$, the slope is positive, so that the sheet thickens at the commencement of the bending. Similarly, when $\lambda_n < .50$, the slope of the $\eta - \kappa$ curve for $\kappa = 0$ is negative, so that the sheet thins. When $\lambda_n = .50$, the slope $\left(\frac{d\eta}{d\kappa} \right)_{\kappa = 0}$, so that no change in thickness occurs at the beginning of the

bending. The behaviour described above has been found to be true for all the calculations performed and would indicate that the position of the neutral layer λ_n will determine, at least at the onset of the process, how the sheet thickness will alter.

APPENDIX VII

BENDING OF LAMINATED SHEET, COMPOSED OF RIGID-PLASTIC,
STRAINHARDENING MATERIALS WITHOUT BAUSCHINGER EFFECTVII.1 Determination of the Effective Strain of an Arbitrary Layer in the Bent Sheet

The material has a stress-strain curve

$$\bar{\sigma} = H \left(\int d\bar{\epsilon} \right)$$

If the material should have a Bauschinger effect, the function $H \left(\int d\bar{\epsilon} \right)$ should not be unique for the same values of $\bar{\epsilon} = \int d\bar{\epsilon}$. The equivalent stress $\bar{\sigma}$ is influenced by the straining path that is necessary to attain the effective strain $\bar{\epsilon}$ in that case. Indeed, a value of $\bar{\epsilon}$ reached by unidirectional straining should give rise to a different $\bar{\sigma}$ than the ones found for the same values of $\bar{\epsilon}$, but reached through a straining path that contains at least one straining reversal. However, since it is assumed that the material shows no Bauschinger effect, the equivalent yield stress $\bar{\sigma}$ is solely dependent on the magnitude of $\bar{\epsilon}$, and not on the straining path that was followed to reach that equivalent strain.

The equivalent strain increment was defined in Section 3.2.8, and equation (3.2.2) indicates that

$$d\bar{\epsilon} = \frac{2}{\sqrt{3}} |d\epsilon_{\phi}|$$

so that it is fully determined when the tangential strain increment is

known. The tangential strain for any layer in the sheet is given by

$$\epsilon_{\phi} = \lambda_n \frac{r}{r_0} \quad (3.2.6)$$

$$\text{or} \quad \epsilon_{\phi} = \frac{1}{2} \lambda_n \left[\left(1 - \frac{\kappa}{2}\right)^2 + 2\lambda\kappa \right] - \lambda_n \eta \quad (I.9)$$

For the layer in the sheet that has been subjected to a continuous length increase, the straining has been unidirectional, and, since

$$d\bar{\epsilon} = \frac{2}{\sqrt{3}} d\epsilon_{\phi}$$

$$\bar{\epsilon} = \int d\bar{\epsilon} = \frac{2}{\sqrt{3}} \int d\epsilon_{\phi} = \frac{2}{\sqrt{3}} \epsilon_{\phi}$$

$$\text{Hence} \quad \bar{\epsilon} = \frac{2}{\sqrt{3}} \lambda_n \frac{r}{r_0}$$

The effective strain for these layers can thus be determined quite easily. Layers in the sheet that are monotonously subjected to tangential compression, have

$$d\bar{\epsilon} = -\frac{2}{\sqrt{3}} d\epsilon_{\phi}$$

so that

$$\bar{\epsilon} = -\frac{2}{\sqrt{3}} \lambda_n \frac{r}{r_0}$$

The determination of $\bar{\epsilon}$ is not that simple for layers that have undergone

one or more reversals in tangential straining. This arises from the fact that the current value of $|\epsilon_\phi|$ for such a layer will always be less than the effective strain $\bar{\epsilon}$. The value of $\bar{\epsilon}$ can be determined if the straining path of the layer is known. In fact, it is sufficient to know the tangential strains at which strain reversals occurred. We will handle this in detail with some examples to avoid any confusion.

Figure VII.1 plots the yield condition for plane strain

$$\sigma_\phi - \sigma_r = \bar{\sigma} \quad \text{for } r > r_n$$

$$\sigma_\phi - \sigma_r = -\bar{\sigma} \quad \text{for } r < r_n$$

as a function of the equivalent tangential strain, which we will define as

$$\bar{\epsilon}_\phi = \frac{\sqrt{3}}{2} \bar{\epsilon}$$

so that

$$\bar{\epsilon}_\phi = \int |d\epsilon_\phi|$$

It is clear that for point A, which has gone through unidirectional tangential straining,

$$\bar{\epsilon}_\phi^A = \epsilon_\phi^A$$

and that for point B, gone through unidirectional compressive straining,

$$\bar{\epsilon}_{\phi}^B = - \bar{\epsilon}_{\phi}^B$$

Figure VII.2 shows the straining path of a layer that has first undergone compressive straining, down to a strain $\epsilon_{\phi c}$, followed by a strain reversal. tangential straining was carried out to point C, tangential strain is still compressive, and further to D, with tensile tangential strain. It can be verified that

$$\bar{\epsilon}_{\phi}^C = - 2\epsilon_{\phi c} + \epsilon_{\phi}^C$$

$$\bar{\epsilon}_{\phi}^D = - 2\epsilon_{\phi c} + \epsilon_{\phi}^D$$

Figure VII.3 shows the straining path of a layer, first strained in tension up to a strain of $\epsilon_{\phi t}$, and then strained in compression to point E, with the tangential strain still positive, and further to point F, with the tangential strain compressive. It is clear that,

$$\bar{\epsilon}_{\phi}^E = 2\epsilon_{\phi t} - \epsilon_{\phi}^E$$

$$\bar{\epsilon}_{\phi}^F = 2\epsilon_{\phi t} - \epsilon_{\phi}^F$$

Figure VII.4 shows the path for a layer first strained in tension up to $\epsilon_{\phi t}$, then in compression till the tangential strain decreased to $\epsilon_{\phi c}$ and then again in tension until the final tangential strain reached ϵ_{ϕ}^G (point G). Although this is more difficult to follow, it can be shown that

$$\bar{\epsilon}_{\phi}^G = 2\epsilon_{\phi t} - 2\epsilon_{\phi c} + \epsilon_{\phi}^G$$

Going through the above examples, it can be seen that the current tangential strain ϵ_{ϕ} for a layer gives a contribution ϵ_{ϕ} to the equivalent tangential strain when that layer is situated to the outside of the neutral layer.

Similarly, when the layer is situated to the inside of the neutral layer, the contribution of the tangential strain ϵ_{ϕ} to the equivalent tangential strain is $-\epsilon_{\phi}$. Note that ϵ_{ϕ} being positive or negative is irrelevant, only the position of the layer compared to the neutral layer position is important. The above examples also show that a tangential strain $\epsilon_{\phi t}$ in the layer when the straining is reversed from tensile to compressive, gives a contribution $+2\epsilon_{\phi t}$ to the equivalent tangential strain. Similarly, a tangential strain $\epsilon_{\phi c}$ in the layer when the straining is reversed from compressive to tensile gives a contribution $-2\epsilon_{\phi c}$. Note that the signs of $\epsilon_{\phi t}$ and $\epsilon_{\phi c}$ themselves have no influence. It can be concluded that

$$\bar{\epsilon}_{\phi} = 2 \sum_i \epsilon_{\phi t i} - 2 \sum_j \epsilon_{\phi c j} + \text{sgn}(\sigma_{\phi} - \sigma_r) \epsilon_{\phi}$$

in which $\epsilon_{\phi t i}$ is the tangential strain at the i th strain reversal from tensile to compressive, in which $\epsilon_{\phi c j}$ is the tangential strain at the j th strain reversal from compressive to tensile, and in which $\text{sgn}(\sigma_{\phi} - \sigma_r)$ equals $+1$ when $\sigma_{\phi} > \sigma_r$ and equals -1 when $\sigma_{\phi} < \sigma_r$. The equivalent strain for a layer that has undergone strain reversal is therefore,

$$\bar{\epsilon} = \frac{2}{\sqrt{3}} \bar{\epsilon}_{\phi} = \frac{2}{\sqrt{3}} \left[2 \sum_i \epsilon_{\phi t i} - 2 \sum_j \epsilon_{\phi c j} + \text{sgn}(\sigma_{\phi} - \sigma_r) \epsilon_{\phi} \right]$$

ϵ_ϕ can still be expressed with (3.2.6) or (I.9), but a convenient way to express $\epsilon_{\phi ti}$ and $\epsilon_{\phi cj}$ must be found. It is sufficient to remember that a layer can only undergo a reversal of stress when it coincides with the neutral layer. The tangential strain of that layer is at that stage in the bending equal to $\lambda_n \frac{r_n}{r_o} = \lambda_n \rho$. Hence,

$$\bar{\epsilon} = \frac{2}{\sqrt{3}} \left[\sum_i \lambda_n \rho_{ti} - 2 \sum_j \lambda_n \rho_{cj} + \text{sgn}(\sigma_\phi - \sigma_r) \lambda_n \frac{r_n}{r_o} \right]$$

where ρ_{ti} is the ρ -value of the bent sheet when the layer coincides with the neutral layer and goes for the i th time from tensile to compressive straining. Similarly, ρ_{cj} is the ρ -value when the layer goes for the j th time from compressive to tensile straining. Every layer in the bent sheet is defined by its volume fraction λ . A layer coincides with the neutral layer when $\lambda_n = \lambda$. Figure VII.5 indicates how, by knowing the $\lambda_n - \kappa$ and $\rho - \kappa$ curve of the previous deformation process, all the values of ρ_{ti} and ρ_{cj} can be found for an arbitrary layer λ . Take the layer indicated by λ in figure VII.5. At the commencement of bending, the layer is situated to the outside of the neutral layer. As bending proceeds, the neutral layer moves up in the bent sheet (this behaviour is possible in laminated strainhardening sheet as explained in Chapter 5). The neutral layer crosses the layer λ at point A. The straining in layer λ is then reversed from tensile to compressive. The corresponding κ -value is given by A' . Moving to the $(\rho - \kappa)$ plot, A' value for κ gives the value A'' for ρ . This ρ values gives a contribution $\frac{2}{\sqrt{3}} 2 \lambda_n \rho_{A''}$ to the equivalent strain. During further bending, λ_n crosses λ a second time, at point B. The corresponding ρ -value is $\rho_{B''}$, and since λ changes this time from compressive to tensile straining, the contribution to $\bar{\epsilon}$ is $\frac{2}{\sqrt{3}} 2 \lambda_n \rho_{B''}$. Further bending up to the current κ -value doesn't show any strain reversals. Layer λ is therefore

currently in tensile straining, and its tangential strain gives a contribution $+\frac{2}{\sqrt{3}} \epsilon_{\phi}$ to $\bar{\epsilon}$. The equivalent strain for layer λ is then

$$\bar{\epsilon} = \frac{2}{\sqrt{3}} \left[\ell_n \rho_{A''}^2 - \ell_n \rho_{B''}^2 + \frac{1}{2} \ell_n \left[\left(1 - \frac{\kappa}{2}\right)^2 + 2 \lambda \kappa \right] - \ell_n \eta \right]$$

In general,

$$\bar{\epsilon} = \frac{2}{\sqrt{3}} \ell_n \left[\frac{\prod_i \rho_{ti}^2}{\prod_j \rho_{cj}^2} \frac{\left(1 - \frac{\kappa}{2}\right)^2 + 2 \lambda \kappa}{\eta} \right]$$

(Π means product).

It was indicated in this section how the equivalent strain for all layers in the bent sheet can be found. For layers that have undergone monotonous straining, it is straightforward. For all the layers which have ever coincided with the neutral layer, it involves determining the ρ -values for which this happened together with recording how the straining changed, from compression to tension or the reverse. In actual computer calculations, this effective strain determination makes it necessary to store the values of λ_n and ρ in computer memory. Since only discrete values for κ , λ_n and ρ can be stored, the actual determination of the exact ρ -values needed in the calculations of $\bar{\epsilon}$ for an arbitrary layer λ is done by using a second order approximation to the $(\lambda_n - \kappa)$ and $(\rho - \kappa)$ curves in the immediate neighbourhood of the required value.

VII.2 Description of Laminates

The sheet is composed of n laminates. The same convention for the numbering of laminates is used as in Appendix V, Section V.2. The

boundary surfaces between laminates are similarly defined by the volume fraction of material embraced by the surface and the inside surface of the bend. The inside surface of laminate i is characterised by v_{i1} , the outside by v_{i2} . A corresponding notation will be used for the laminate boundary radii during bending, which are respectively r_{i1} and r_{i2} . The inside and outside radii of the bent sheet are then r_{11} and r_{n2} .

The stress-strain curve in uniaxial tension will be characterised by three parameters, A_i , B_i and n_i . Two types of stress-strain curves will be considered, type 1,

$$\bar{\sigma}^i = H_1^i (\bar{\epsilon}) = A_i + B_i \bar{\epsilon}^{n_i}$$

and type 2,

$$\bar{\sigma}^i = H_2^i (\bar{\epsilon}) = A_i (B_i + \bar{\epsilon})^{n_i}$$

VII.3 Yield Condition and Equilibrium Equation

The general yield condition for laminate i is

$$\left. \begin{aligned} \sigma_\phi^i - \sigma_r^i &= \frac{2}{\sqrt{3}} \bar{\sigma}^i & r_n < r \leq r_{n2} \\ \sigma_\phi^i - \sigma_r^i &= -\frac{2}{\sqrt{3}} \bar{\sigma}^i & r_{11} \leq r < r_n \end{aligned} \right\} \text{and } r_{i1} < r < r_{i2}$$

Radial equilibrium for the plane strain case can be expressed as

$$\left. \begin{aligned}
 r \frac{d \sigma_r^i}{dr} &= \frac{2}{\sqrt{3}} \bar{\sigma}^i & r_n \leq r \leq r_{n2} \\
 r \frac{d \sigma_r^i}{dr} &= -\frac{2}{\sqrt{3}} \bar{\sigma}^i & r_{i1} \leq r \leq r_n
 \end{aligned} \right\} r_{i1} \leq r \leq r_{i2}$$

The sheet thickness can be divided into four zones, see figure VII.6. The material in zone I is subjected to monotonous tangential tension, zone II to monotonous tangential compression. Zone III consists of layers that have undergone at least one strain reversal, and are currently situated to the outside of the neutral layer. Zone IV layers have also undergone at least one strain reversal, and are current to the inside of the neutral layer. Of course, all these zones will not always be present in the bent sheet. At the commencement of bending, only zones I and II exist, see figure VII.7. When the neutral layer has moved monotonously to the inside of the sheet, only zones I, II and III exist, as indicated in Figure VII.8. Bending laminated sheet, it is possible that the neutral layer moves first to the outside of the bend, as in Figure VII.9. Only zones I, II and IV exist then. When the neutral layer starts to move to the inside, we come to the case of Figure VII.6, with the four zones. The outermost position that the neutral layer has ever been in the previous bending process will be indicated by the maximum value λ_n has ever reached, and noted as λ_{max} . The same applies for the innermost position of the neutral layer, noted as λ_{min} . With this λ -value corresponds current radii values r_{max} and r_{min} . Hence, the division in zones is as follows

$$\text{zone I} \quad \lambda_{\max} \leq \lambda \leq 1 \quad \text{or} \quad r_{\max} \leq r \leq r_{n2}$$

$$\text{zone II} \quad 0 \leq \lambda \leq \lambda_{\min} \quad r_{11} \leq r \leq r_{\min}$$

$$\text{zone III} \quad \lambda_n \leq \lambda \leq \lambda_{\max} \quad r_n \leq r \leq r_{\max}$$

$$\text{zone IV} \quad \lambda_{\min} \leq \lambda \leq \lambda_n \quad r_{\min} \leq r \leq r_n$$

The yield condition in the different zones is different, due to the different method of calculation of $\bar{\epsilon}$, the equivalent strain.

VII.3.1 Stress-Strain Curve Type 1: $H_1^i(\bar{\epsilon}) = A_i + B_i \bar{\epsilon}^{n_i}$

The yield condition for laminate i is

$$\text{zone I} \quad \sigma_\phi - \sigma_r = \frac{2}{\sqrt{3}} A_i + \frac{2}{\sqrt{3}} B_i \left(\frac{2}{\sqrt{3}} \epsilon_\phi\right)^{n_i}$$

$$\text{zone II} \quad \sigma_\phi - \sigma_r = -\frac{2}{\sqrt{3}} A_i - \frac{2}{\sqrt{3}} B_i \left(-\frac{2}{\sqrt{3}} \epsilon_\phi\right)^{n_i}$$

$$\text{zone III} \quad \sigma_\phi - \sigma_r = \frac{2}{\sqrt{3}} A_i + \frac{2}{\sqrt{3}} B_i \left(2 \sum_k \ell_n \rho_{tk} - 2 \sum_j \ell_n \rho_{cj} + \epsilon_\phi\right)^{n_i}$$

$$\text{zone IV} \quad \sigma_\phi - \sigma_r = -\frac{2}{\sqrt{3}} A_i - \frac{2}{\sqrt{3}} B_i \left(\frac{2}{\sqrt{3}} \left(2 \sum_k \ell_n \rho_{tk} - 2 \sum_j \ell_n \rho_j - \epsilon_\phi\right)\right)^{n_i}$$

$$\text{Substituting } \alpha_i = \frac{2}{\sqrt{3}} A_i$$

$$\beta_i = \left(\frac{2}{\sqrt{3}}\right)^{n_i+1} B_i$$

$$\epsilon_\phi = \ell_n \frac{r}{r_0}$$

gives for the yield condition

$$\text{zone I } \sigma_{\phi} - \sigma_r = \alpha_i + \beta_i \left(\ell_n \frac{r}{r_0} \right)^{n_i}$$

$$\text{zone II } \sigma_{\phi} - \sigma_r = -\alpha_i - \beta_i \left(-\ell_n \frac{r}{r_0} \right)^{n_i}$$

$$\text{zone III } \sigma_{\phi} - \sigma_r = \alpha_i + \beta_i \left(2 \sum_k \ell_n \rho_{tk} - 2 \sum_j \ell_n \rho_{cj} + \ell_n \frac{r}{r_0} \right)^{n_i}$$

(VII.3.1)

$$\text{zone IV } \sigma_{\phi} - \sigma_r = -\alpha_i - \beta_i \left(2 \sum_k \ell_n \rho_{tk} - 2 \sum_j \ell_n \rho_{cj} - \ell_n \frac{r}{r_0} \right)^{n_i}$$

The combined yield condition-equilibrium equation can be found by substituting

$$\sigma_{\phi} - \sigma_r = r \frac{d\sigma_r}{dr}$$

in the above equations.

VII.3.2 Stress-Strain Curve Type 2: $H_2^i(\bar{\epsilon}) = A_i (B_i + \bar{\epsilon})^{n_i}$

The yield condition for laminate i is

$$\text{zone I } \sigma_{\phi} - \sigma_r = \frac{2}{\sqrt{3}} A_i \left(B_i + \frac{2}{\sqrt{3}} \epsilon_{\phi} \right)^{n_i}$$

$$\text{zone II } \sigma_{\phi} - \sigma_r = -\frac{2}{\sqrt{3}} A_i \left(B_i - \frac{2}{\sqrt{3}} \epsilon_{\phi} \right)^{n_i}$$

$$\text{zone III } \sigma_{\phi} - \sigma_r = \frac{2}{\sqrt{3}} A_i \left(B_i + \frac{2}{\sqrt{3}} \left(2 \sum_k \ell_n \rho_{tk} - 2 \sum_j \ell_n \rho_{cj} + \varepsilon_{\phi} \right) \right)^{n_i}$$

$$\text{zone IV } \sigma_{\phi} - \sigma_r = -\frac{2}{\sqrt{3}} A_i \left(B_i + \frac{2}{\sqrt{3}} \left(2 \sum_k \ell_n \rho_{tk} - 2 \sum_j \ell_n \rho_{cj} - \varepsilon_{\phi} \right) \right)^{n_i}$$

Substituting

$$\alpha_i = A_i \left(\frac{2}{\sqrt{3}} \right)^{n_i + 1}$$

$$\beta_i = \frac{\sqrt{3}}{2} B_i$$

$$\varepsilon_{\phi} = \ell_n \frac{r}{r_0}$$

gives for the yield condition

$$\text{zone I } \sigma_{\phi} - \sigma_r = \alpha_i \left(\beta_i + \ell_n \frac{r}{r_0} \right)^{n_i}$$

$$\text{zone II } \sigma_{\phi} - \sigma_r = -\alpha_i \left(\beta_i - \ell_n \frac{r}{r_0} \right)^{n_i}$$

$$\text{zone III } \sigma_{\phi} - \sigma_r = \alpha_i \left(\beta_i + 2 \sum_k \ell_n \rho_{tk} - 2 \sum_j \ell_n \rho_{cj} \right.$$

$$\left. + \ell_n \frac{r}{r_0} \right)^{n_i}$$

(VII.3.2.)

$$\text{zone IV } \sigma_{\phi} - \sigma_r = -\alpha_i \left(\beta_i + 2 \sum_k \ell_n \rho_{tk} - 2 \sum_j \ell_n \rho_{cj} \right.$$

$$\left. - \ell_n \frac{r}{r_0} \right)^{n_i}$$

Substituting

$$\sigma_{\phi} - \sigma_r = r \frac{d\sigma_r}{dr}$$

in the yield condition gives the combined yield condition-equilibrium equations.

VII.4 Initial Conditions

The initial conditions for the integration of the sheet thickness equation are

$$\kappa = 0$$

$$\eta = 1$$

and the exact position of the neutral layer, λ_n , at the beginning of bending. This original neutral layer position can be determined by using the method described in Appendix V, Section V.3. All formula used there remain valid for a stress-strain curve of type 1, $H_1^i(\bar{\epsilon}) = A_i + B_i \bar{\epsilon}^{n_i}$. For a stress-strain curve of type 2, $H_2^i(\bar{\epsilon}) = A_i (B_i + \bar{\epsilon})^{n_i}$, the symbol α_i in the formulas of Section V.3 must be replaced by $\alpha_i \beta_i^{n_i}$. The original bending moment is also given by the formulas of Section V.3, unchanged for stress-strain curve type 1, changed as indicated above for a stress-strain curve of type 2.

VII.5 Solution Method

The general method of approach is explained in Section 3.2.8. The variables κ , η and λ_n are used to describe the bending process. The sheet thickness equation to be integrated is

$$\frac{d\eta}{d\kappa} = -\frac{1}{2} \frac{\eta}{\kappa} \left[\frac{1 - 2\lambda_n - \kappa/2}{2\kappa\lambda_n + (1 - \frac{\kappa}{2})} \right] \quad (3.2.20)$$

The initial conditions are given in Section VII.4. The second dependent variable λ_n will be determined in function of κ and η by integrating the equilibrium equations across the sheet thickness.

The solution will be given for a case when all the four zones, as described in Section VII.3, are present in the sheet. If some of them are absent, the analysis is slightly simplified. The analysis for these simpler cases is not given here, but it is obvious how to proceed in these cases.

The current position of the neutral layer is given by λ_n , the maximum position of the neutral layer in the previous bending is given by λ_{\max} , and the minimum position by λ_{\min} . λ_n , λ_{\min} and λ_{\max} indicate the boundaries between the four zones. The neutral layer occurs currently in laminate ℓ_n , so that

$$\mu_{\ell_n 1} < \lambda_n < \mu_{\ell_n 2}$$

The minimum neutral layer position occurs in laminate ℓ_{\min} , so that

$$\mu_{\ell_{\min 1}} < \lambda_{\min} < \mu_{\ell_{\min 2}}$$

The maximum neutral layer position is situated in laminate ℓ_{\max} , so that

$$\mu_{\ell_{\max 1}} < \lambda_{\max} < \mu_{\ell_{\max 2}}$$

VII.5.1 Solution for Stress-Strain Curve Type 1: $H_1^i(\bar{\epsilon}) = A_i + B_i \bar{\epsilon}^{-n_i}$

Integration of the equilibrium equation, as given in Section VII.3.1, in zone I, with as initial boundary condition

$$\left(\sigma_r^n\right)_{r=r_{n2}} = 0$$

and application of the laminate jumping as explained in Section V.4, yields

$$\begin{aligned} \sigma_r^{iI} = & \sum_{p=i}^n \alpha_p \ell_n \frac{\max(r_{p1}, r)}{r_{p2}} \\ & + \sum_{p=i}^n \frac{\beta_p}{n_p + 1} \left(\ell_n \frac{\max(r_{p1}, r)}{r_o} \right)^{n_p + 1} \\ & - \sum_{p=i}^n \frac{\beta_p}{n_p + 1} \left(\ell_n \frac{r_{p2}}{r_o} \right)^{n_p + 1} \end{aligned} \quad \text{(VII.5.1)}$$

The value of the radial stress at the inside boundary of zone I is then

$$\left(\sigma_r^{\max I}\right)_{r=r_{\max}} = \sum_{p=\ell_{\max}}^n \alpha_p \ell_n \frac{\max(r_{p1}, r_{\max})}{r_{p2}}$$

$$\begin{aligned}
& + \sum_{p = \ell_{\max}}^n \frac{\beta_p}{n_p + 1} \left[\left(\ell_n \frac{\max(r_{p1}, r_{\max})}{r_o} \right)^{n_p + 1} \right. \\
& \left. - \left(\ell_n \frac{r_{p2}}{r_o} \right)^{n_p + 1} \right]
\end{aligned} \tag{VII.5.2}$$

Integration of the equilibrium condition in zone II, with initial boundary condition

$$(\sigma_r^I)_{r = r_{11}} = 0$$

gives in a similar way

$$\begin{aligned}
\sigma_r^{iII} = & - \sum_{p = 1}^i \alpha_p \ell_n \frac{\min(r_{p2}, r)}{r_{p1}} \\
& - \sum_{p = 1}^i \frac{\beta_p}{n_p + 1} \left(- \ell_n \frac{r_{p1}}{r_o} \right)^{n_p + 1} \\
& + \sum_{p = 1}^i \frac{\beta_p}{n_p + 1} \left(- \ell_n \frac{\min(r_{p2}, r)}{r_o} \right)^{n_p + 1}
\end{aligned} \tag{VII.5.3}$$

The value of the radial stress at the outside boundary of zone II is then

$$(\sigma_r^{\ell_{\min} I})_{r = r_{\min}} = - \sum_{p = 1}^{\ell_{\min}} \alpha_p \ell_n \frac{\min(r_{p2}, r_{\min})}{r_{p1}}$$

$$\begin{aligned}
& + \sum_{p=1}^{\ell_{\min}} \frac{\beta_p}{n_p + 1} \left(- \ell_n \frac{\min(r_{p2}, r_{\min})}{r_o} \right)^{n_p + 1} \\
& - \sum_{p=1}^{\ell_{\min}} \frac{\beta_p}{n_p + 1} \left(- \ell_n \frac{r_{p1}}{r_o} \right)^{n_p + 1} \tag{VII.5.4}
\end{aligned}$$

The radial stress at the boundary between zones I and III, and the zones II and IV can be analytically calculated with equations (VII.5.2) and (VII.5.4). All the radii can be expressed in function of κ and η using the formulas provided in Appendix I. The current position of the neutral layer, λ_n , or ρ , is not needed to calculate these radial stresses. To find the current λ_n -value, the equilibrium has still to be integrated over zones III and IV. The equilibrium equations for laminate i in these zones can be expressed as follows

$$\text{zone III } d \sigma_r^{iIII} = \alpha_i \frac{dr}{r} + \beta_i \left[2 \sum_k \ell_n \rho_{tk} - 2 \sum_j \ell_n \rho_{cj} + \ell_n \frac{r}{r_o} \right]^{n_i} \frac{dr}{r} \tag{VII.5.5}$$

$$\text{zone IV } d \sigma_r^{iIV} = - \alpha_i \frac{dr}{r} - \beta_i \left[2 \sum_k \ell_n \rho_{tk} - 2 \sum_j \ell_n \rho_{cj} - \ell_n \frac{r}{r_o} \right]^{n_i} \frac{dr}{r} \tag{VII.5.6}$$

These equations cannot be analytically integrated, since the strains at the points of strain reversals are different for different layers, and are not analytically known. Hence, integration of the equilibrium equations

is performed numerically, using the Runge-Kutta method. The starting condition for the integration of (VII.5.5) is the radial stress at $r = r_{\max}$, given by equation (VII.5.2). Integration is performed for decreasing values of the layer radius r . When crossing a material boundary, the starting condition for the new equilibrium equation is provided by the radial stress at the boundary. The starting condition for the integration of (VII.5.6) is given by equation (VII.5.4).

Integration is done for increasing values of the layer radius r . The position of the neutral layer is found by determining for which layer the radial stress computed by integration in zone III or zone IV is identical. Once λ_n as a function of κ , η and the previous bending behaviour is found, the integration of the sheet-thickness equation (3.2.20) can be performed, so that η , λ_n and ρ as a function of κ are known.

VII.5.2 Solution Method for Stress-Strain Curve Type 2: $H_2^i(\bar{\epsilon}) = A_i(B_i + \bar{\epsilon})^{n_i}$

The same method as described in Section VII.5.1 is used. The most important formulas follow here. Integration in zone I leads to

$$\sigma_r^{iI} = \sum_{p=i}^n \frac{\alpha_p}{n_p + 1} \left(\beta_p + \ell_n \frac{\max(r_{p1}, r)}{r_o} \right)^{n_p + 1} \quad (\text{VII.5.7})$$

$$- \sum_{p=i}^n \frac{\alpha_p}{n_p + 1} \left(\beta_p + \ell_n \frac{r_{p2}}{r_o} \right)^{n_p + 1}$$

$$\begin{aligned}
 (\sigma_r^{\max})_{r=r_{\max}}^{\ell \text{ max I}} &= \sum_{p=\ell_{\max}}^n \frac{\alpha_p}{n_p+1} (\beta_p + \ell_n \frac{\max(r_{p1}, r_{\max})}{r_o})^{n_p+1} \\
 &- \sum_{p=\ell_{\max}}^n \frac{\alpha_p}{n_p+1} (\beta_p + \ell_n \frac{r_{p2}}{r_o})^{n_p+1}
 \end{aligned}
 \tag{VII.5.8}$$

Integration in zone II leads to

$$\begin{aligned}
 \sigma_r^{\text{III}} &= \sum_{p=1}^i \frac{\alpha_p}{n_p+1} (\beta_p - \ell_n \frac{\min(r_{p2}, r)}{r_o})^{n_p+1} \\
 &- \sum_{p=1}^i \frac{\alpha_p}{n_p+1} (\beta_p - \ell_n \frac{r_{p1}}{r_o})^{n_p+1}
 \end{aligned}
 \tag{VII.5.9}$$

$$\begin{aligned}
 (\sigma_r^{\min})_{r=r_{\min}}^{\ell \text{ min II}} &= \sum_{p=1}^{\ell_{\min}} \frac{\alpha_p}{n_p+1} (\beta_p - \ell_n \frac{\min(r_{p2}, r_{\min})}{r_o})^{n_p+1} \\
 &- \sum_{p=1}^{\ell_{\min}} \frac{\alpha_p}{n_p+1} (\beta_p - \ell_n \frac{r_{p1}}{r_o})^{n_p+1}
 \end{aligned}
 \tag{VII.5.10}$$

(VII.5.8) and (VII.5.10) are the boundary conditions to start integration in zone III and IV. The equilibrium condition in these zones is

$$\text{zone III d } \sigma_r^{\text{III}} = \alpha_i (\beta_i + 2 \sum_k \ell_n \rho_{tk} - 2 \sum_j \ell_n \rho_{cj})$$

$$+ \lambda_n \left(\frac{r}{r_0} \right)^{n_i} \frac{dr}{r} \quad (\text{VII.5.11})$$

$$\begin{aligned} \text{zone IV } d \sigma_r^{iIV} = & - \alpha_i (\beta_i + 2 \sum_k \lambda_n \rho_{tk} - 2 \sum_j \lambda_n \rho_{cj} \\ & - \lambda_n \left(\frac{r}{r_0} \right)^{n_i} \frac{dr}{r} \end{aligned} \quad (\text{VII.5.12})$$

The value of λ_n is found by numerically integrating (VII.5.11) and (VII.5.12), and determining for what layer the radial stress found by the two integrations coincides. Integration of sheet thickness equation is straightforward, since λ_n is known.

VII.6 Stress Distribution and Bending Moment

The values of the radial stress in zones I or II can be analytically determined by formulas (VII.5.1) and (VII.5.3) or (VII.5.7) and (VII.5.9). The radial stress in zones III or IV must be determined by numerical integration of (VII.5.5) and (VII.5.6) or (VII.5.11) and (VII.5.12). The tangential stress follows out of (VII.3.1) or (VII.3.2) and requires the knowledge of the radial stress and the previous deformation behaviour (to calculate the equivalent strain). The bending moment can be determined when the tangential stress distribution across the sheet is known.

$$M = \int_{r_i}^{r_y} \sigma_\phi r dr = \frac{r_y^2 - r_i^2}{2} \int_0^1 \sigma_\phi d\lambda$$

Numerical calculation of

$$\int_0^1 \sigma_\phi dr$$

is straightforward. However, it was found that the calculation accuracy was very bad for small values of κ , i.e., large radii of curvature r . Calculation of the moment around the neutral layer instead of around the centre of curvature solved the problem. It can be shown, by differentiating (3.2.11), that

$$rdr = d\lambda \left(\frac{r_y^2 - r_i^2}{2} \right)$$

When we call $z = r - r_n$, $z_i = r_i - r_n$, $z_y = r_y - r_n$ then

$$M = \int_{z_i}^{z_y} \sigma_\phi z dz$$

$$dz = dr$$

$$zdz = d\lambda \left(\frac{r_y^2 - r_i^2}{2} \right) - r_n \frac{d\lambda}{r} \left(\frac{r_y^2 - r_i^2}{2} \right)$$

Hence

$$M = \left(\frac{r_y^2 - r_i^2}{2} \right) \int_{z_i}^{z_y} \sigma_\phi \left(1 - \frac{r_n}{r} \right) d\lambda$$

in which r and r_n are expressed in function of λ .

VII.7 Program BENDING

A FORTRAN program to calculate the plane strain bending of laminated strainhardening sheet without Bauschinger effect, is listed below. Comments on the accuracy of this program can be found in Appendix IX.

APPENDIX VIII

BENDING OF A RIGID-PLASTIC STRAINHARDENING SHEET,
WITH BAUSCHINGER EFFECT AS SUGGESTED BY CRAFOORD

The rationale for the introduction of this simplified Bauschinger effect is given in CRAFOORD [33] and is also treated in Chapter 5. The solution method for a sheet with that behaviour follows the general solution method outlined in Chapter 3.

VIII.1 Stress-Strain Curve and Effective Yield Stress

As explained in Chapter 5, the stress-strain curve for layers to the inside of the neutral layer (zone II in figure 5.11) or to the outside of the unelongated layer (zone I) is

$$\bar{\sigma} = H(\bar{\epsilon}) \quad r_i \leq r \leq r_n \quad \text{zone II}$$

$$\bar{\sigma} = H(\bar{\epsilon}) \quad r_o \leq r \leq r_y \quad \text{zone I}$$

and for layers that are situated between neutral and unelongated layers (zone III),

$$\bar{\sigma} = H(\bar{\epsilon} = 0) \quad r_n \leq r \leq r_o \quad \text{zone III}$$

This was applied to two different types of strainhardening curves.

$$\text{type 1: } H_1(\bar{\epsilon}) = A + B\bar{\epsilon}^{-n} \quad (\text{VIII.1.1})$$

$$\text{type 2: } H_2(\bar{\epsilon}) = A(B + \bar{\epsilon})^n \quad (\text{VIII.1.2})$$

The effective yield stress for the different zones is then

$$\text{type 1: } \left. \begin{array}{l} \text{zone I} \\ \text{zone II} \end{array} \right\} \bar{\sigma} = A + B\bar{\epsilon}^n$$

$$\text{zone III } \bar{\sigma} = A$$

$$\text{type 2: } \left. \begin{array}{l} \text{zone I} \\ \text{zone II} \end{array} \right\} \bar{\sigma} = A(B + \bar{\epsilon})^n$$

$$\text{zone III } \bar{\sigma} = AB^n$$

VIII.2 Yield Condition and Equilibrium Equation

The general yield condition is

$$\sigma_\phi - \sigma_r = \frac{2}{\sqrt{3}} \bar{\sigma} \quad r_n < r \leq r_y \quad (3.2.3A)$$

$$\sigma_\phi - \sigma_r = \frac{2}{\sqrt{3}} \bar{\sigma} \quad r_i \leq r < r_n \quad (3.2.3B)$$

and the radial equilibrium equation for plane strain is

$$r \frac{d\sigma_r}{dr} = \frac{2}{\sqrt{3}} \bar{\sigma} \quad r_n \leq r \leq r_y \quad (3.2.1A)$$

$$r \frac{d\sigma_r}{dr} = -\frac{2}{\sqrt{3}} \bar{\sigma} \quad r_i \leq r \leq r_n \quad (3.2.1B)$$

VIII.2.1 Stress Strain Curve Type 1: $H_1(\bar{\epsilon}) = A + B\bar{\epsilon}^n$

The yield condition becomes

$$\left. \begin{aligned}
 \text{zone I} \quad \sigma_\phi - \sigma_r &= \frac{2}{\sqrt{3}} A + \frac{2}{\sqrt{3}} B\bar{\epsilon}^n & r_o \leq r \leq r_y \\
 \text{zone III} \quad \sigma_\phi - \sigma_r &= \frac{2}{\sqrt{3}} A & r_n < r \leq r_o \\
 \text{zone II} \quad \sigma_\phi - \sigma_r &= -\frac{2}{\sqrt{3}} A - \frac{2}{\sqrt{3}} B\bar{\epsilon}^n & r_i \leq r < r_n
 \end{aligned} \right\} \quad (\text{VIII.2.1})$$

(3.2.2) and (3.2.6) together yield

$$\left. \begin{aligned}
 \text{zone I} \quad \bar{\epsilon} &= \frac{2}{\sqrt{3}} \epsilon_\phi = \frac{2}{\sqrt{3}} \ell_n \frac{r}{r_o} & r_o \leq r \leq r_y \\
 \text{zone II} \quad \bar{\epsilon} &= -\frac{2}{\sqrt{3}} \epsilon_\phi = -\frac{2}{\sqrt{3}} \ell_n \frac{r}{r_o} & r_i \leq r \leq r_n
 \end{aligned} \right\} \quad (\text{VIII.2.2})$$

$\bar{\epsilon}$ in zone III is not needed, since the yield condition in zone III is independent of $\bar{\epsilon}$. This is a great simplification in comparison with a strainhardening material without this simplified Bauschinger effect. In such a material the value of $\bar{\epsilon}$ for the layers that have undergone a strain reversal is difficult to determine. It will be seen that since $\bar{\sigma}$ is assumed to be independent of $\bar{\epsilon}$ in zone III the resulting analysis is very much simplified. Substitution of the values for the effective strain $\bar{\epsilon}$ for zones I and II in (VII.2.1) leads to

$$\left. \text{zone I} \quad \sigma_\phi - \sigma_r = \frac{2}{\sqrt{3}} A + \frac{2}{\sqrt{3}} B \left(\frac{2}{\sqrt{3}} \ell_n \frac{r}{r_o} \right)^n \quad r_o \leq r \leq r_y \right\}$$

$$\begin{array}{l}
 \text{zone II } \sigma_{\phi} - \sigma_r = \frac{2}{\sqrt{3}} A \quad r_n < r \leq r_o \\
 \text{zone III } \sigma_{\phi} - \sigma_r = -\frac{2}{\sqrt{3}} A - \frac{2}{\sqrt{3}} B \left(\frac{2}{\sqrt{3}} \ell_n \frac{r}{r_o} \right)^n \quad r_i \leq r < r_n
 \end{array} \quad \left. \vphantom{\begin{array}{l} \text{zone II} \\ \text{zone III} \end{array}} \right\} \text{(VIII.2.3)}$$

Substituting

$$\begin{array}{l}
 \alpha = \frac{2}{\sqrt{3}} A \\
 \beta = \frac{2}{\sqrt{3}} B \left(\frac{2}{\sqrt{3}} \right)^n = B \left(\frac{2}{\sqrt{3}} \right)^{n+1}
 \end{array} \quad \left. \vphantom{\begin{array}{l} \alpha \\ \beta \end{array}} \right\} \text{(VIII.2.4)}$$

in (VIII.2.3) simplifies these expressions to

$$\begin{array}{l}
 \text{zone I } \sigma_{\phi} - \sigma_r = \alpha + \beta \left(\ell_n \frac{r}{r_o} \right)^n \quad r_o \leq r \leq r_y \\
 \text{zone II } \sigma_{\phi} - \sigma_r = \alpha \quad r_n < r \leq r_o \\
 \text{zone III } \sigma_{\phi} - \sigma_r = -\alpha - \beta \left(-\ell_n \frac{r}{r_o} \right)^n \quad r_i \leq r < r_n
 \end{array} \quad \left. \vphantom{\begin{array}{l} \text{zone I} \\ \text{zone II} \\ \text{zone III} \end{array}} \right\} \text{(VIII.2.5)}$$

The combined yield condition-equilibrium equations (3.2.1A) and (3.2.1B) are for this case

$$\begin{array}{l}
 \text{zone I } r \frac{d\sigma_r}{dr} = \alpha + \beta \left(\ell_n \frac{r}{r_o} \right)^n \quad r_o \leq r \leq r_y \\
 \text{zone III } r \frac{d\sigma_r}{dr} = \alpha \quad r_n \leq r \leq r_o \\
 \text{zone II } r \frac{d\sigma_r}{dr} = -\alpha - \beta \left(-\ell_n \frac{r}{r_o} \right)^n \quad r_i \leq r \leq r_n
 \end{array} \quad \left. \vphantom{\begin{array}{l} \text{zone I} \\ \text{zone III} \\ \text{zone II} \end{array}} \right\} \text{(VIII.2.6)}$$

VIII.2.2 Stress Strain Curve Type 2: $H_2(\bar{\epsilon}) = A(B + \bar{\epsilon})^n$

The yield condition is

$$\begin{array}{ll}
 \text{zone I} & \sigma_\phi - \sigma_r = \frac{2}{\sqrt{3}} A(B + \bar{\epsilon})^n & r_o \leq r \leq r_y \\
 \text{zone III} & \sigma_\phi - \sigma_r = \frac{2}{\sqrt{3}} AB^n & r_n < r \leq r_o \\
 \text{zone II} & \sigma_\phi - \sigma_r = -\frac{2}{\sqrt{3}} A(B + \bar{\epsilon})^n & r_i \leq r < r_n
 \end{array} \quad \left. \vphantom{\begin{array}{l} \text{zone I} \\ \text{zone III} \\ \text{zone II} \end{array}} \right\} \text{(VIII.2.7)}$$

Using (VIII.2.2) and substituting

$$\begin{array}{l}
 \alpha = \frac{2}{\sqrt{3}} A \left(\frac{2}{\sqrt{3}} \right)^n = A \left(\frac{2}{\sqrt{3}} \right)^{n+1} \\
 \beta = \frac{\sqrt{3}}{2} B
 \end{array} \quad \left. \vphantom{\begin{array}{l} \alpha \\ \beta \end{array}} \right\} \text{(VIII.2.8)}$$

in (VIII.2.7) gives

$$\begin{array}{ll}
 \text{zone I} & \sigma_\phi - \sigma_r = \alpha \left(\beta + \ell_n \frac{r}{r_o} \right)^n & r_o \leq r \leq r_y \\
 \text{zone III} & \sigma_\phi - \sigma_r = \alpha \beta^n & r_n < r \leq r_o \\
 \text{zone II} & \sigma_\phi - \sigma_r = -\alpha \left(\beta - \ell_n \frac{r}{r_o} \right)^n & r_i \leq r < r_n
 \end{array} \quad \left. \vphantom{\begin{array}{l} \text{zone I} \\ \text{zone III} \\ \text{zone II} \end{array}} \right\} \text{(VIII.2.9)}$$

The combined yield condition-equilibrium equations are then

$$\text{zone I} \quad r \frac{d\sigma_r}{dr} = \alpha \left(\beta + \ell_n \frac{r}{r_o} \right)^n \quad r_o \leq r \leq r_y$$

$$\begin{array}{ll}
 \text{zone III } r \frac{d\sigma_r}{dr} = \alpha\beta^n & r_n \leq r \leq r_o \\
 \text{zone II } r \frac{d\sigma_r}{dr} = -\alpha\left(\beta - \lambda_n \frac{r}{r_o}\right)^n & r_i \leq r \leq r_n
 \end{array} \quad \left. \vphantom{\begin{array}{l} \text{zone III} \\ \text{zone II} \end{array}} \right\} \text{(VIII.2.10)}$$

VIII.3 Initial Conditions

The initial conditions for the integration of the sheet thickness equation are known, namely

$$\kappa = 0$$

$$\eta = 1$$

$$\rho = 1$$

Since the tensile and compressive stress-strain curves are identical, the neutral layer at the beginning of the bending coincides with the central layer. Thus

$$\lambda_n = 0.5$$

The tangential stress at the commencement of bending is, for stress-strain curve of type 1,

$$\sigma_\phi = +\alpha \quad \lambda > \lambda_n$$

$$\sigma_\phi = -\alpha \quad \lambda < \lambda_n$$

and, hence, the original bending moment is

$$M = \int_{r_i}^{r_y} \sigma_{\phi} r dr = t_o^2 \int_0^1 \sigma_{\phi} \lambda d\lambda = t_o^2 \frac{\alpha}{4}$$

For a stress-strain curve of type 2, the tangential stress at the beginning of the bending is

$$\sigma_{\phi} = + \alpha \beta^n \quad \lambda > \lambda_n$$

$$\sigma_{\phi} = - \alpha \beta^n \quad \lambda > \lambda_n$$

and the original bending moment is

$$M = t_o^2 \frac{\alpha \beta^n}{4}$$

VIII.4 Solution Method

The general method of approach explained in Section 3.2.8 is used here. The variables κ , η and ρ are used to characterise the bend. The sheet thickness equation to integrate is

$$\frac{d\eta}{d\kappa} = - \frac{1}{2} \frac{\eta}{\kappa} \left(\frac{1 - \frac{\kappa^2}{4}}{\eta^2 \rho^2} - 1 \right) \quad (3.2.19)$$

The second dependent variable ρ will be determined by integrating (VIII.2.6) or (VIII.2.10) along the sheet thickness, and requiring that the radial stress at the neutral layer be unique. Formulas will be given for the two stress strain curves used.

VIII.4.1 Solution With Stress-Strain Curve Type 1: $H_1(\bar{\epsilon}) = A + B\bar{\epsilon}^n$

The combined yield condition-equilibrium equations that apply are equations (VIII.2.6). Integration of the equation that applies in zone I, with boundary condition

$$(\sigma_r)_{r=r_y} = 0$$

gives

$$\begin{aligned} \sigma_r^I = \alpha \ell_n \frac{r}{r_y} + \frac{\beta}{n+1} \left(\ell_n \frac{r}{r_o} \right)^{n+1} \\ - \frac{\beta}{n+1} \left(\ell_n \frac{r_y}{r_o} \right)^{n+1} \end{aligned} \quad \text{(VIII.4.1)}$$

The radial stress at the unelongated layer is

$$(\sigma_r^I)_{r=r_o} = \alpha \ell_n \frac{r_o}{r_y} - \frac{\beta}{n+1} \left(\ell_n \frac{r_y}{r_o} \right)^{n+1}$$

Integration of equation (VIII.2.6) applicable in zone III, with boundary condition

$$(\sigma_r^{III})_{r=r_o} = (\sigma_r^I)_{r=r_o}$$

yields

$$\sigma_r^{III} = \alpha \ell_n \frac{r}{r_y} - \frac{\beta}{n+1} \left(\ell_n \frac{r}{r_o} \right)^{n+1} \quad \text{(VIII.4.2)}$$

The radial stress at the neutral layer is

$$(\sigma_r^{III})_{r=r_n} = \alpha \ell_n \frac{r_n}{r_y} - \frac{\beta}{n+1} (\ell_n \frac{r_y}{r_o})^{n+1} \quad (\text{VIII.4.3})$$

Integration of equation (VIII.2.6) in zone II, with boundary condition

$$(\sigma_r^{II})_{r=r_i} = 0$$

results in

$$\sigma_r^{II} = -\alpha \ell_n \frac{r}{r_i} + \frac{\beta}{n+1} (-\ell_n \frac{r}{r_o})^{n+1} - \frac{\beta}{n+1} (-\ell_n \frac{r_i}{r_o})^{n+1} \quad (\text{VIII.4.4})$$

The radial stress at the neutral layer is then also given by

$$(\sigma_r^{II})_{r=r_n} = -\alpha \ell_n \frac{r_n}{r_i} + \frac{\beta}{n+1} (-\ell_n \frac{r_n}{r_o})^{n+1} - \frac{\beta}{n+1} (-\ell_n \frac{r_i}{r_o})^{n+1} \quad (\text{VIII.4.5})$$

Since the radial stress at the neutral layer is continuous, (VIII.4.3)

and (VIII.4.5) must have the same value, so that

$$\alpha \ell_n \frac{r_n}{r_y} - \frac{\beta}{n+1} (\ell_n \frac{r_y}{r_o})^{n+1} = -\alpha \ell_n \frac{r_n}{r_i} + \frac{\beta}{n+1} (-\ell_n \frac{r_n}{r_o})^{n+1}$$

$$-\frac{\beta}{n+1} \left(-\ell_n \frac{r_i}{r_o} \right)^{n+1}$$

or

$$2\alpha \ell_n \frac{r_n}{r_o} - \alpha \ell_n \frac{r_y}{r_o} - \alpha \ell_n \frac{r_i}{r_o} - \frac{\beta}{n+1} \left(\ell_n \frac{r_y}{r_o} \right)^{n+1} \quad (\text{VIII.4.6})$$

$$-\frac{\beta}{n+1} \left(-\ell_n \frac{r_n}{r_o} \right)^{n+1} + \frac{\beta}{n+1} \left(-\ell_n \frac{r_i}{r_o} \right)^{n+1} = 0$$

Substituting $\rho = \frac{r_n}{r_o}$, and expressing all radii as a function of κ , η , ρ with the formulas (I.3), (I.4), (I.5) and (I.6), brings (VIII.4.6) in the following form.

$$2\alpha \ell_n \rho - \frac{\beta}{n+1} \left(-\ell_n \rho \right)^{n+1} - \alpha \left[\ell_n \frac{1 - \frac{\kappa}{2}}{\eta} + \ell_n \frac{1 + \frac{\kappa}{2}}{\eta} \right] \quad (\text{VIII.4.7})$$

$$+ \frac{\beta}{n+1} \left[\left(-\ell_n \left(\frac{1 - \frac{\kappa}{2}}{\eta} \right) \right)^{n+1} - \left(\ell_n \left(\frac{1 + \frac{\kappa}{2}}{\eta} \right) \right)^{n+1} \right] = 0$$

Equation (VIII.4.7) can be written as $g(\eta, \kappa, \rho) = 0$. Sheet thickness equation (3.2.19) is of the form $f(\eta, \kappa, \rho) = \frac{d\eta}{d\kappa}$. These two equations are sufficient to determine η and ρ is function of κ . For every value of η and κ , ρ is implicitly given by (VIII.4.7), and could be determined by solving (VIII.4.7) using an iterative procedure. It was decided, however, to convert the system (3.2.19), (VIII.4.7) to a system of two first order differential equations. This is done by differentiating (VIII.4.7) to κ . This gives

$$\begin{aligned}
\frac{dg(\eta, \kappa, \rho)}{d\kappa} = 0 &= [2\alpha + B(-\ell_n \rho)^n] \frac{1}{\rho} \frac{d\rho}{d\kappa} \\
&+ \frac{\alpha\kappa}{2(1 - \frac{\kappa^2}{4})} + \frac{\beta}{2(1 - \frac{\kappa^2}{2})} (-\ell_n \frac{1 - \frac{\kappa}{2}}{\eta})^n \\
&- \frac{\beta}{2(1 + \frac{\kappa}{2})} (\ell_n \frac{1 + \frac{\kappa}{2}}{\eta})^n \\
&+ \frac{1}{\eta} \frac{d\eta}{d\kappa} [2\alpha + B(-\ell_n \frac{1 - \frac{\kappa}{2}}{\eta})^n \\
&\quad + B(\ell_n \frac{1 + \frac{\kappa}{2}}{\eta})^n]
\end{aligned}$$

$\frac{d\rho}{d\kappa}$ can now be expressed as a function of $\frac{d\eta}{d\kappa}$, η , κ , ρ . The system of two differential equations of first order that has to be solved is

$$\left\{ \begin{aligned} \frac{d\eta}{d\kappa} &= -\frac{1}{2} \frac{\eta}{\kappa} \left(\frac{1 - \frac{\kappa^2}{4}}{\eta^2 \rho^2} - 1 \right) \end{aligned} \right. \quad (3.2.19)$$

$$\left\{ \begin{aligned} \frac{d\rho}{d\kappa} &= \frac{-\rho h(\eta, \kappa, \rho)}{2\alpha + \beta(-\ell_n \rho)^n} \end{aligned} \right. \quad (VIII.4.8)$$

with

$$\begin{aligned}
h(\eta, \kappa, \rho) &= \frac{\alpha\kappa}{2 - \frac{\kappa}{2}} + \frac{\beta}{2 - \kappa} (-\ell_n \frac{1 - \frac{\kappa}{2}}{\eta})^n \\
&\quad - \frac{\beta}{2 + \kappa} (\ell_n \frac{1 + \frac{\kappa}{2}}{\eta})^n
\end{aligned}$$

$$-\frac{1}{2} \frac{1}{\kappa} \left(\frac{1 - \frac{\kappa^2}{4}}{\eta^2 \rho^2} - 1 \right) 2\alpha + \beta \left(-\ell_n \frac{1 - \frac{\kappa}{2}}{\eta} \right)^n$$

$$+ \beta \left(\ell_n \frac{1 + \frac{\kappa}{2}}{\eta} \right)^n$$

This system of two differential equations (3.2.19) and (VIII.4.8) will be solved using a Runge-Kutta numerical integration technique.

Say that the system to solve is

$$\left\{ \begin{array}{l} \frac{dy}{dx} = F(x, y, z) \\ \frac{dz}{dx} = G(x, y, z) \end{array} \right.$$

Take as starting point x, y, z and h as step size for integration to x .

Compute then the following values

$$k_1 = hF(x, y, z)$$

$$\ell_1 = hG(x, y, z)$$

$$k_2 = hF\left(x + \frac{1}{2}h, y + \frac{1}{2}k_1, z + \frac{1}{2}\ell_1\right)$$

$$\ell_2 = hG\left(x + \frac{1}{2}h, y + \frac{1}{2}k_1, z + \frac{1}{2}\ell_1\right)$$

$$k_3 = hF\left(x + \frac{1}{2}h, y + \frac{1}{2}k_2, z + \frac{1}{2}\ell_2\right)$$

$$\ell_3 = hG\left(x + \frac{1}{2}h, y + \frac{1}{2}k_2, z + \frac{1}{2}\ell_2\right)$$

$$k_4 = hF(x + h, y + k_3, z + \ell_3)$$

$$\ell_4 = hG (x + h, y + k_3, z + \ell_3)$$

$$\kappa = \frac{1}{6} (k_1 + 2k_2 + 2k_3 + k_4)$$

$$\ell = \frac{1}{6} (k_1 + 2k_2 + 2k_3 + k_4)$$

Then the new calculated point is $x + h, y + k, z + \ell$. This point is used as starting point for the next integration step, etc. This technique can be applied to the system (3.2.19), (VIII.4.8) by putting $\kappa = x, \eta = y, \rho = z$. The initial conditions are known, namely $\kappa = 0, \eta = 1$ and $\rho = 1$.

VIII.4.2 Solution with Stress-Strain Curve Type 2: $H_2(\bar{\epsilon}) = A(B + \bar{\epsilon})^n$

The derivation is exactly of the same type as the one used for the stress-strain curve type 1 given in Section VIII.4.1. Only the most important equations will be given. The equations to integrate are (VIII.2.10). Integration in the different zones yields

$$\sigma_r^I = \frac{\alpha}{n+1} \left(\beta + \ell_n \frac{r}{r_0} \right)^{n+1} - \frac{\alpha}{n+1} \left(\beta + \ell_n \frac{r_1}{r_0} \right)^{n+1} \quad (\text{VIII.4.9})$$

$$\sigma_r^{III} = \alpha \beta^n \ell_n \frac{r}{r_0} + \frac{\alpha}{n+1} \beta^{n+1} - \frac{\alpha}{n+1} \left(\beta + \ell_n \frac{r_1}{r_0} \right)^{n+1} \quad (\text{VIII.4.10})$$

$$\sigma_r^{II} = \frac{\alpha}{n+1} \left(\beta - \ell_n \frac{r}{r_0} \right)^{n+1} - \frac{\alpha}{n+1} \left(\beta - \ell_n \frac{r_1}{r_0} \right)^{n+1} \quad (\text{VIII.4.11})$$

The radial stress at the neutral layer is continuous, hence

$$(\sigma_r^{II})_{r=r_n} = (\sigma_r^{III})_{r=r_n}$$

or

$$\alpha \beta^n \ell_n \frac{r_n}{r_o} + \frac{\alpha}{n+1} \beta^{n+1} - \frac{\alpha}{n+1} \left(\beta + \ell_n \frac{r_y}{r_o} \right)^{n+1} =$$

$$\frac{\alpha}{n+1} \left(\beta - \ell_n \frac{r_n}{r_o} \right)^{n+1} - \frac{\alpha}{n+1} \left(\beta - \ell_n \frac{r_i}{r_o} \right)^{n+1}$$

Expressing all radii in function of κ , η , ρ yields

$$0 = g(\eta, \kappa, \rho) = -\alpha \beta^n \ell_n \rho + \frac{\alpha}{n+1} (\beta - \ell_n \rho)^{n+1}$$

$$- \frac{\alpha}{n+1} \beta^{n+1} + \frac{\alpha}{n+1} \left(\beta + \ell_n \frac{1 + \frac{\kappa}{2}}{\eta} \right)^{n+1}$$

$$- \frac{\alpha}{n+1} \left(\beta - \ell_n \frac{1 - \frac{\kappa}{2}}{\eta} \right)^{n+1}$$

Differentiation of this expression to κ , and expression of $\frac{d\rho}{d\kappa}$ in function of $\frac{d\eta}{d\kappa}$, κ , η , ρ leads to the differential equation (VIII.4.12). The system of two differential equations, (3.2.19) and (VIII.4.12) is solved in a similar way as the system arrived at in Section VIII.4.1. The system of differential equations is

$$\left\{ \begin{array}{l} \frac{d\eta}{d\kappa} = -\frac{1}{2} \frac{\eta}{\kappa} \left(\frac{1 - \frac{\kappa^2}{4}}{\eta^2 \rho^2} - 1 \right) \quad (3.2.19) \\ \frac{d\rho}{d\kappa} = \frac{\rho h(\eta, \kappa, \rho)}{\beta^n + (\beta - \ell_n \rho)^n} \quad (VIII.4.12) \end{array} \right.$$

with

$$h(\eta, \kappa, \rho) = (\beta + \ell_n \frac{1 + \frac{\kappa}{2}}{\eta})^n \left[\frac{1}{2 + \kappa} + \frac{1}{2\kappa} \left(\frac{1 - \frac{\kappa^2}{4}}{\eta^2 \rho^2} - 1 \right) \right] \\ + (\beta - \ell_n \frac{1 - \frac{\kappa}{2}}{\eta})^n \left[\frac{1}{\kappa - 2} + \frac{1}{2\kappa} \left(\frac{1 - \frac{\kappa^2}{4}}{\eta^2 \rho^2} - 1 \right) \right]$$

VIII.5 Stress Distributions and Bending Moment

VIII.5.1 Stress-Strain Curve Type 1: $H_1(\bar{\epsilon}) = A + B\bar{\epsilon}^n$

The radial stresses across the sheet thickness are given by (VIII.4.1), (VIII.4.2) and (VIII.4.4). All the radii in these formulas can be easily expressed in function of κ , η , ρ , which are known after solving a system of two differential equations, as indicated in Section VIII.4. The tangential stresses across the sheet thickness are then also known. They are

$$\left. \begin{array}{ll} \text{zone I} & \sigma_{\phi}^I = \sigma_r^I + \alpha + \beta \left(\ell_n \frac{r}{r_0} \right)^n & r_0 \leq r \leq r_y \\ \text{zone III} & \sigma_{\phi}^{III} = \sigma_r^{III} + \alpha & r_n < r \leq r_0 \\ \text{zone II} & \sigma_{\phi}^{II} = \sigma_r^{II} - \alpha - \beta \left(-\ell_n \frac{r}{r_0} \right)^n & r_i \leq r < r_n \end{array} \right\} \quad \text{(VIII.5.1)}$$

The bending moment can be determined by

$$M = \int_{r_i}^{r_y} \sigma_{\phi} r dr \quad \text{(VIII.5.2)}$$

It can be seen that this equation will contain terms of the type

$$\int \left(\beta_n \frac{r}{r_0} \right)^n r dr$$

When n is an integer number, these integrals can be solved by partial integration. But since n , the strainhardening index, is a material constant, n is in general not an integer. In that case, partial integration results in an infinite series. For that reason, the bending moment is calculated numerically. The integral of $\sigma_\phi(r)$ across the sheet thickness is calculated by dividing the distance between inner and outer sheet radius in about a hundred equal intervals, calculating the tangential stress at the end points of these intervals and applying the trapezium rule. This yields the bending moment, M .

VIII.5.2 Stress-Strain Curve Type 2: $H_2(\bar{\epsilon}) = A(B + \bar{\epsilon})^n$

The radial stresses across the sheet thickness are given by (VIII.4.9), (VIII.4.10) and (VIII.4.11). The tangential stresses are

$$\left. \begin{array}{ll} \text{zone I} & \sigma_\phi^I = \sigma_r^I + \alpha \left(\beta + \beta_n \frac{r}{r_0} \right)^n \quad r_0 \leq r \leq r_y \\ \text{zone III} & \sigma_\phi^{III} = \sigma_r^{III} + \alpha \beta^n \quad r_n < r \leq r_0 \\ \text{zone II} & \sigma_\phi^{II} = \sigma_r^{II} - \alpha \left(\beta - \beta_n \frac{r}{r_0} \right)^n \quad r_i \leq r < r_n \end{array} \right\} \quad \text{(VIII.5.3)}$$

The bending moment can again be determined by equation (VIII.5.2). The same remark as made in Section VIII.5.2 applies here, and numerical calculations of the bending moment is required.

VIII.6 Program MONOSH

The following program performs all the calculations required for the solution of the bending of a rigid-plastic strainhardening sheet, with Bauschinger effect as suggested by Crafoord. The accuracy of the program will be discussed in Appendix IX.

APPENDIX IX

ACCURACY OF COMPUTER PROGRAMS

A rigorous analytic solution for the pure bending of a rigid-plastic material is, up to now, only known for the bending of a rigid-nonstrainhardening monometal. The solution for that case is treated in Appendix III. As a first check on the accuracy of the different computing methods used in the programs BINSH, TRINSH, BENDING and MONOSH, the bending of a single nonstrainhardening sheet was calculated. The results of these calculations are shown in Table IX.1. It is seen that all programs give a correct solution to this bending problem with a high degree of accuracy. The only values that deviate substantially from the correct ones are the bending moments calculated by the program MONOSH. In that program, the bending moment is calculated numerically around the centre of curvature of the bend. The moment is arrived at by taking the difference of two quantities determined by numerical integration, thus the error of the difference is likely to exceed the error of the individual integrals. When the moment is calculated around the neutral layer, the moment is the sum of the two integrals, and these increase in relative error does not occur. Improvement of the moment calculations in MONOSH can be arrived at by using the same technique as used in BENDING (see Appendix VII).

The bending of a nonstrainhardening bimetal was calculated with programs BINSH, TRINSH and BENDING. The influence of the step size of the relative curvature, κ , when calculating the sheet thickness variation

was checked for program BINSH, while programs TRINSH and BENDING were used to evaluate the sheet thickness of the same bimetal with a single step size of 0.01. The results of these computations are shown in Table IX.2. It is seen that the accuracy of the computations increases with decreasing step size. The accuracy for program BINSH with a step size of 0.01 is sufficient for graphical representation of the bending behaviour, and hence this step size was used for the results presented in Chapter 4 on the bending of nonstrainhardening bimetals. It is also clear that programs TRINSH and BENDING give essentially the same bending behaviour as BINSH for this case.

The bending of a nonstrainhardening trimetal was computed with TRINSH and BENDING, and the results are presented in Table IX.3. The step size 0.01 for the relative curvature, κ , was used for the results presented in Chapter 4 on the bending of trimetals, and is seen from Table IX.3 to be sufficiently small for graphical presentation of results. Table IX.3 also shows that the difference between the results given by programs BENDING and TRINSH increases for higher values of the relative curvature κ . This is due to the fact that BENDING requires smaller step sizes than the other programs to give accurate results, as will be explained further.

Except for the nonstrainhardening monometal, the results of program MONOSH cannot be checked with other programs. The influence of the step size for the relative curvature κ on the results of strainhardening sheets with Crafoord Bauschinger effect can be seen in Table IX.4 and IX.5. It can be concluded that program MONOSH gives satisfactory results for even large step size. This cannot be said from the other programs. This is probably due to the inherent simplicity and elegance of the computing

method, which is much singler than in TRINSH or BENDING.

Finally, the influence of the **step size** for the relative curvature κ on the results for the bending of a strainhardening bimetal is featured in Table IX.6. As can be seen, small **step sizes** are required to get results with some accuracy. In addition to that, every step consumes much more computer time compared to the other programs. Therefore, a large amount of computer time must be used due to the method used to find the effective strain for layers in the sheet which have undergone a stress reversal. Furthermore, for those layers, the radial equilibrium equation has to be integrated numerically. It follows that the bigger the zone with stress reversal in the sheet, the more computer time consuming on integration step becomes. The small accuracy for big integration step sizes is also caused by the method for effective strain calculation. A small error in neutral layer position in the first integration steps will be retained in further calculations of the deformation process, causing an oscillation superimposed on the real values of the variables.

When the integration **step size** is not small, the amplitude of this oscillation can be bigger than the change in the variable value between different steps, so that results only can be determined by taking averages over different integration steps. This oscillation effect in the $\lambda_n - \kappa$ curve can be reduced to a negligible amount by decreasing the **step size**. However, this is only feasible to a certain extent since the computation time required increases very drastically. The author has tried to compromise by changing the integration step during the computations. At the commencement of the bending process, small steps are used, and these are gradually increased when κ increases. (The exact scheme used is given as note to Table IX.6). This variable **step size** scheme has the advantage that

the early bending behaviour is computed fairly accurate, while the results for κ -values above 1.0 are rather inaccurate (\pm 20 percent). The bending behaviour for high κ -values is only of theoretical interest, since it is very difficult to achieve bends of this severity in practice. Furthermore, these bends will not be uniform (see Crafoord [33]). The results given in Chapters 5 and 6 are calculated using the variable step size integration scheme, and the big step size used for $\kappa > 1.0$ explains why the bending moment is not very accurately known for these values of relative curvature.

TABLE IX.1

BENDING OF A NONSTRAINHARDENING MONOMETAL
CALCULATED BY DIFFERENT PROGRAMS*

κ	Computed Values				Computing Method (Program)
	η	ρ	λ _n	M/t ₀ ²	
.10	1	.998 749 218	.475	.288 675 1	analytical BINSH TRINSH BENDING MONOSH
	1.000 000 000	.998 749 218	.475 000 0	.288 675 1	
	1.000 000 0	.998 749 2	.474 999 4	.288 689 6	
	.999 974 5	.998 770 6	.474 959 4	.288 571 9	
	1.000 000	.998 749	.475 000	.274 250	
.50	1	.968 245 837	.375	.288 675 1	analytical BINSH TRINSH BENDING MONOSH
	1.000 000	.968 245 837	.375 000 0	.288 675 1	
	.999 999 7	.968 244 4	.374 996 7	.288 690 3	
	.999 841 1	.968 331 6	.374 868 1	.288 168 7	
	1.000 000	.968 246	.375 000	.274 474	
1.0	1	.866 025 404	.250	.288 675 1	analytical BINSH TRINSH BENDING MONOSH
	1.000 000 000	.866 025 404	.250 000 0	.288 675 1	
	.999 998 5	.866 017 2	.249 991 7	.288 693 3	
	.999 610 2	.866 320 3	.249 963 0	.287 503 0	
	1.000 000	.866 025	.250 000	.278 369	
1.50	1	.661 437 828	.125	.288 675 1	analytical BINSH TRINSH BENDING MONOSH
	1.000 000	.661 437 828	.125 000 0	.288 675 1	
	.999 994 1	.661 394 2	.124 979 0	.288 704 0	
	-	-	-	-	
	1.000 000 0	.661 438	.125 000	.283 451	

* Step size for the relative curvature in the integrations of the sheet thickness equation is .01. The effective yield stress $\bar{\sigma}$ is one. In programs BENDING and MONOSH, this is realised with the stress strain curve

$$\bar{\sigma} = 1 (1 + \bar{\epsilon})^{10-10}$$

TABLE IX.2

BENDING OF A NONSTRAINHARDENING BIMETAL*

κ	Computed Values							Step size $\Delta\kappa$	Computing Method	
	η			ρ			λ_n			M/t_o^2
.10	1.010	704	338	1.001	237	181	.607 762 2	.406 658 0	.1	BINSH
	1.011	759	354	1.000	193	137	"	.407 507 5	.05	"
	1.012	286	862	.999	671	931	"	.407 932 5	.025	"
	1.012	603	366	.999	359	469	"	.408 187 6	.01	"
	1.012	708	868	.999	255	358	"	.408 272 7	.005	"
	1.012	793	269	.999	172	085	"	.408 340 7	.001	"
	1.012	599	4	.999	363	3	.607 761 9	.408 198 3	.01	TRINSH
	1.012	588	9	.999	308	6	.607 094 8	.408 510 7	.01	BENDING
.50	1.068	280	294	.981	355	187	.536 563 7	.466 154 8	.1	BINSH
	1.069	395	410	.980	331	876	"	.467 128 5	.05	"
	1.069	952	967	.979	821	020	"	.467 615 7	.025	"
	1.070	287	502	.979	514	763	"	.467 908 2	.01	"
	1.070	399	013	.979	412	719	"	.468 005 7	.005	"
	1.070	488	222	.979	331	100	"	.468 083 7	.001	"
	1.070	267	8	.979	532	1	.536 562 2	.467 907 4	.01	TRINSH
	1.070	210	3	.979	209	8	.535 721 2	.468 250 2	.01	BENDING
1.00	1.148	222	561	.873	620	230	.378 115 3	.566 147 8	.1	BINSH
	1.149	431	612	.872	701	296	"	.567 340 7	.05	"
	1.150	036	146	.872	242	547	"	.567 937 7	.025	"
	1.150	395	733	.871	969	904	"	.568 292 9	.01	"
	1.150	515	859	.871	878	861	"	.568 411 6	.005	"
	-	-	-	-	-	-	-	-	.001	"
	1.150	392	4	.871	959	1	.378 099 8	.568 336 8	.01	TRINSH
	1.150	167	8	.869	566	6	.375 147 4	.566 933 1	.01	BENDING
1.50	1.213	290	233	.645	042	522	.183 333 3	.642 148 1	.1	BINSH
	1.214	567	798	.644	364	023	"	.643 501 1	.05	"
	1.215	206	590	.644	025	303	"	.644 178 2	.025	"
	1.215	586	555	.643	823	995	"	.644 581 1	.01	"
	1.215	713	488	.643	756	773	"	.644 715 7	.005	"
	-	-	-	-	-	-	-	-	.001	"
	1.215	610	6	.643	756	9	.183 298 9	.644 685 0	.01	TRINSH
	1.213	890	1	.638	073	7	.179 143 3	.637 036 8	.025	BENDING

*1-2 bimetal, with $\mu = 0.50$, $A_1 = 1$, $A_2 = 2$. In program BENDING, the stress strain curve used is $\bar{\sigma} = A (B + \bar{\epsilon})^n$ with $B = 1$, $n = 10^{-10}$ and $A = 1$ for laminate 1 on the inside of the bent sheet, and $A = 2$ for laminate 2.

TABLE IX.3

BENDING OF A NONSTRAINHARDENING TRIMETAL*

κ	Computed Values											Computing method			
	η	λ_n			ρ			M/t_o^2			Step size $\Delta\kappa$				
.10	1.007	489	4	.999	258	5	.555	150	6	.527	960	9	.1	TRINSH	
	1.008	245	1	.998	523	9	.555	297	1	.525	315	0	.05	"	
	1.008	622	7	.998	153	8	.555	334	3	.524	835	3	.025	"	
	1.008	849	0	.997	930	9	.555	344	8	.524	824	0	.01	"	
	1.008	924	4	.937	856	5	.555	346	3	.524	867	0	.005	"	
	1.008	984	7	.997	796	9	.555	346	8	.524	918	4	.001	"	
	1.008	893	7	.997	800	0	.554	464	0	.522	701	4	.01	BENDING	
.40	1.022	748	6	.964	436	7	.416	172	7	.557	646	2	.1	TRINSH	
	1.023	289	3	.964	178	2	.416	806	4	.554	405	4	.05	"	
	1.023	550	8	.963	995	8	.416	967	7	.553	713	3	.025	"	
	1.023	704	4	.963	869	2	.417	013	4	.553	603	2	.01	"	
	1.023	754	9	.963	824	2	.417	019	9	.553	618	2	.005	"	
	1.023	795	2	.963	787	1	.417	022	0	.553	649	0	.001	"	
	1.023	481	6	.963	960	4	.416	713	9	.550	387	2	.01	BENDING	
.80	1.011	731	2	.851	436	8	.238	783	4	.536	171	7	.1	TRINSH	
	1.012	011	8	.852	365	2	.240	043	9	.532	736	1	.05	"	
	1.012	094	9	.852	582	3	.240	366	6	.531	880	3	.025	"	
	1.012	135	2	.852	632	3	.240	458	2	.531	651	6	.01	"	
	1.012	145	9	.852	635	5	.240	471	4	.531	623	7	.005	"	
	-	-	-	-	-	-	-	-	-	-	-	-	-	.001	"
	1.001	629	1	.852	269	0	.239	596	6	.526	705	3	.01	BENDING	
1.50	.939	712	4	.615	239	0	.090	584	9	.422	297	9	.1	TRINSH	
	.939	816	6	.617	599	7	.091	466	5	.420	002	0	.05	"	
	.940	312	8	.617	930	9	.091	705	7	.419	794	9	.025	"	
	.940	443	3	.618	038	9	.091	776	3	.419	719	3	.01	"	
	.940	459	2	.618	056	9	.019	786	7	.419	705	2	.005	"	
	-	-	-	-	-	-	-	-	-	-	-	-	-	.007	"
	.937	735	4	.612	350	9	.089	077	4	.406	476	5	.25	BENDING	

* 2-1-2 TRIMETAL, with $\mu_{21} = .20$ and $\mu_{31} = .60$

In BENDING, the stress-strain curve $\bar{\sigma} = A (B + \bar{\epsilon})^n$ is used, with $B = 1$ and $n = 10^{-10}$, and $A = 2$ for laminates 1 and 3, and $A = 1$ for laminate 2.

TABLE IX.4
 BENDING OF STRAIN HARDENING MONOMETAL WITH
 CRAFOORD BAUSCHINGER EFFECT AND STRESS STRAIN
 CURVE $\bar{\sigma} = 1 (0.01 + \bar{\epsilon})^{0.5}$
 (PROGRAM MONOSH)

κ	Computed Values				Step size $\Delta\kappa$
	η	ρ	λ_n	M/t_0^2	
.10	.998 959	.999 306	.470 167	-	.1
	.999 484	.998 119	.463 566	-	.05
	.999 514	.998 060	.463 281	-	.025
	.999 516	.998 055	.463 258	.060 4062	.01
	.999 517	.998 055	.463 256	-	.005
	.999 517	.998 055	.463 256	-	.001
.40	.988 482	.967 654	.343 637	-	.1
	.988 575	.967 528	.343 552	-	.05
	.988 582	.967 517	.343 543	-	.025
	.988 583	.967 517	.343 542	.108 546	.01
	.988 583	.967 517	.343 542	-	.005
	.988 583	.967 517	.343 542	-	.001
.80	.950 806	.873 685	.206 295	-	.1
	.950 869	.873 618	.206 285	-	.05
	.950 875	.873 612	.206 284	-	.025
	.950 875	.873 611	.206 284	.140793	.01
	.950 875	.873 611	.206 284	-	.005
	.950 875	.873 611	.206 284	-	.001
1.50	.799 544	.546 704	.042 856 2	-	.1
	.799 578	.546 694	.042 859 3	-	.05
	.799 581	.546 692	.042 859 5	-	.025
	.799 582	.546 692	.042 859 5	.138206	.01
	.799 582	.546 692	.042 859 5	-	.001

TABLE IX.5

BENDING OF STRAINHARDENING MONOMETAL
 WITH CRAFOORD BAUSCHINGER EFFECT AND
 STRESS-STRAIN CURVE $\bar{\sigma} = 1 + 1\bar{\epsilon}^{0.5}$
 (PROGRAM MONOSH)

κ	Computed Values				Step size $\Delta\kappa$
	η	ρ	λ_n	M/t_o^2	
.10	.999 852	.998 631	.472 342	-	.1
	.999 886	.998 606	.472 432	-	.05
	.999 893	.998 600	.472 440	-	.025
	.999 894	.998 598	.472 440	.326 924	.01
	.999 894	.998 598	.472 440	-	.005
	.999 895	.998 598	.472 440	-	.001
.40	.996 974	.975 856	.383 174	-	.1
	.997 019	.975 812	.383 177	-	.05
	.997 027	.975 805	.383 176	-	.025
	.997 028	.975 803	.383 176	.377 821	.01
	.997 028	.975 803	.383 175	-	.005
	.997 028	.975 803	.383 175	-	.001
.80	.984 325	.897 207	.262 464	-	.1
	.984 369	.897 165	.262 461	-	.05
	.984 376	.897 157	.262 461	-	.025
	.984 377	.897 156	.262 460	.411 756	.01
	.984 378	.897 156	.262 460	-	.005
	.984 378	.897 156	.262 460	-	.001
1.50	.920 367	.584 132	.075 5103	-	.1
	.920 405	.584 110	.075 5108	-	.05
	.920 410	.584 106	.075 5107	-	.025
	.920 411	.584 105	.075 5107	.402896	.01
	.920 412	.584 105	.075 5107	-	.005
	-	-	-	-	.001

TABLE IX.6

BENDING OF STRAINHARDENING
BIMETAL* (PROGRAM BENDING)

κ	Computed Values				Step size** $\Delta\kappa$
	η	ρ	λ_n	M/t_o^2	
.05	1.004 926 4	.997 988 2	.551 929 5	.149 607 9	.05
	1.003 387 3	.995 885 0	.478 922 5	.150 787 3	.025
	1.003 874 4	.997 205 6	.515 144 9	.150 848 6	.01
	1.003 974 7	.996 752 9	.508 047 7	.150 973 9	.005
	1.004 294 6	.996 651 8	.512 399 2	.151 492 7	.001
	1.004 274 7	.996 759 7	.514 169 8	.151 492 7	VAR
.10	1.004 123 9	.993 738 8	.465 892 0	.178 928 6	.1
	1.003 696 9	.991 869 1	.442 959 0	.178 685 1	.05
	1.004 260 6	.994 346 1	.473 336 1	.179 771 8	.025
	1.004 473 9	.994 356 7	.475 560 3	.179 829 5	.01
	1.004 592 5	.994 161 5	.474 780 5	.179 892 3	.005
	1.004 834 8	.993 958 1	.475 144 1	.180 285 2	VAR
.20	1.001 092 9	.986 603 8	.413 789 5	.216 322 4	.1
	1.003 220 9	.986 920 9	.425 743 2	.218 293 6	.05
	1.003 681 6	.987 646 9	.431 605 0	.218 783 9	.025
	1.003 775 6	.987 578 6	.431 725 2	.218 814 2	.01
	1.003 953 3	.988 037 7	.434 880 8	.219 034 0	.005
	1.004 176 3	.988 089 3	.436 230 8	.319 365 5	VAR
.50	.992 490 3	.951 919 3	.330 091 6	.285 593 6	.1
	.994 270 7	.952 282 9	.333 981 3	.287 418 5	.05
	.994 901 6	.951 185 8	.333 052 3	.287 617 0	.025
	.995 028 5	.951 055 5	.333 035 4	.287 687 7	.01
	.995 097 3	.954 228 7	.339 146 1	.288 845 1	VAR
1.00	.960 950 5	.818 165 1	.184 068 0	.331 061 1	.1
	.964 638 9	.825 166 4	.191 798 2	.338 137 8	.05
	.965 675 4	.829 087 2	.195 503 5	.340 923 3	.025
	.964 740 6	.837 778 6	.201 625 2	.343 702 0	VAR
1.50	.915 213 7	.587 838 9	.075 647 4	.339 888 6	.05
	.909 669 3	.555 537 1	.064 294 6	.317 581 0	VAR

* The stress strain curve used is $\bar{\sigma} = A (B + \bar{\epsilon})^n$ with
 $A = 1.8$, $B = 10^{-10}$, $n = .36$ for inside laminate 1.
 $A = 2.0$, $B = .09$, $n = .43$ for outside laminate 2.

The laminate boundary is defined by $\mu_{21} = .82$.

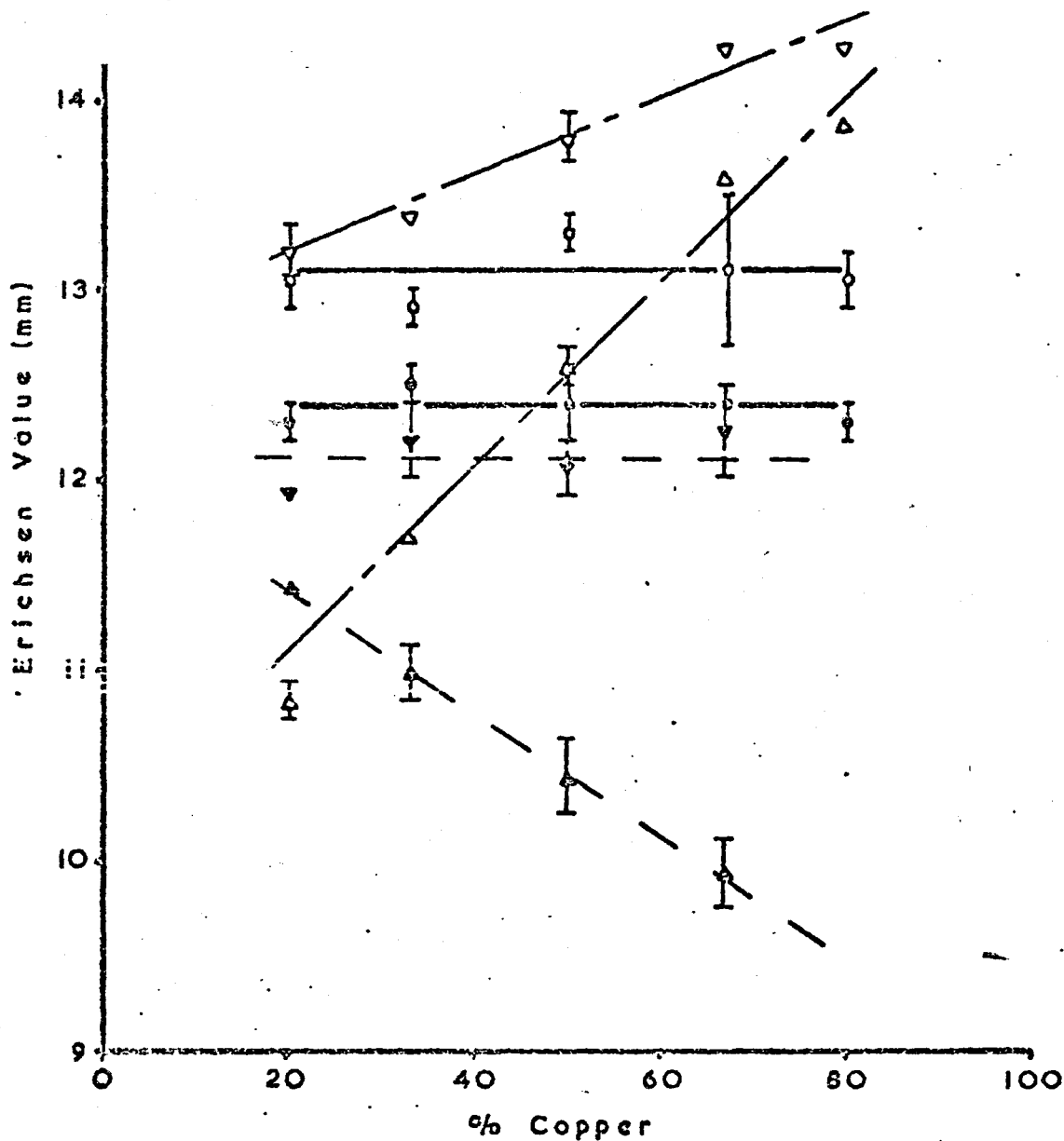
Table IX.6 (continued)

** A constant stepsize is used if a numerical value is given.
A variable stepsize is used when VAR is indicated in the column.
The following stepsize scheme was used.

$\Delta\kappa = .0005$	0	$< \kappa < .002$
.0010	.002	$< \kappa < .01$
.0025	.01	$< \kappa < .02$
.0050	.02	$< \kappa < .05$
.010	.05	$< \kappa < .10$
.025	.10	$< \kappa < .50$
.05	.50	$< \kappa < 1.00$
.10	1.00	$< \kappa < 2.0$

VARIATION OF ERICHSEN VALUE WITH PER CENT COPPER AND SHEET THICKNESS FOR THE ROLL BONDED COPPER-MILD STEEL BIMETALS

from Hawkins and Wright [20]



- Copper on outside.
- Steel on outside.
- △△ Results on copper or steel components respectively.
- ▽▽ Results corrected to 1.83 m.m's (0.072 ins.)

fig 1.1

THICKNESS SURVEYS ON CUPS DRAWN FROM 65 mm DIAMETER BLANKS

from Hawkins and Wright [20]

50% copper - 50% steel bimetal

25%-50%-25% trimetal

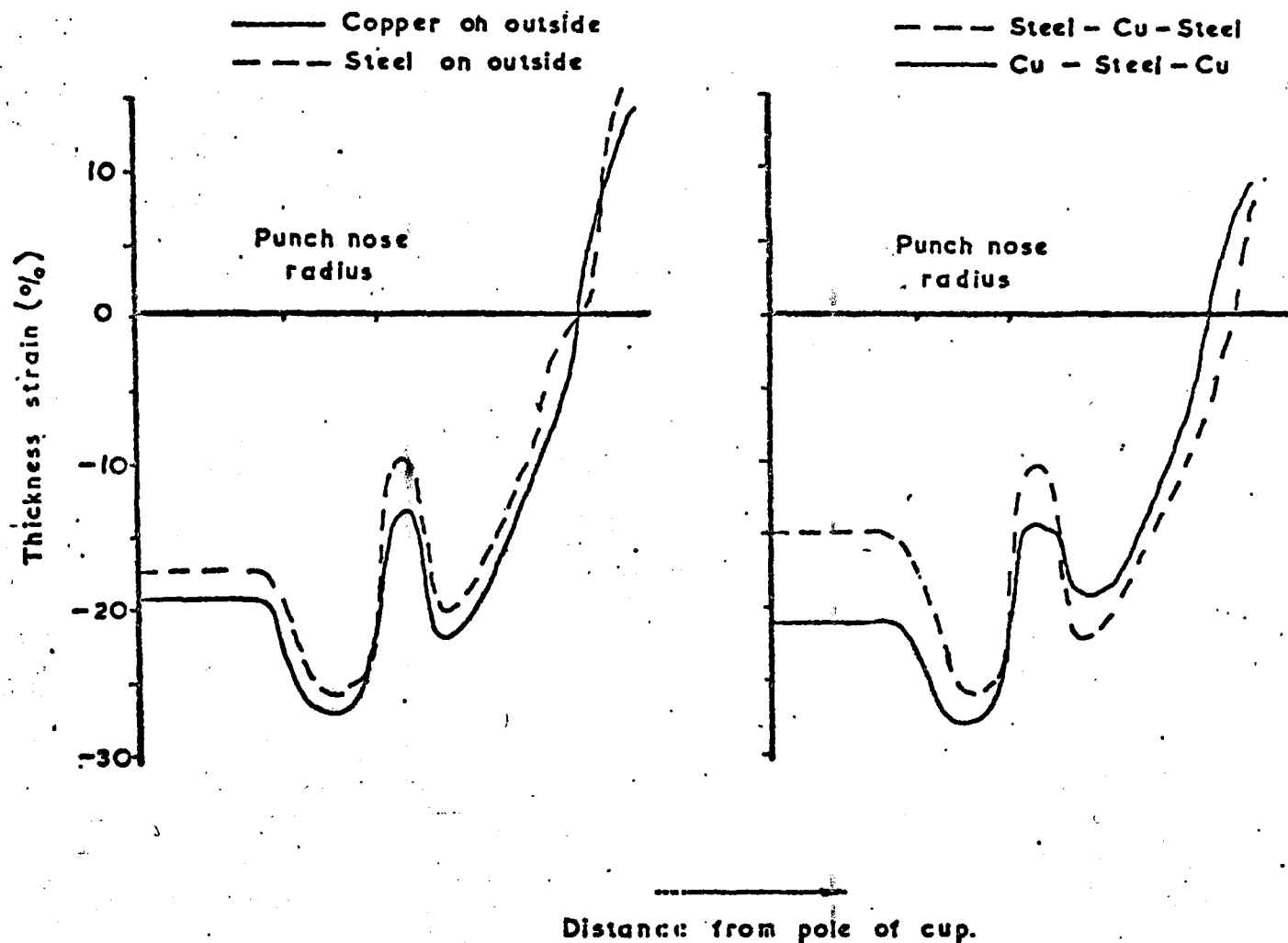
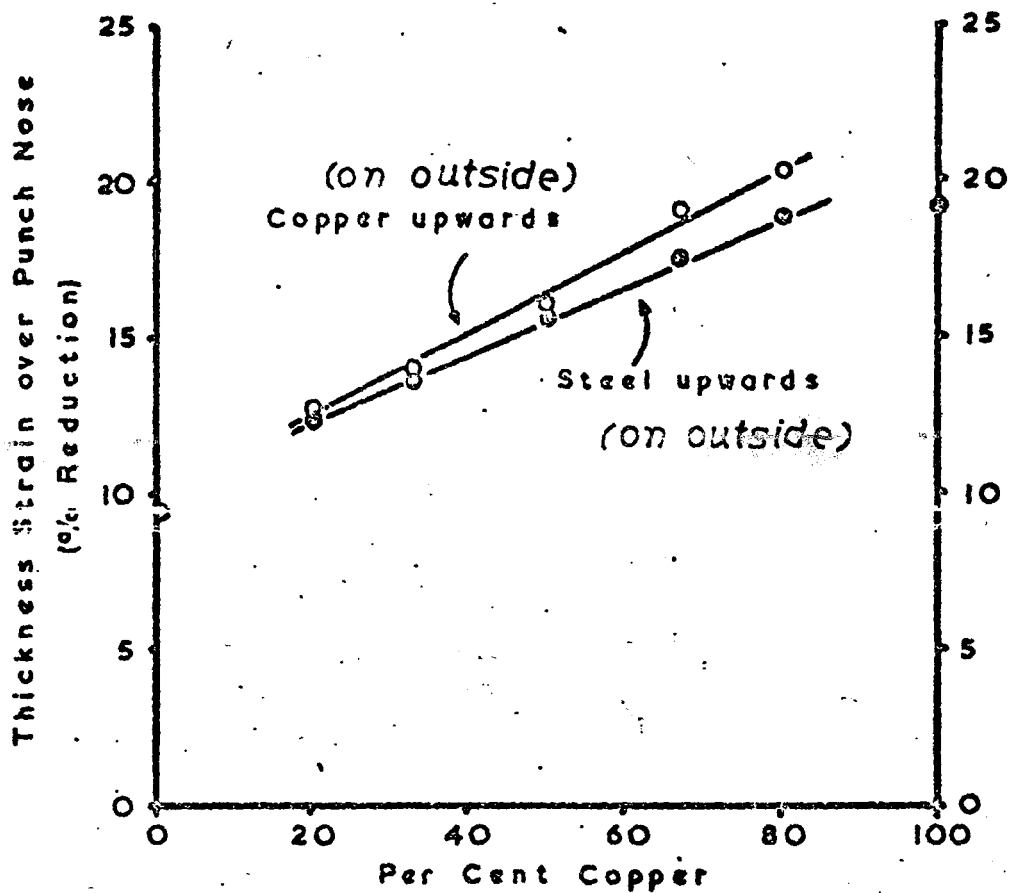


fig 1.2

VARIATION OF THICKNESS STRAIN OVER THE PUNCH NOSE WITH PER CENT COPPER

from Hawkins and Wright [20]



deep drawing of roll bonded copper-mild steel bimetal

fig 1.3

STRESSES ACTING ON A SEGMENT OF A CUP DURING DEEP DRAWING

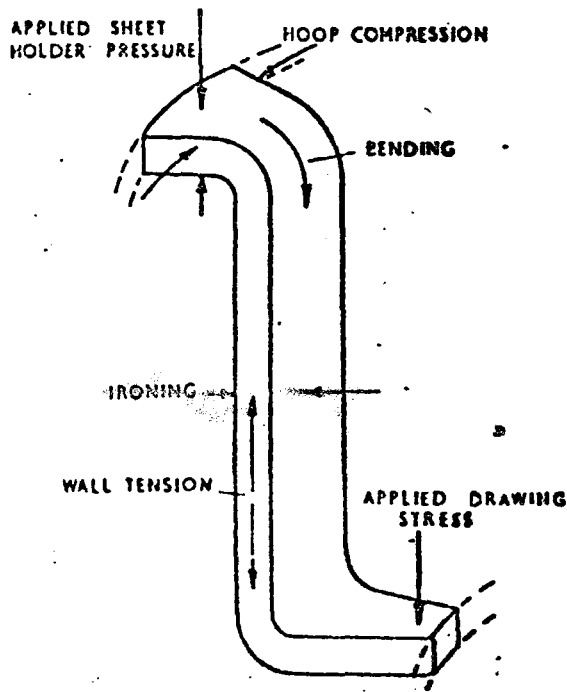
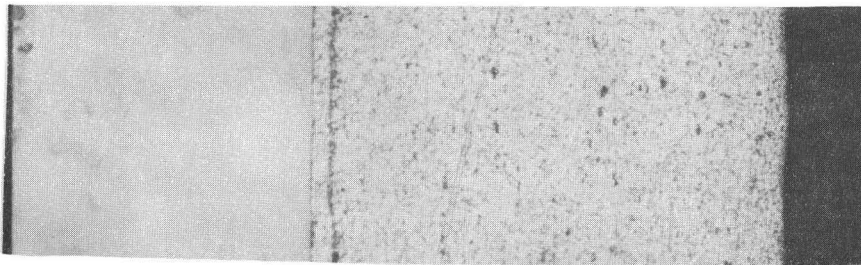


fig 1.4

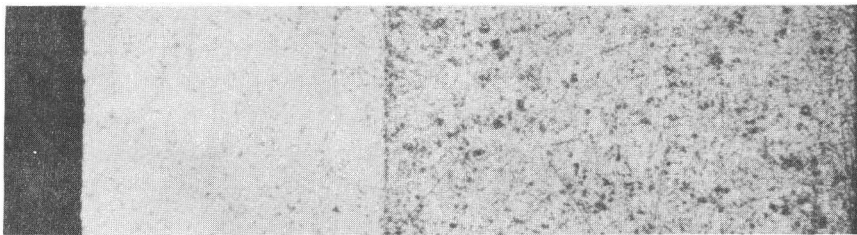
PHOTOMICROGRAPHS OF LAMINATED MATERIALS



434SS / C22AL / 5052 AL

material
B

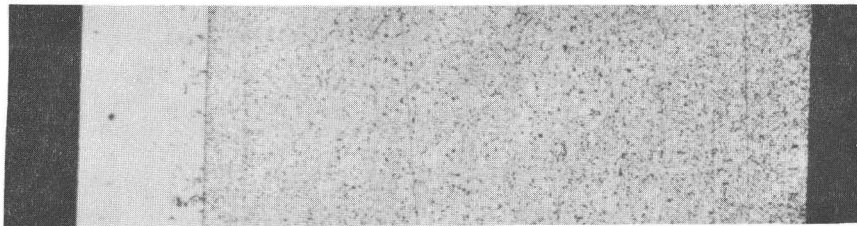
0.05 in



201SS / C22AL 5052AL

material
C

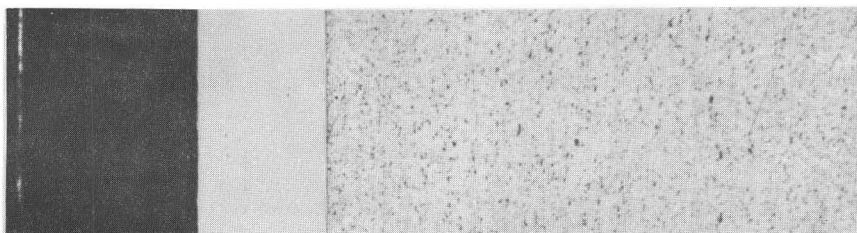
0.05 in



304SS/ C22AL 3003AL

material
D

0.01 in



304SS/ C22AL 3003AL

material
DD

0.01 in



430SS/ C22AL /ZINC

material
E

0.01 in

fig 2.1

TENSILE TEST SPECIMEN

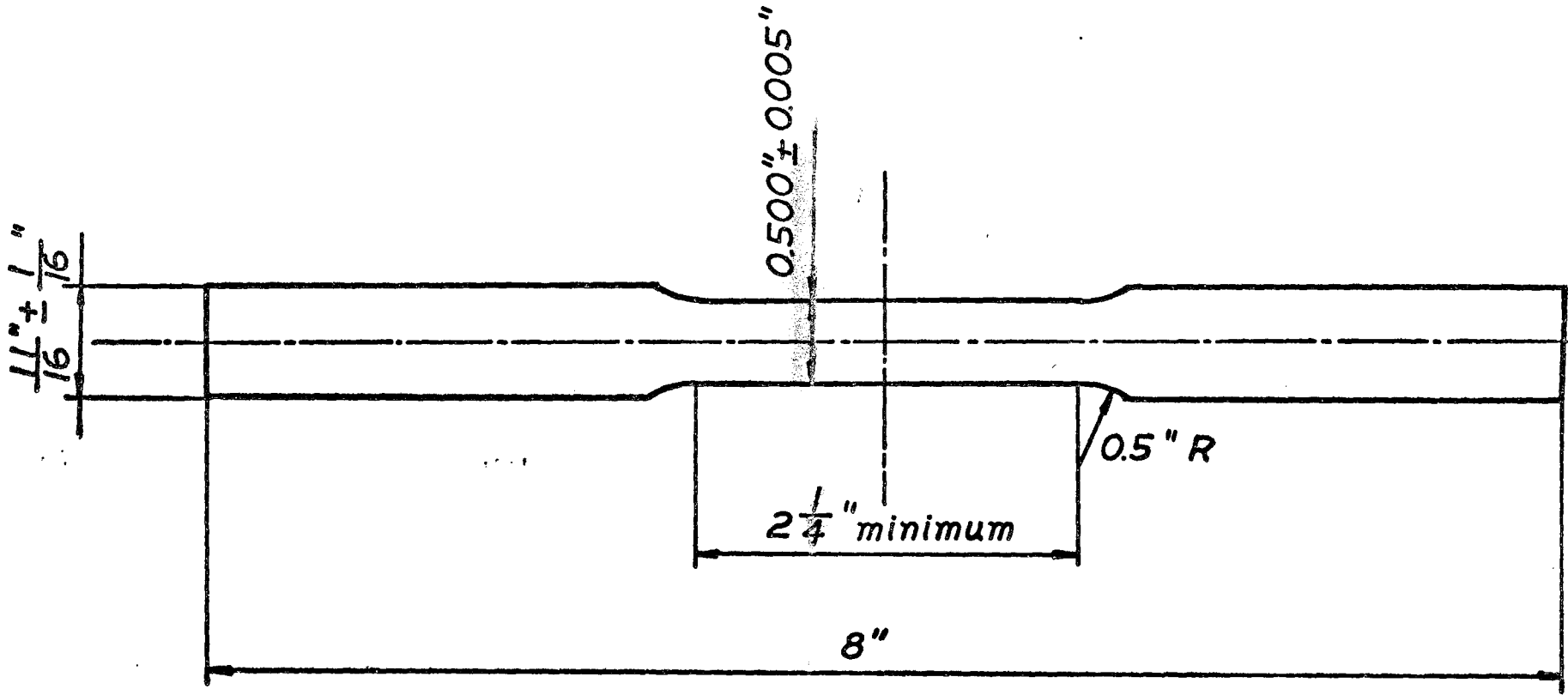


fig 2.2

STRESS STRAIN CURVE MATERIAL B

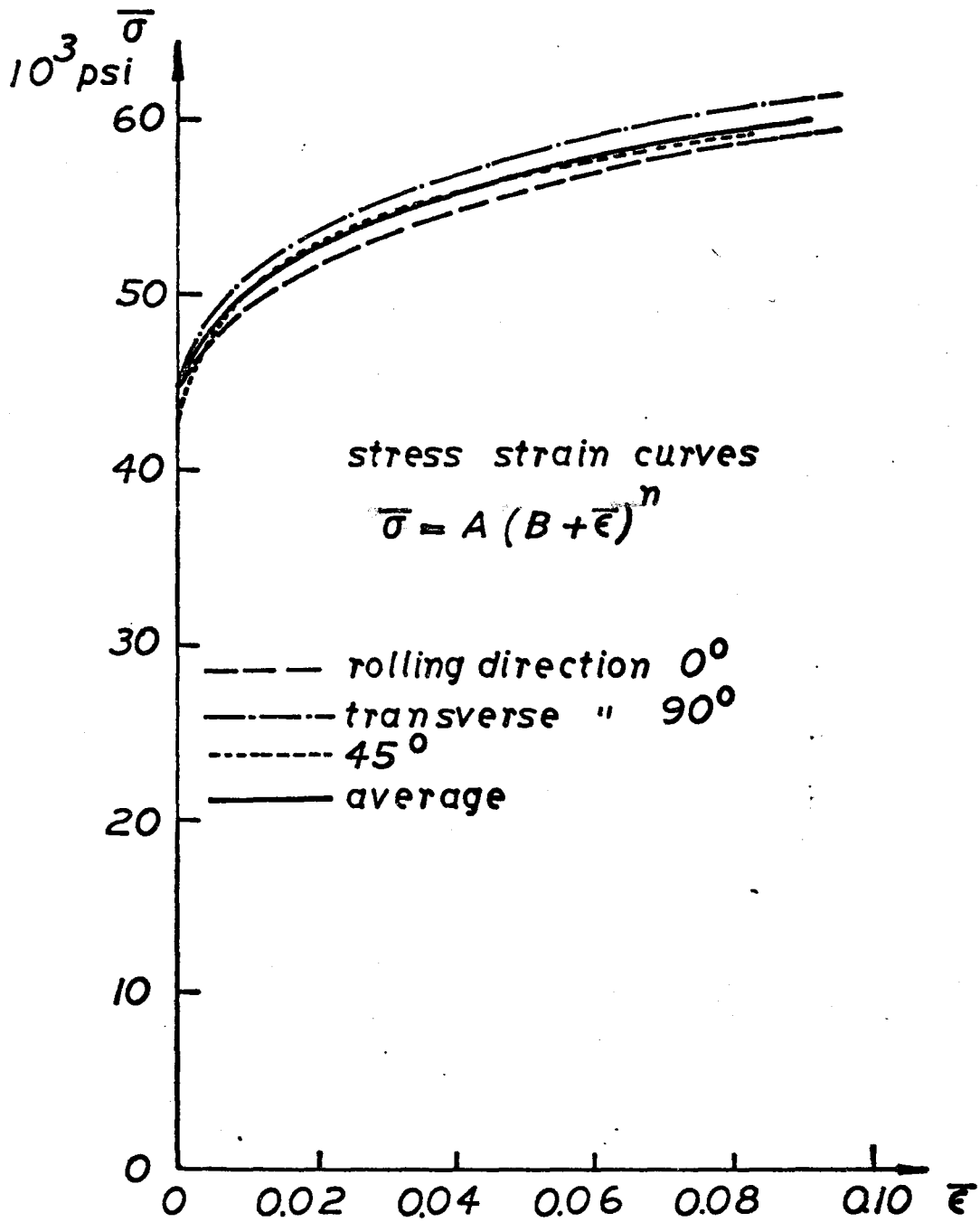


fig 2.3

STRESS STRAIN CURVE

MATERIAL C

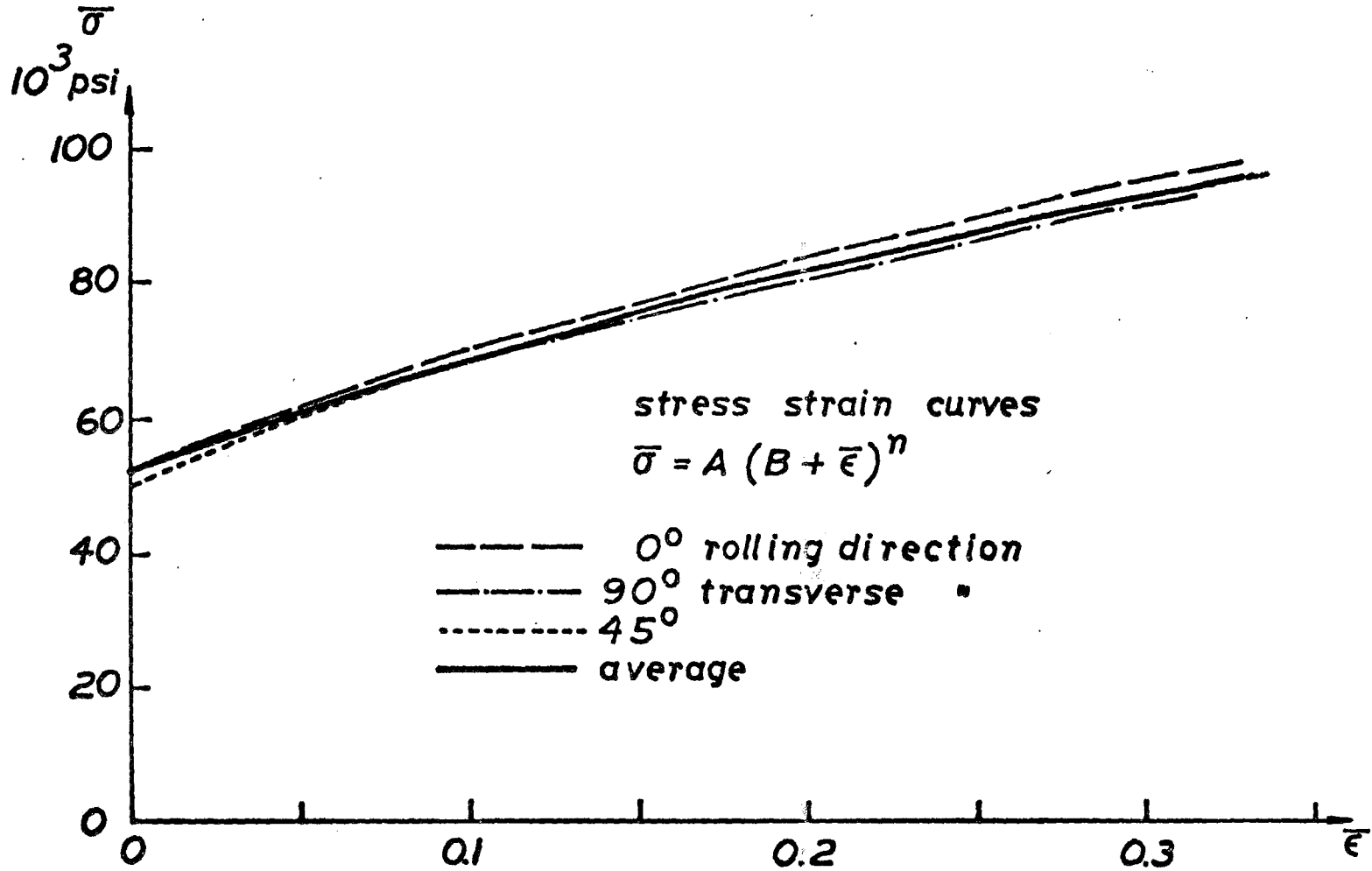


fig 2.4

STRESS STRAIN CURVE

MATERIAL D

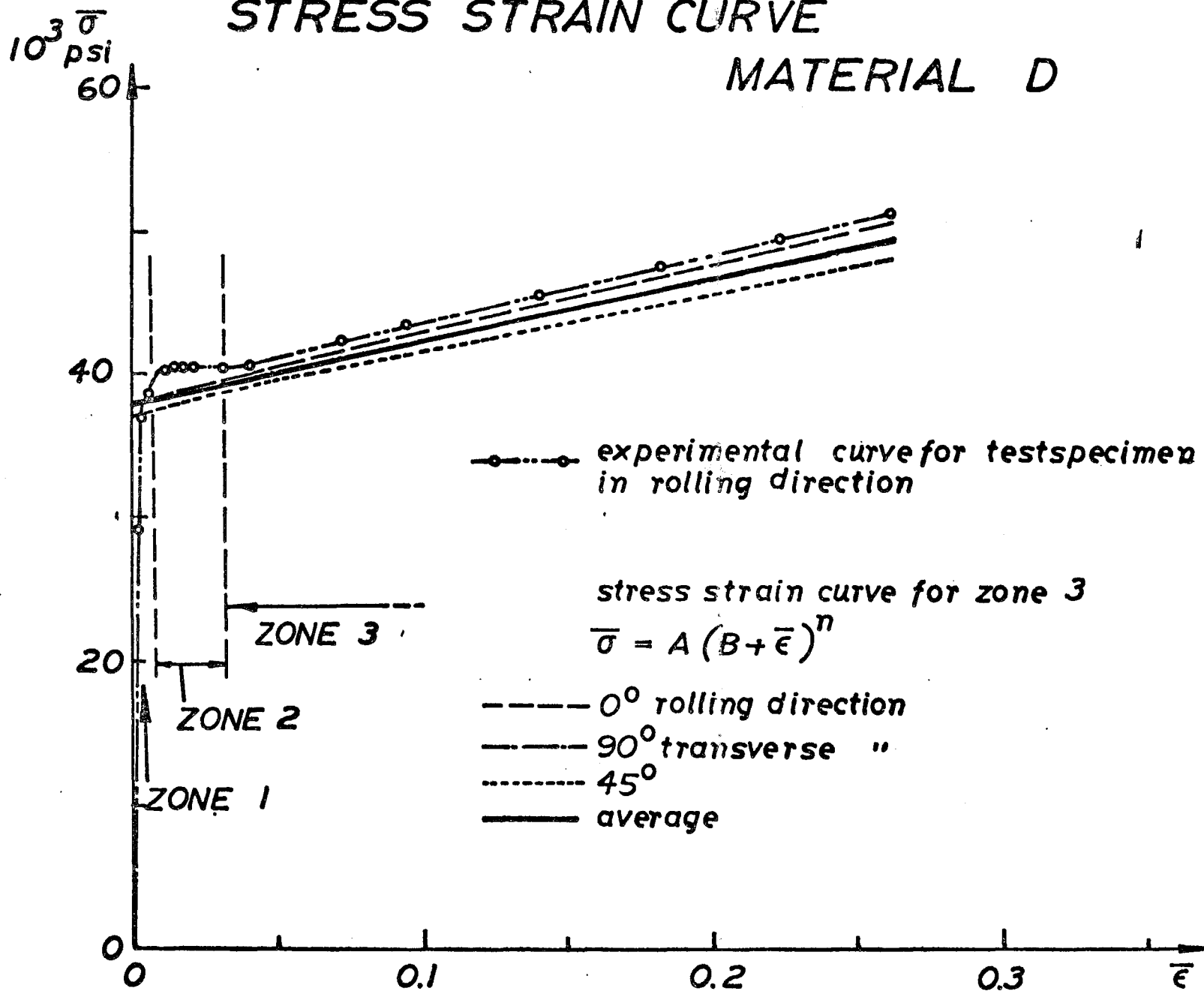


fig 2.5

STRESS STRAIN CURVE MATERIAL D-SS

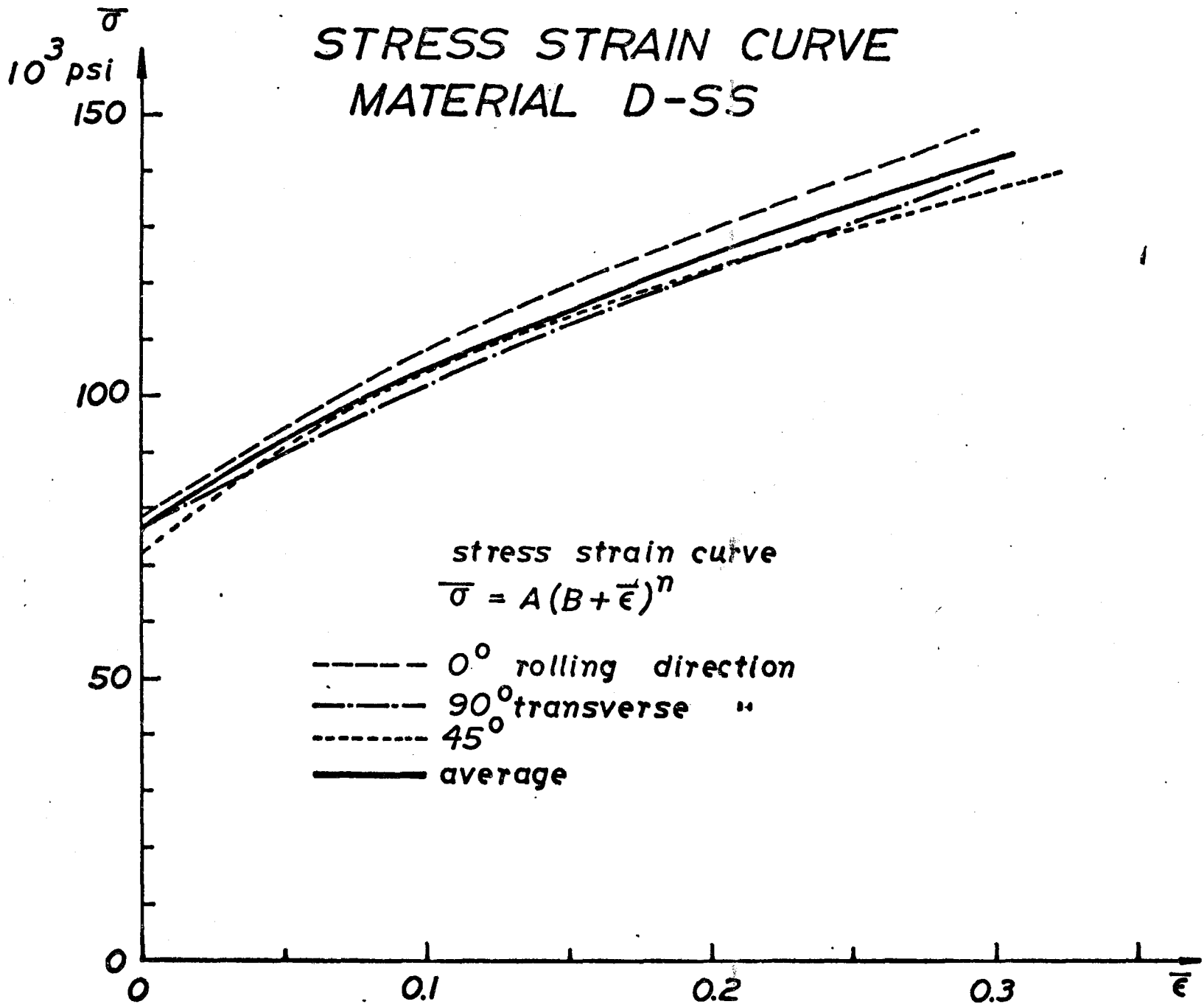


fig 2.6

STRESS STRAIN CURVE MATERIAL D-AL

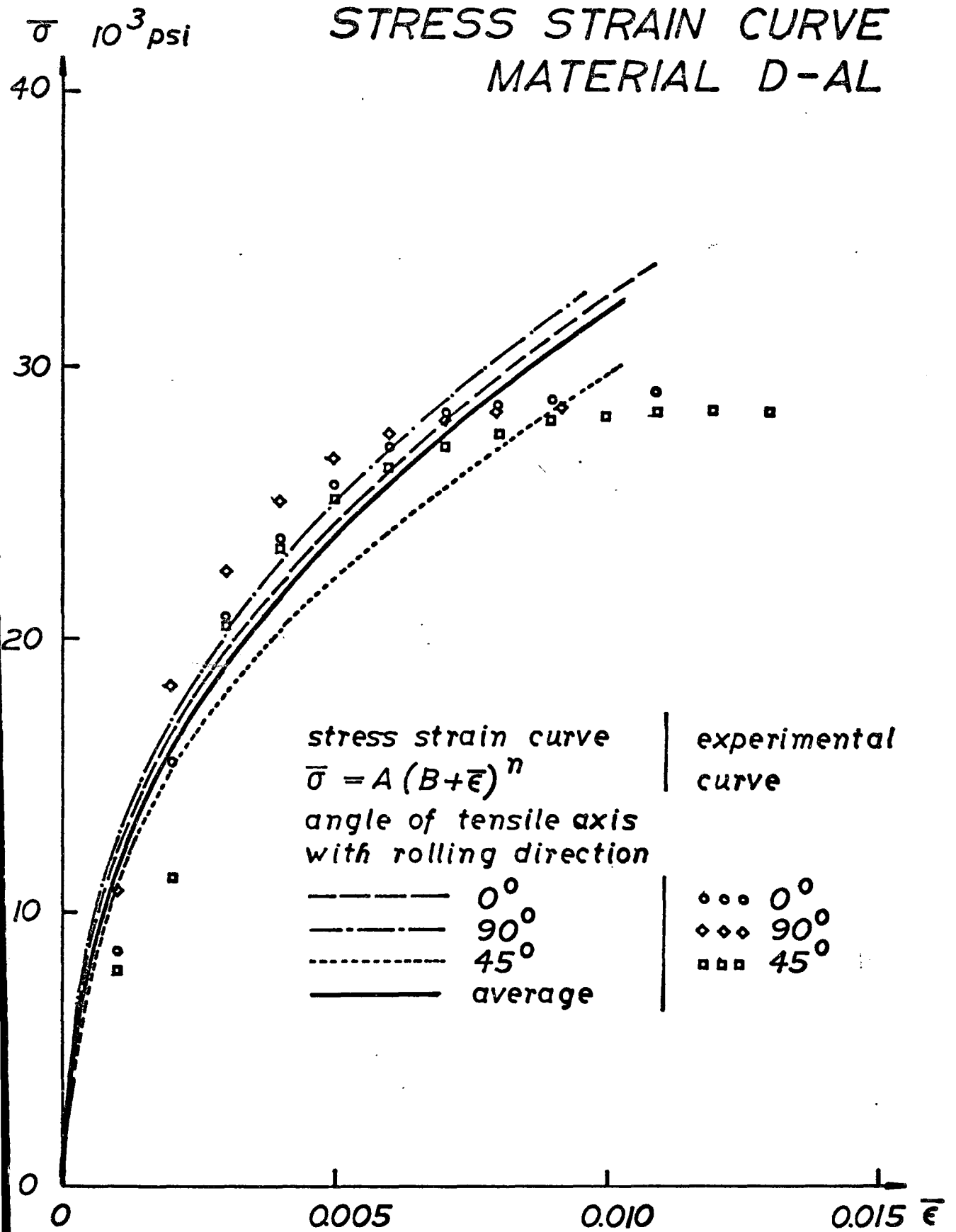


fig 2.7

STRESS STRAIN CURVE

MATERIAL DD

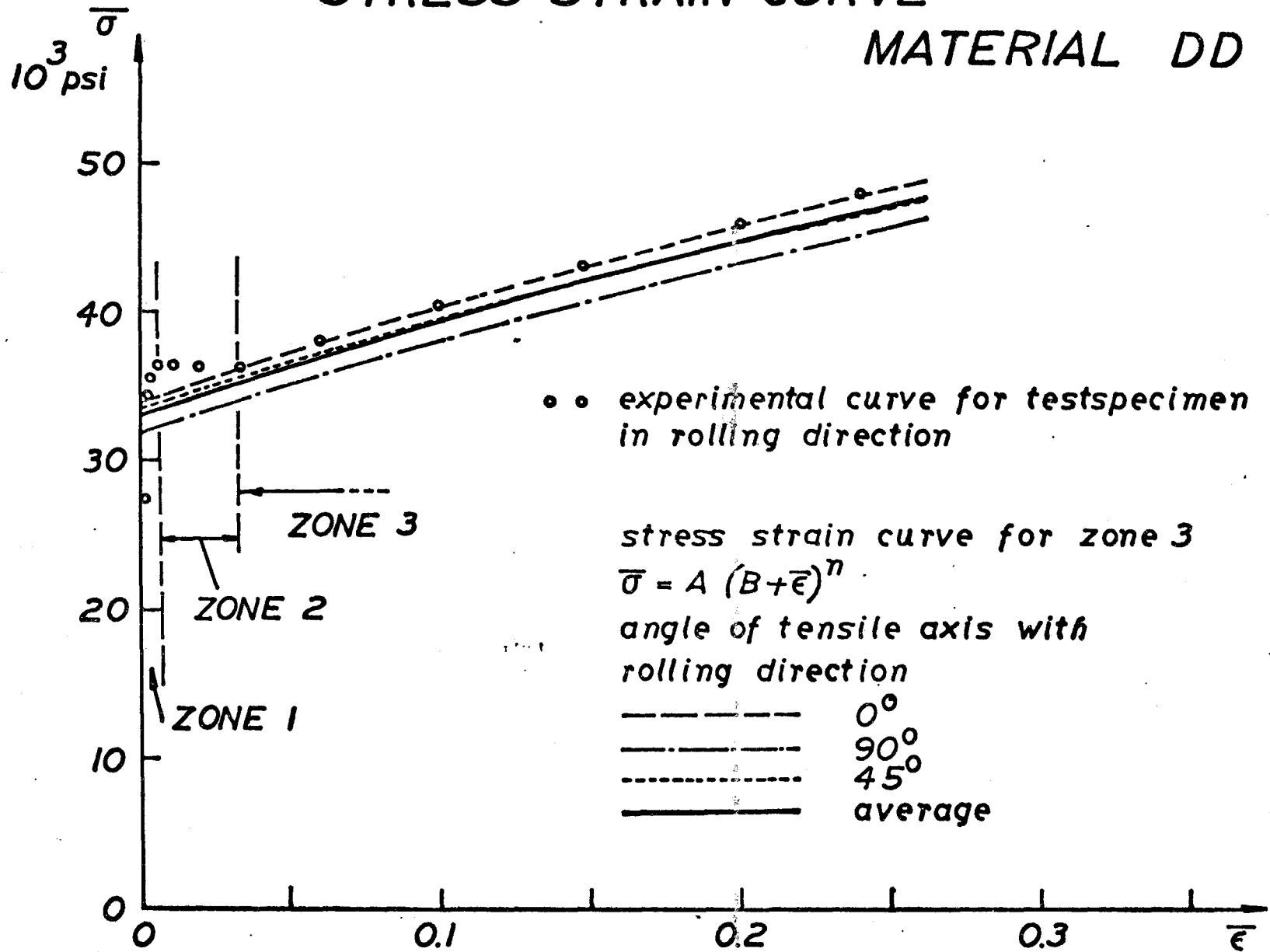


fig 2.8

STRESS STRAIN CURVE MATERIAL E

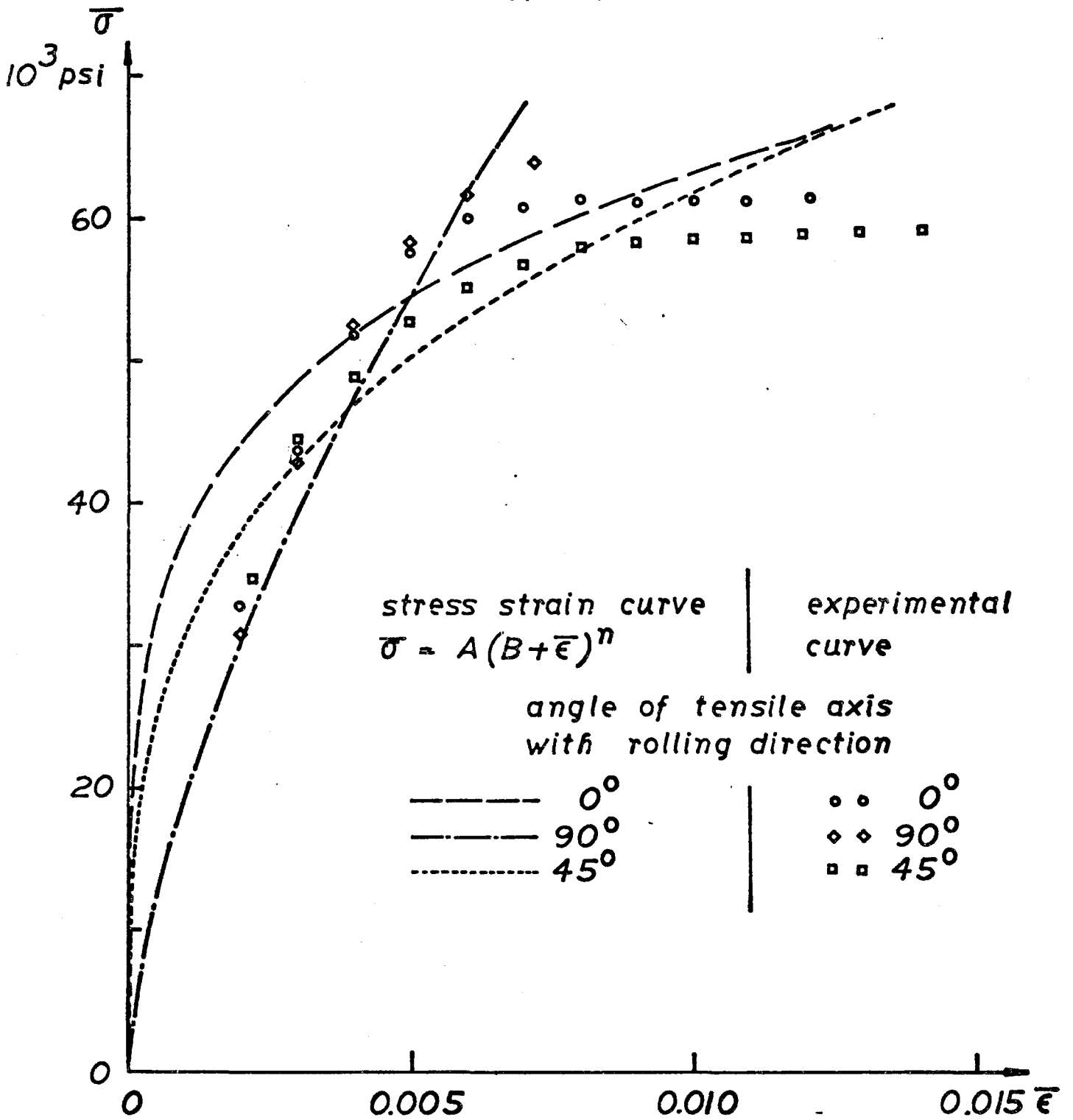


fig 2.9

TYPICAL LOAD-ELONGATION CURVE IN TENSILE TESTS OF MATERIAL D

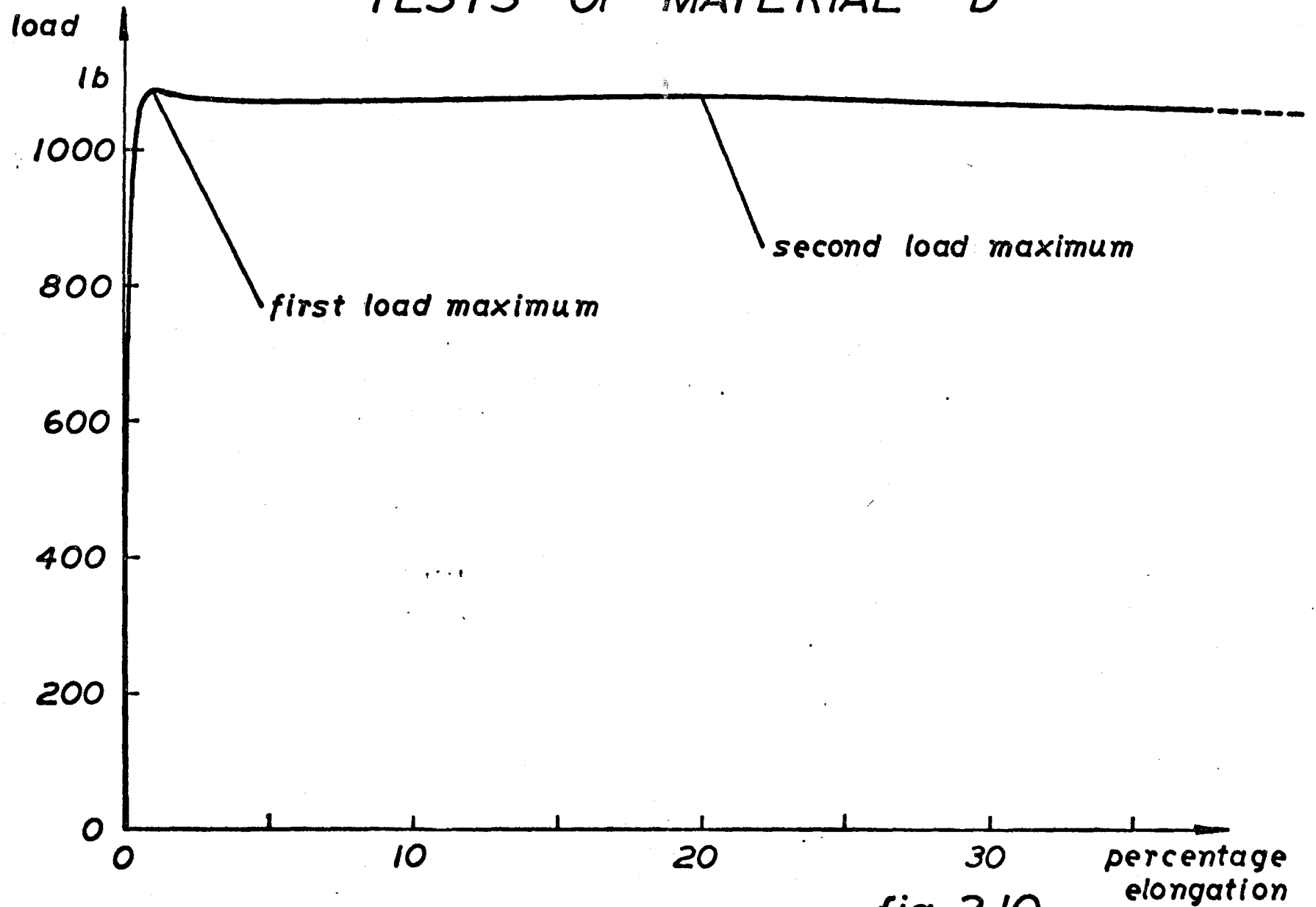


fig 2.10

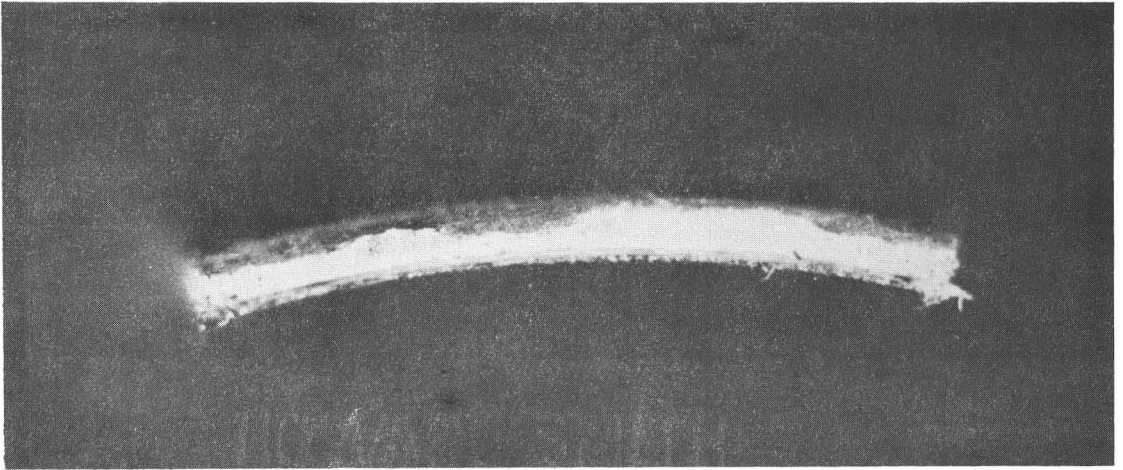


FIG. 2.11 (a) - CURLING ABOUT THE LONGITUDINAL AXIS

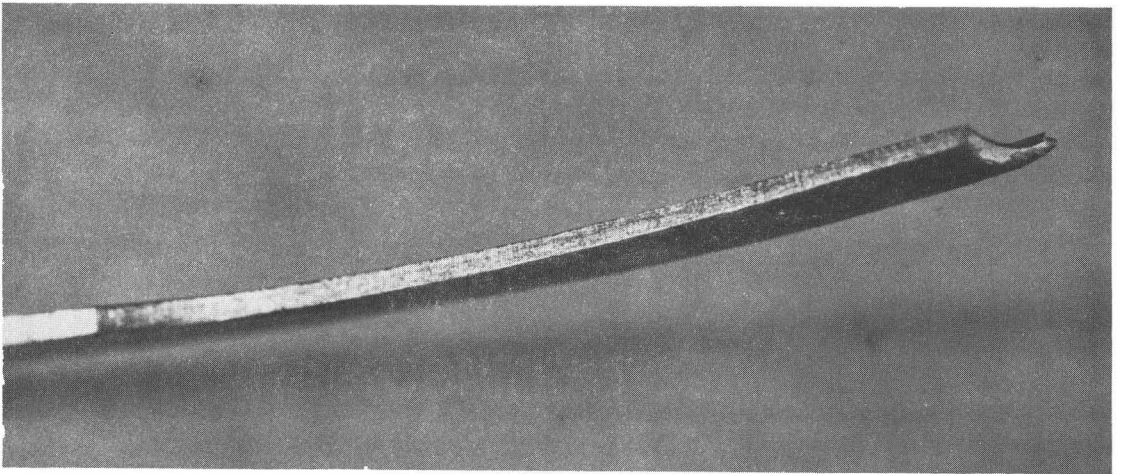


FIG. 2.11 (b)

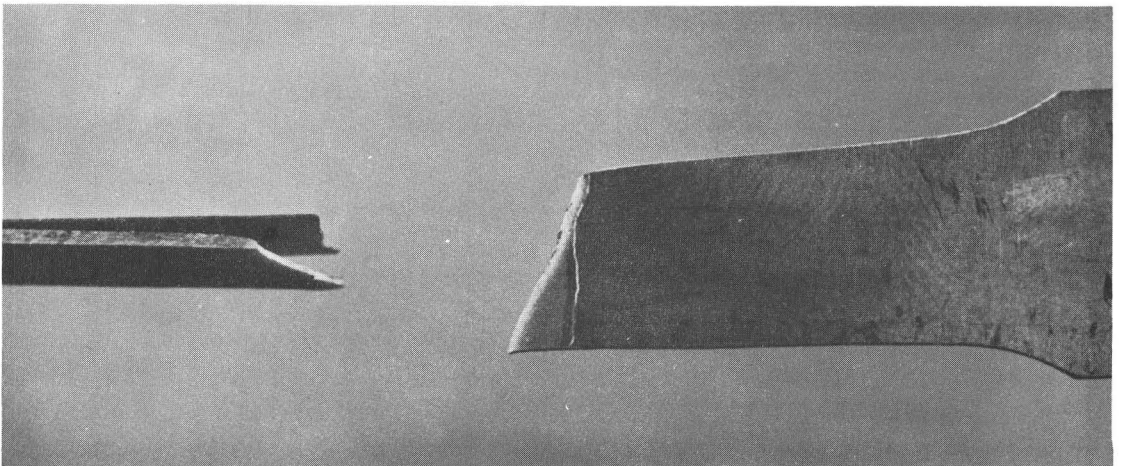


FIG. 2.12

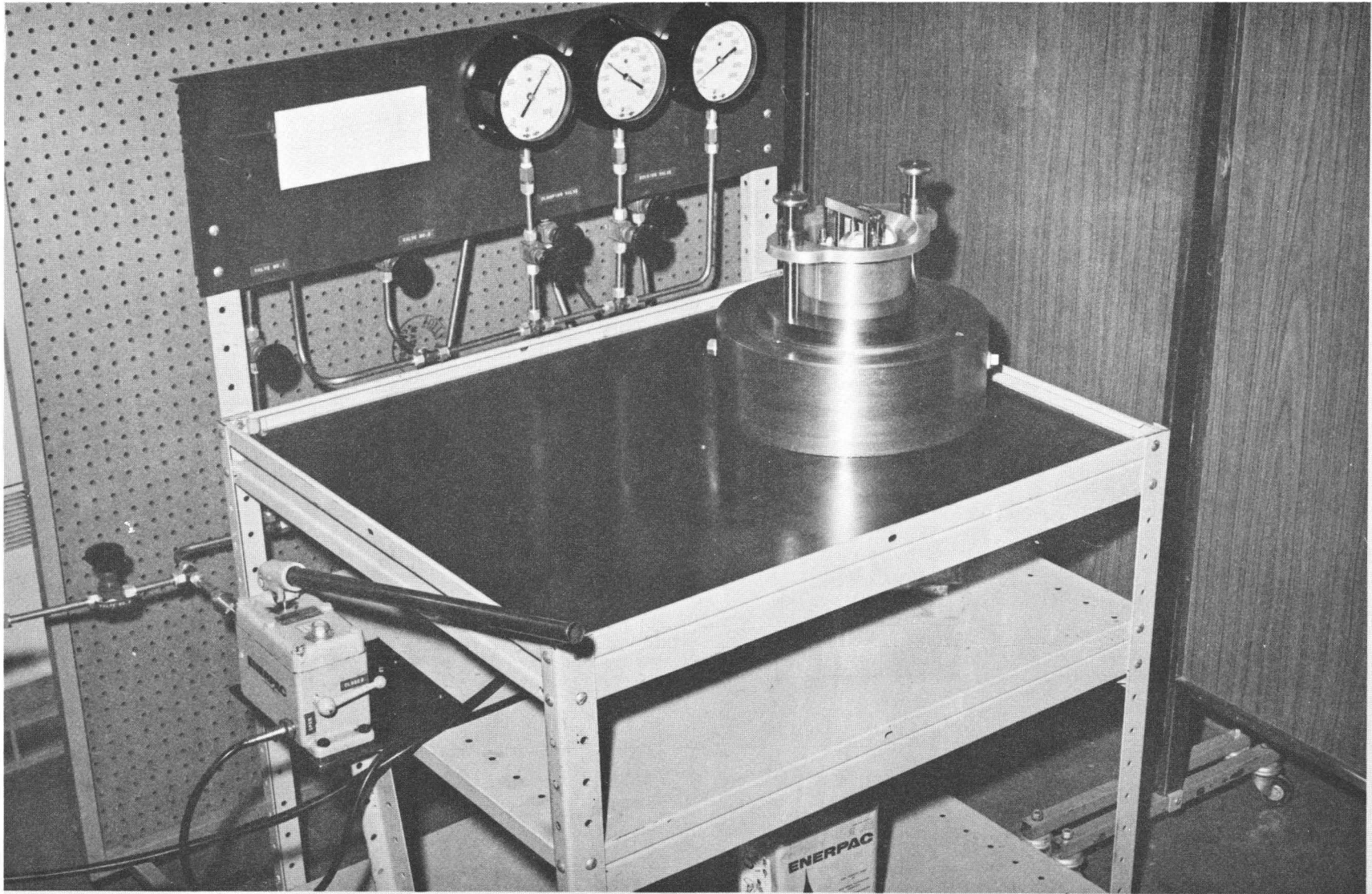


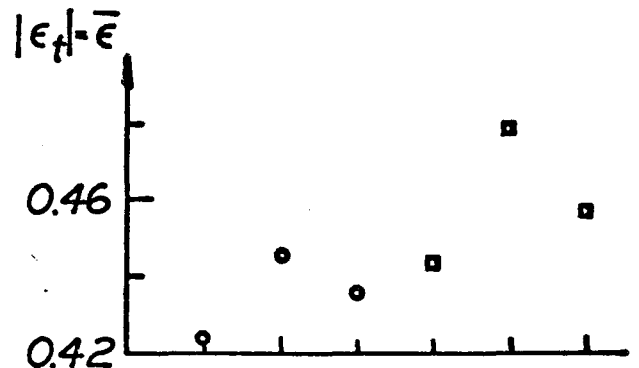
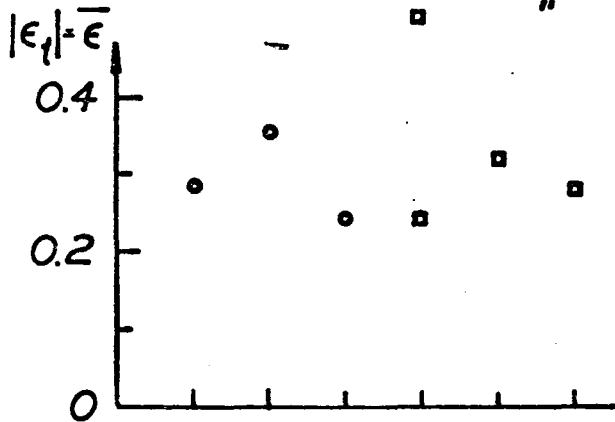
Figure 2.13 Biaxial test equipment.

INFLUENCE OF SHEET ORIENTATION ON CIRCULAR BULGE TEST RESULTS

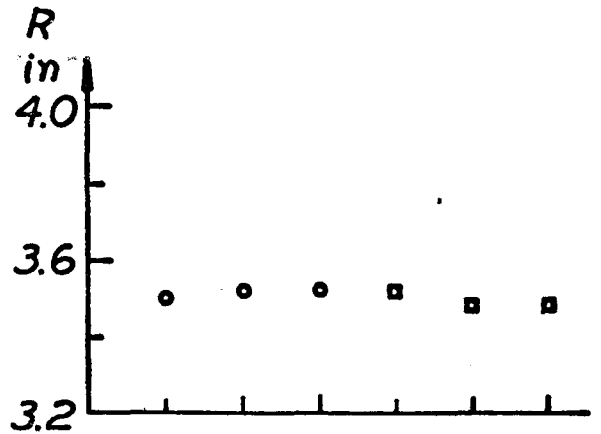
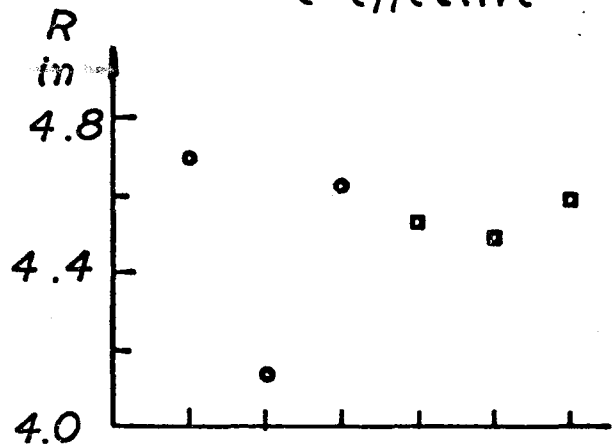
MATERIAL B

MATERIAL C

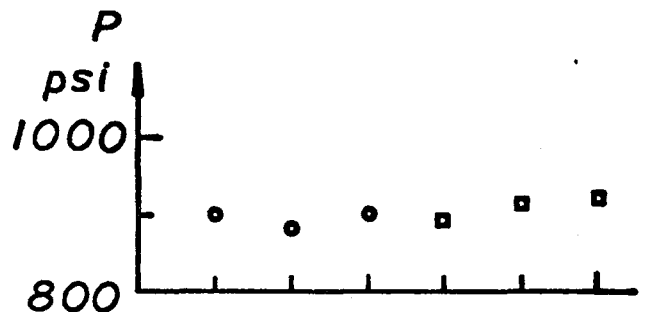
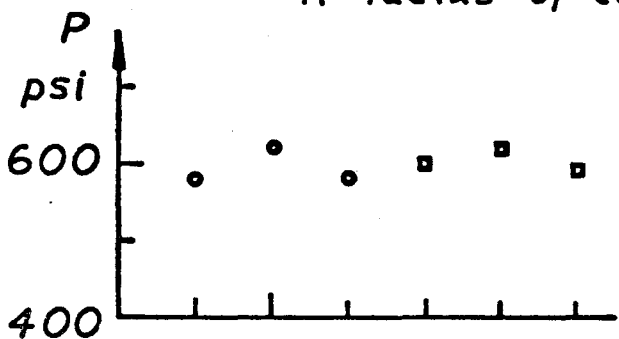
○ stainless steel on outside of bulge
 □ " " inside " "



ϵ_t thickness strain at pole at failure
 $\bar{\epsilon}$ effective " " " " " "



R radius of curvature at pole at failure



P hydraulic pressure at failure

fig 2.14

fig 2.15

INFLUENCE OF SHEET ORIENTATION ON CIRCULAR BULGE TEST RESULTS

MATERIAL D MATERIAL DD

○ stainless steel on outside of bulge
 □ " " " " inside " "

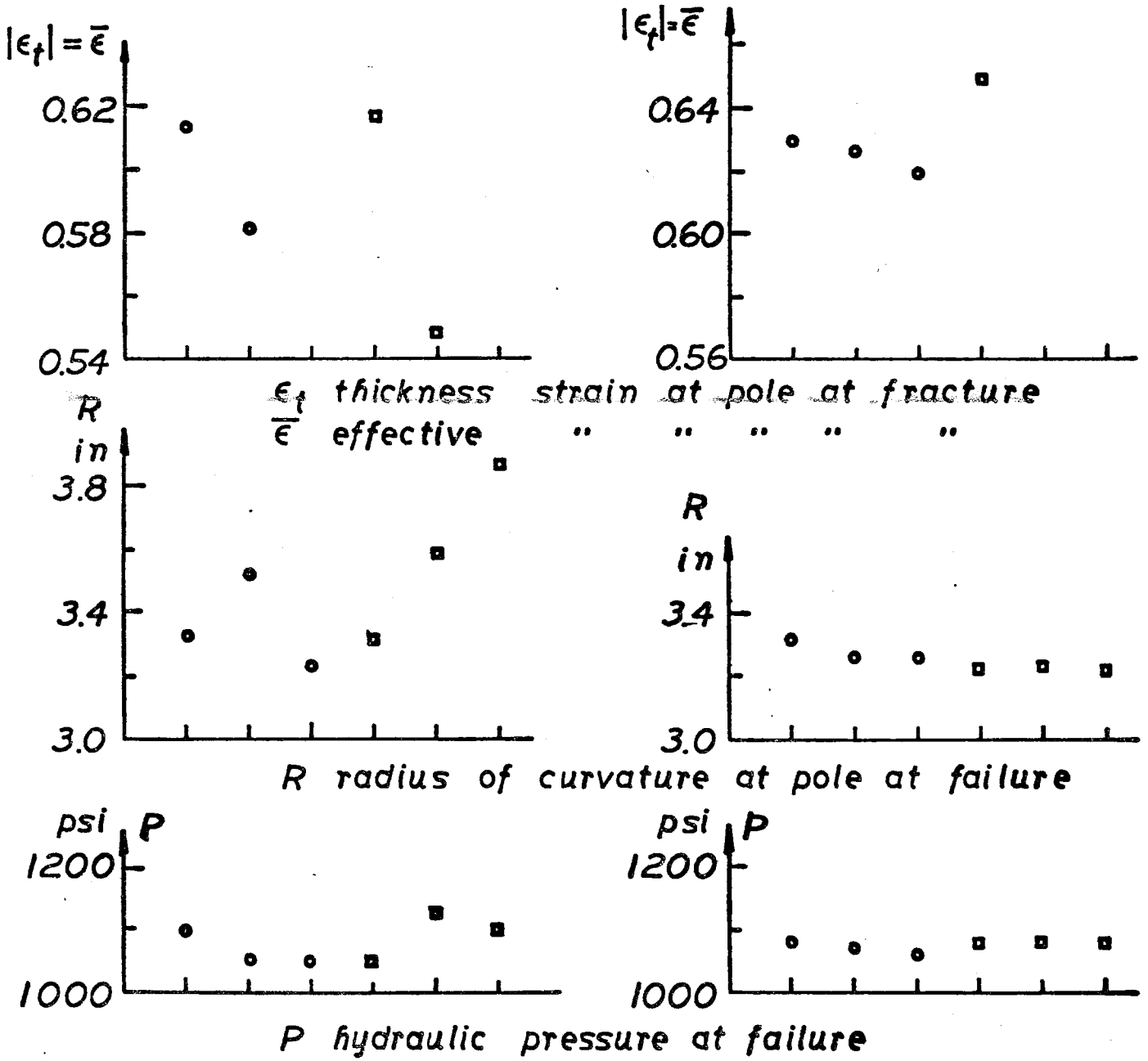
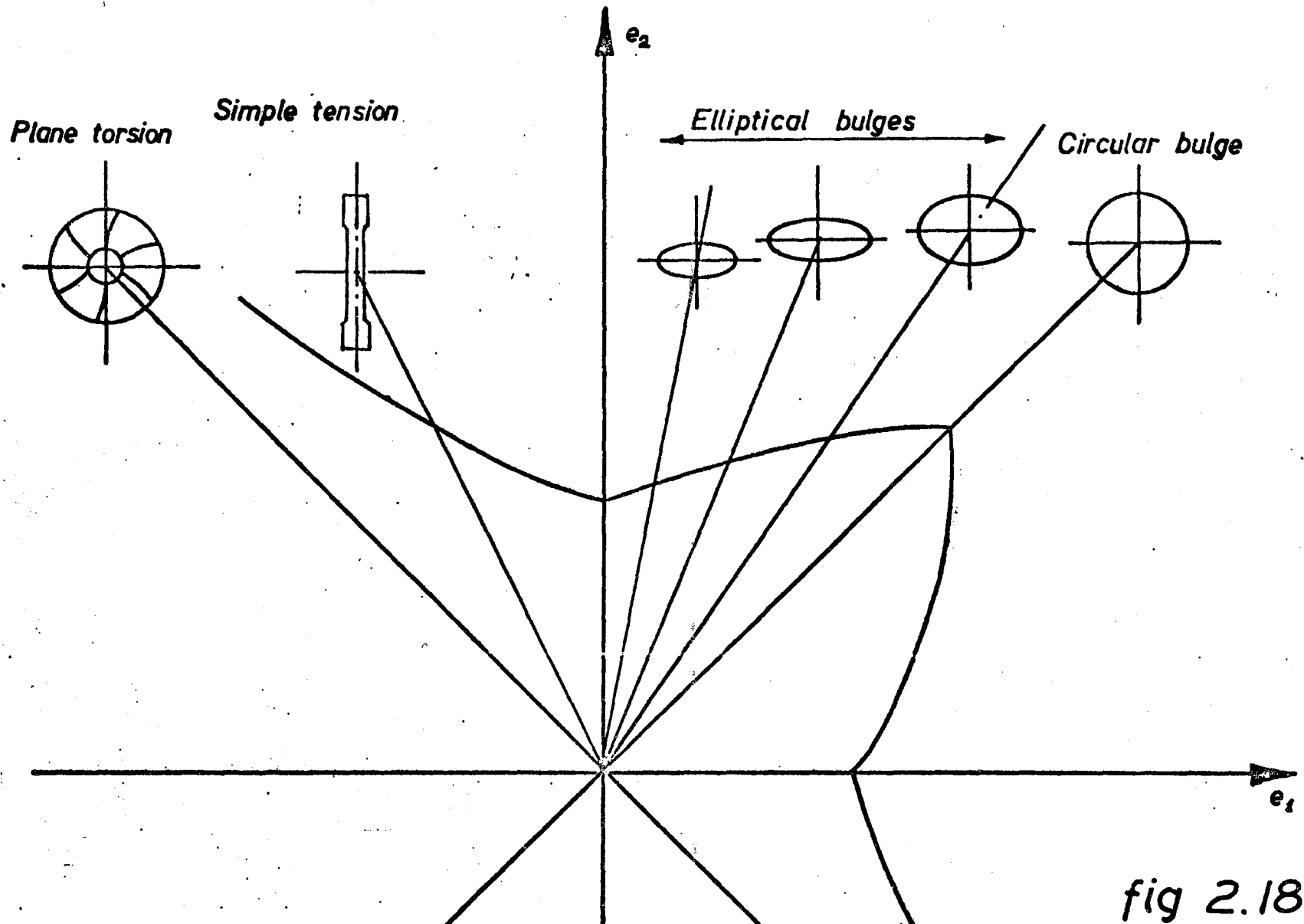


fig 2.16

fig 2.17

FORMING LIMIT DIAGRAM AND ATTAINABLE STRAIN PATHS WITH DIFFERENT LABORATORY TESTS



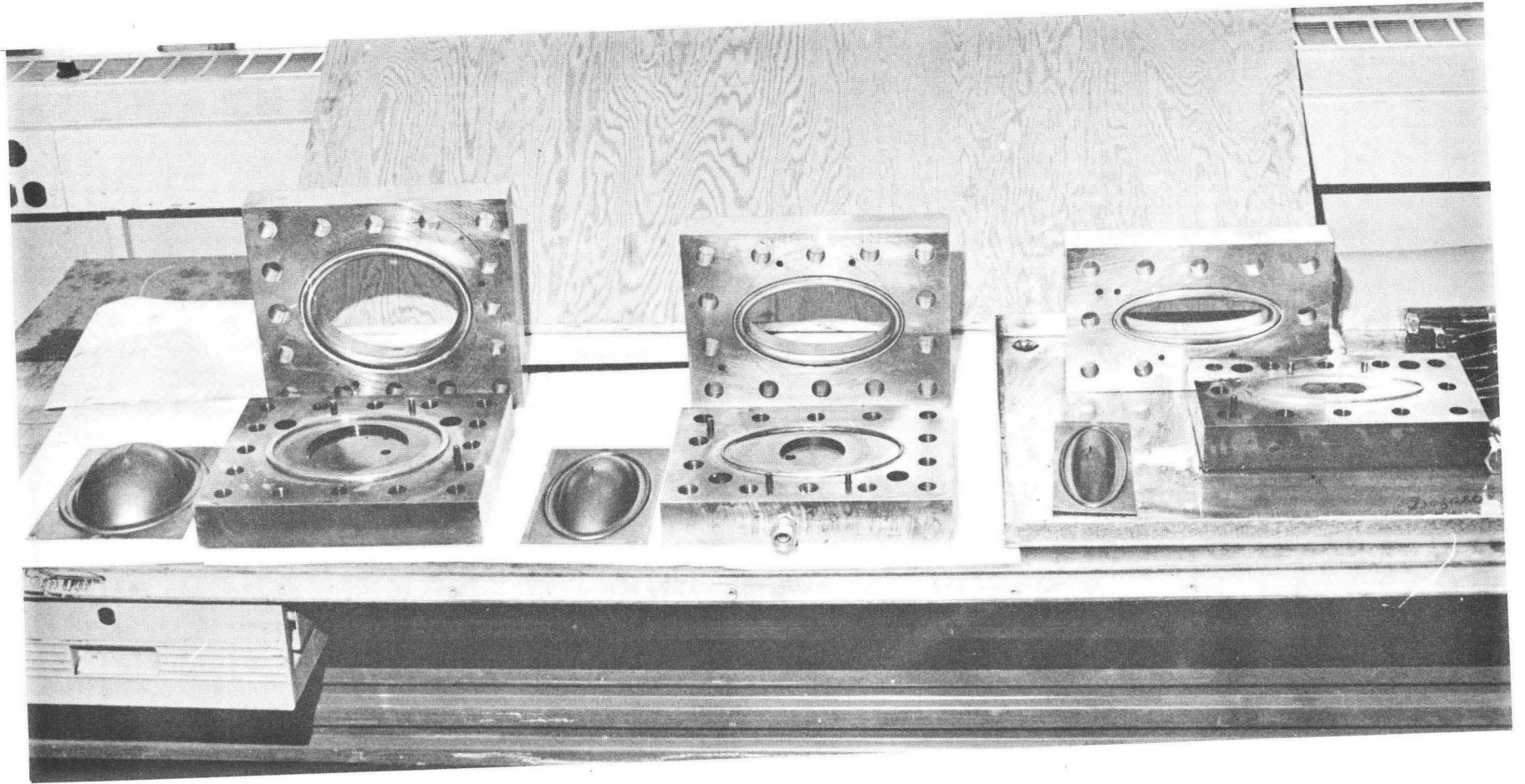
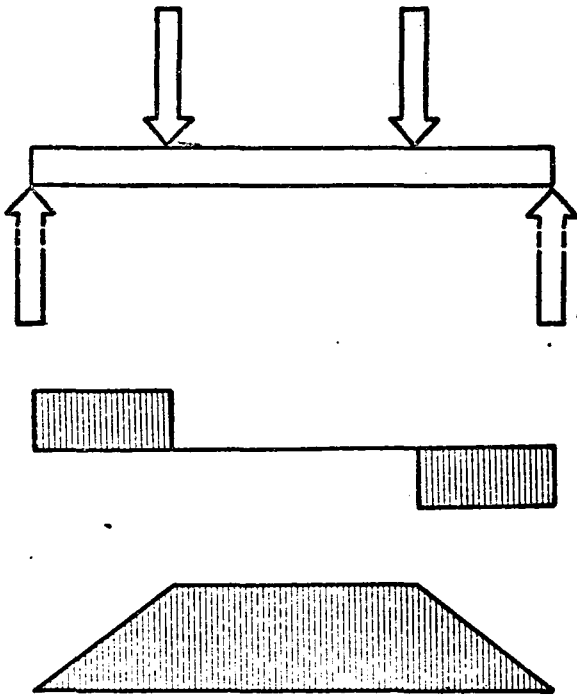


Figure 2-19 Various elliptical dies used in bulge testing

FOUR POINT BEND TEST

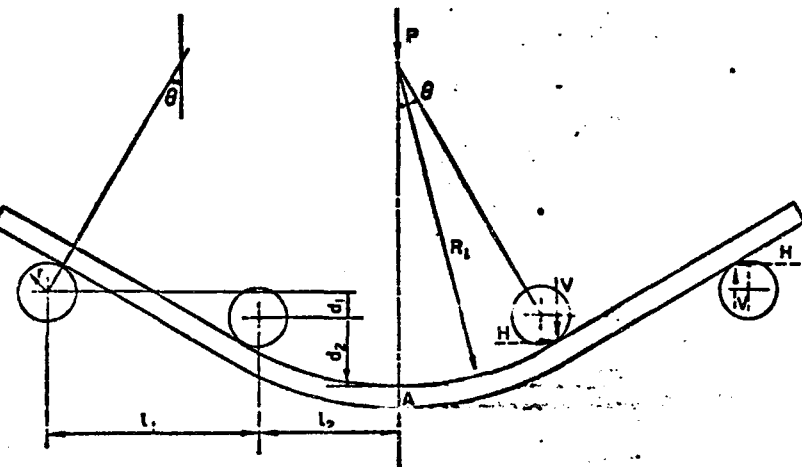


bending method

transverse force

bending moment

fig 3.1



*geometry of four
point bend test
loading rig and
specimen*

fig 3.2

STRESSES ON AN ELEMENT
IN THE BENDING ZONE
according to Hill

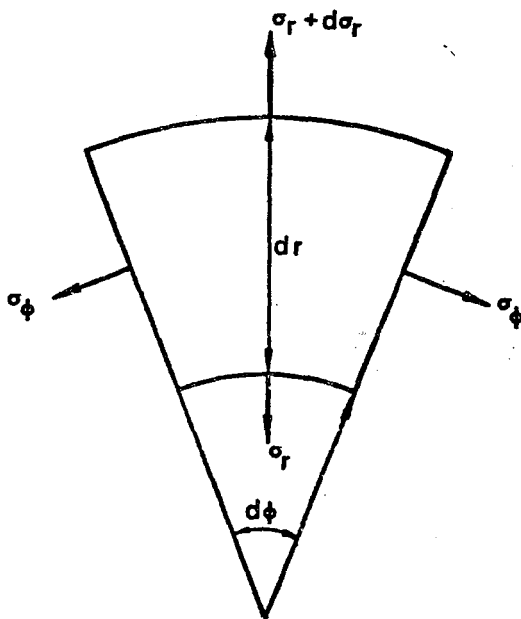


fig 3.3

STRESS DISTRIBUTION IN BENDING
 NON STRAINHARDENING MONOMETAL
 FOR RELATIVE CURVATURE $\kappa = 1$.

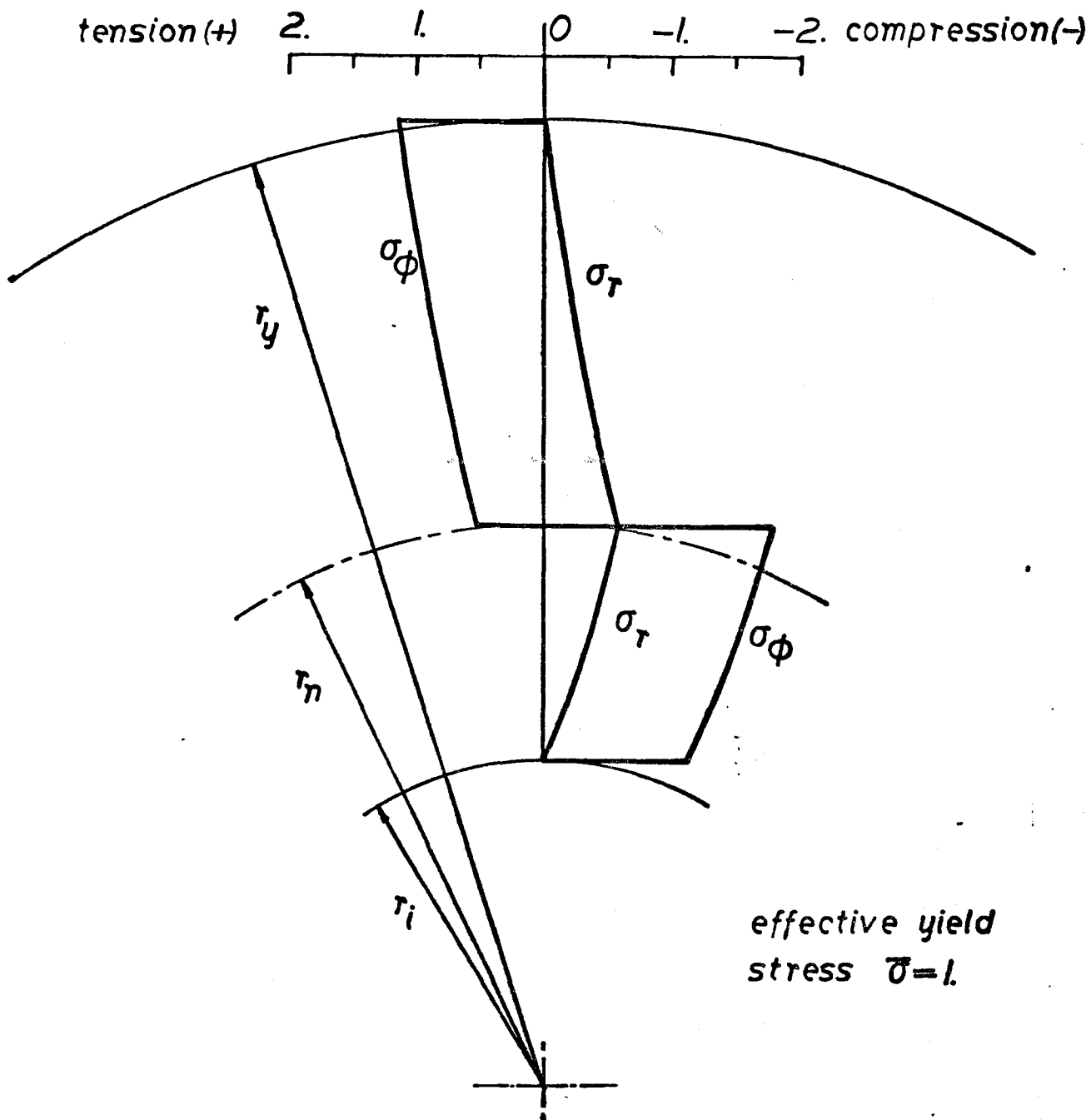


fig 3.4

STRESS DISTRIBUTION IN BENDING NON STRAINHARDENING 4-1-4 (20-40-40) TRIMETAL

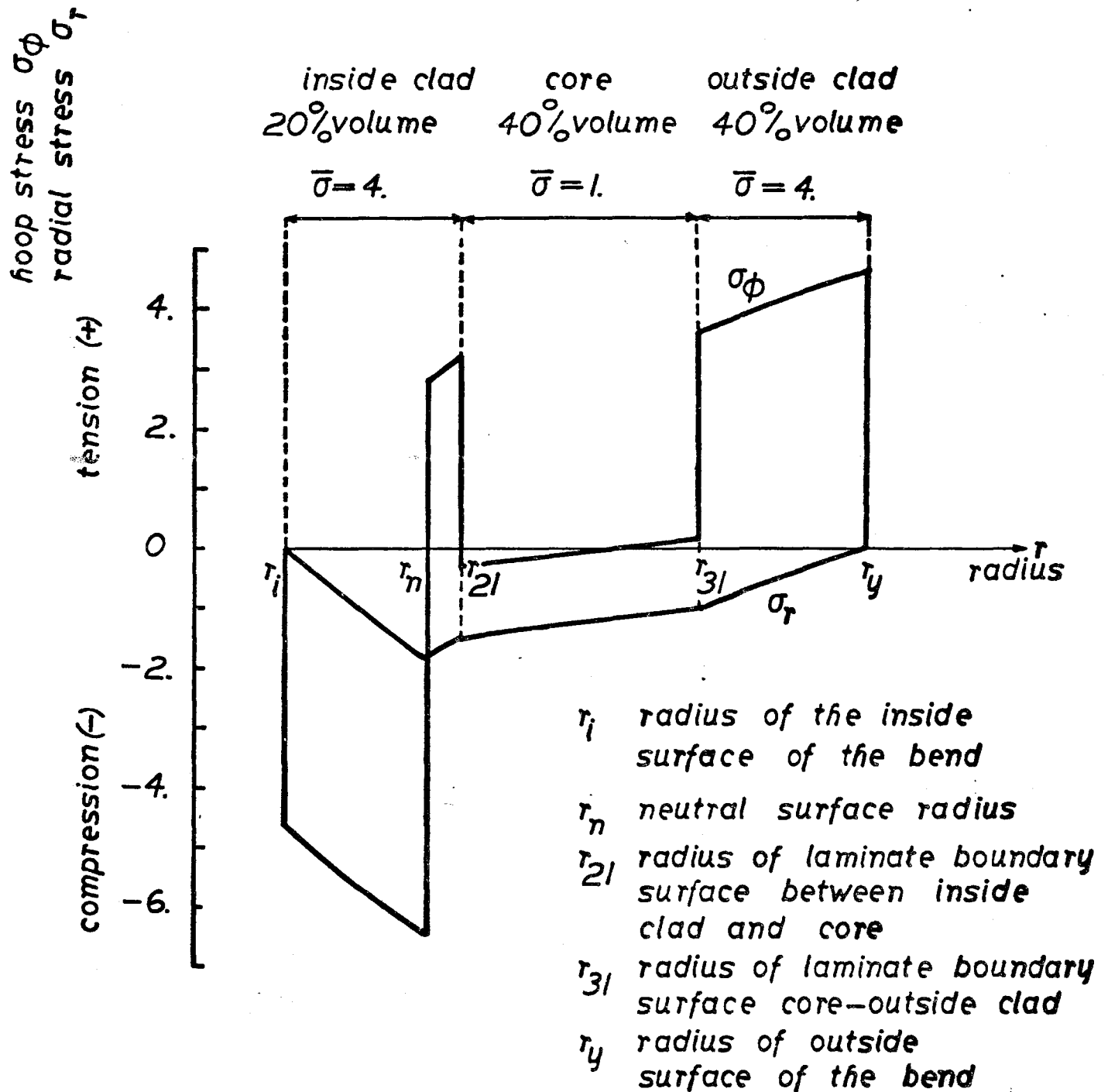


fig 3.5

STRESS DISTRIBUTION IN BENDING NONSTRAINHARDENING MONOMETAL

$$\bar{\sigma} = 1.$$

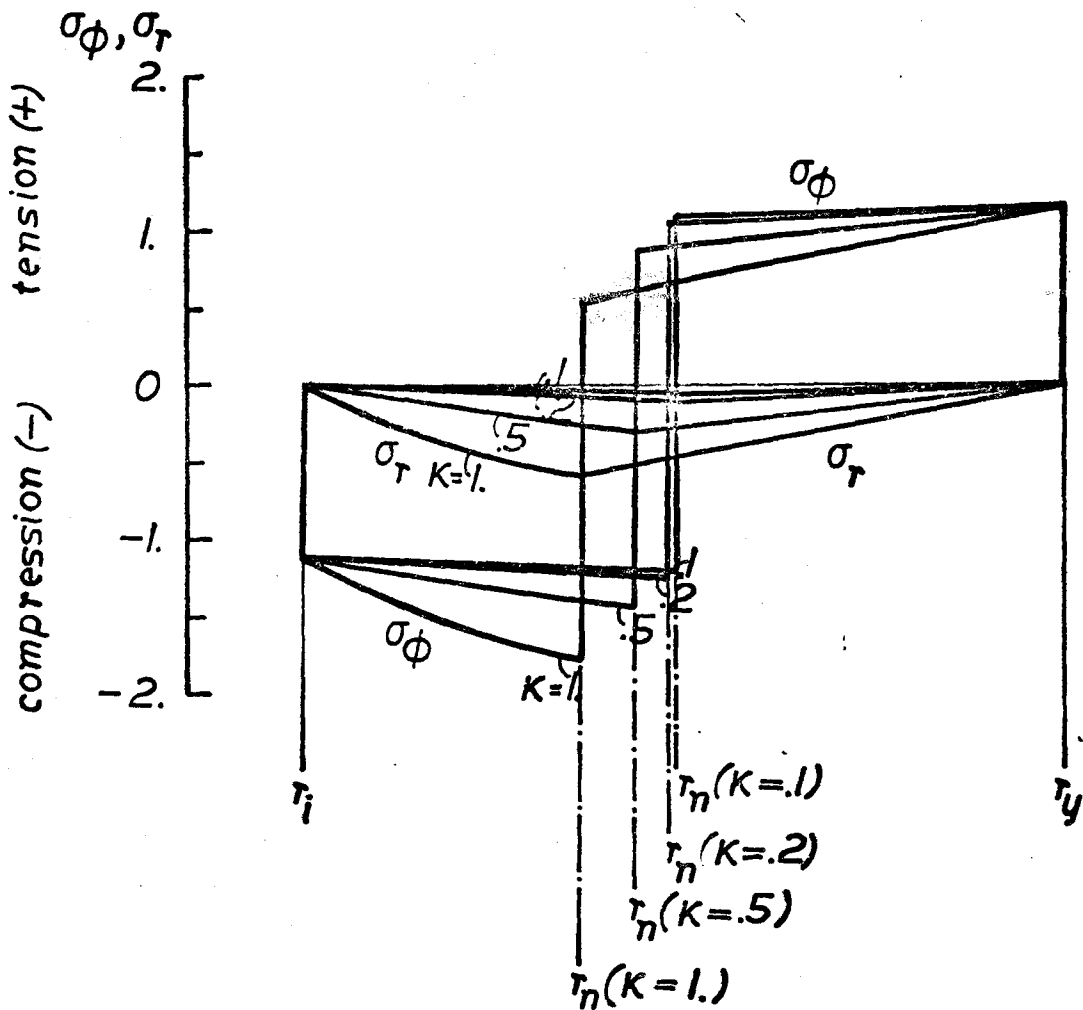


fig 4.1

BENDING MOMENT AND LAYER POSITION
 IN BENDING NON STRAIN HARDENING
 MONOMETAL $\bar{\sigma} = 1$

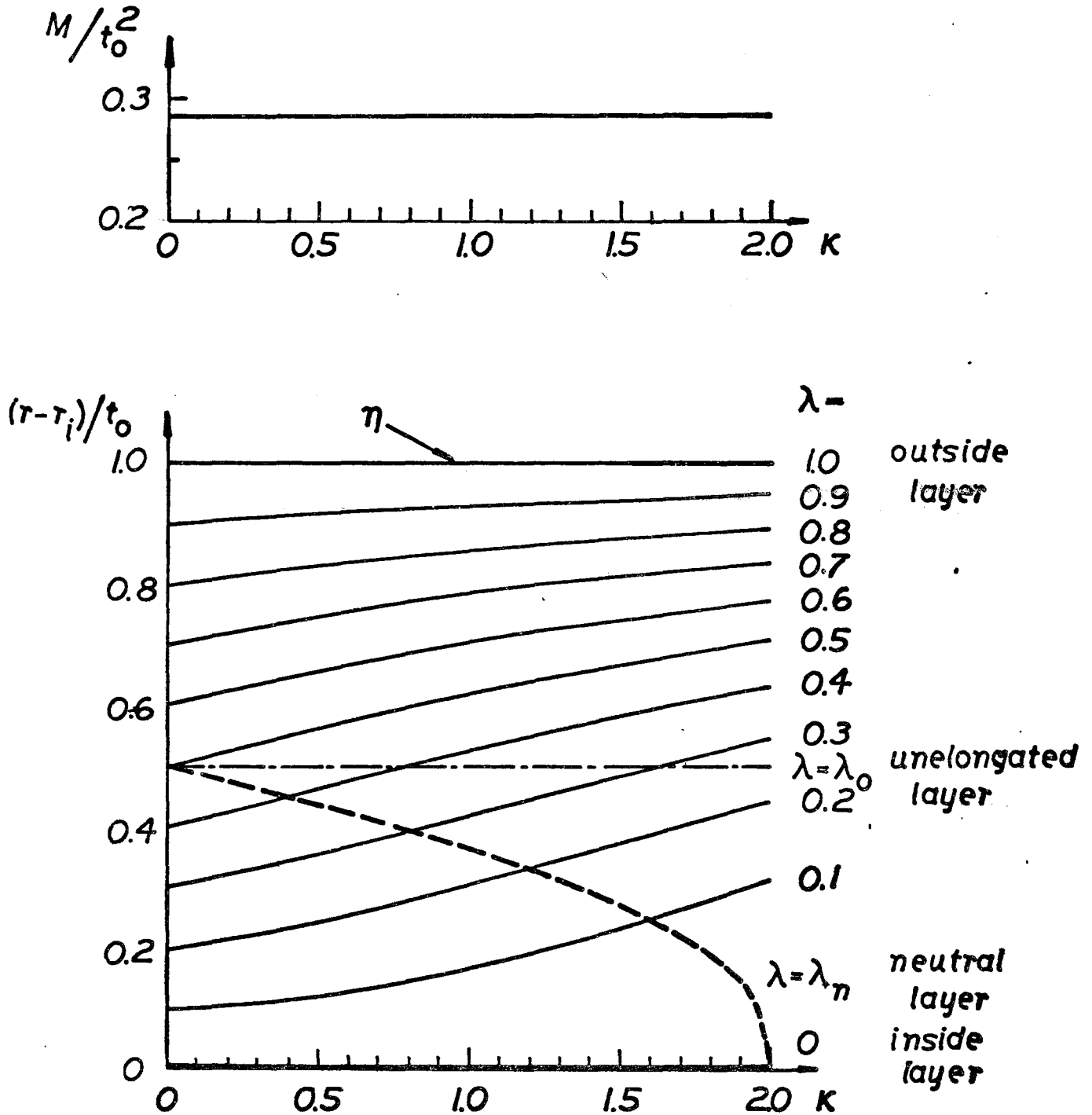


fig 4.2

NEUTRAL LAYER POSITION IN BENDING NON STRAIN HARDENING MONO-AND BIMETALS

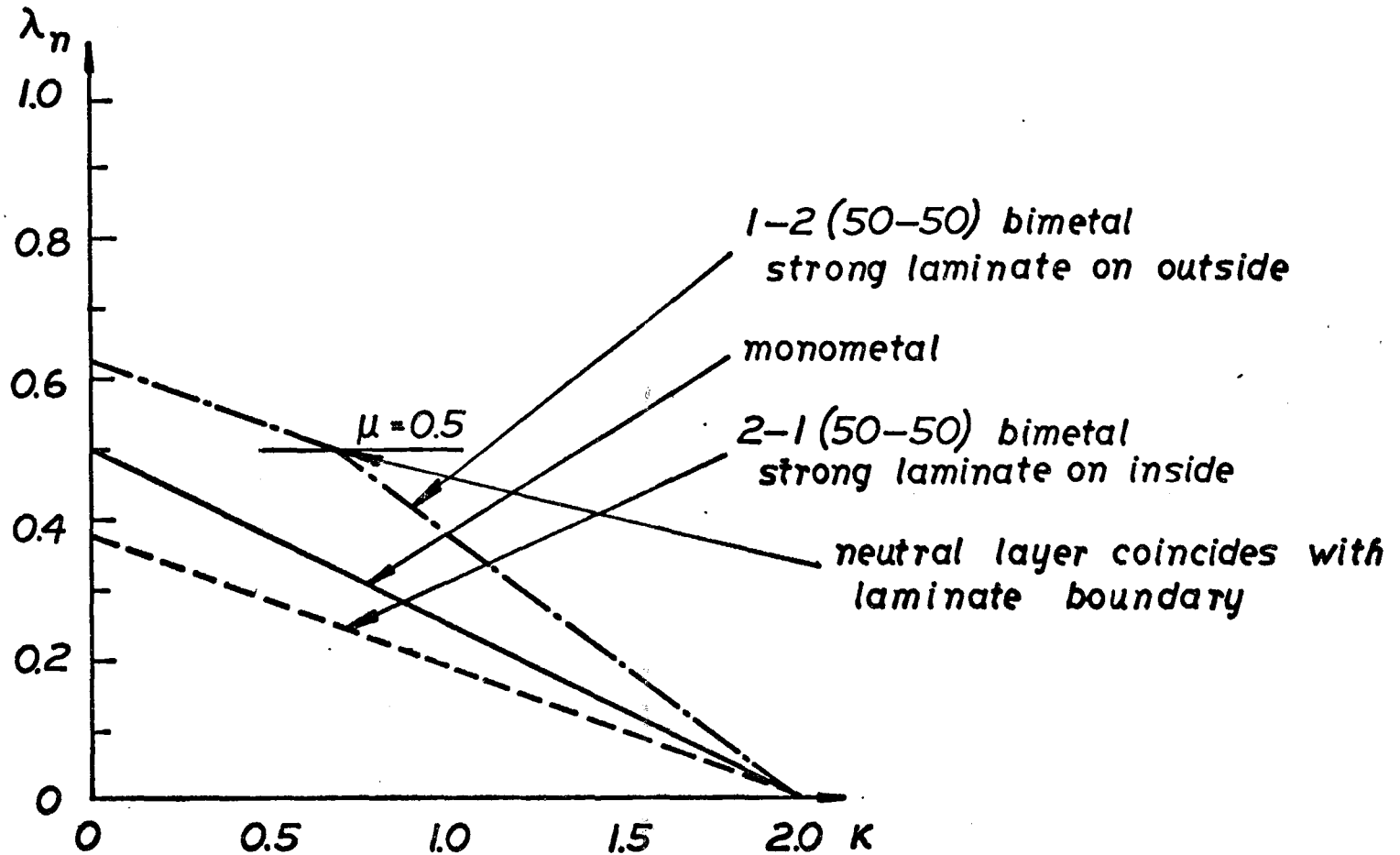


fig 4.2BIS

STRAINPROCESS IN BENDING NONSTRAINHARDENING MONOMETAL

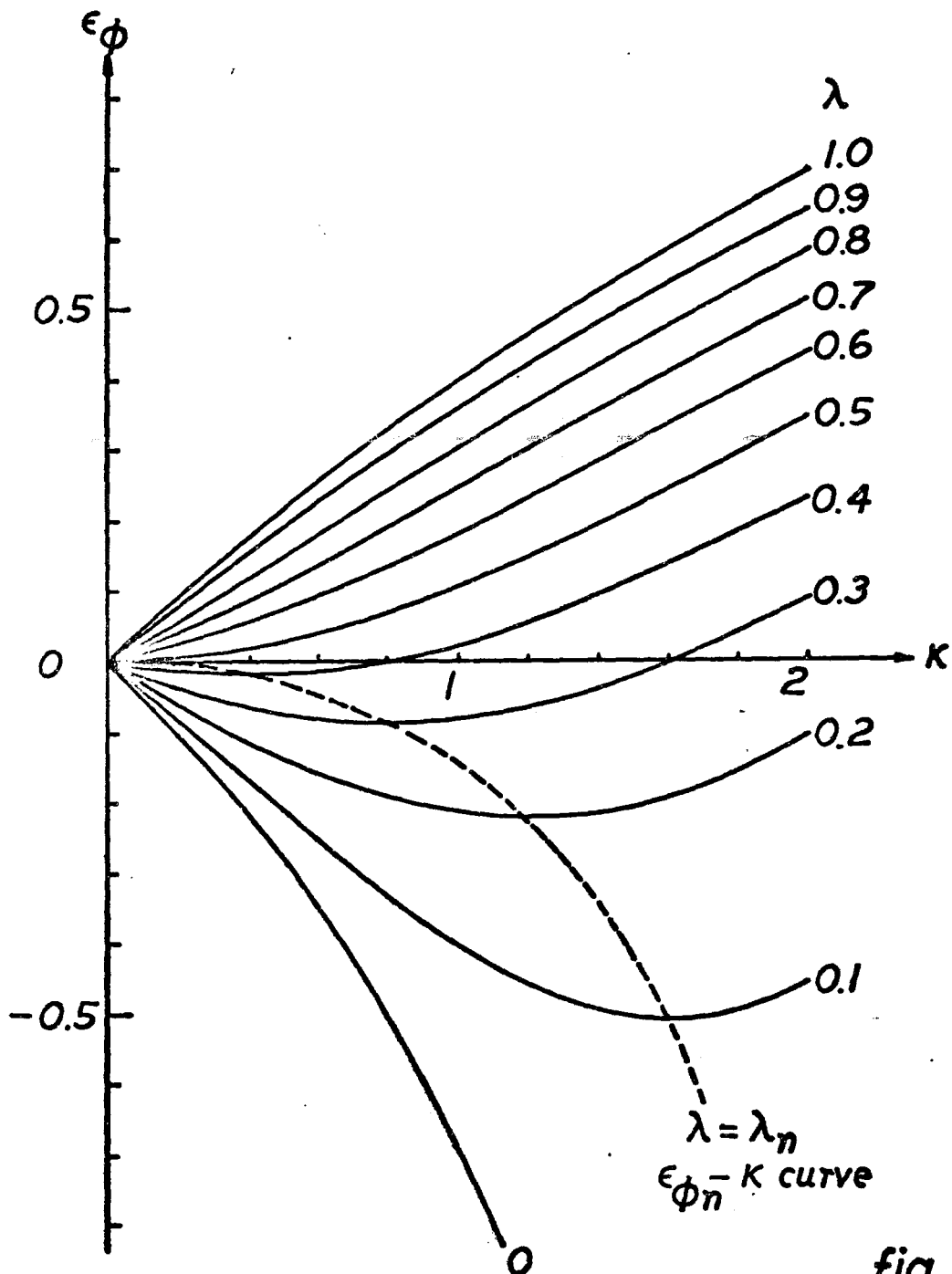


fig 4.3

BENDING OF NON STRAIN HARDENING 1-2 50-50 BIMETAL : PARAMETERS

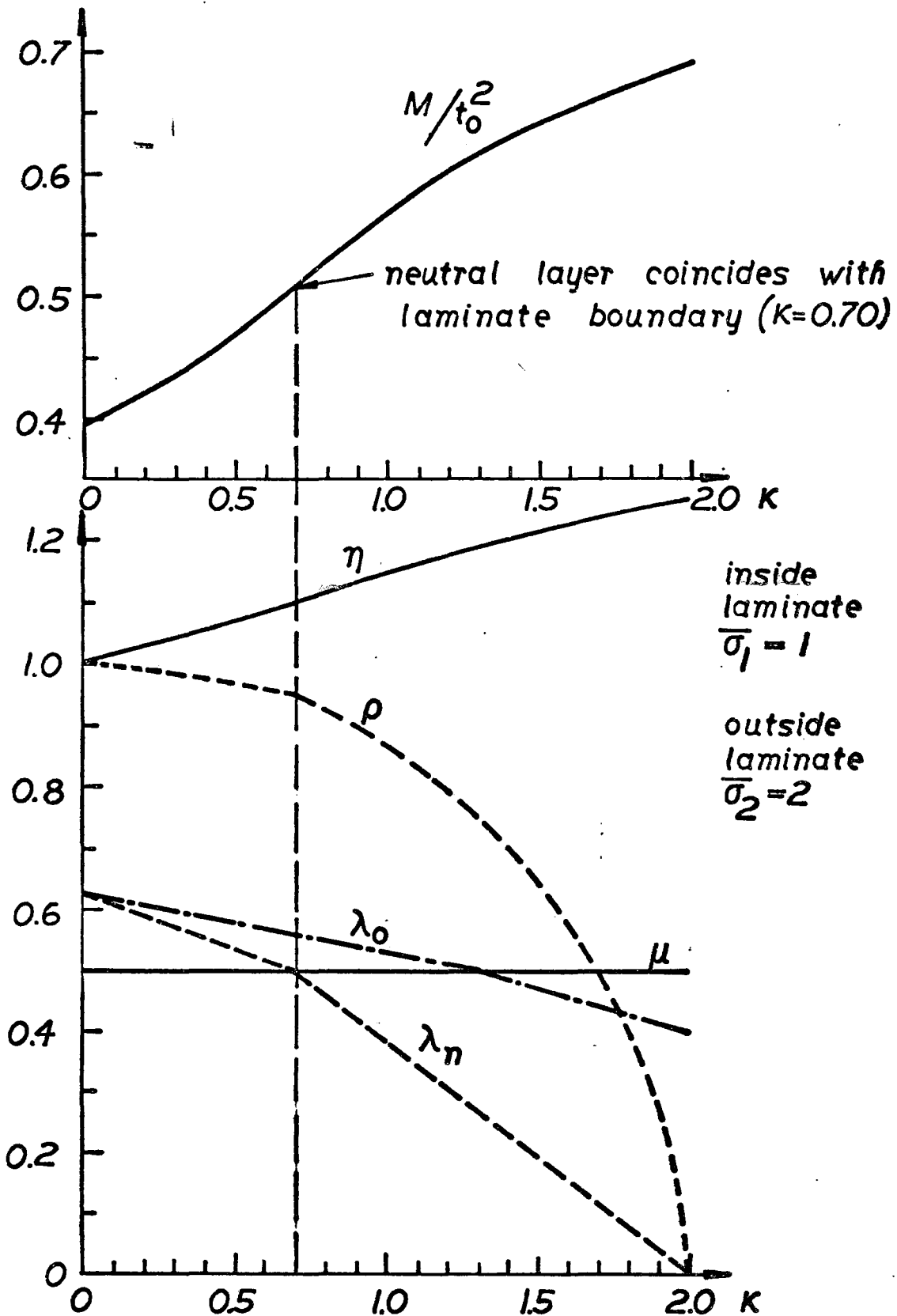


fig 4.4

BENDING MOMENT AND LAYER POSITION IN BENDING NON STRAIN HARDENING 1-2 (50-50) BIMETAL

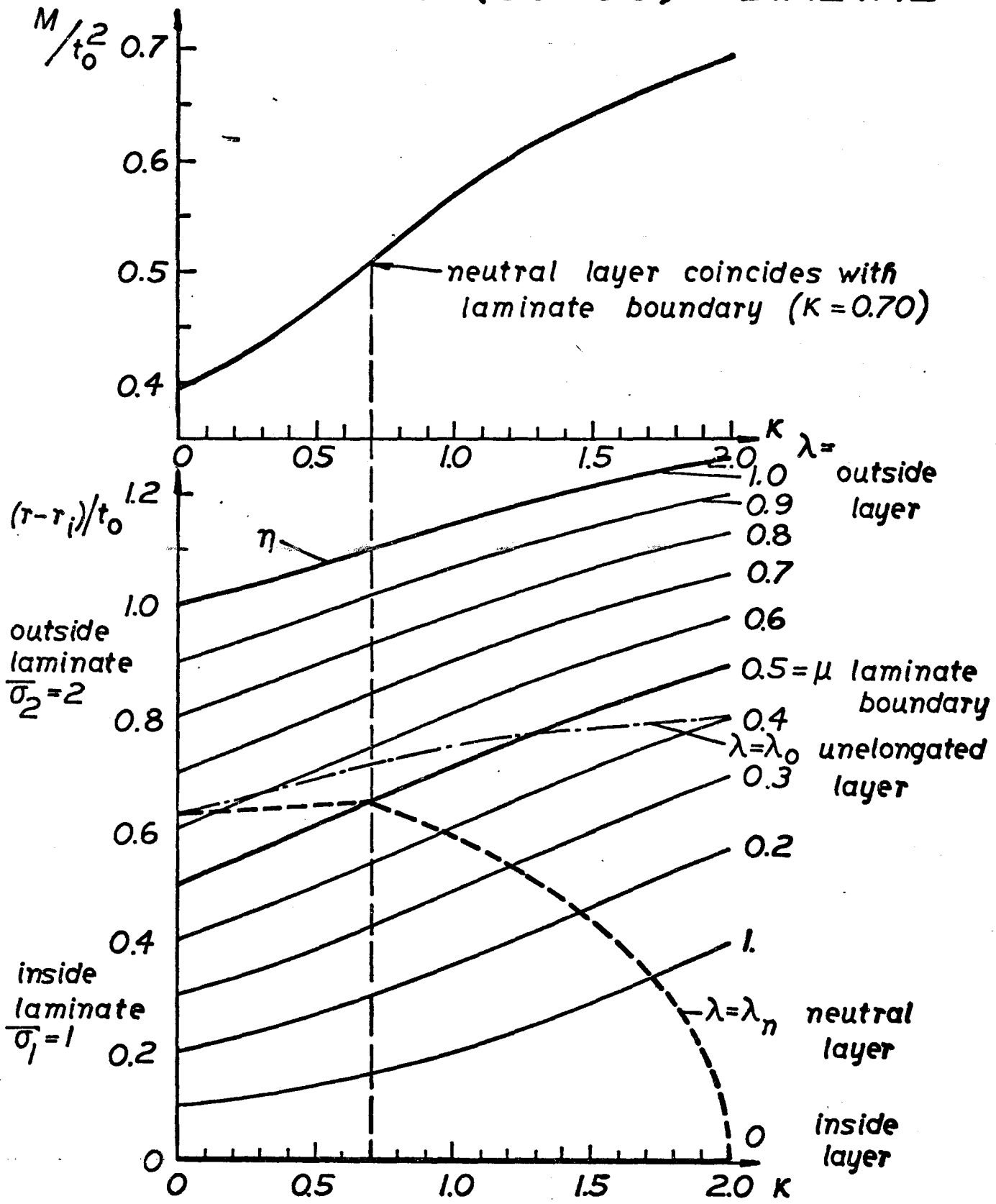


fig 4.5

STRAIN PROCESS IN BENDING
NONSTRAINHARDENING

1-2 BIMETAL

$A_1 = 1$ $A_2 = 2$ $\mu = 0.5$

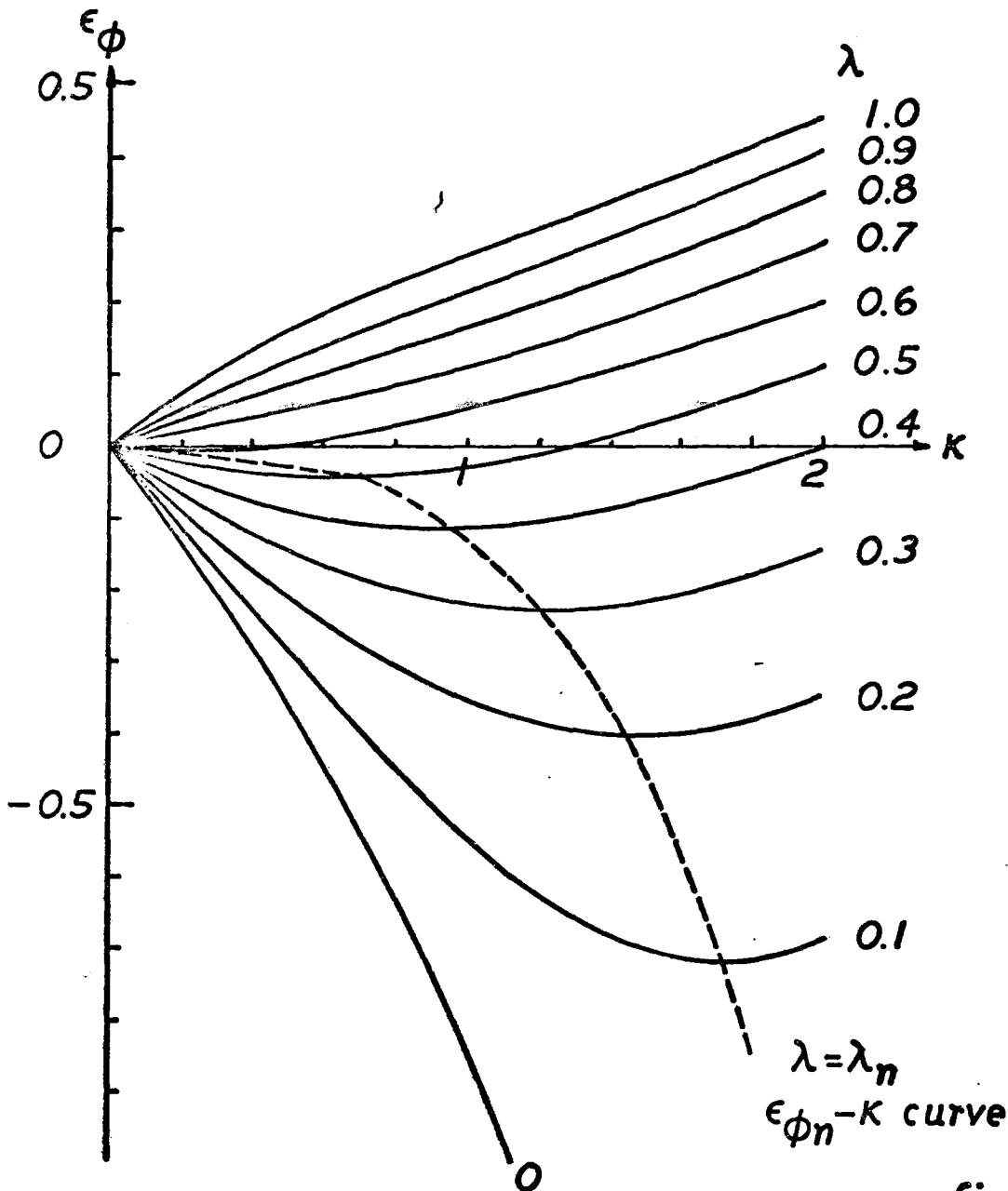
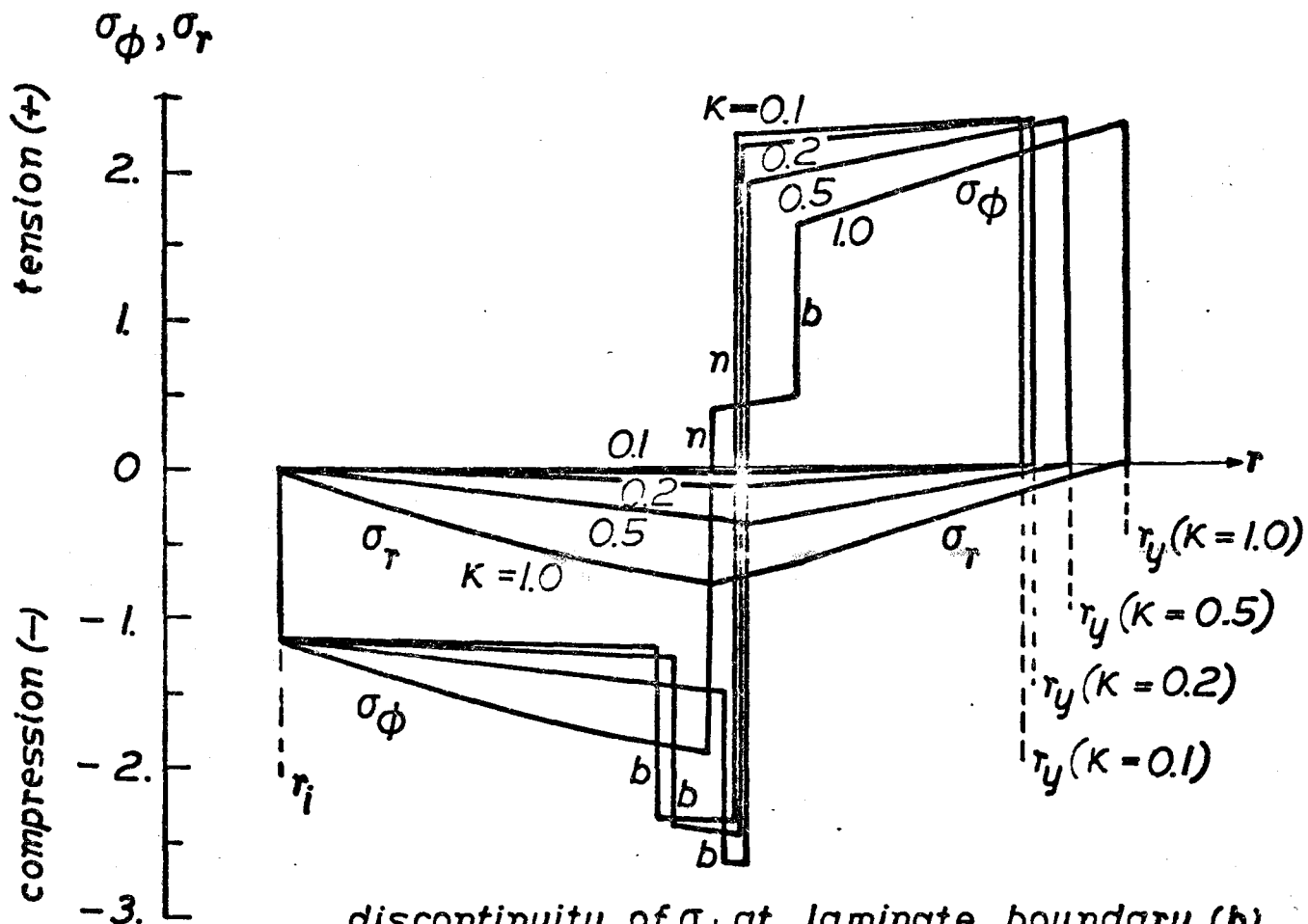


fig 4.6

STRESS DISTRIBUTION IN BENDING NON STRAINHARDENING 1-2 (50-50) BIMETAL



discontinuity of σ_ϕ at laminate boundary (b)
and neutral layer radii (n)

fig 4.7

BENDING OF NON STRAIN HARDENING 2-1 (50-50) BIMETAL : PARAMETERS

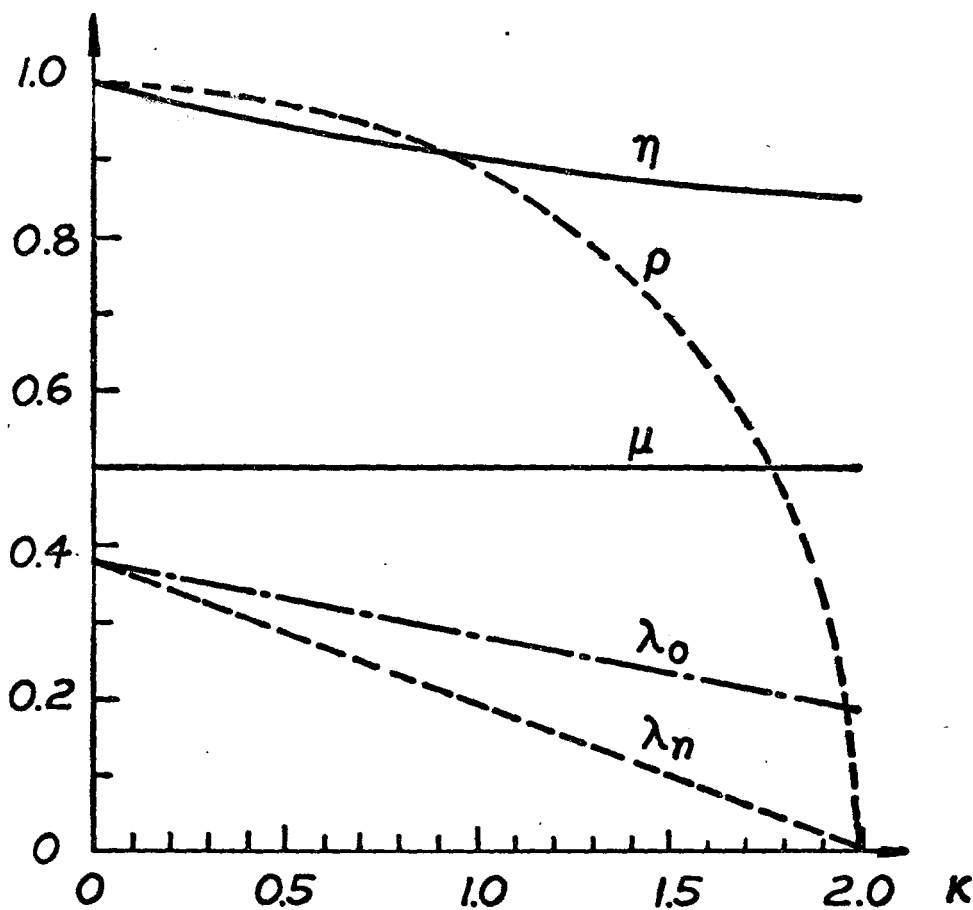
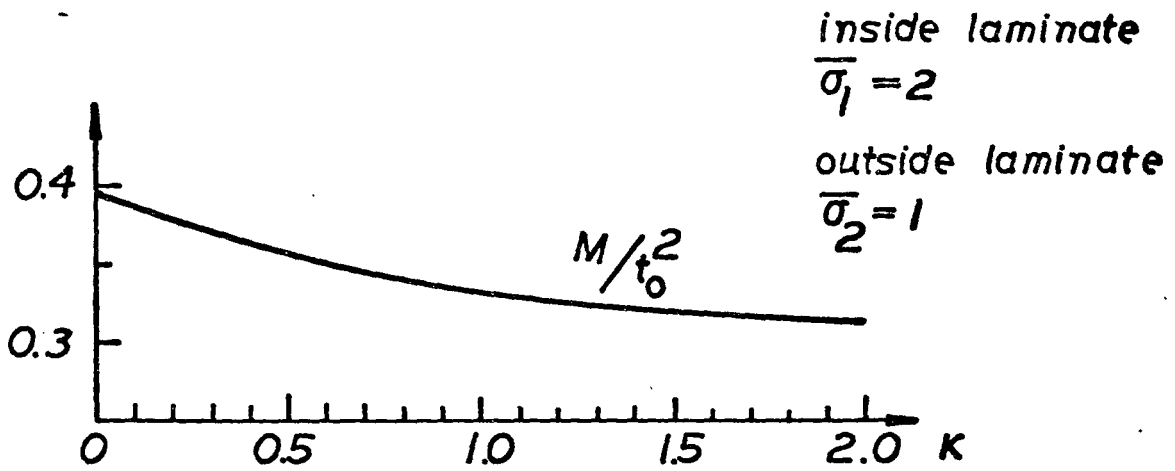


fig 4.8

BENDING MOMENT AND LAYER POSITION IN BENDING NON STRAIN HARDENING 2-1 (50-50) BIMETAL

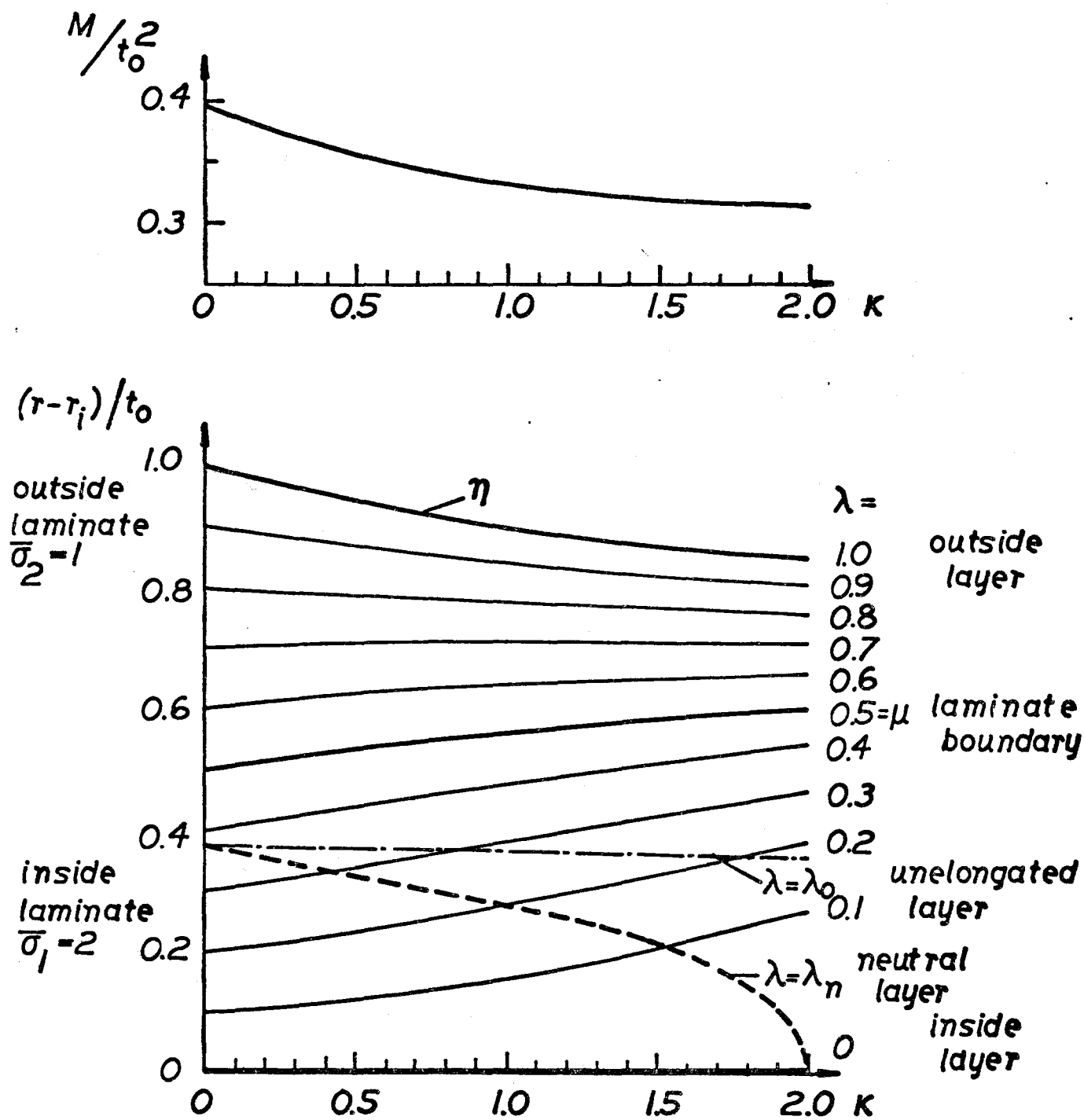


fig 4.9

STRAIN PROCESS IN BENDING NONSTRAINHARDENING

2-1 BIMETAL

$$A_1 = 2 \quad A_2 = 1 \quad \mu = 0.5$$

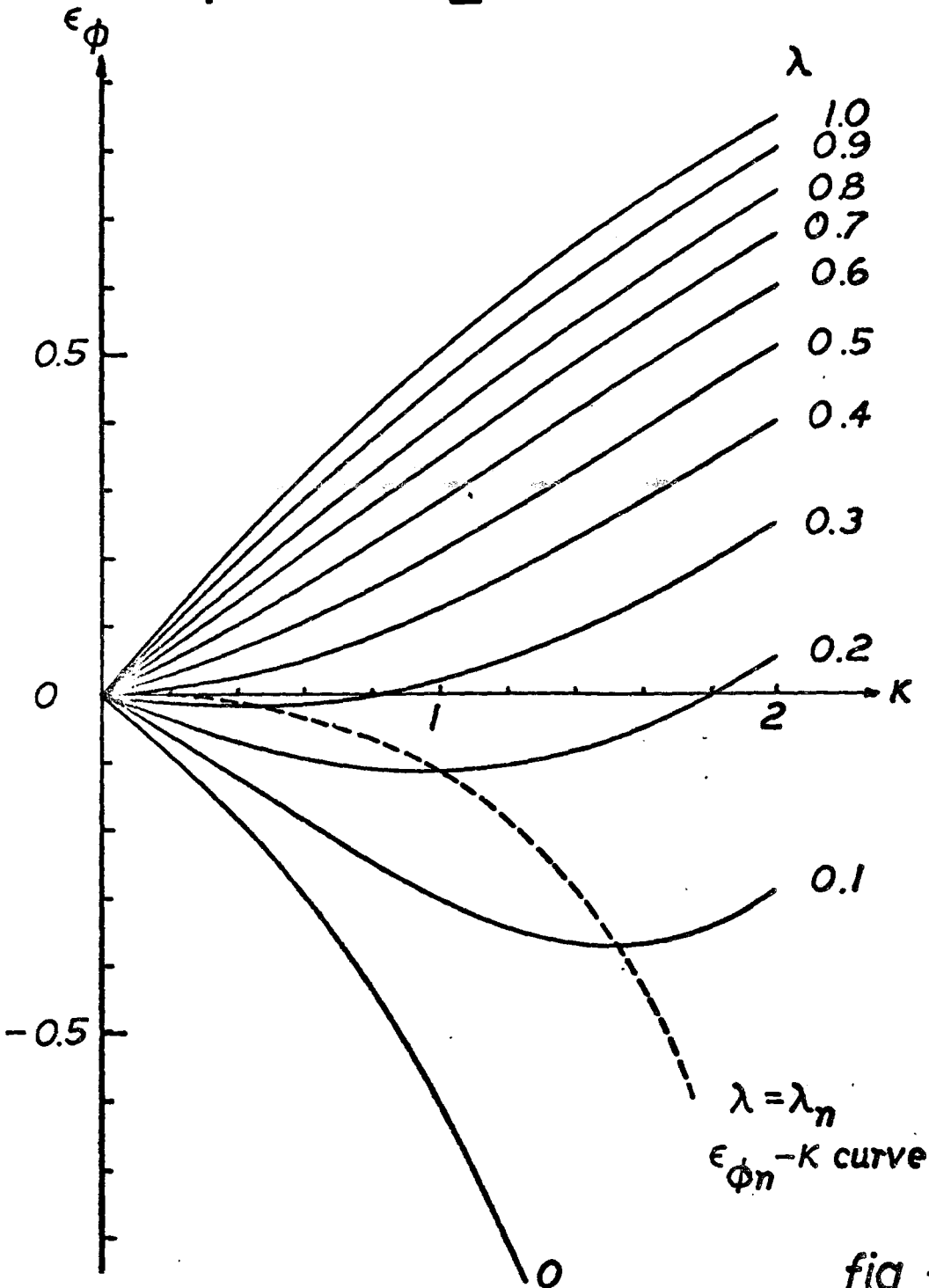


fig 4.10

STRESS DISTRIBUTION IN BENDING NON STRAINHARDENING 2-1 (50-50) BIMETAL

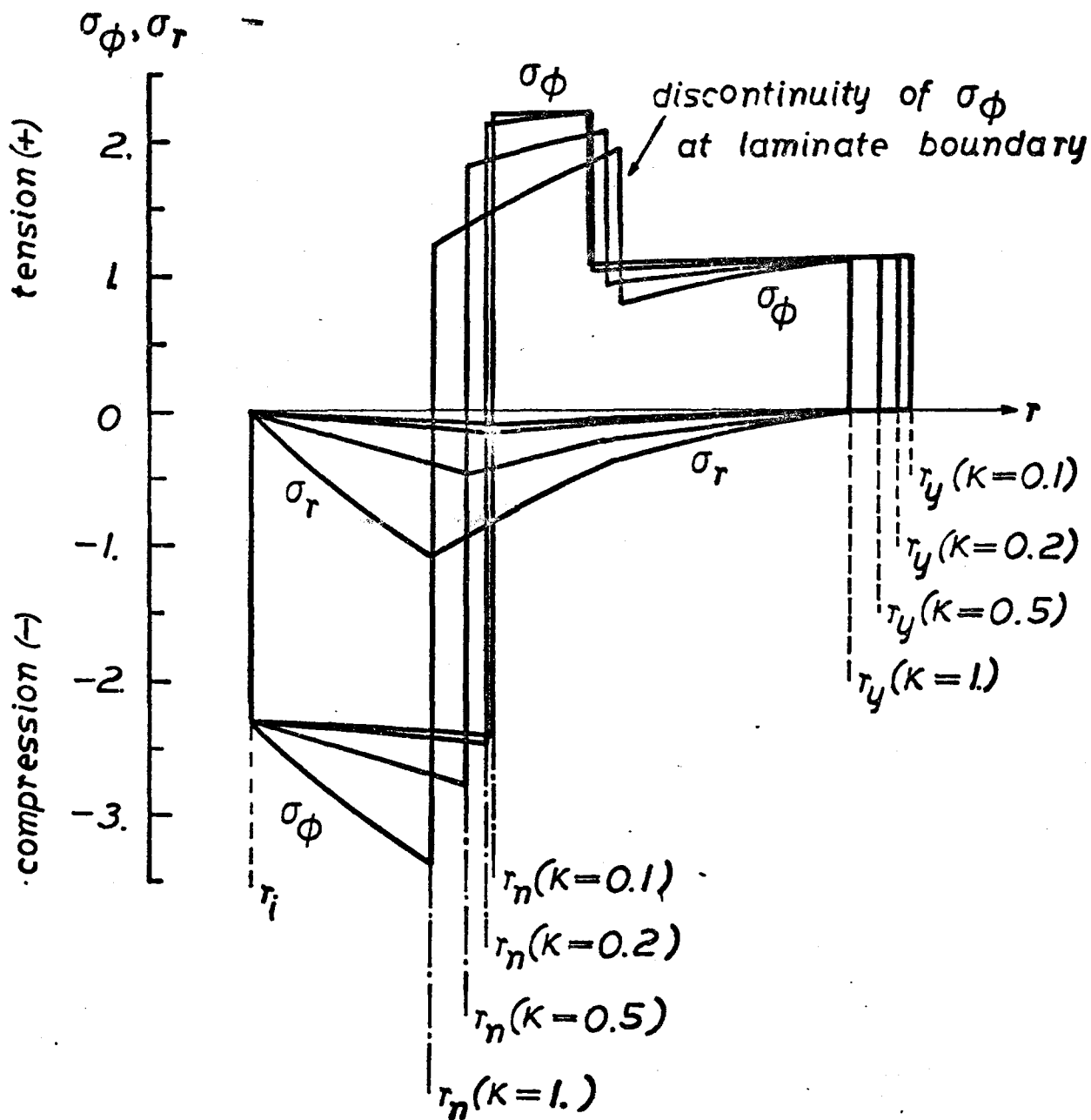


fig 4.11

RELATIVE SHEET THICKNESS AND NEUTRAL LAYER POSITION IN BENDING NON STRAIN HARDENING 2-1 AND 1-2 BIMETALS

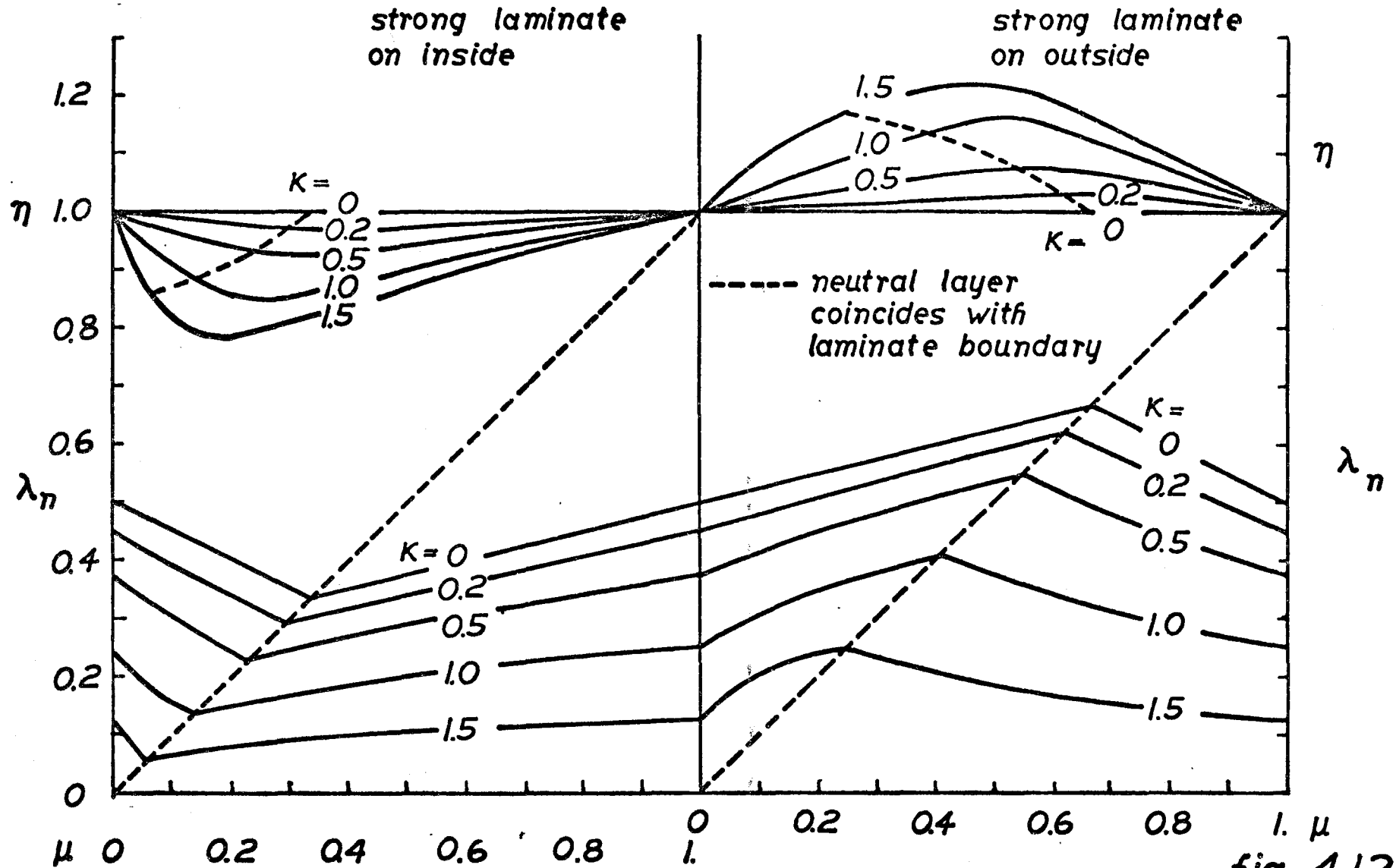


fig 4.12

BENDING MOMENT FOR NON STRAIN HARDENING 2-1 AND 1-2 BIMETALS

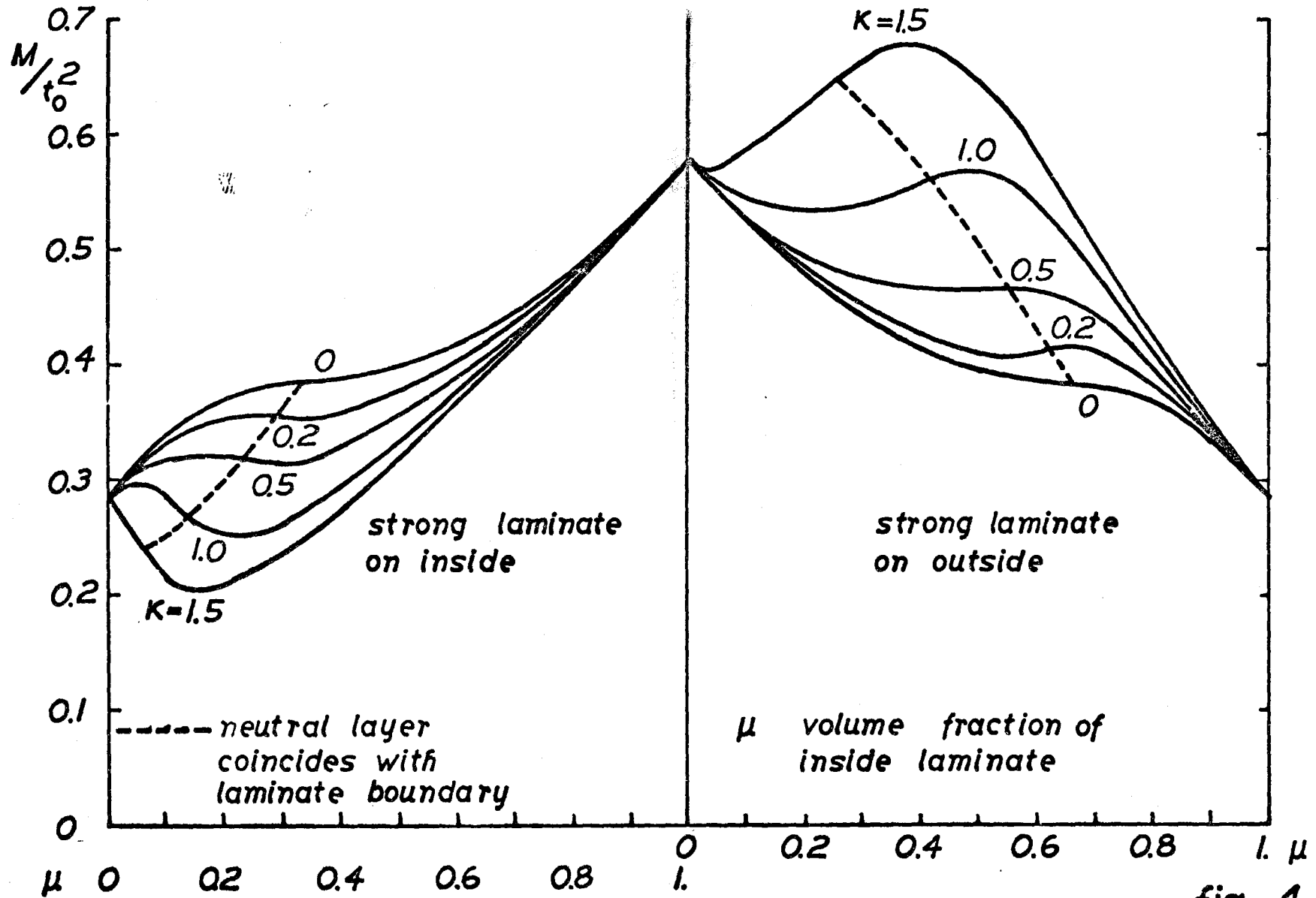


fig 4.13

BENDING MOMENT FOR NON STRAINHARDENING 2-1 AND 1-2 BIMETALS

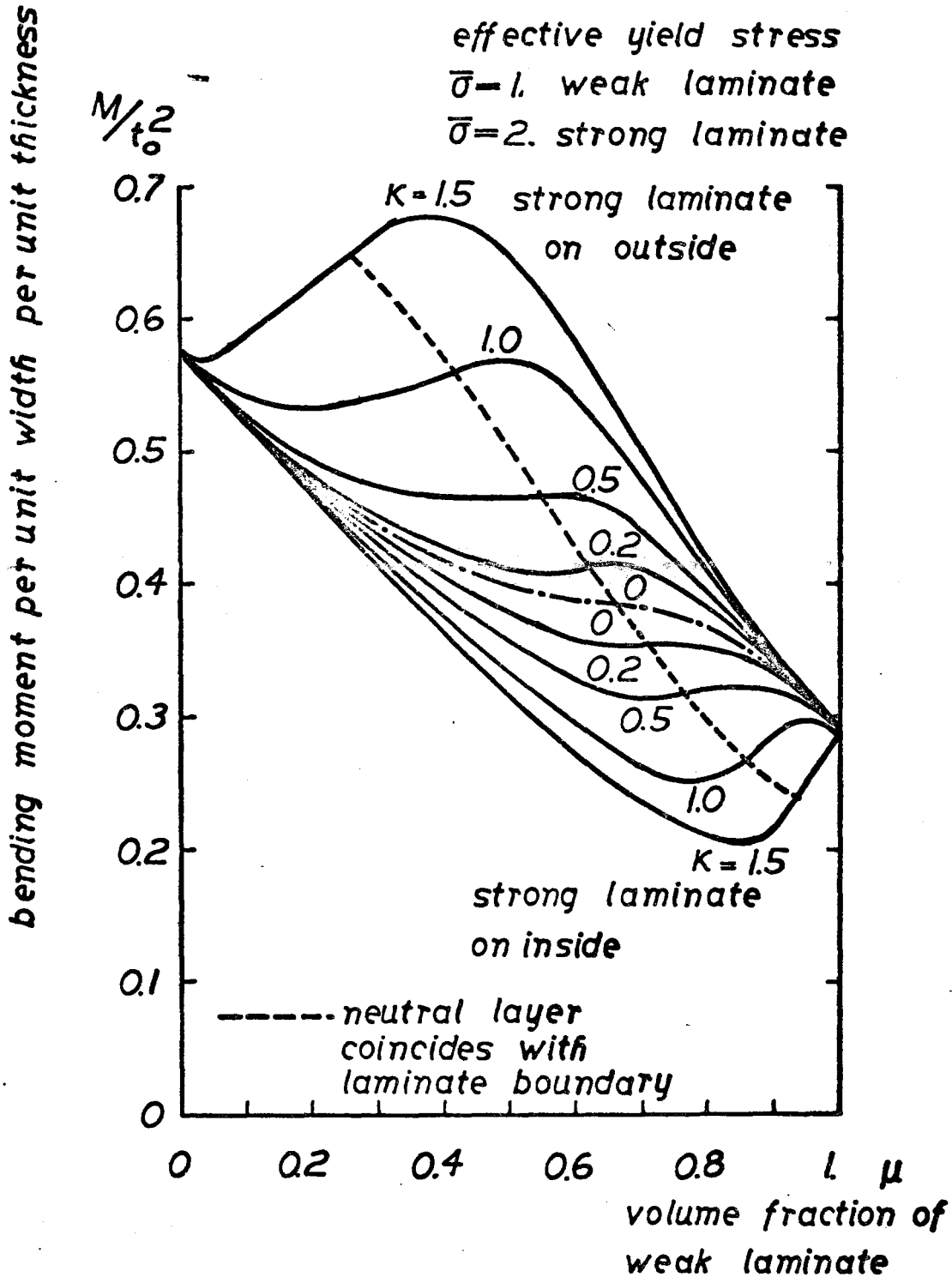


fig 4.14

RATIO OF BENDING MOMENT TO SQUARE OF ORIGINAL SHEET THICKNESS FOR NON STRAIN HARDENING 2-1 AND 1-2 BIMETALS

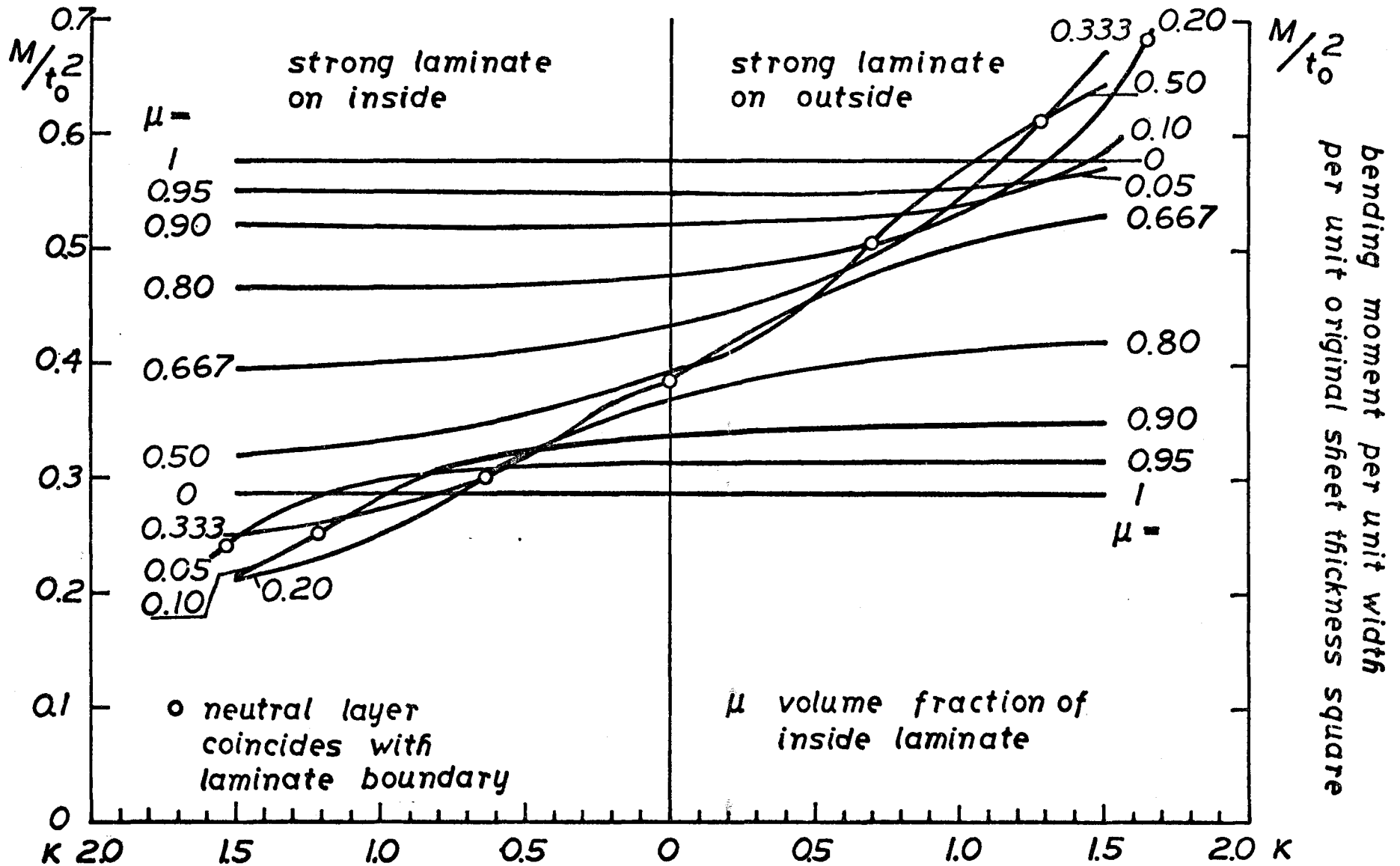


fig 4.15

RATIO OF BENDING MOMENT TO SQUARE OF CURRENT SHEET THICKNESS FOR NON STRAIN HARDENING 2-1 AND 1-2 BIMETALS

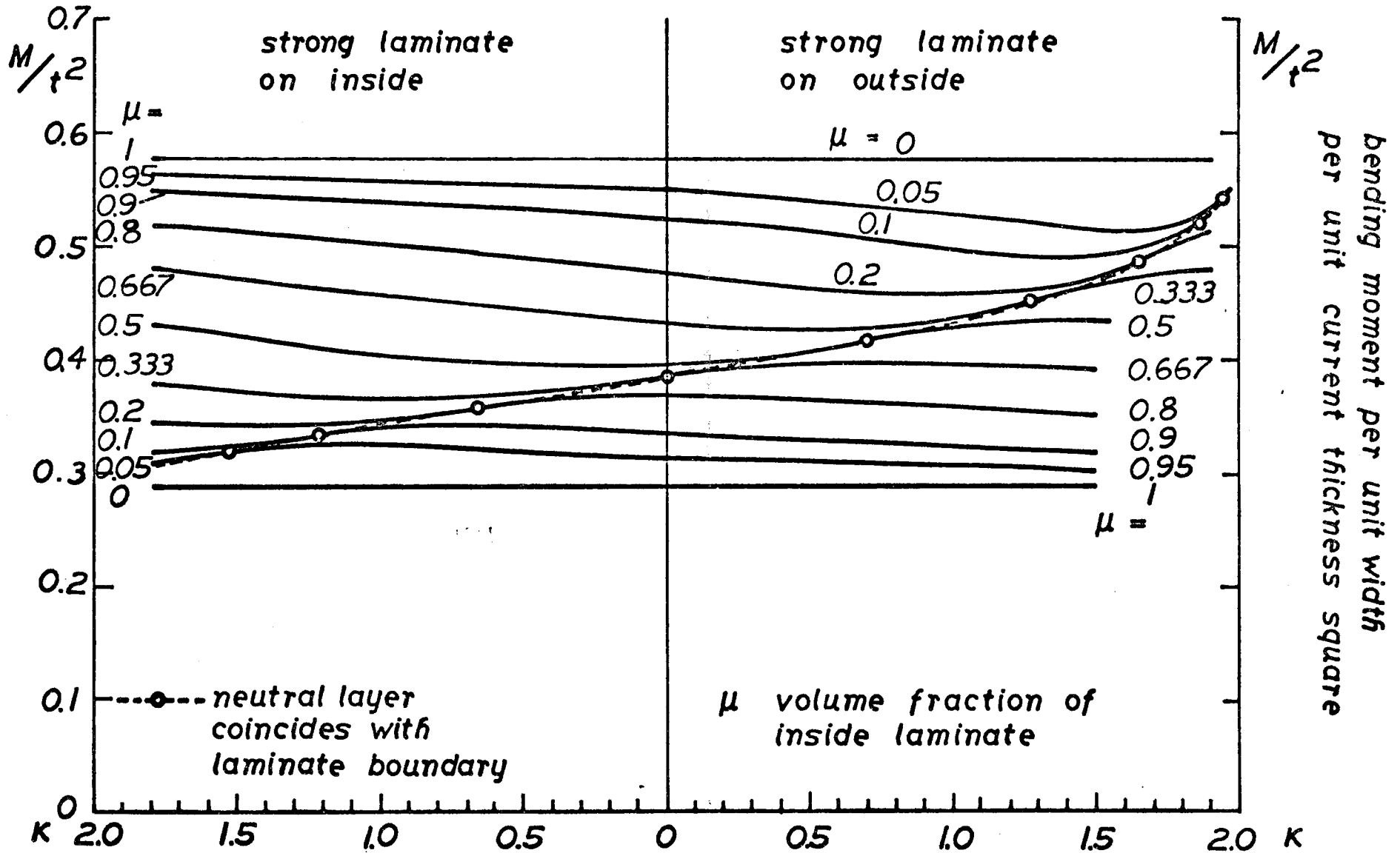
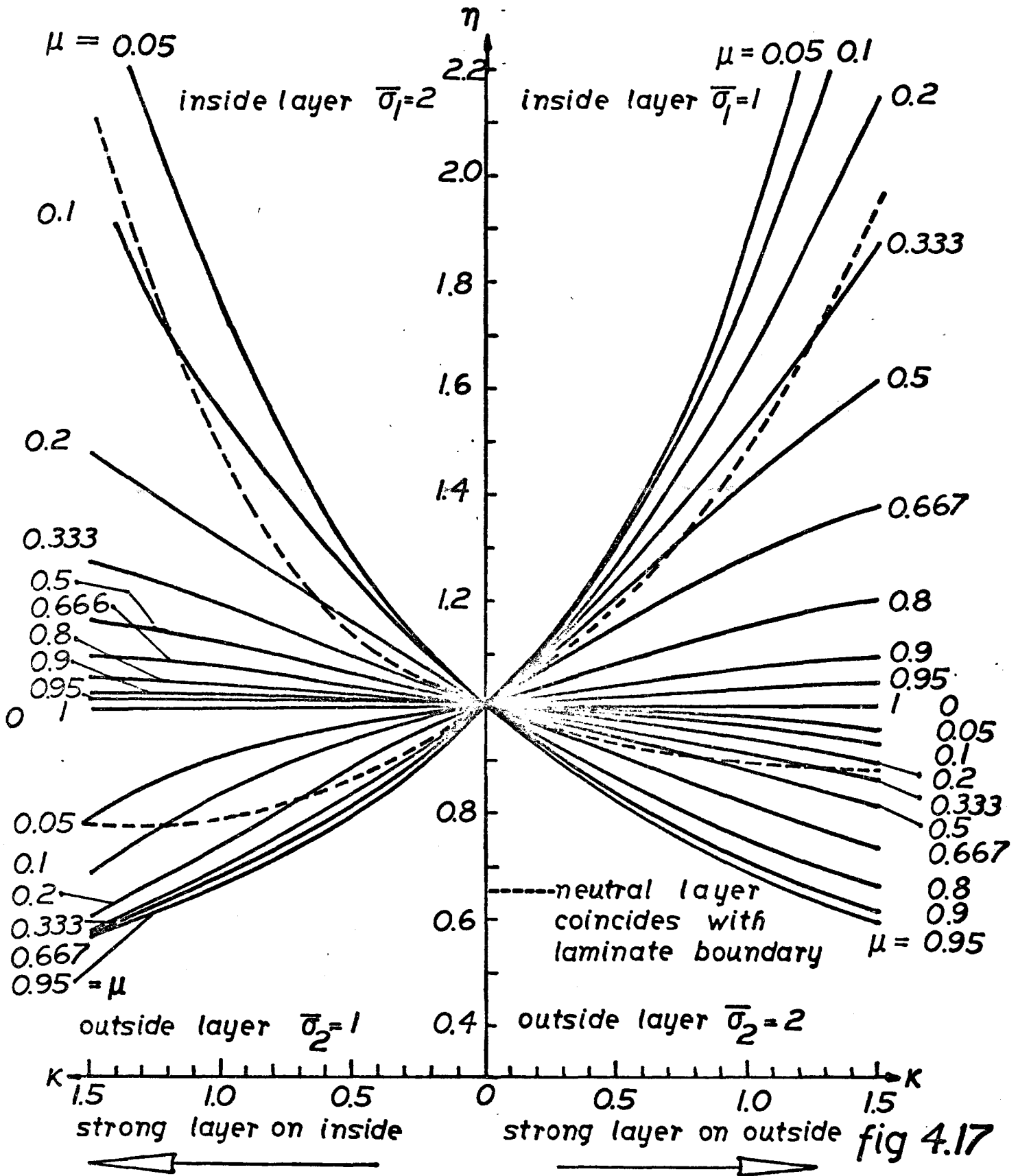
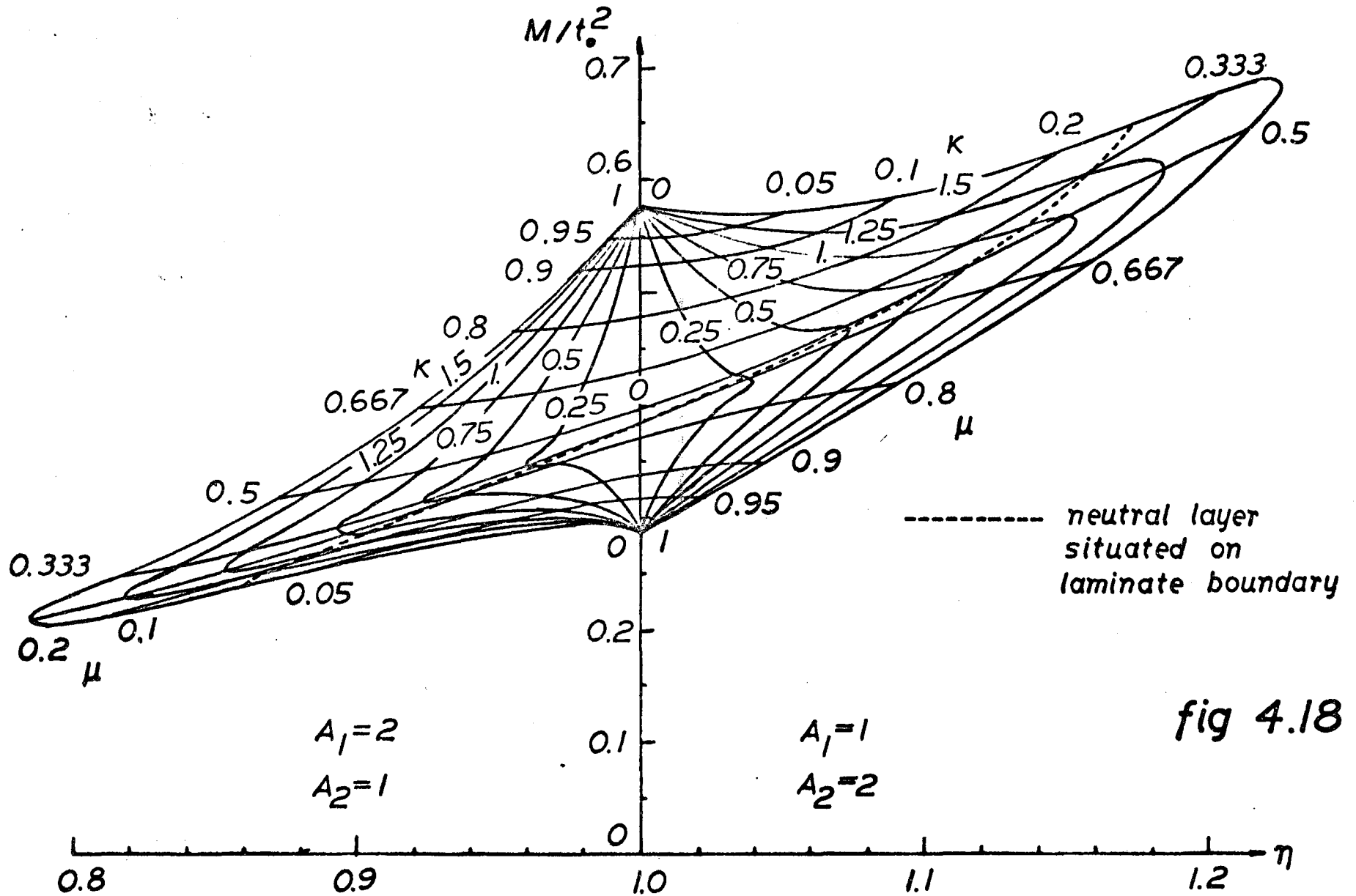


fig 4.16

RELATIVE LAMINATE THICKNESSES IN BENDING NON STRAIN HARDENING 2-1 AND 1-2 BIMETALS



BENDING OF NONSTRAINHARDENING BIMETALS



BENDING MOMENT AND LAYER POSITION IN BENDING NON STRAIN HARDENING 2-1-2 (40-40-20) TRIMETAL

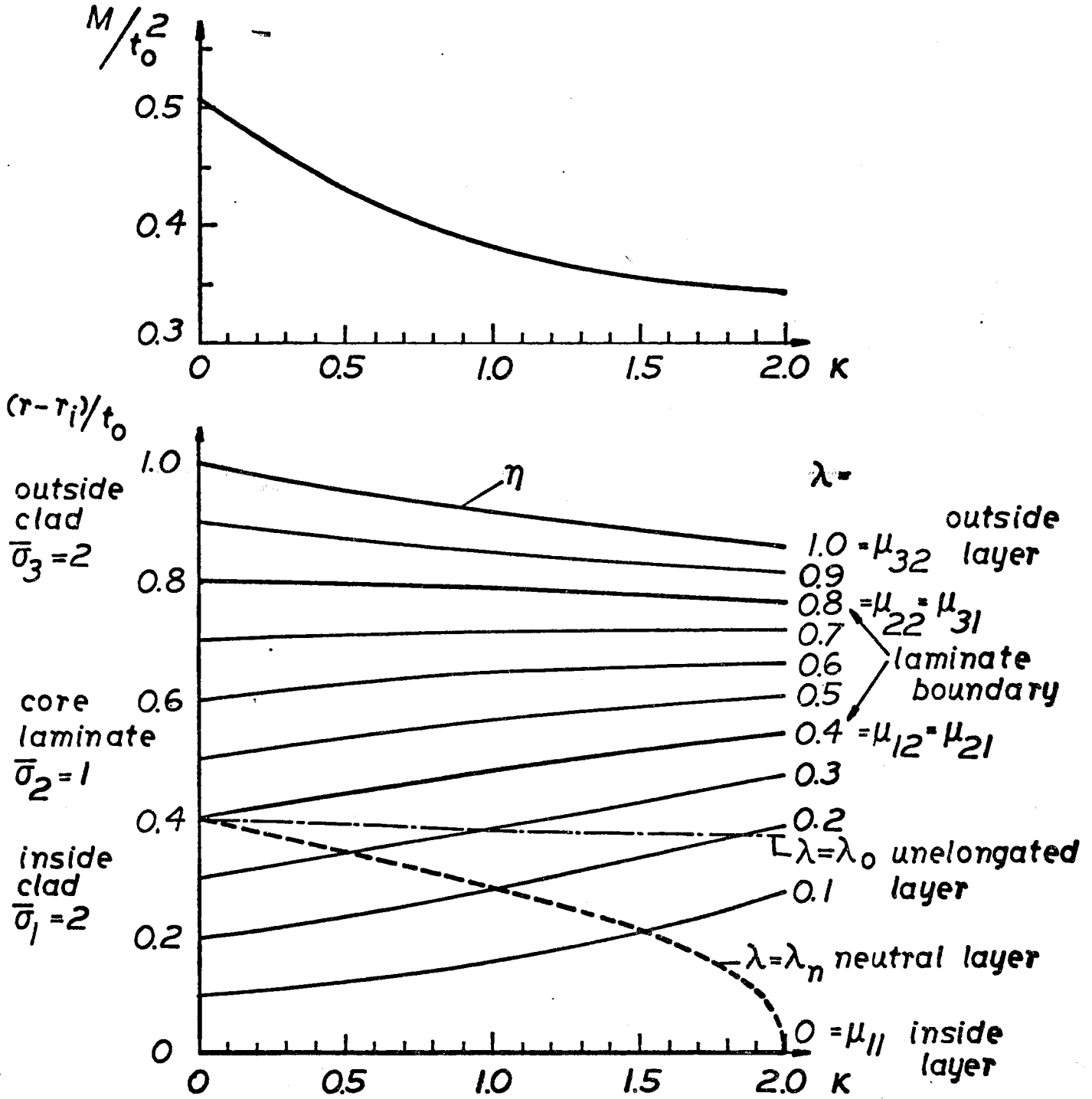


fig 4.19

BENDING MOMENT AND LAYER POSITION IN BENDING NON STRAIN HARDENING 2-1-2 (20-40-40) TRIMETAL

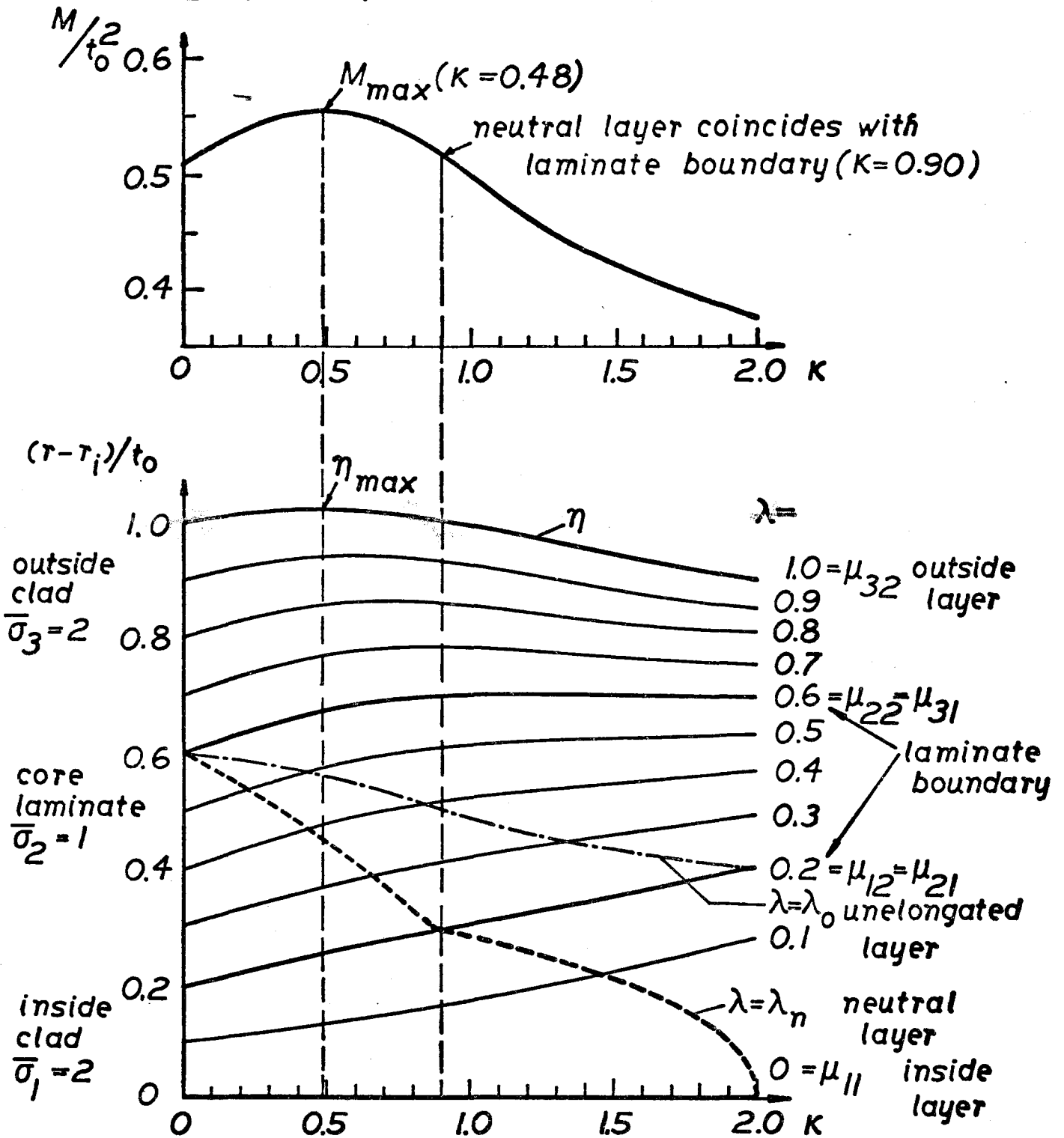
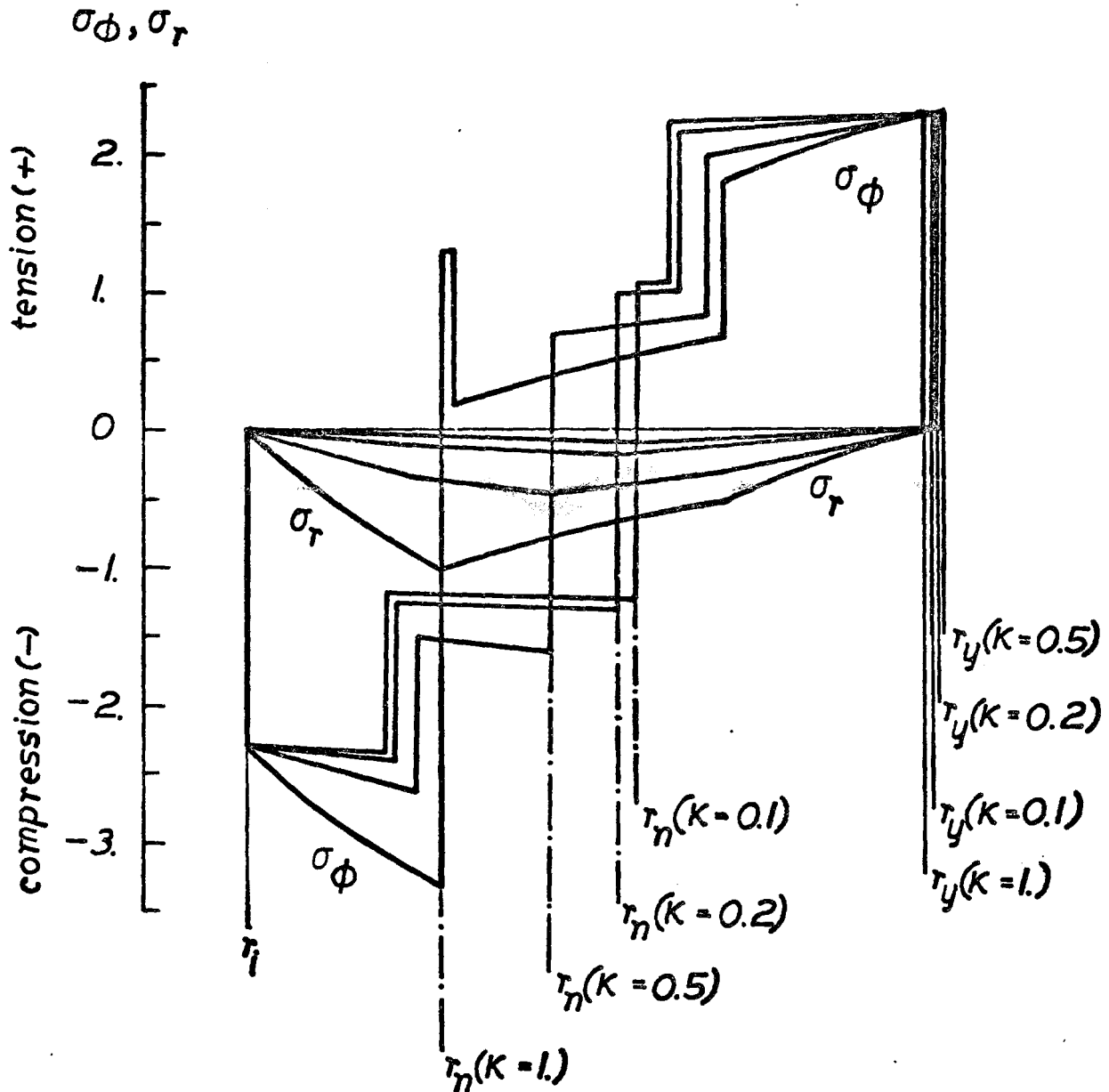


fig 4.20

STRESS DISTRIBUTION IN BENDING NONSTRAINHARDENING 2-1-2 (20-40-40) TRIMETAL



Discontinuity of hoop stress σ_ϕ at laminate boundary and neutral layer

fig 4.21

symmetrical trimetal line

all compositions with
5 percent outside clad

all compositions with
70 percent core

$\frac{\text{percent inside clad}}{\text{percent outside clad}} = 0.25$ line

PERCENTAGE
INSIDE CLAD

PERCENTAGE
OUTSIDE
CLAD

20 percent
inside clad

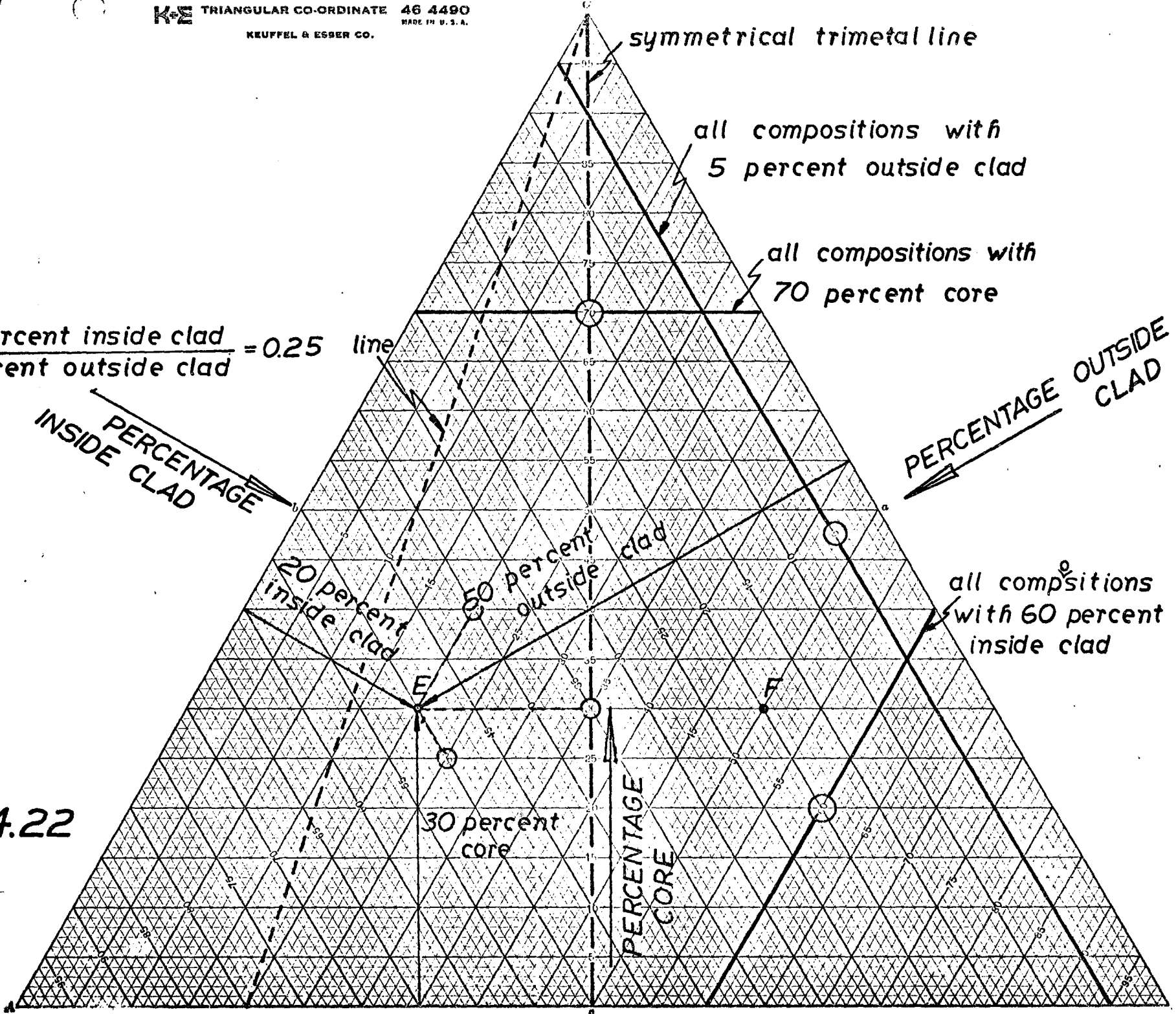
50 percent
outside clad

all compositions
with 60 percent
inside clad

30 percent
core

PERCENTAGE
CORE

fig 4.22



STABILITY OF 2-1-2 NON STRAIN HARDENING TRIMETALS IN BENDING

left: STABLE up to indicated
 value $K_{M_{max}}$
 (relative curvature
 at which bending
 moment is maximum)

percentage
 inside clad ($\bar{\sigma}_1 = 2$)

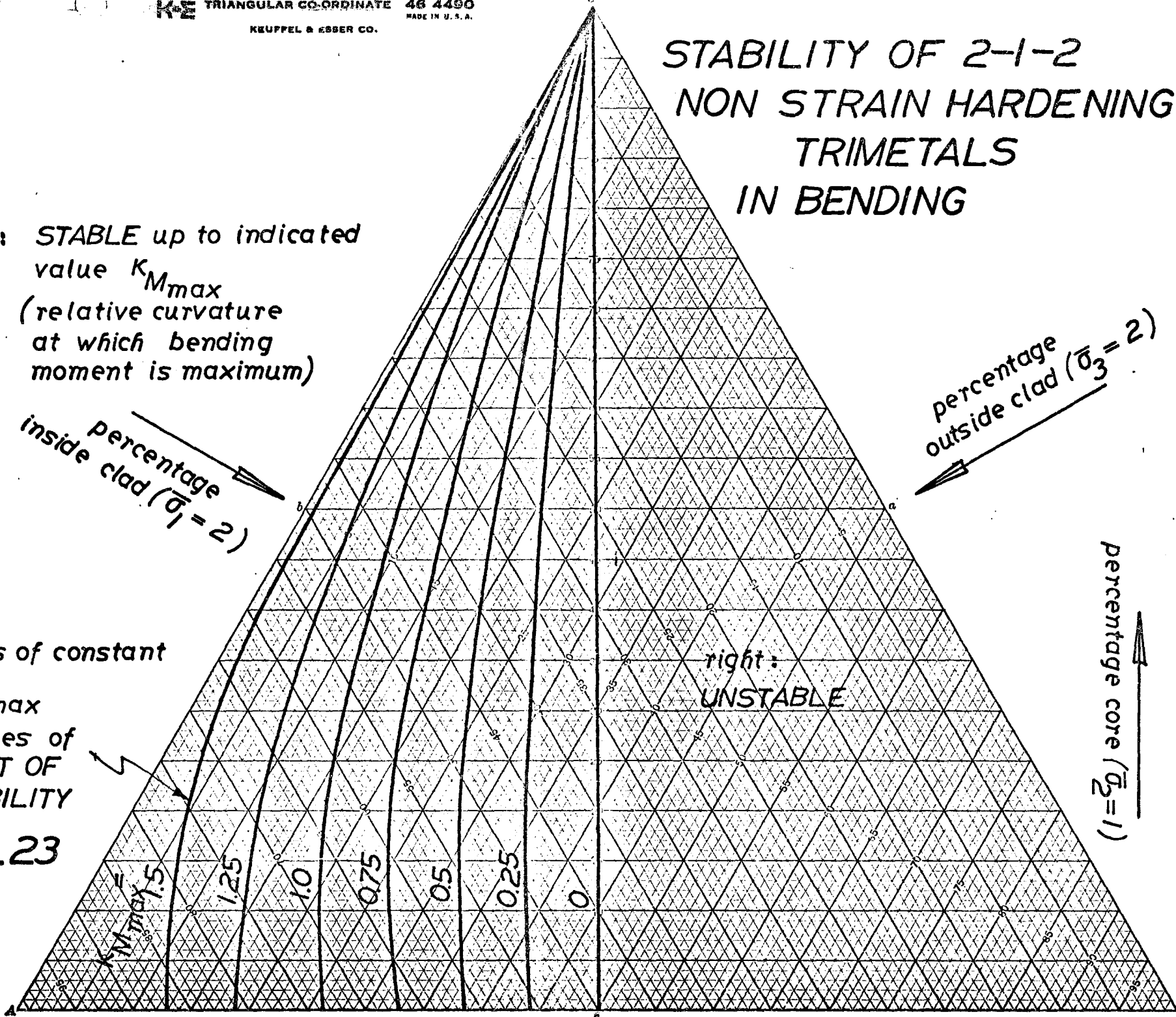
percentage
 outside clad ($\bar{\sigma}_3 = 2$)

lines of constant
 $K_{M_{max}}$
 = lines of
 LIMIT OF
 STABILITY

right:
 UNSTABLE

percentage
 core ($\bar{\sigma}_2 = 1$)

fig 4.23



STABILITY OF NON STRAIN HARDENING 2-1-2 TRIMETALS IN BENDING

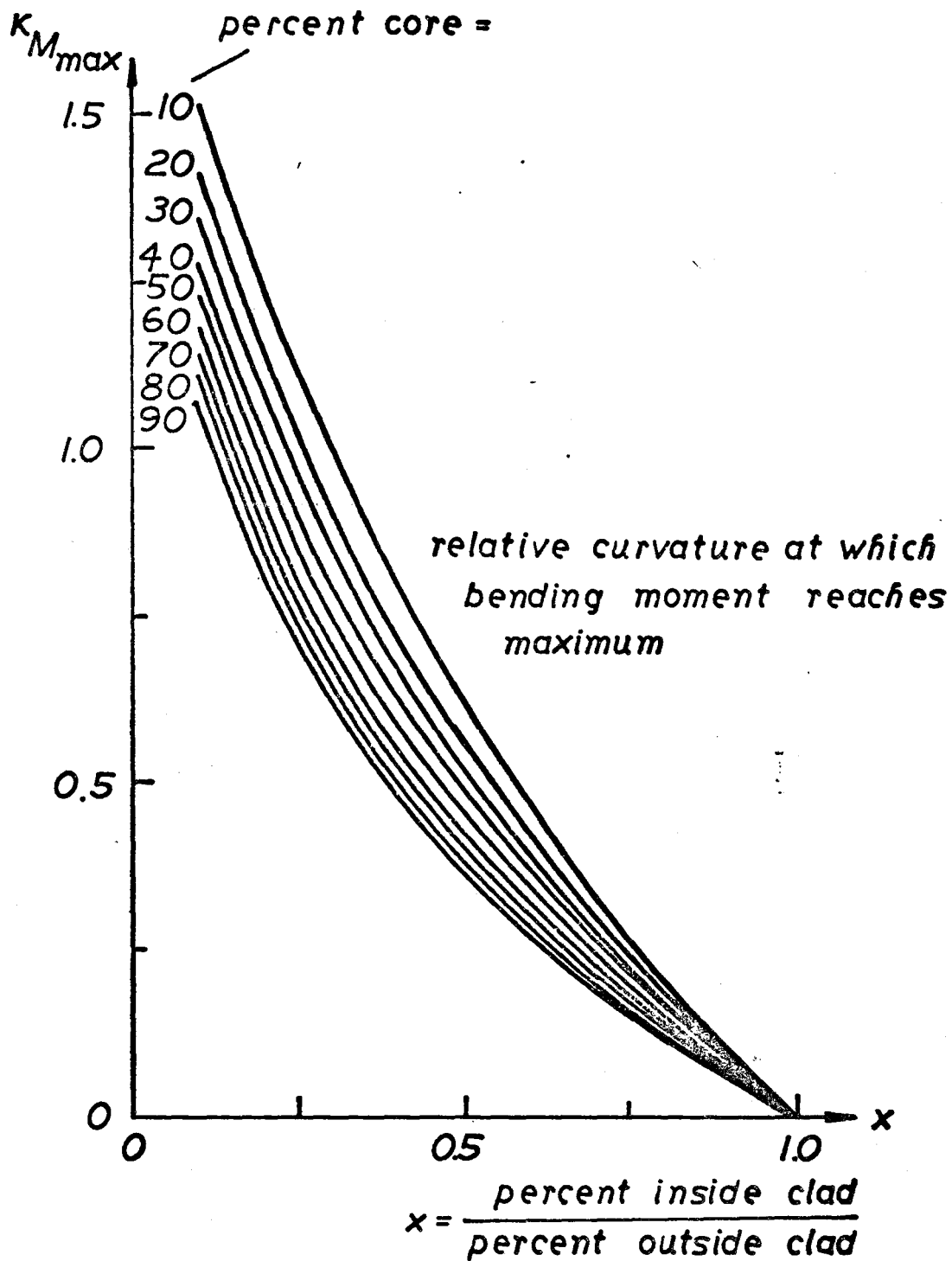
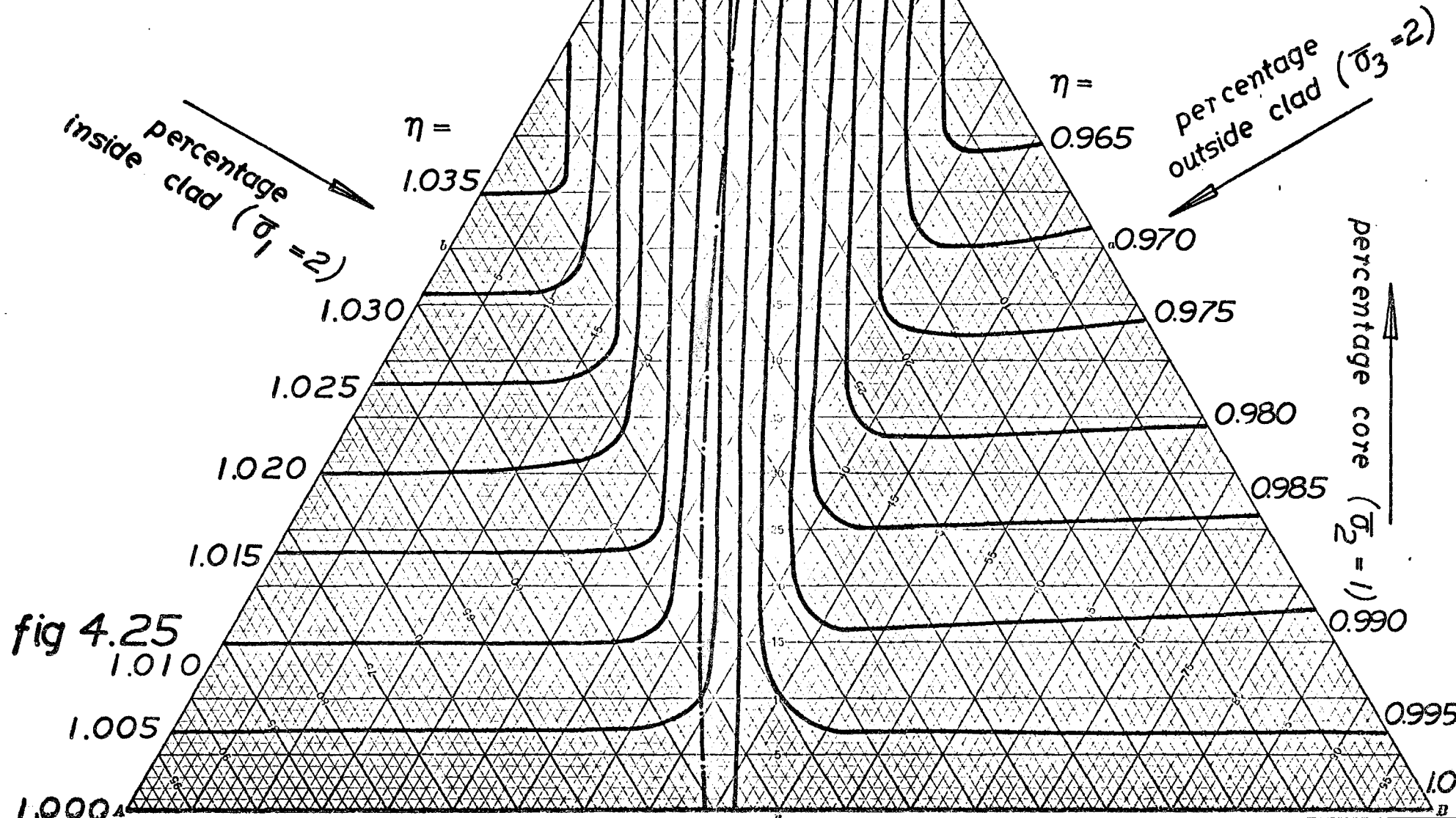


fig 4.24

RELATIVE SHEET THICKNESS IN BENDING 2-1-2 NON STRAIN HARDENING TRI-METALS FOR K=0.25

limit of stability for $K=0.25$ ———



limit of stability for $K=0.5$ -----

RELATIVE SHEET THICKNESS IN BENDING
 2-1-2 NON STRAIN HARDENING TRIME-TALS FOR $K=0.5$

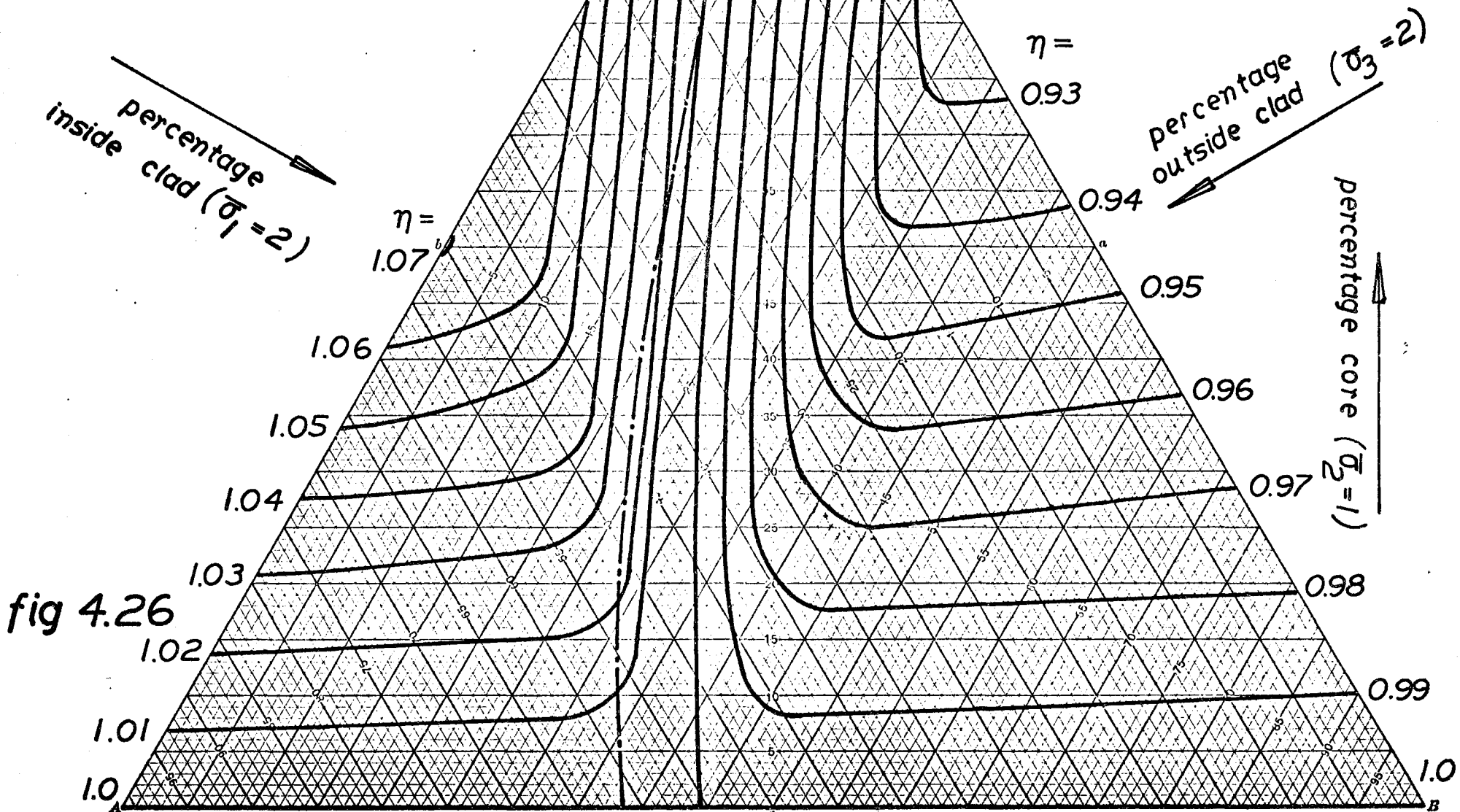
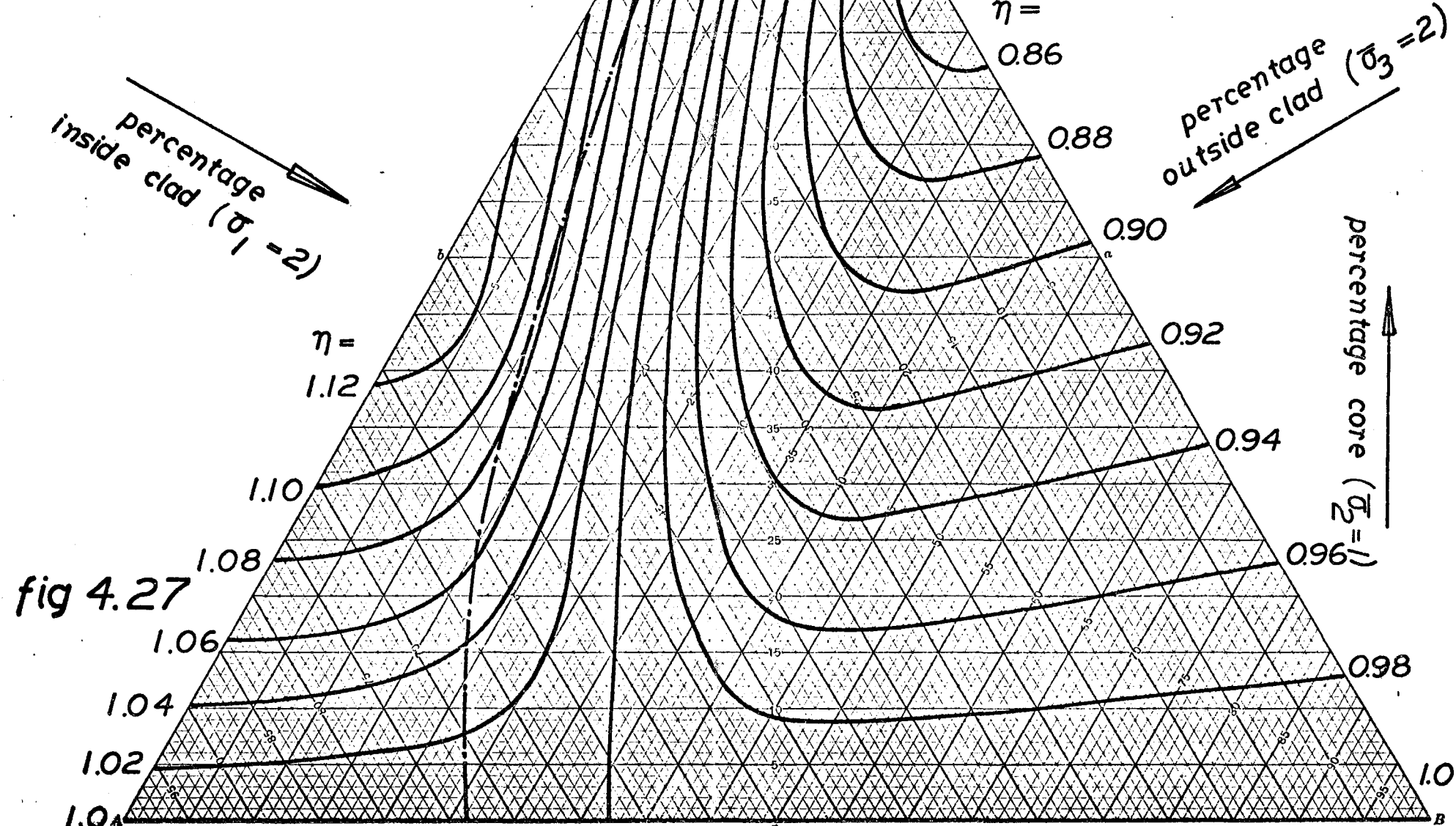


fig 4.26

RELATIVE SHEET
 THICKNESS IN BENDING
 2-1-2 NON STRAIN
 HARDENING TRIME-
 TALS FOR $K=1.0$

limit of stability for $K=1.0$ - - - - -



BENDING MOMENT AND LAYER POSITION IN BENDING NON STRAIN HARDENING 1-2-1 (40-40-20) TRIMETAL

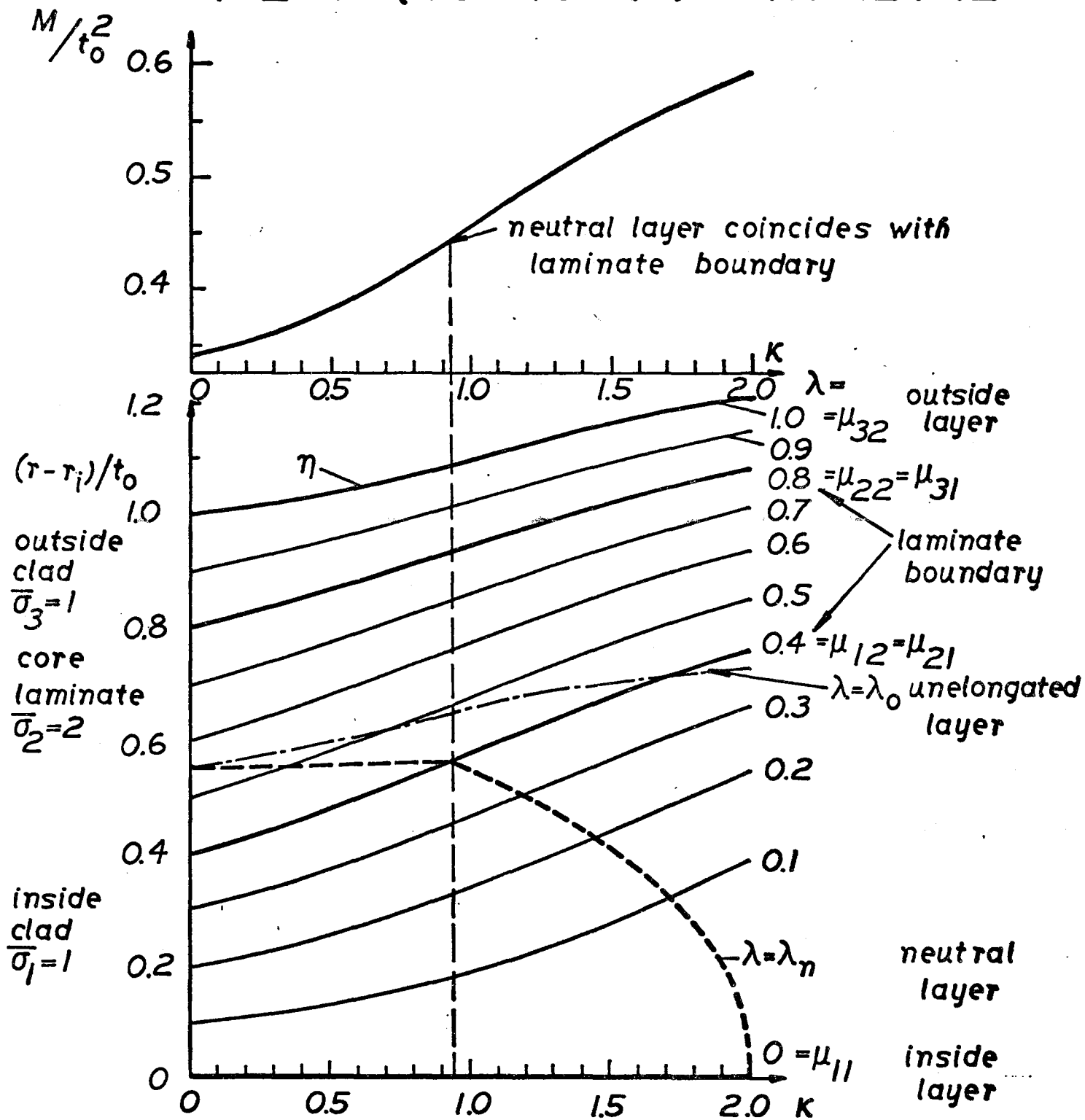


fig 4.28

BENDING MOMENT AND LAYER POSITION IN BENDING NON STRAIN HARDENING 1-2-1 (20-40-40) TRIMETAL

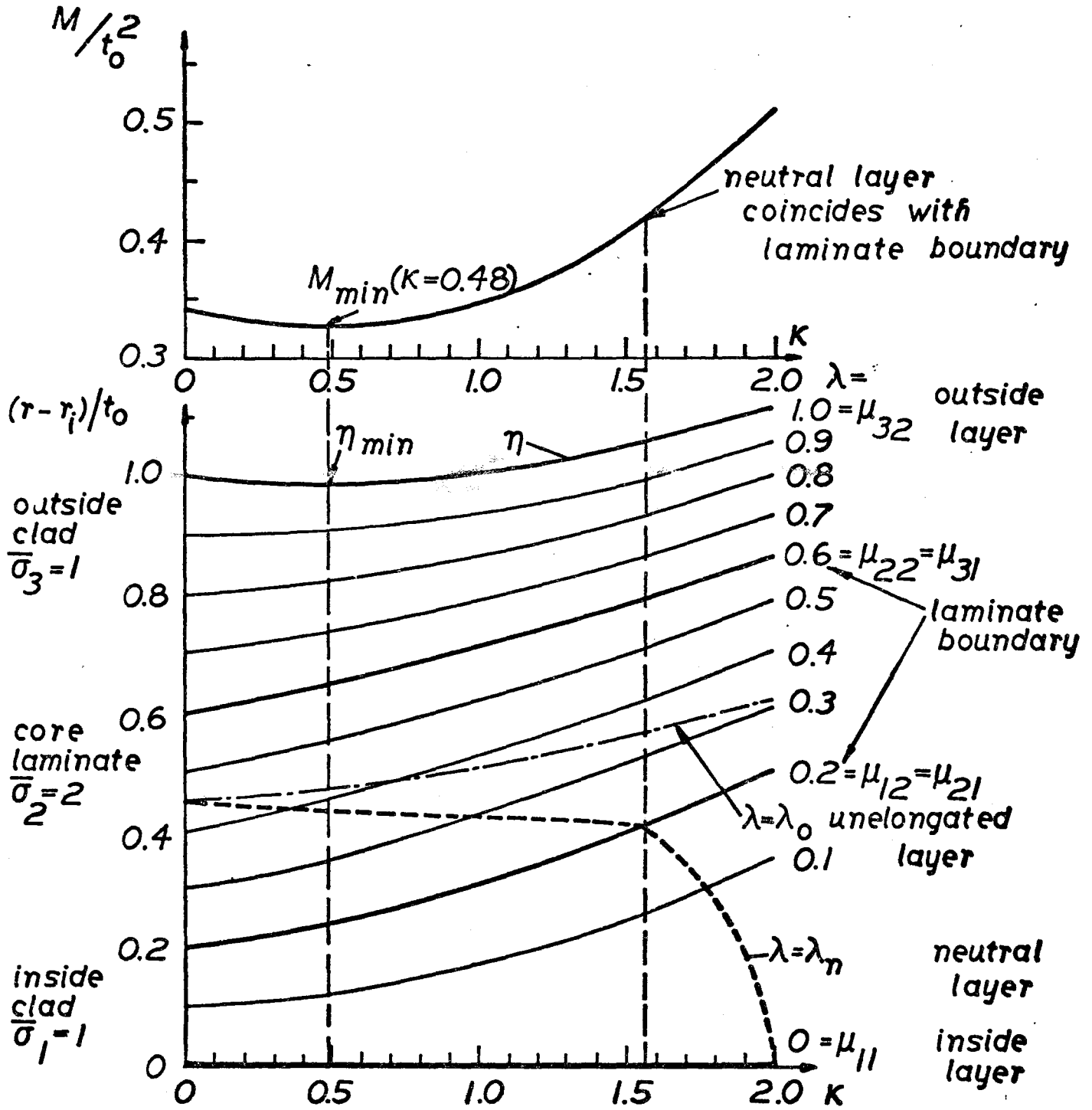


fig 4.29

STABILITY OF 1-2-1 NON STRAINHARDENING TRIMETALS IN BENDING

left: bending moment decreases (UNSTABLE) up to indicated relative curvature $K_{M_{min}}$ at which moment is minimum

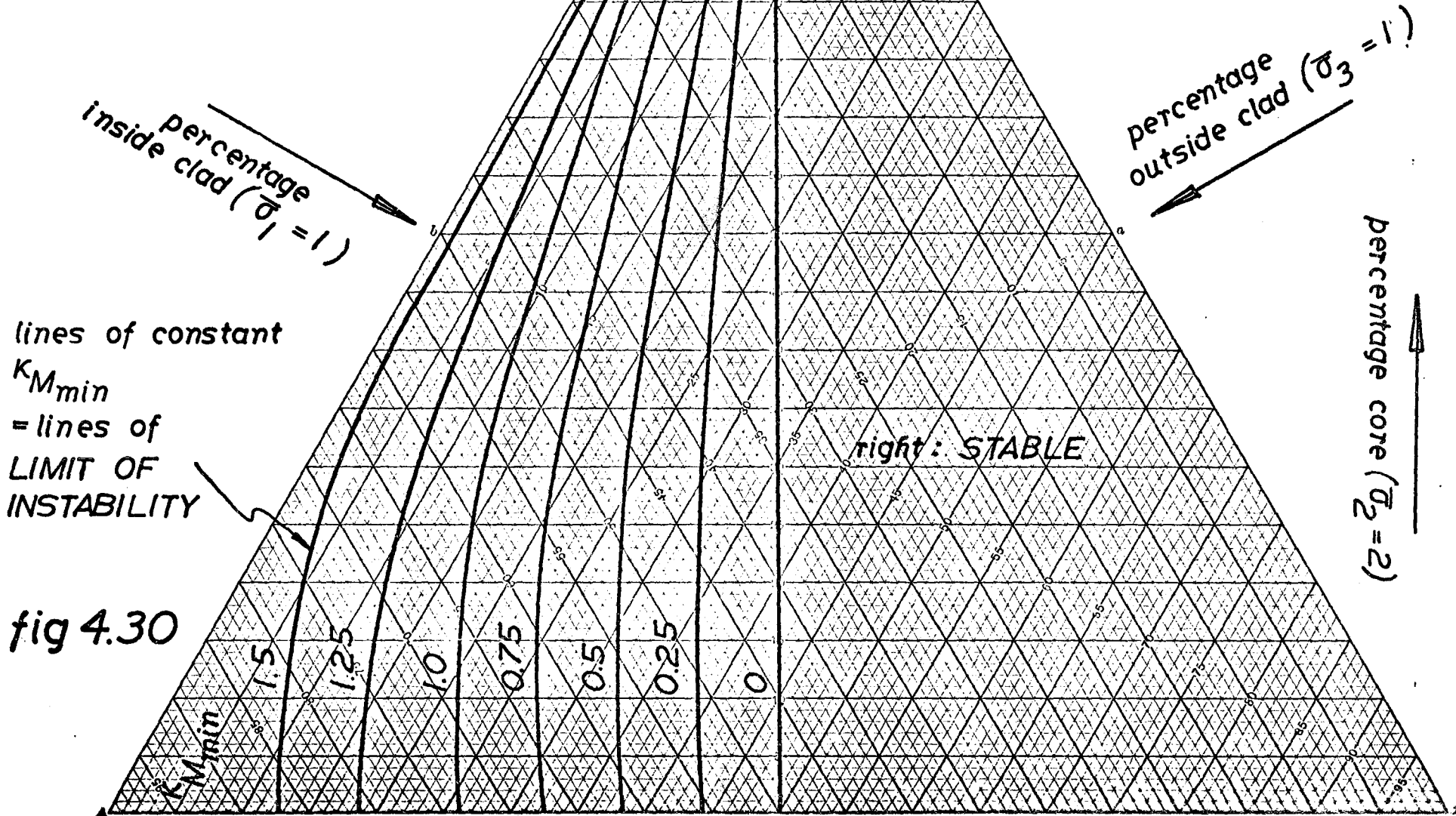


fig 4.30

RELATIVE SHEET THICKNESS IN BENDING
 1-2-1 NON STRAIN HARDENING TRIME-
 TAL FOR $K=0.25$

minimum in bending moment at
 $K=0.25$ for sheet compositions
 on the line $\eta = 1.0$

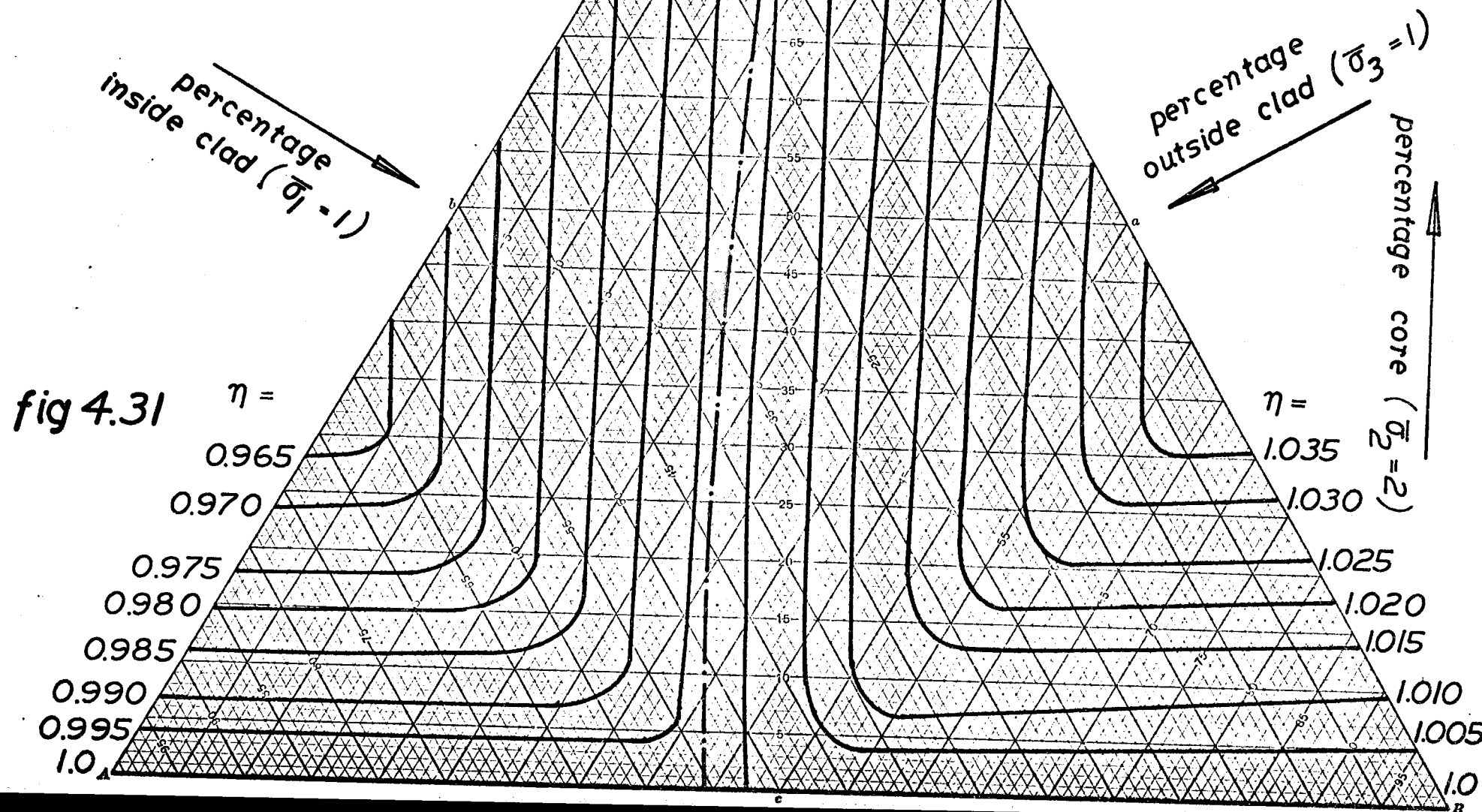


fig 4.31

RELATIVE SHEET THICKNESS IN BENDING
 1-2-1 NON STRAIN HARDENING TRIMETALS FOR K=0.5

— · — · — the bending moment is minimum at $K=0.5$ for trimetals on this line

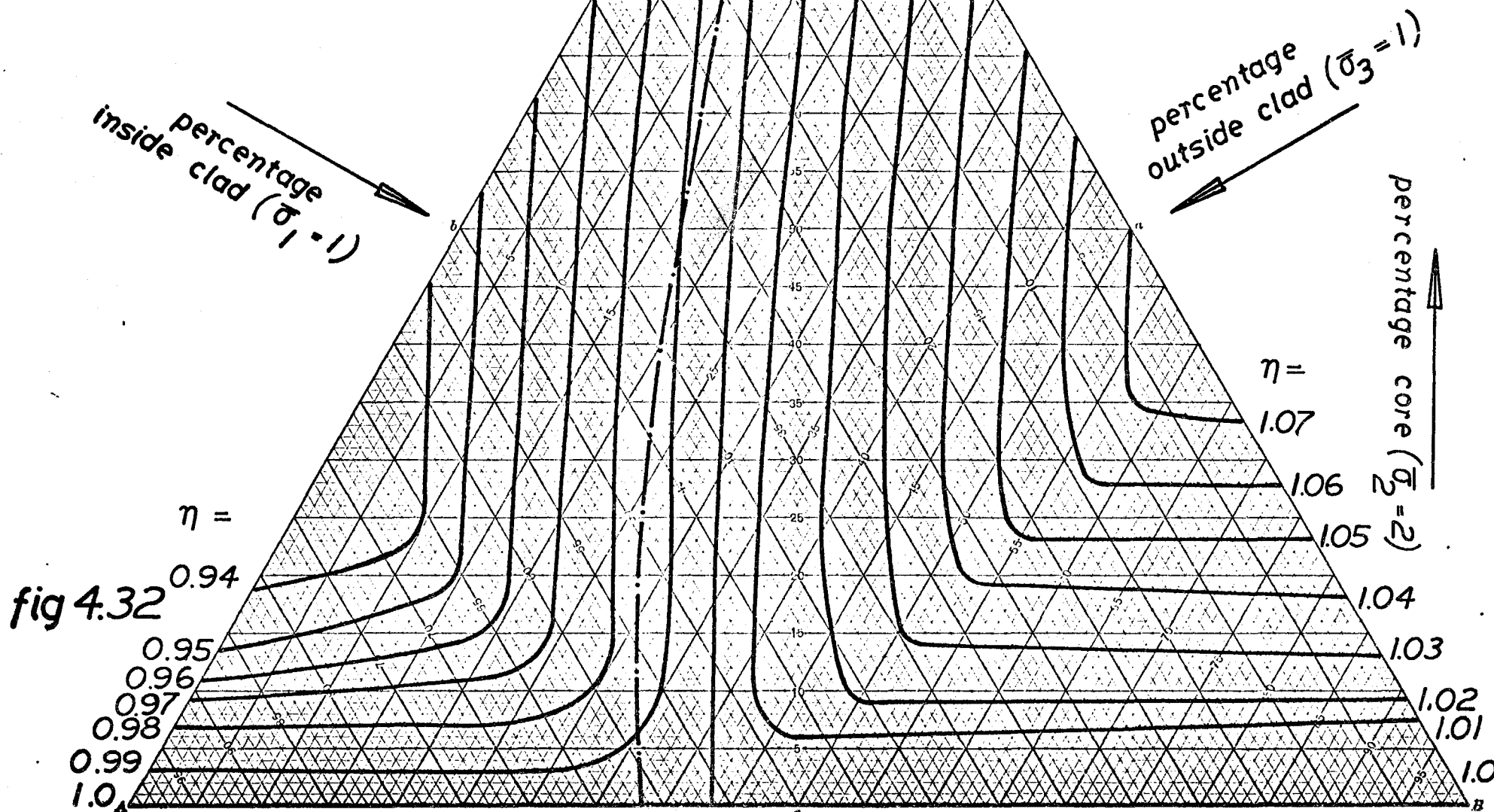
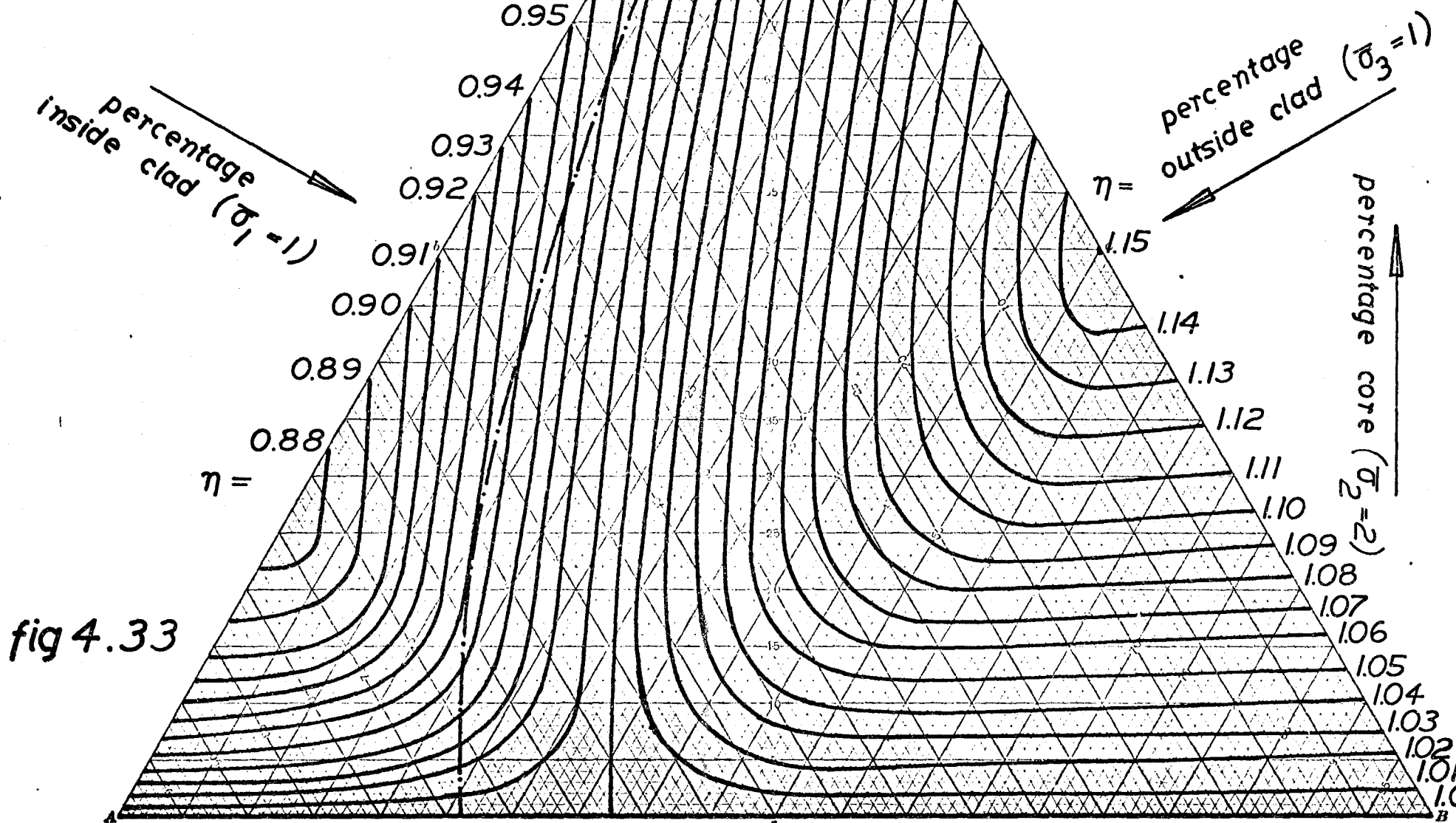


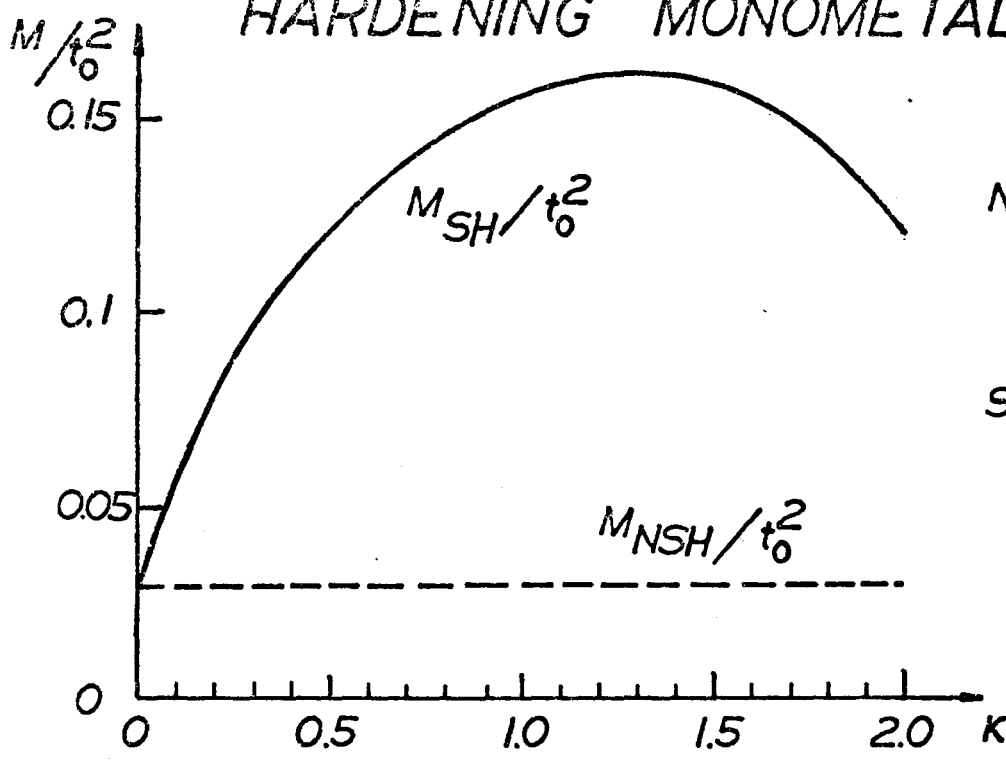
fig 4.32

RELATIVE SHEET THICKNESS IN BENDING
 1-2-1 NON STRAIN HARDENING TRIMETALS FOR K=1.0

..... bending moment reaches minimum at $K=1.0$ for trimetals on this line



COMPARISON BETWEEN THE BENDING OF NON STRAIN HARDENING AND STRAIN HARDENING MONOMETAL



NSH: non strain hardening monometal $\bar{\sigma} = 0.1$

SH: strain hardening monometal $\bar{\sigma} = 1. (0.01 + \bar{\epsilon})^{0.5}$

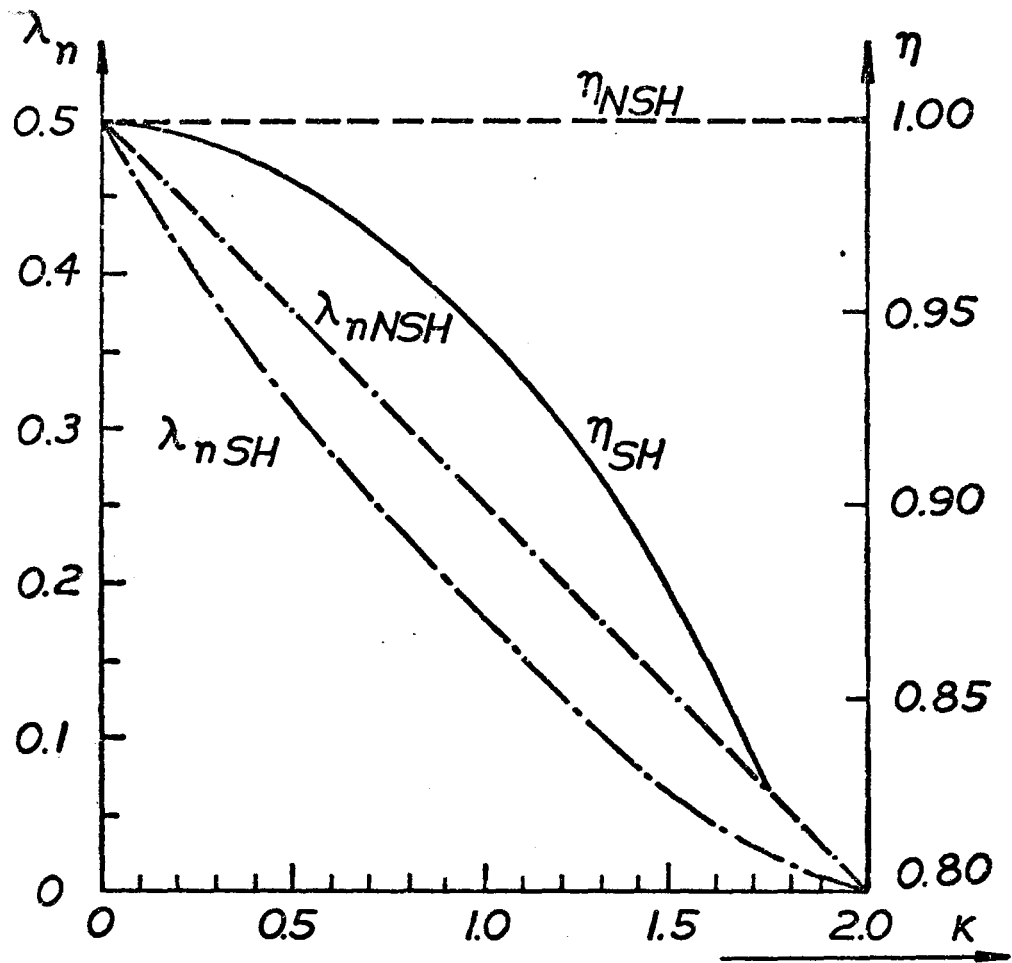


fig 5.1

EFFECTIVE STRESS AND STRAIN DISTRIBUTION
 IN BENDING STRAINHARDENING MONOMETAL WITHOUT
 BAUSCHINGER EFFECT FOR $K=1$.

$$\bar{\sigma} = 1. (0.01 + \bar{\epsilon})^{0.5}$$

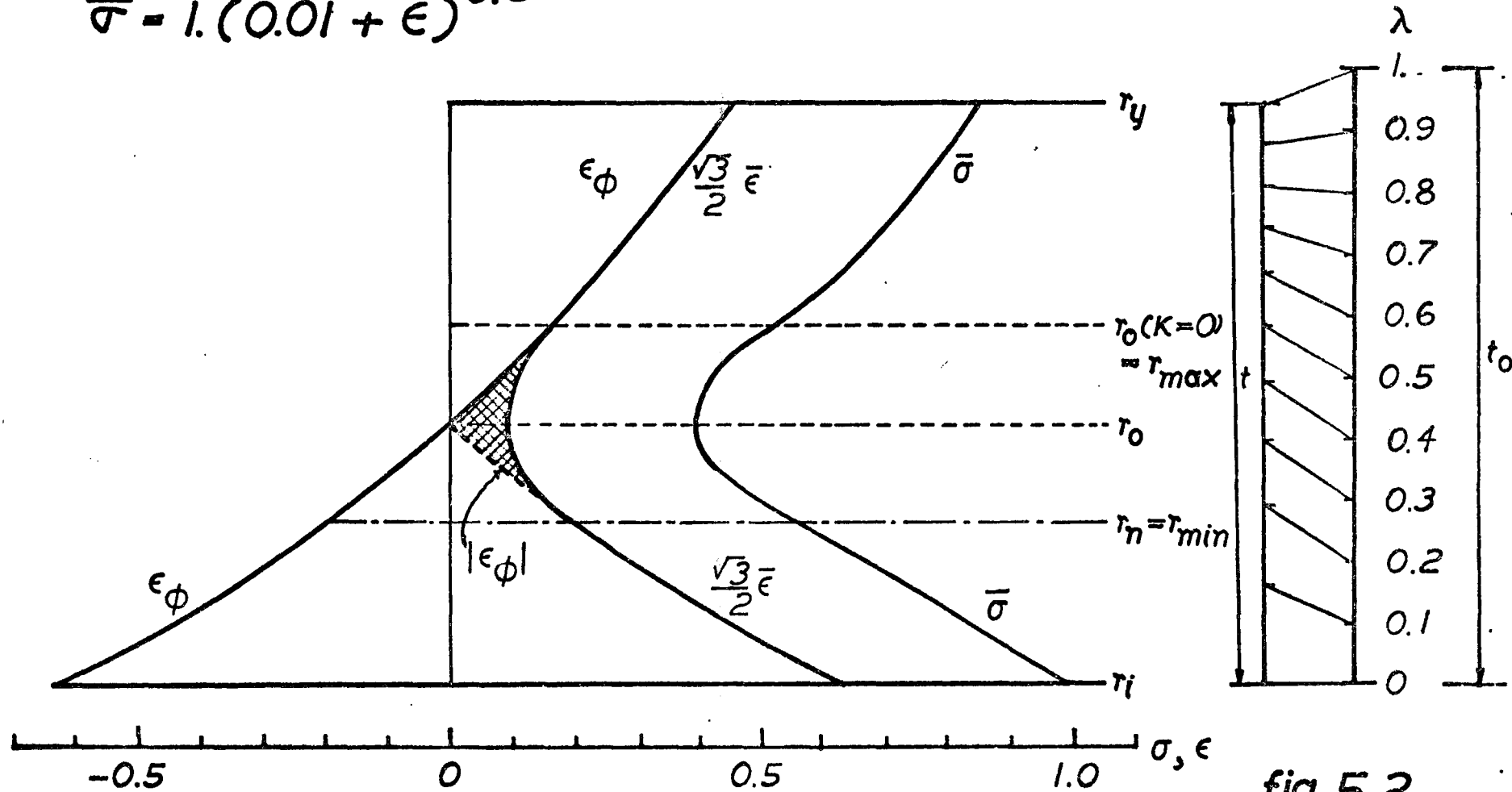
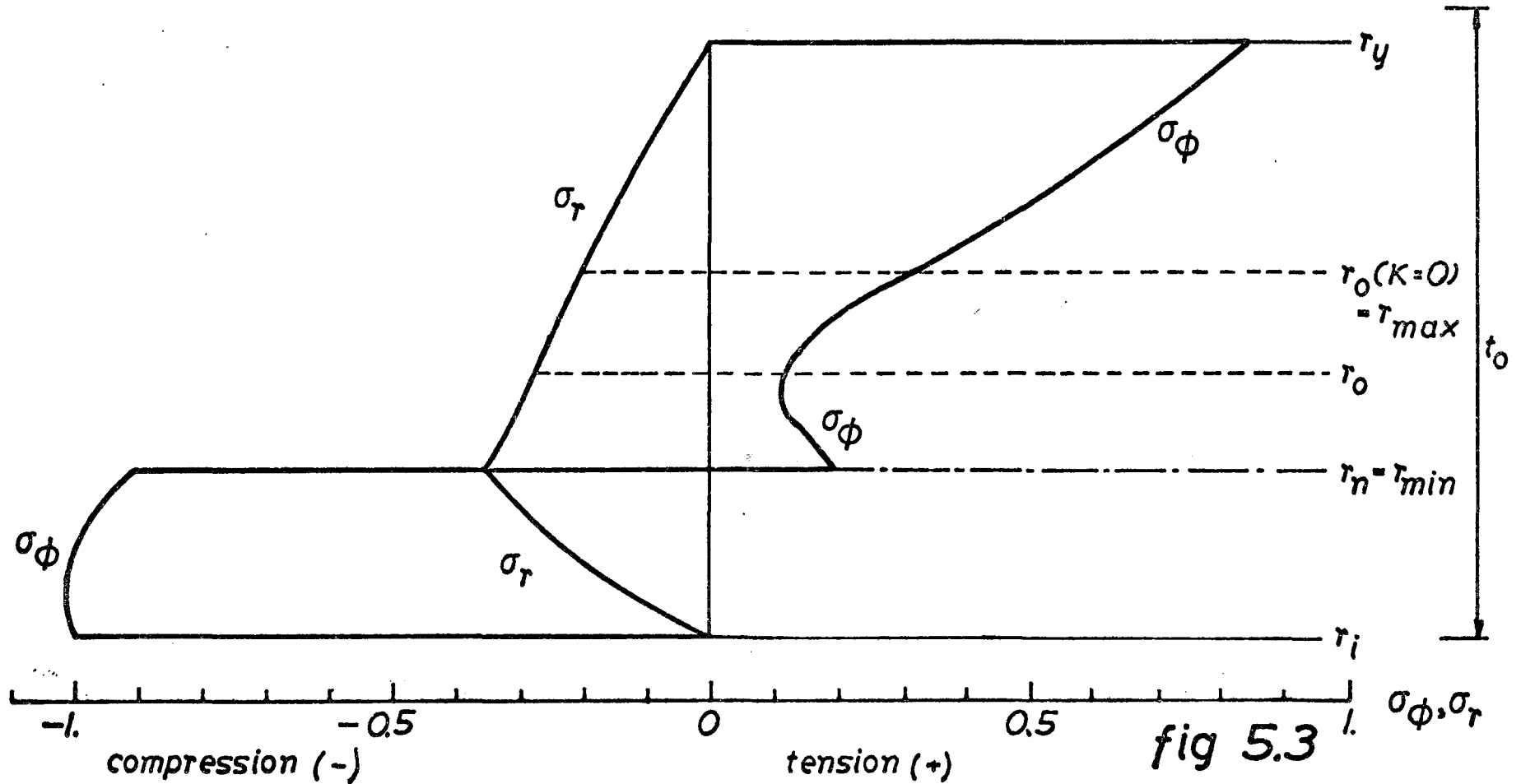


fig 5.2

STRESSDISTRIBUTION IN BENDING STRAINHARDENING
MONOMETAL WITHOUT BAUSCHINGER EFFECT FOR $K=1$.

$$\bar{\sigma} = 1. (0.01 + \bar{\epsilon})^{0.5}$$



BENDING OF A STRAIN HARDENING MONOMETAL INFLUENCE OF PRESTRAIN ON NEUTRAL LAYER POSITION AND RELATIVE SHEET THICKNESS

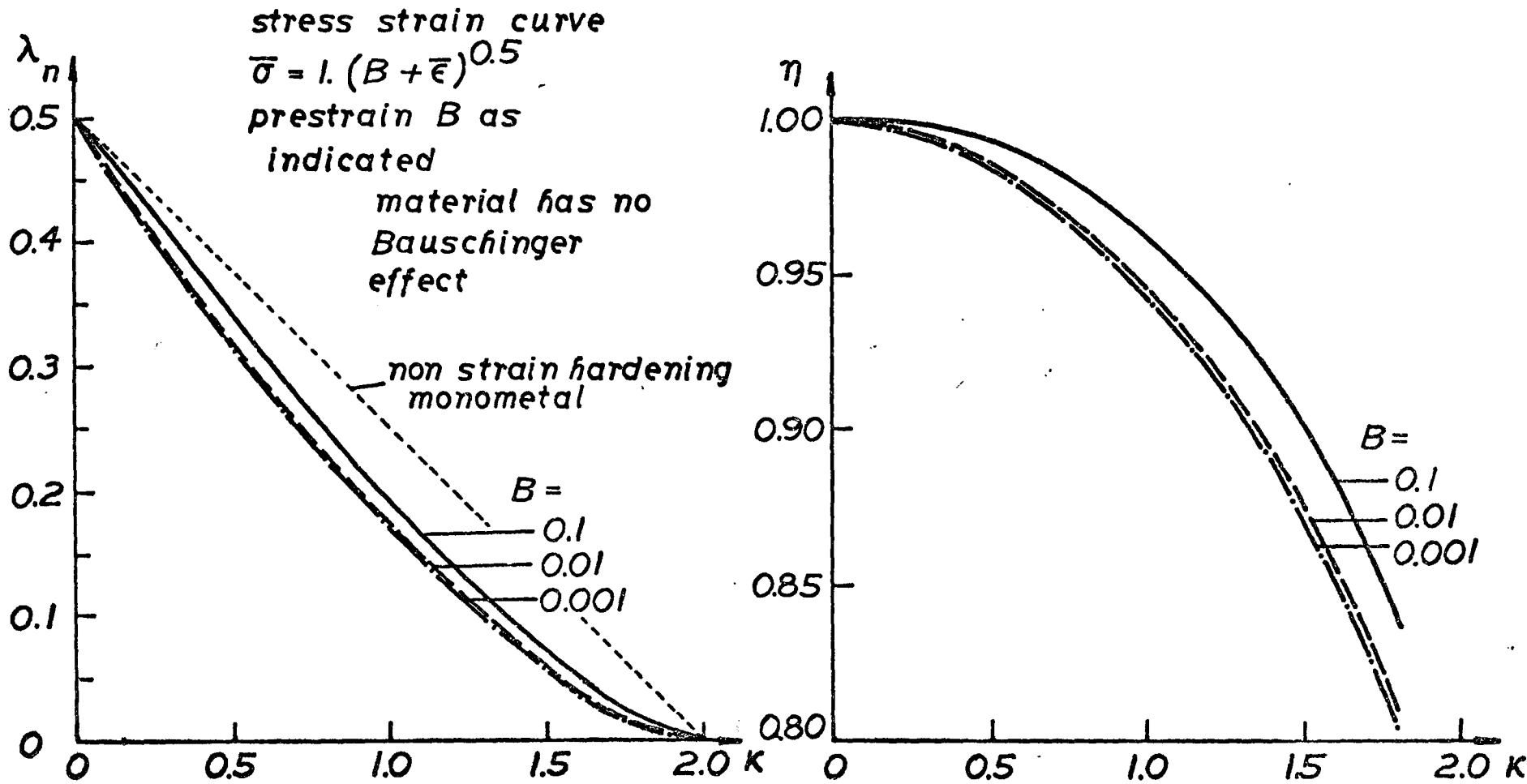
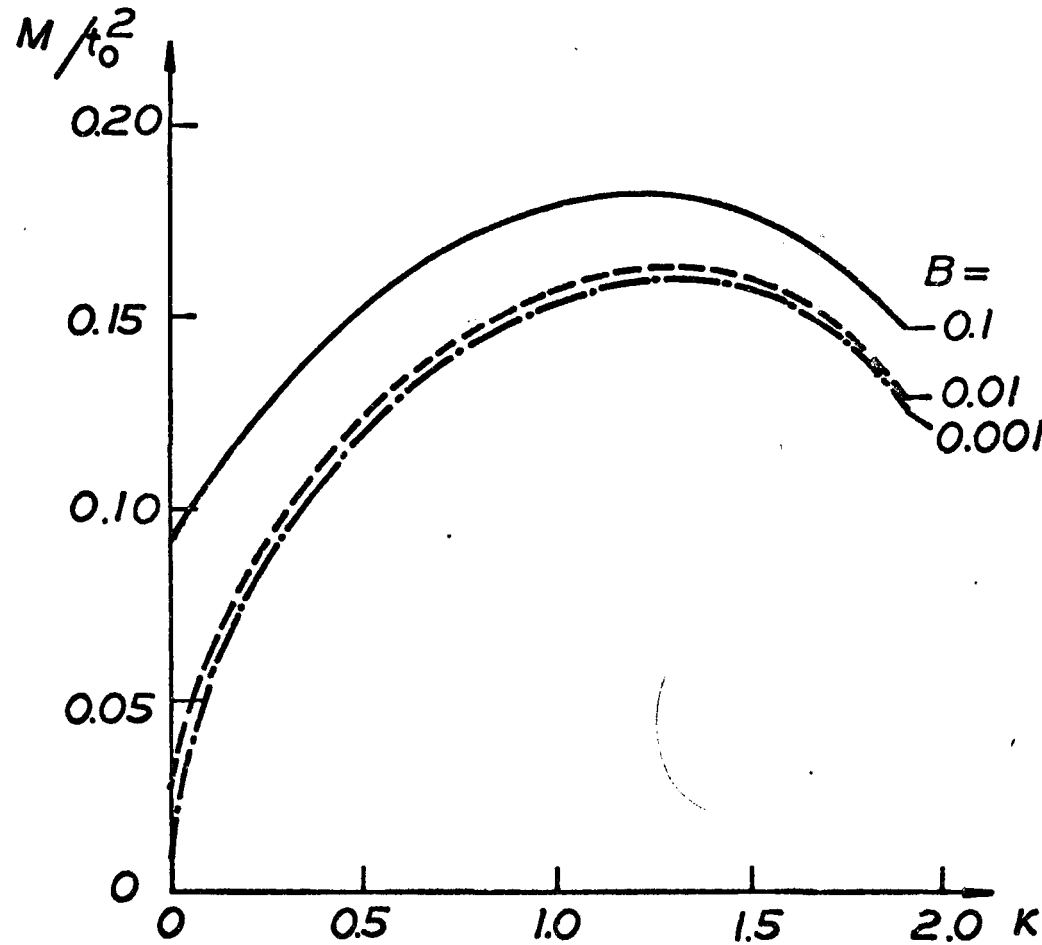


fig 5.4

BENDING OF A STRAINHARDENING MONOMETAL INFLUENCE OF PRESTRAIN ON BENDING MOMENT



stress strain curve
 $\bar{\sigma} = 1. (B + \bar{\epsilon})^{0.5}$
prestrain B as indicated
material has no
Bauschinger effect

fig 5.5

BENDING OF A STRAIN HARDENING MONOMETAL INFLUENCE OF PRESTRAIN ON NEUTRAL LAYER POSITION AND RELATIVE SHEET THICKNESS

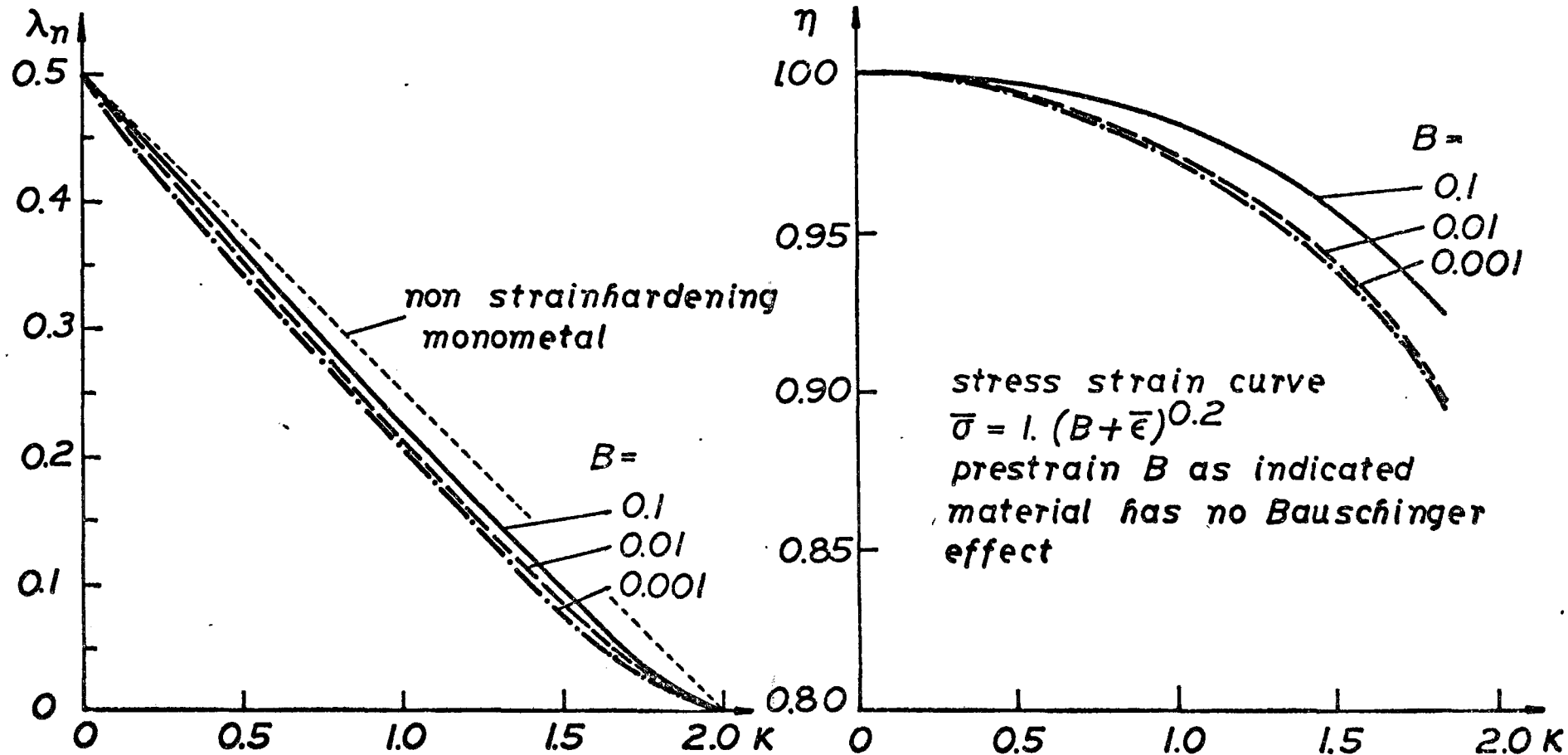


fig 5.6

BENDING OF A STRAIN HARDENING MONOMETAL INFLUENCE OF PRESTRAIN ON BENDING MOMENT

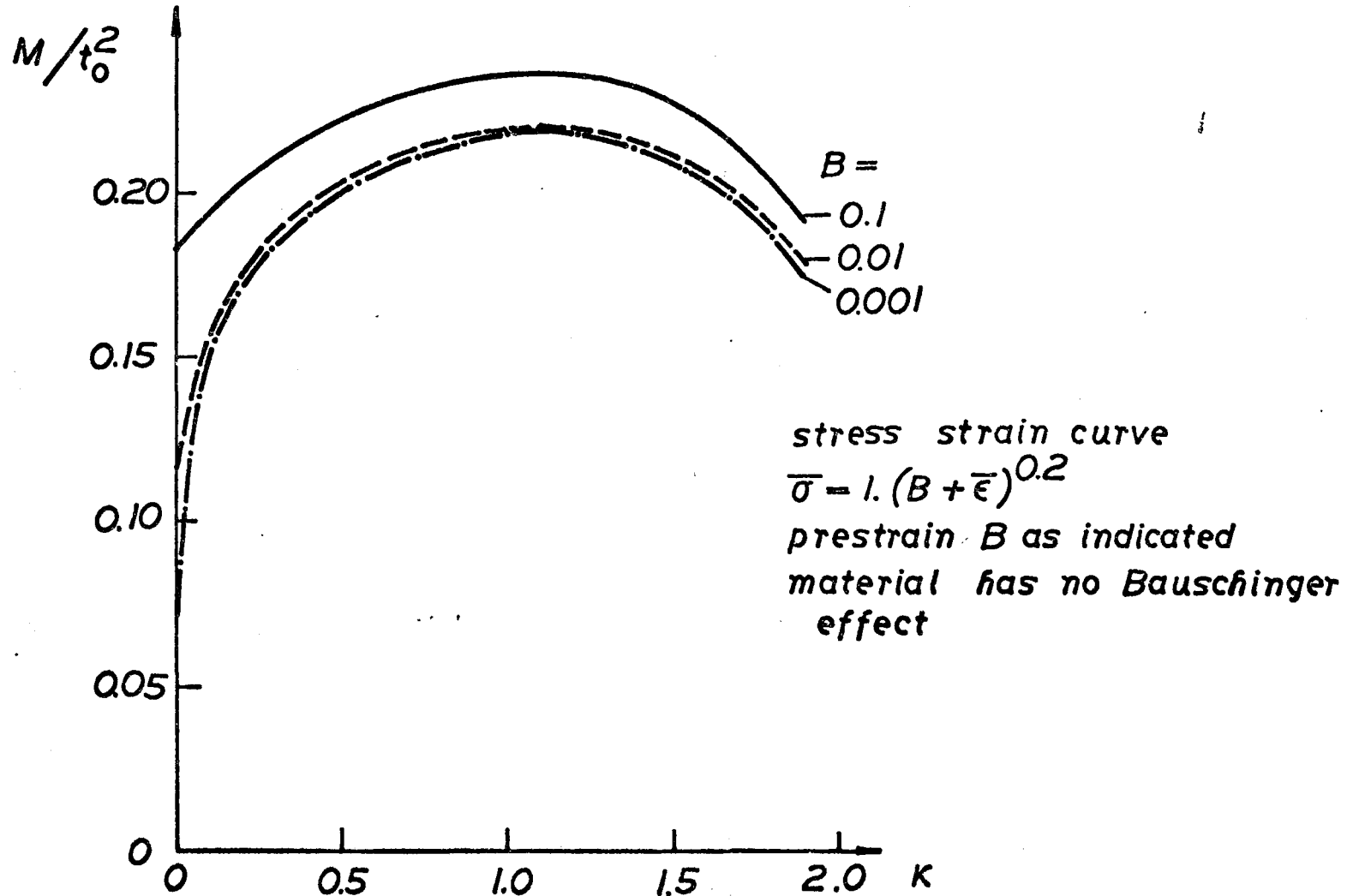


fig 5.7

BAUSCHINGER CURVES FOR BRASS

from Crafoord [33]

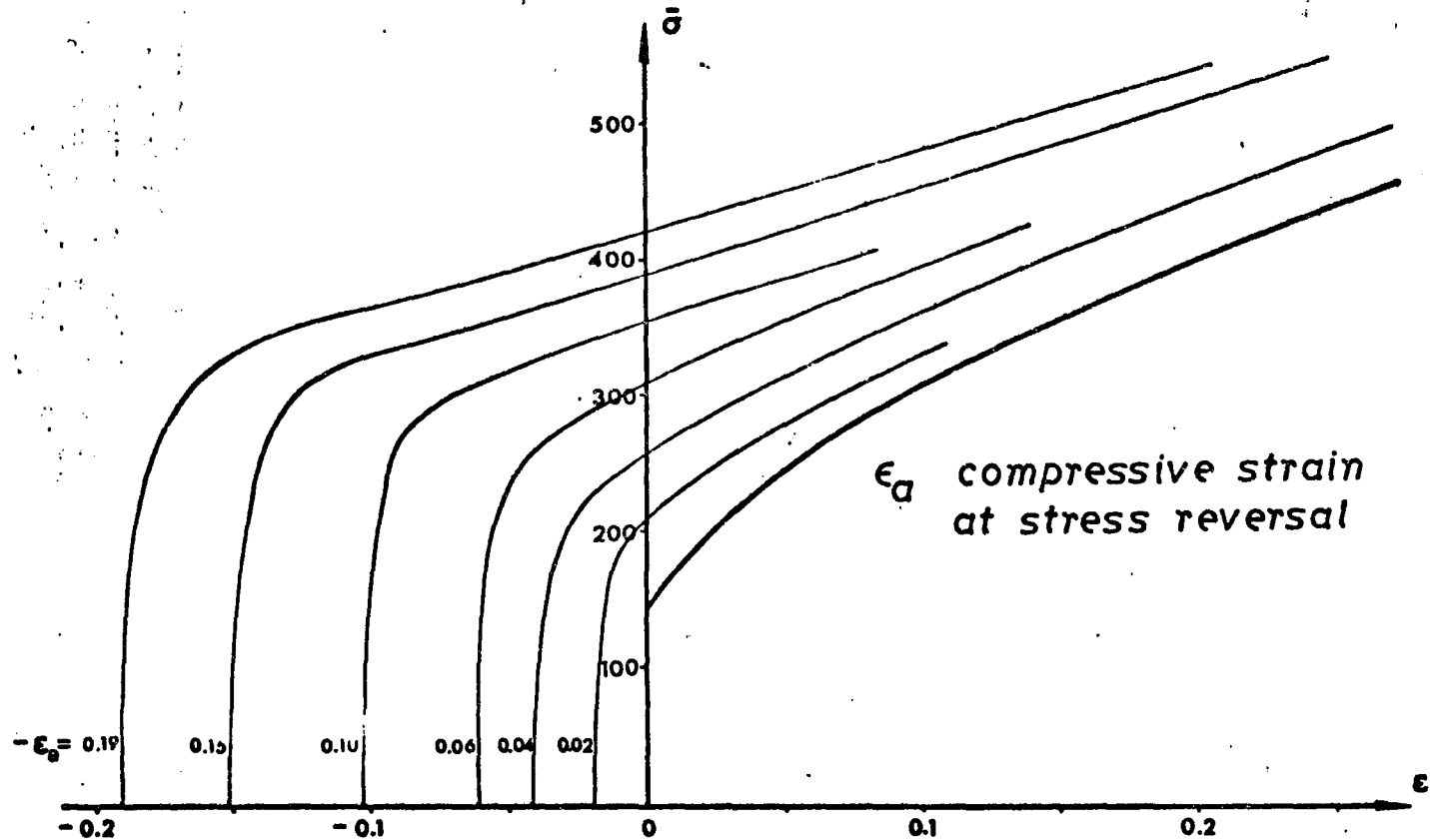


fig 5.8

TRUE STRESS AS A FUNCTION OF EFFECTIVE STRAIN FOR BRASS WITH VARIOUS PRE-STRAINS
from Crafoord [33]

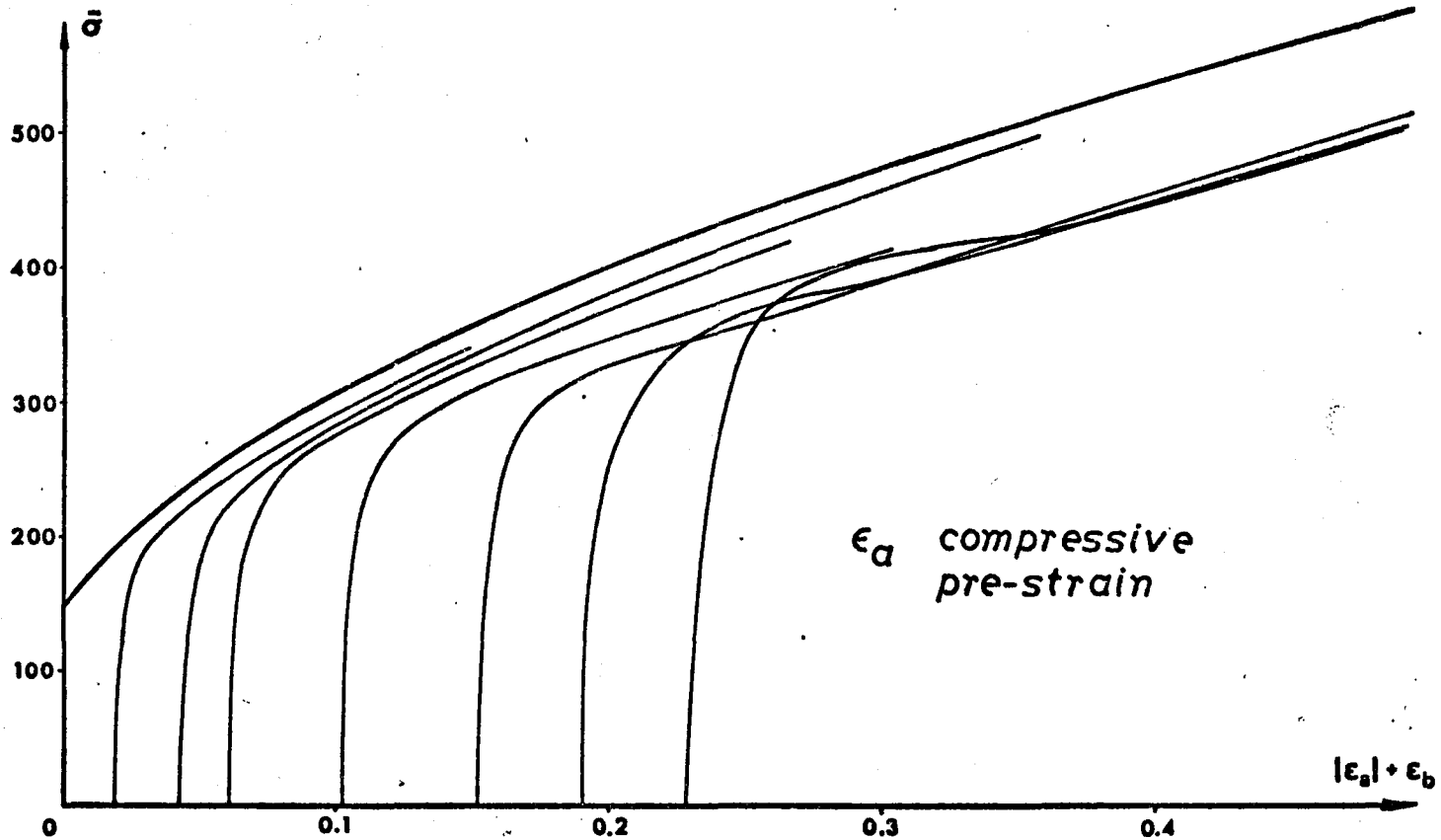


fig 5.9

BAUSCHINGER EFFECT SUB-DIVIDED INTO TWO COMPONENT EFFECTS

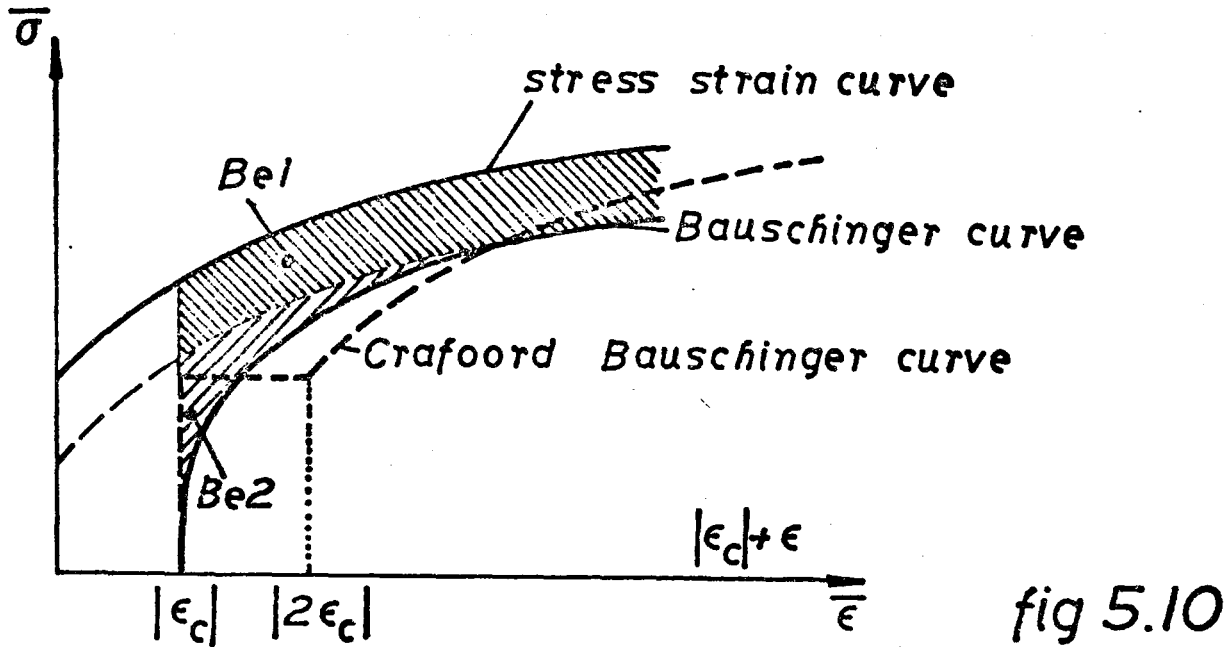


fig 5.10

CRAFOORD BAUSCHINGER EFFECT

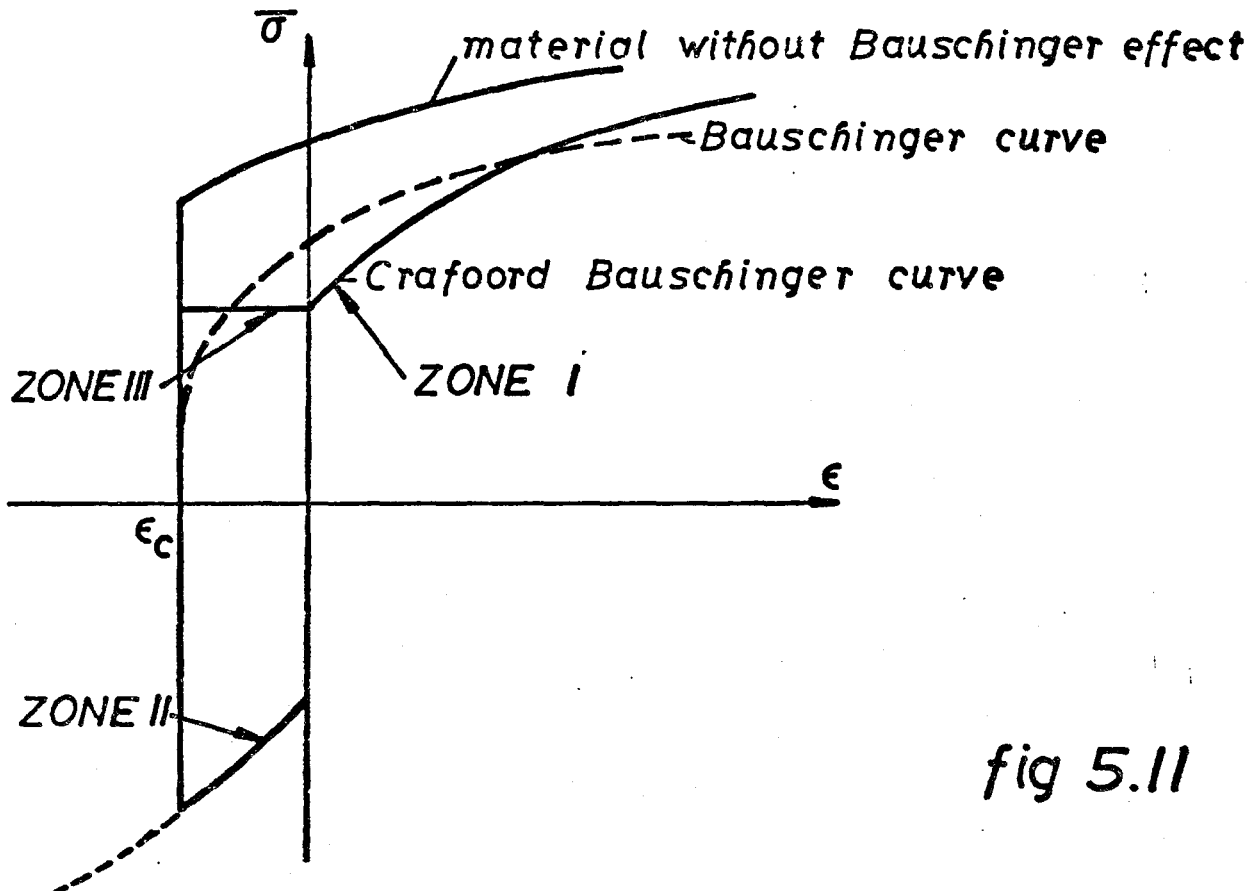


fig 5.11

INFLUENCE OF BAUSCHINGER EFFECT ON THE BENDING OF STRAIN HARDENING MONOMETAL

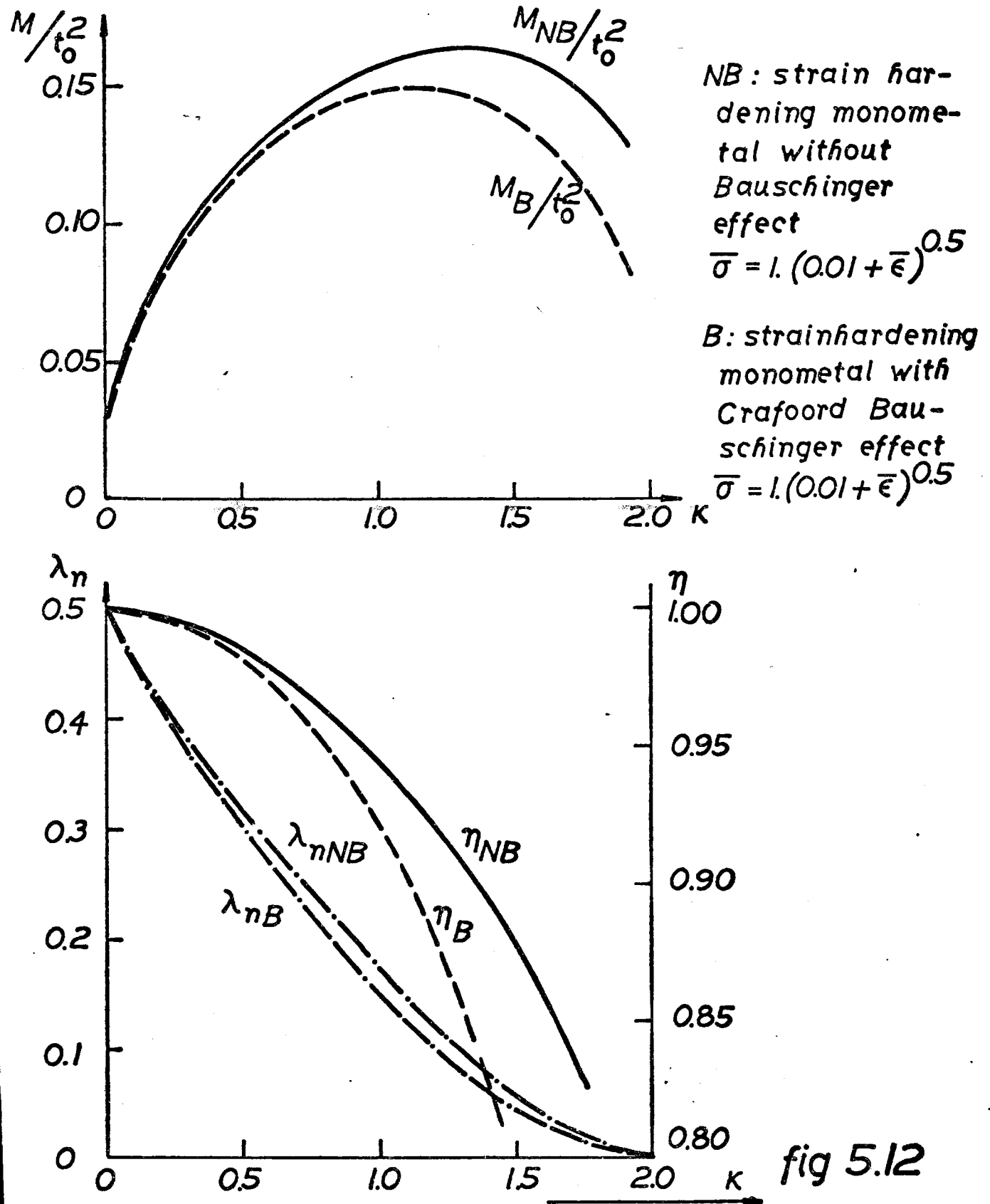


fig 5.12

EFFECTIVE STRESS AND STRAIN DISTRIBUTION
 IN BENDING STRAINHARDENING MONOMETAL WITH
 CRAFTOORD BAUSCHINGER EFFECT FOR $\kappa=1$.

$$\bar{\sigma} = 1. (0.01 + \bar{\epsilon})^{0.5}$$

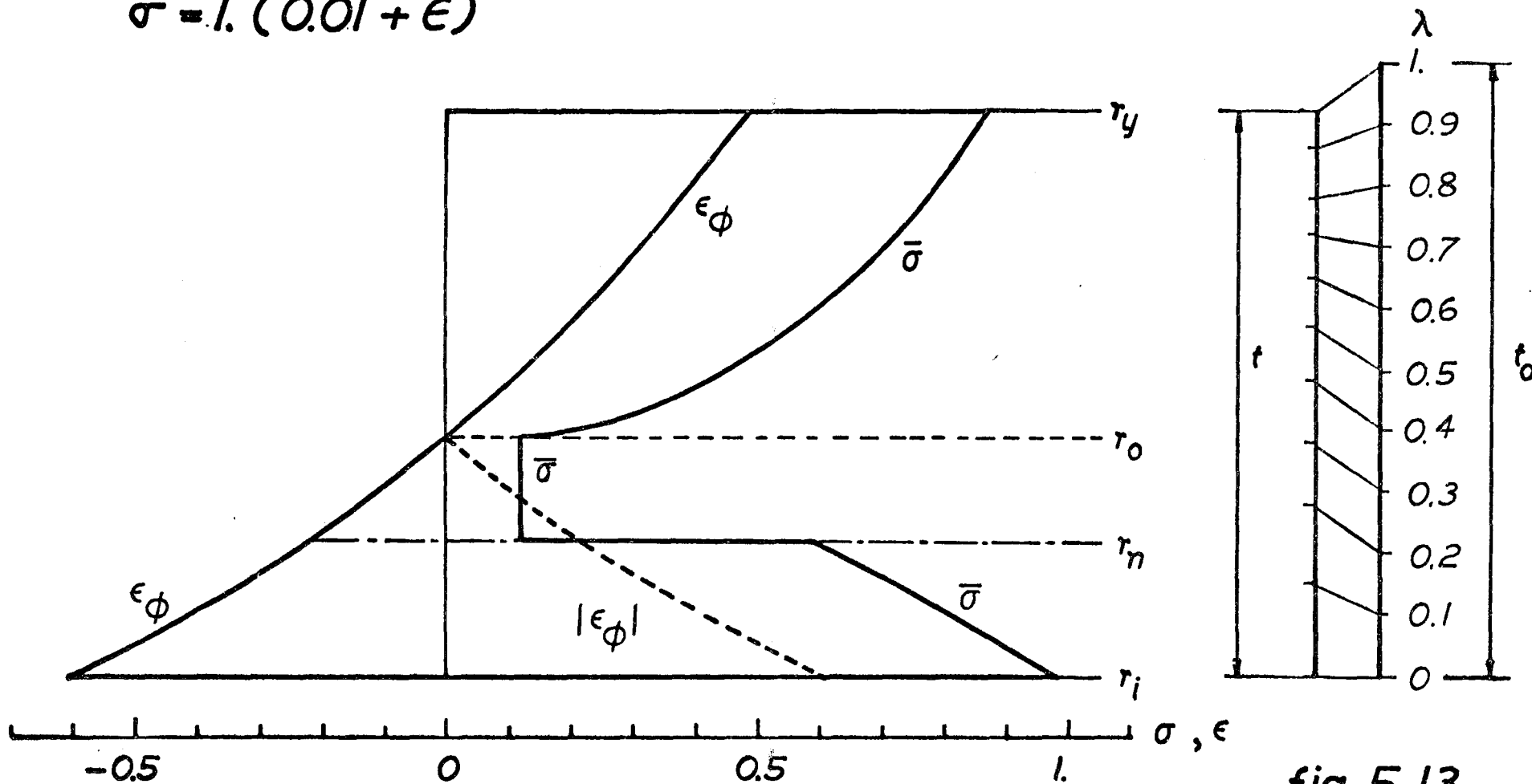
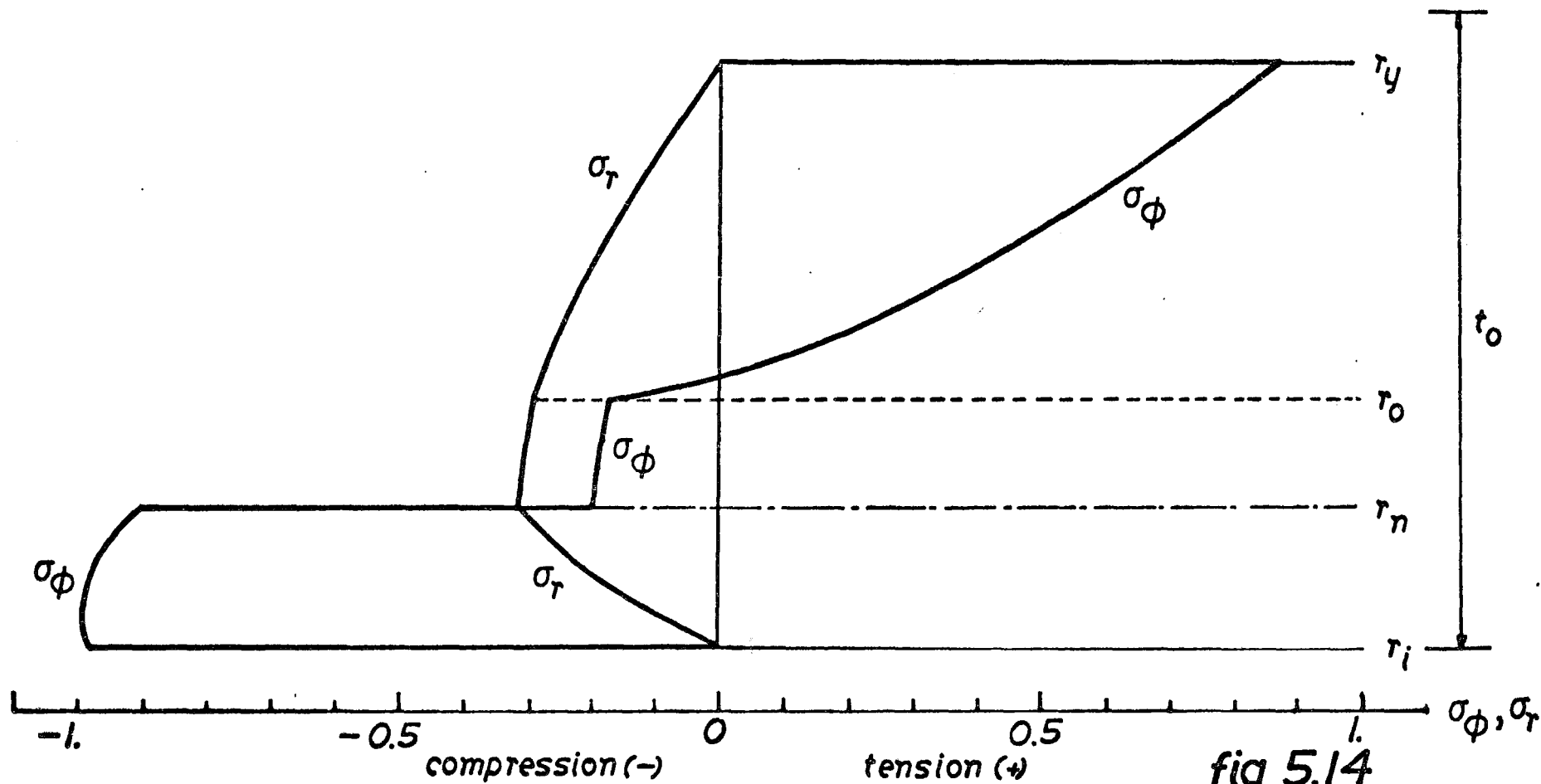


fig 5.13

STRESSDISTRIBUTION IN BENDING STRAINHARDENING
 MONOMETAL WITH GRAFOORD BAUSCHINGER EFFECT
 FOR $K=1$.

$$\bar{\sigma} = 1. (0.01 + \bar{\epsilon})^{0.5}$$



BENDING OF STRAIN HARDENING MONOMETAL WITH CRAFTOORD BAUSCHINGER EFFECT

INFLUENCE OF PRESTRAIN ON NEUTRAL LAYER POSITION AND RELATIVE SHEET THICKNESS

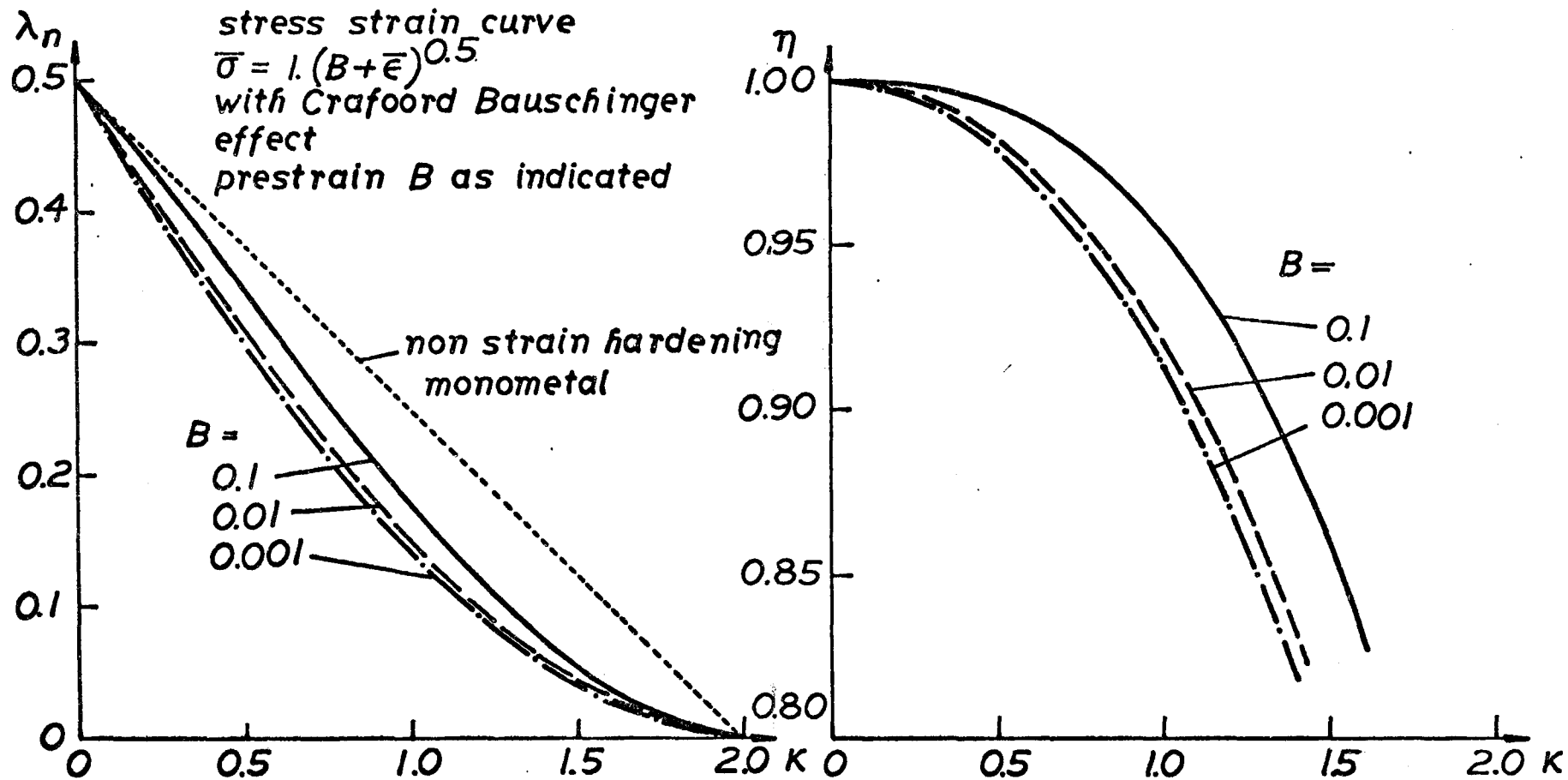
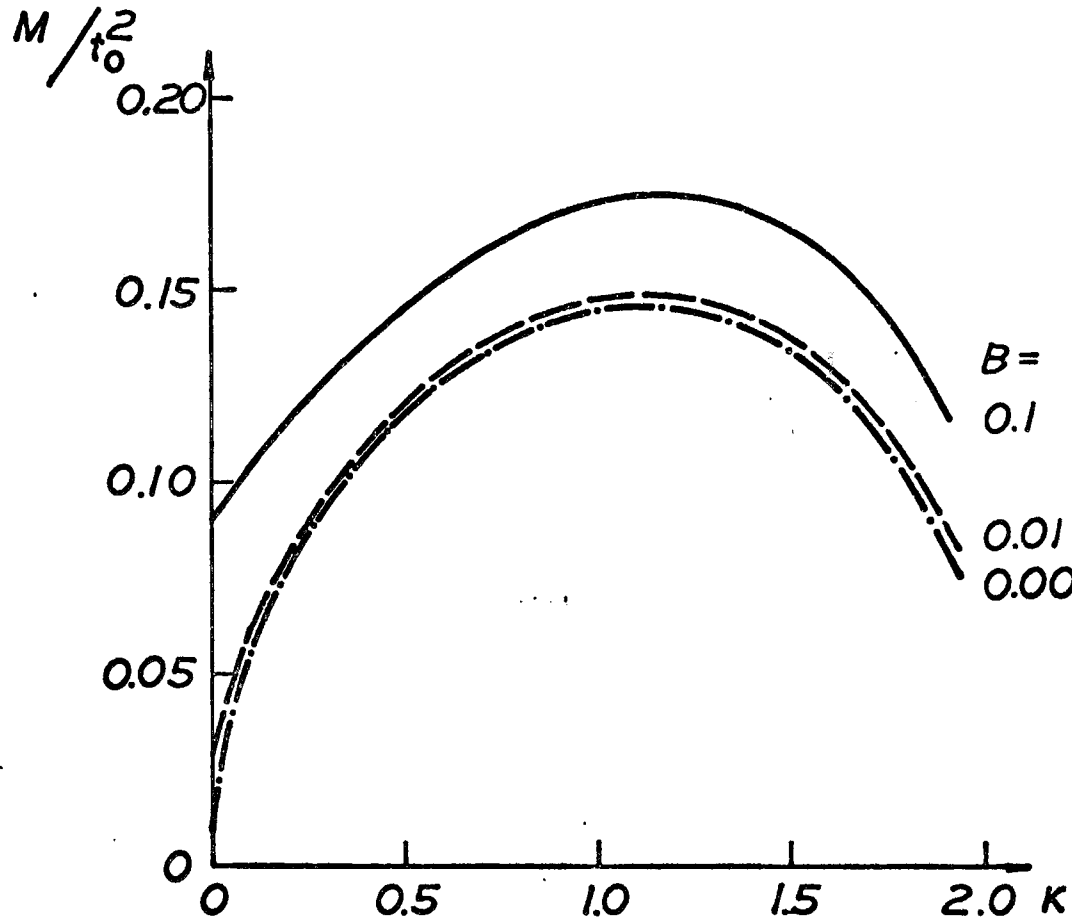


fig 5.15

BENDING OF STRAINHARDENING MONOMETAL
WITH CRAFOORD BAUSCHINGER EFFECT
INFLUENCE OF PRESTRAIN ON BENDING MOMENT



stress strain curve
 $\bar{\sigma} = 1. (B + \bar{\epsilon})^{0.5}$
with Crafoord Bauschinger
effect
prestrain B as indicated

fig 5.16

BENDING OF STRAIN HARDENING MONOMETAL WITH CRAFTOORD BAUSCHINGER EFFECT

INFLUENCE OF PRESTRAIN ON NEUTRAL LAYER POSITION AND RELATIVE SHEET THICKNESS

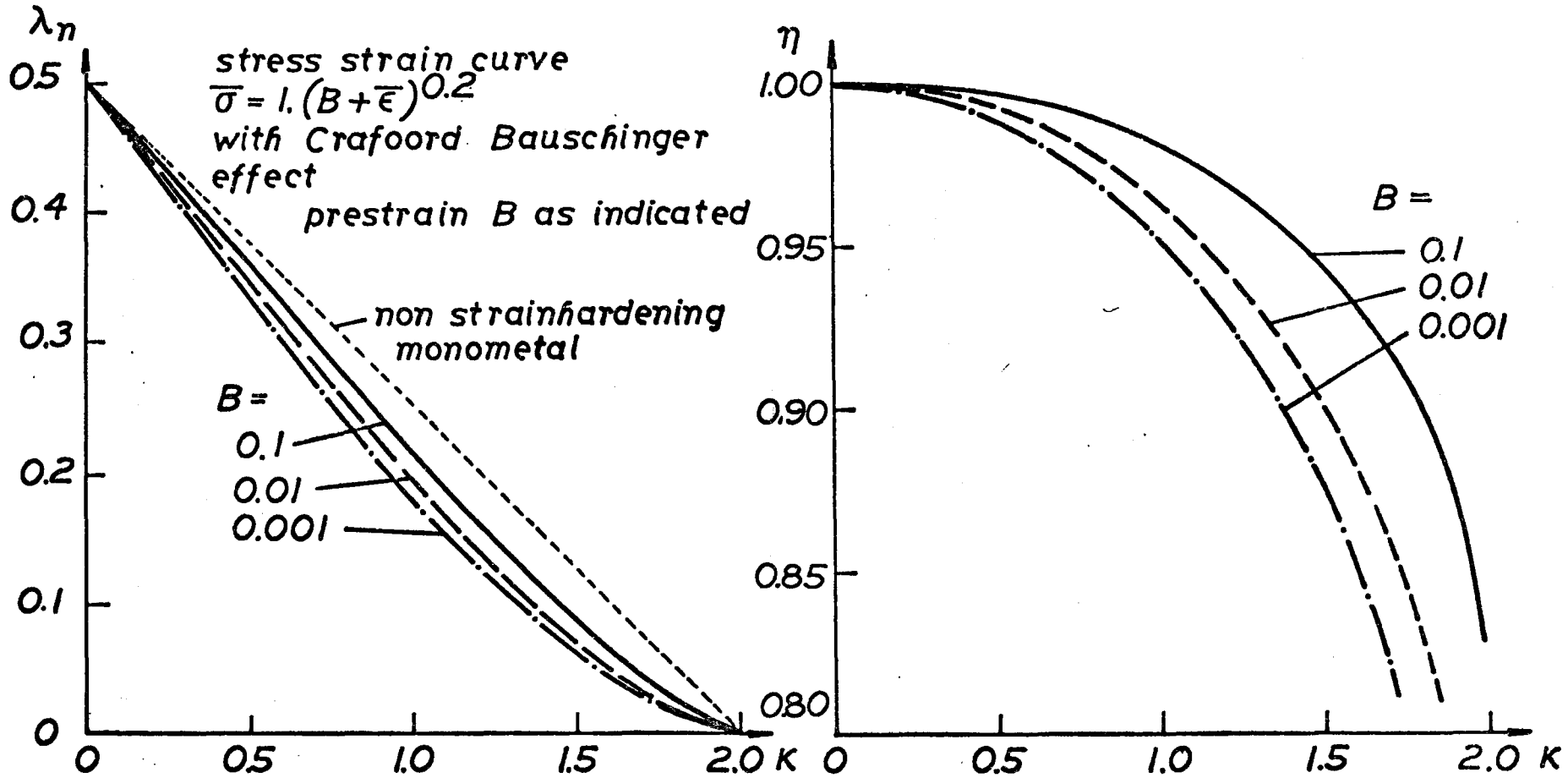


fig 5.17

BENDING OF STRAIN HARDENING MONOMETAL
WITH CRAFOORD BAUSCHINGER EFFECT
INFLUENCE OF PRESTRAIN ON BENDING MOMENT

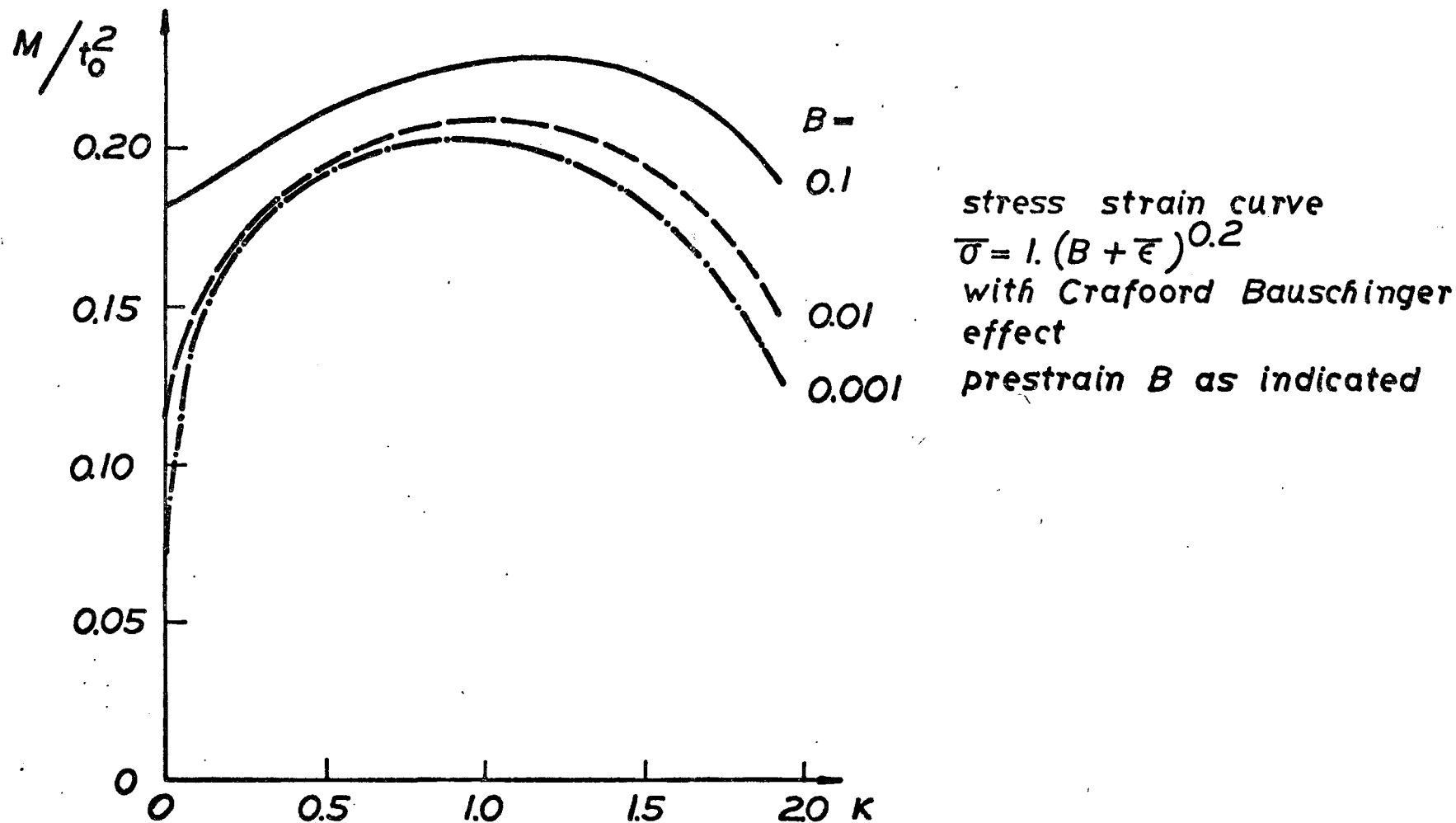
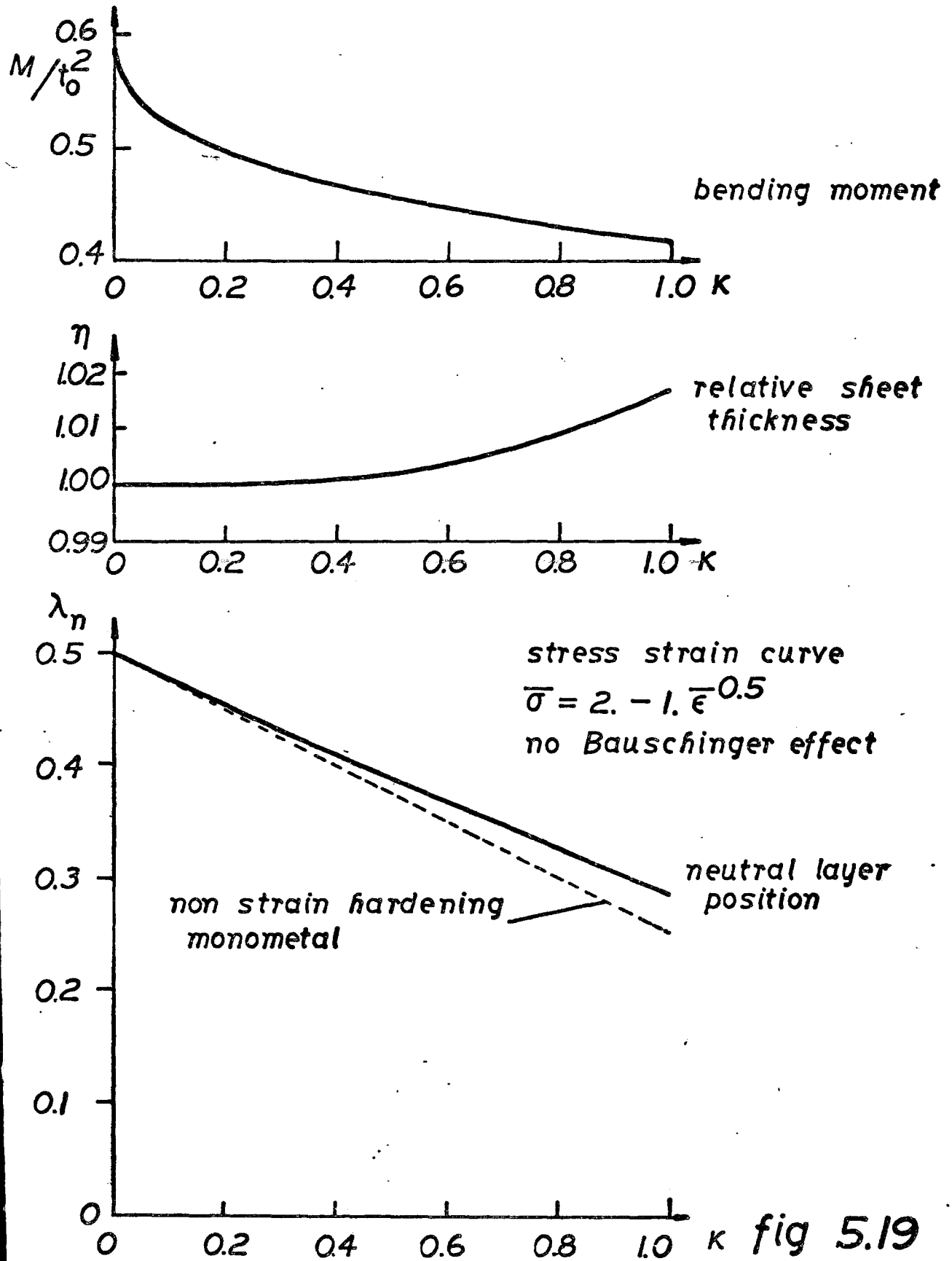


fig 5.18

BENDING OF STRAIN SOFTENING MONOMETAL



STRESSDISTRIBUTION IN BENDING STRAINSOFTENING
 MONOMETAL WITHOUT BAUSCHINGER EFFECT
 FOR $\kappa = 1$.

$$\bar{\sigma} = 2. - 1. \bar{\epsilon}^{0.5}$$

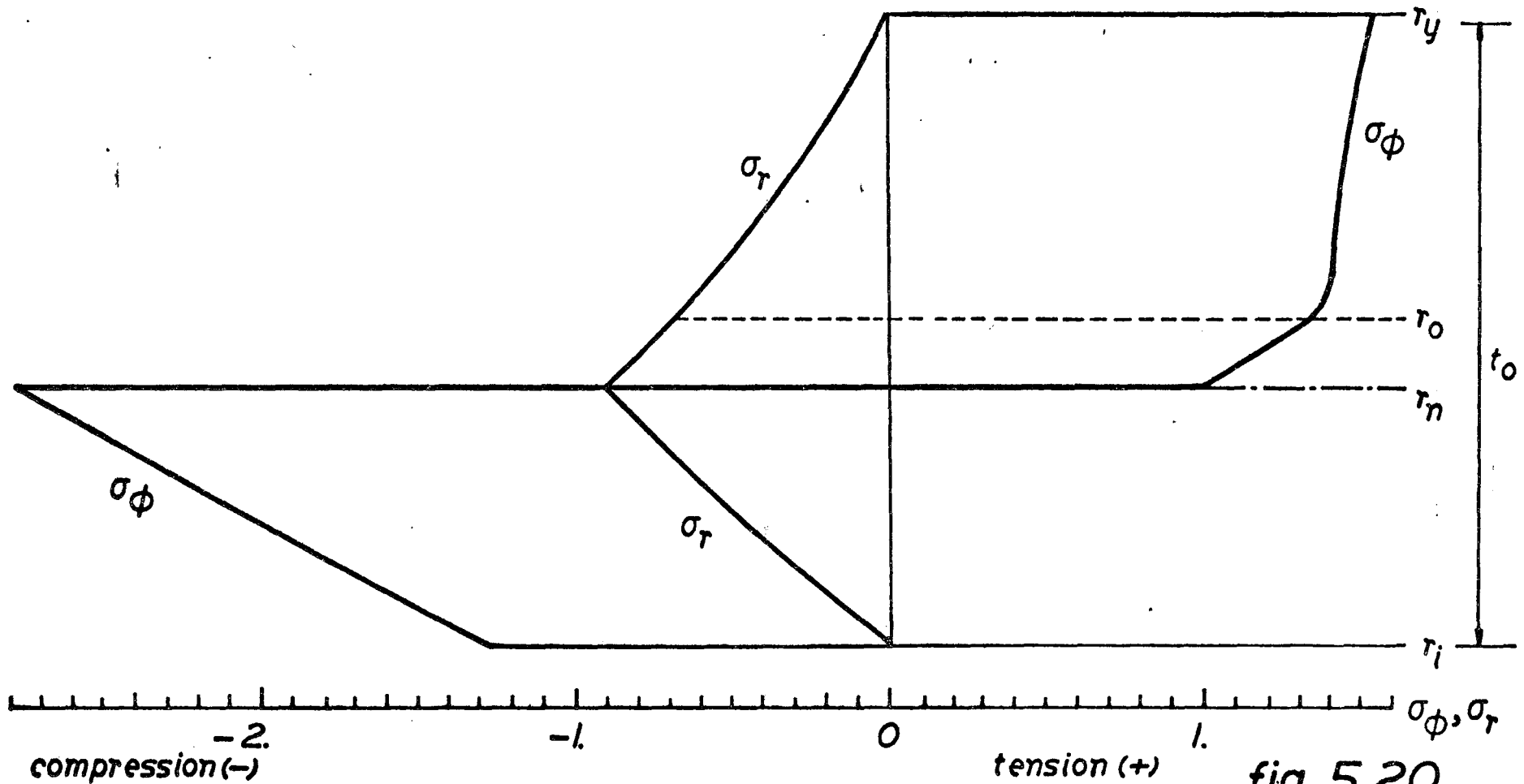


fig 5.20

STRESS STRAIN CURVES

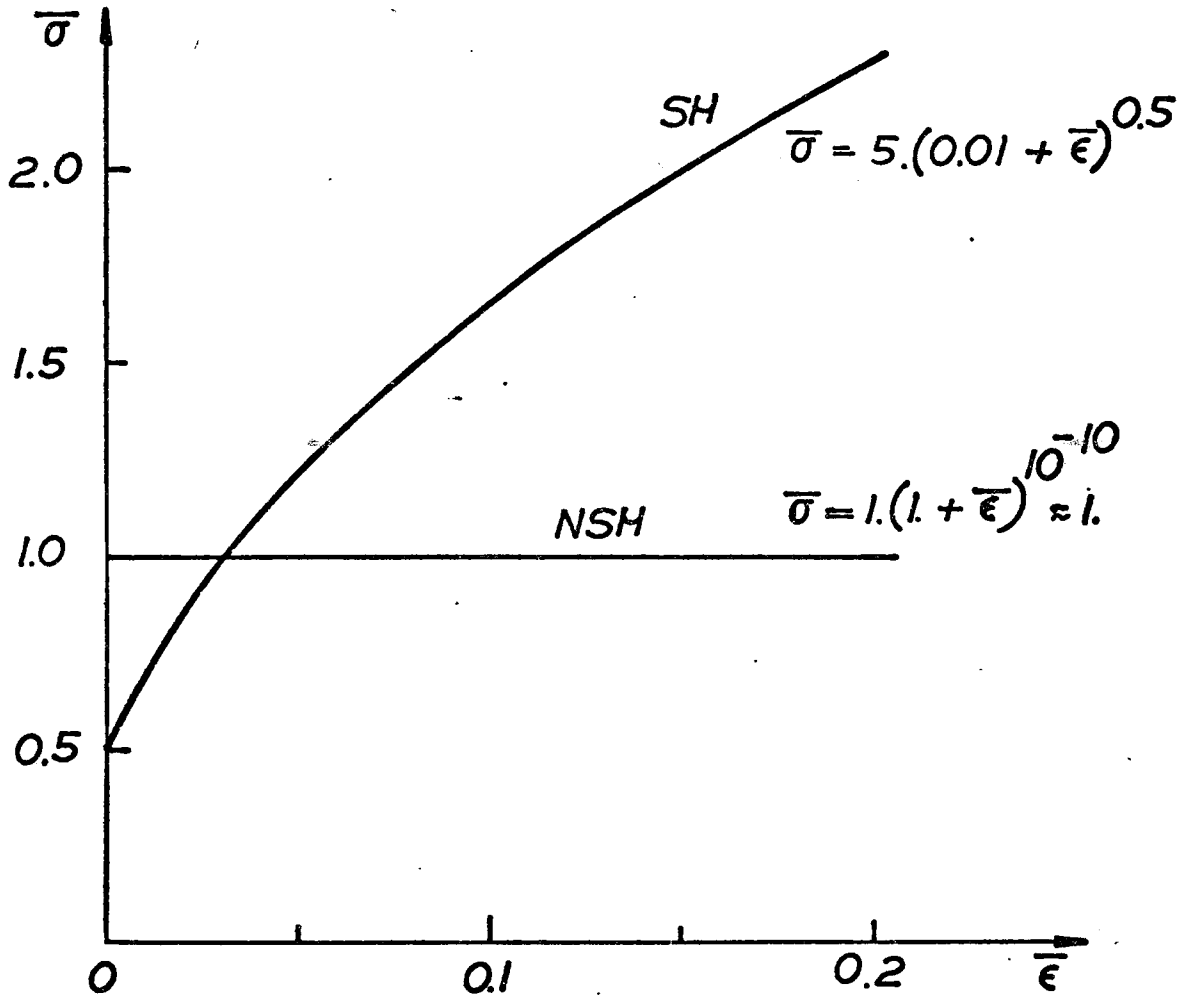
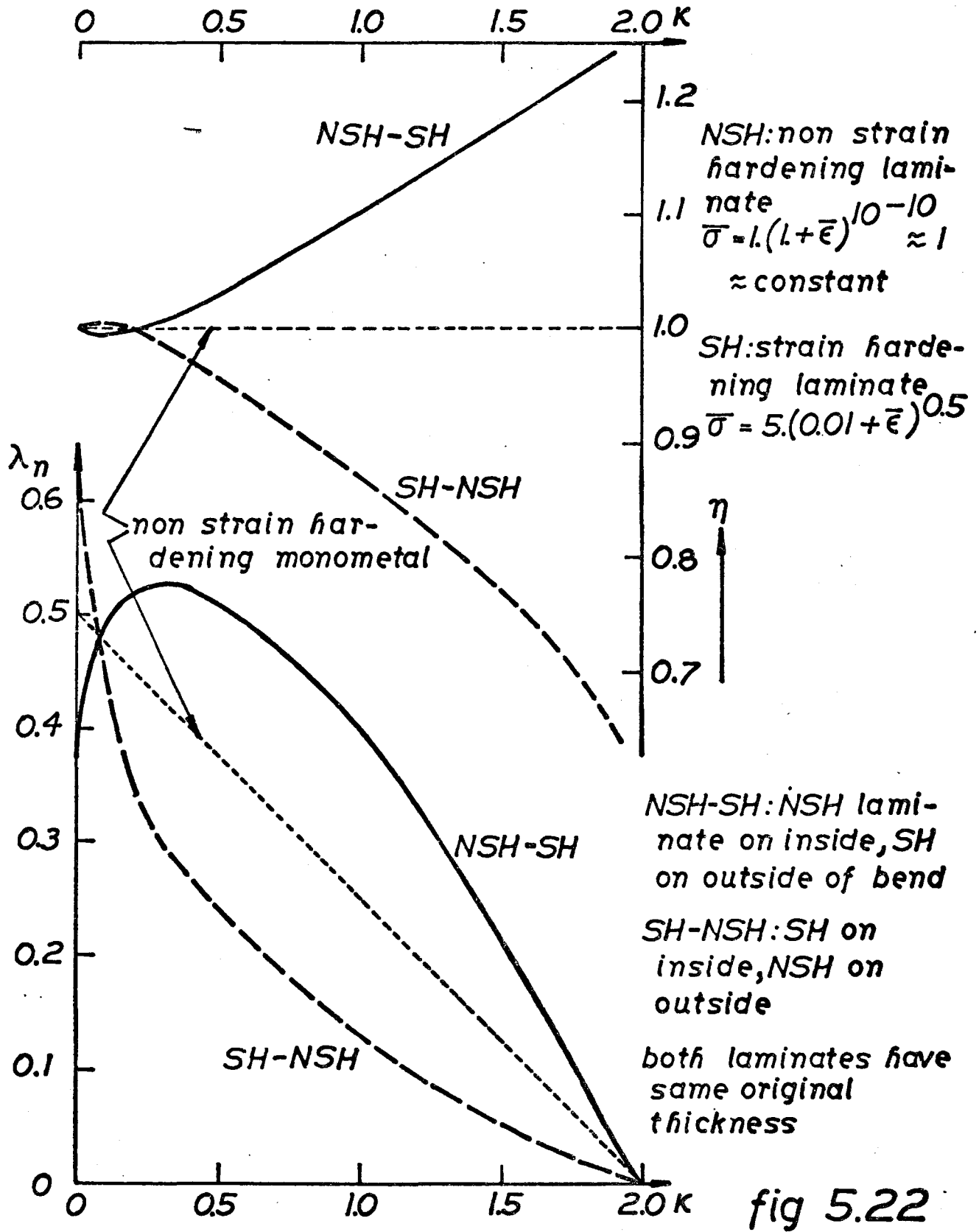


fig 5.21

INFLUENCE OF SHEET ORIENTATION ON BENDING OF STRAIN HARDENING BIMETAL



INFLUENCE OF SHEET ORIENTATION ON BENDING MOMENT OF STRAIN HARDENING BIMETAL

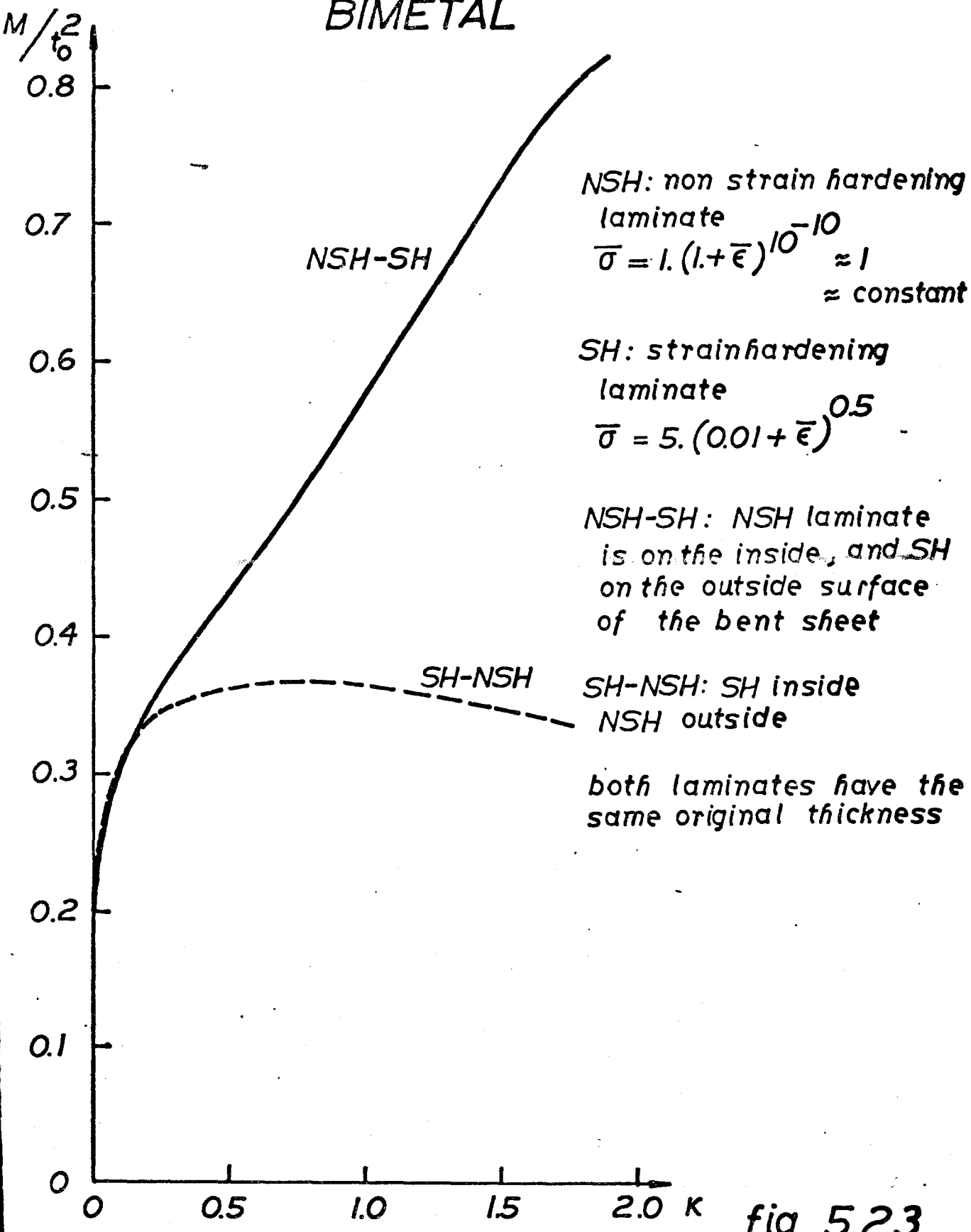


fig 5.23

STRAIN PROCESS IN BENDING STRAINHARDENING BIMETAL

$$\mu_{21} = 0.5$$

$$\bar{\sigma}_1 = 1$$

$$\bar{\sigma}_2 = 5(0.01 + \bar{\epsilon})^{0.5}$$

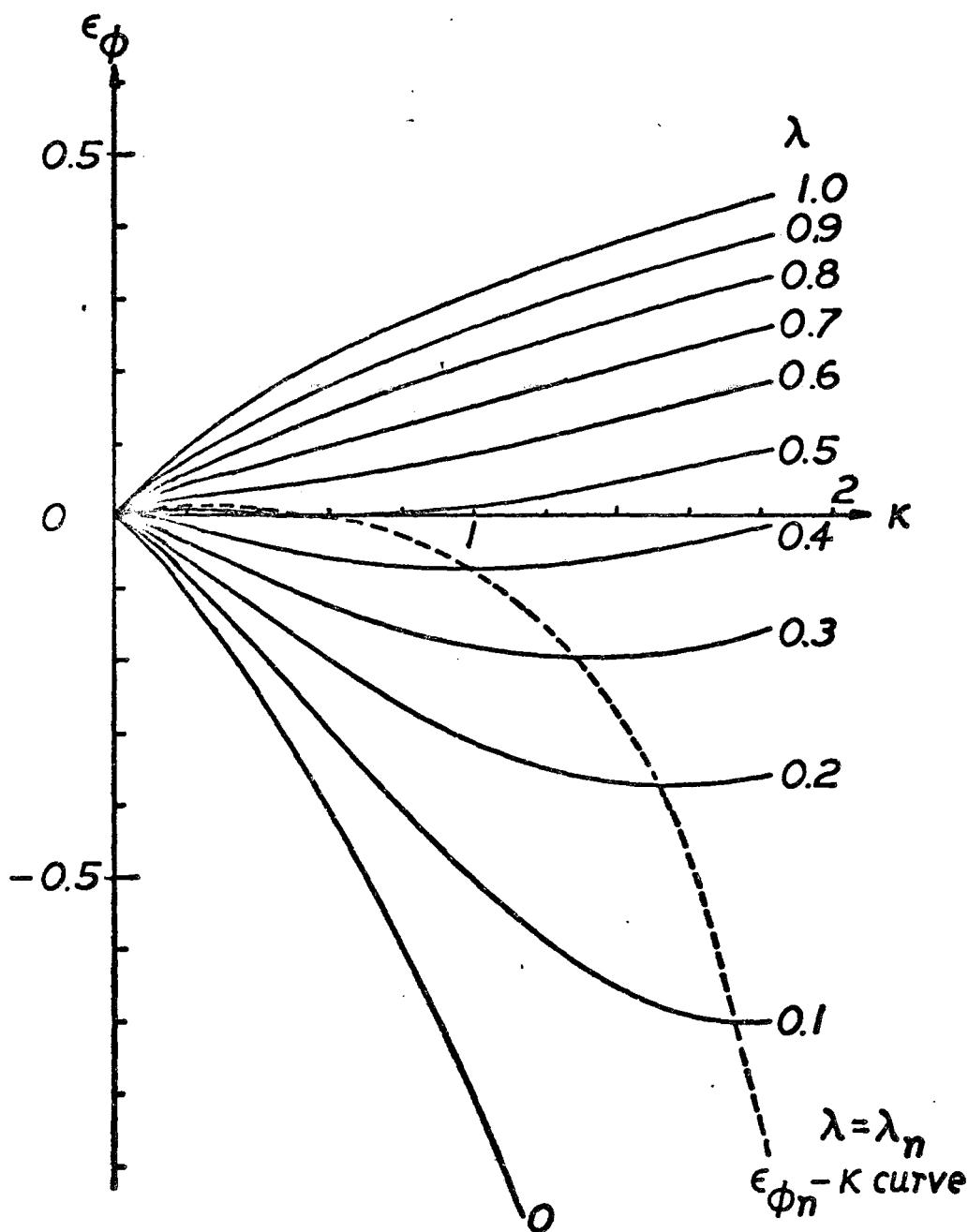
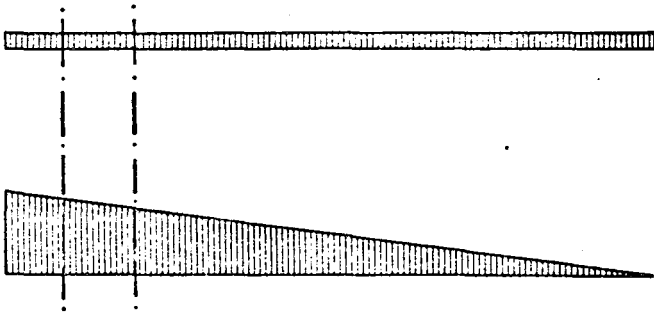
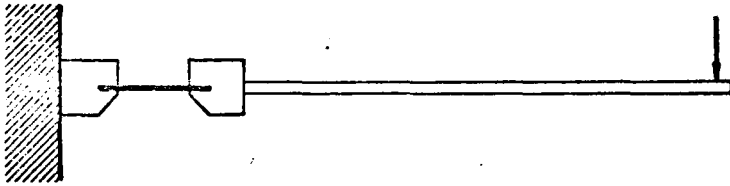


fig 5.24

BEND TEST WITH A FIXED AND MOVABLE JAW



transverse force

bending moment

fig 6.1

BENDING OF MATERIAL D (AL STRAIN HARDENING)

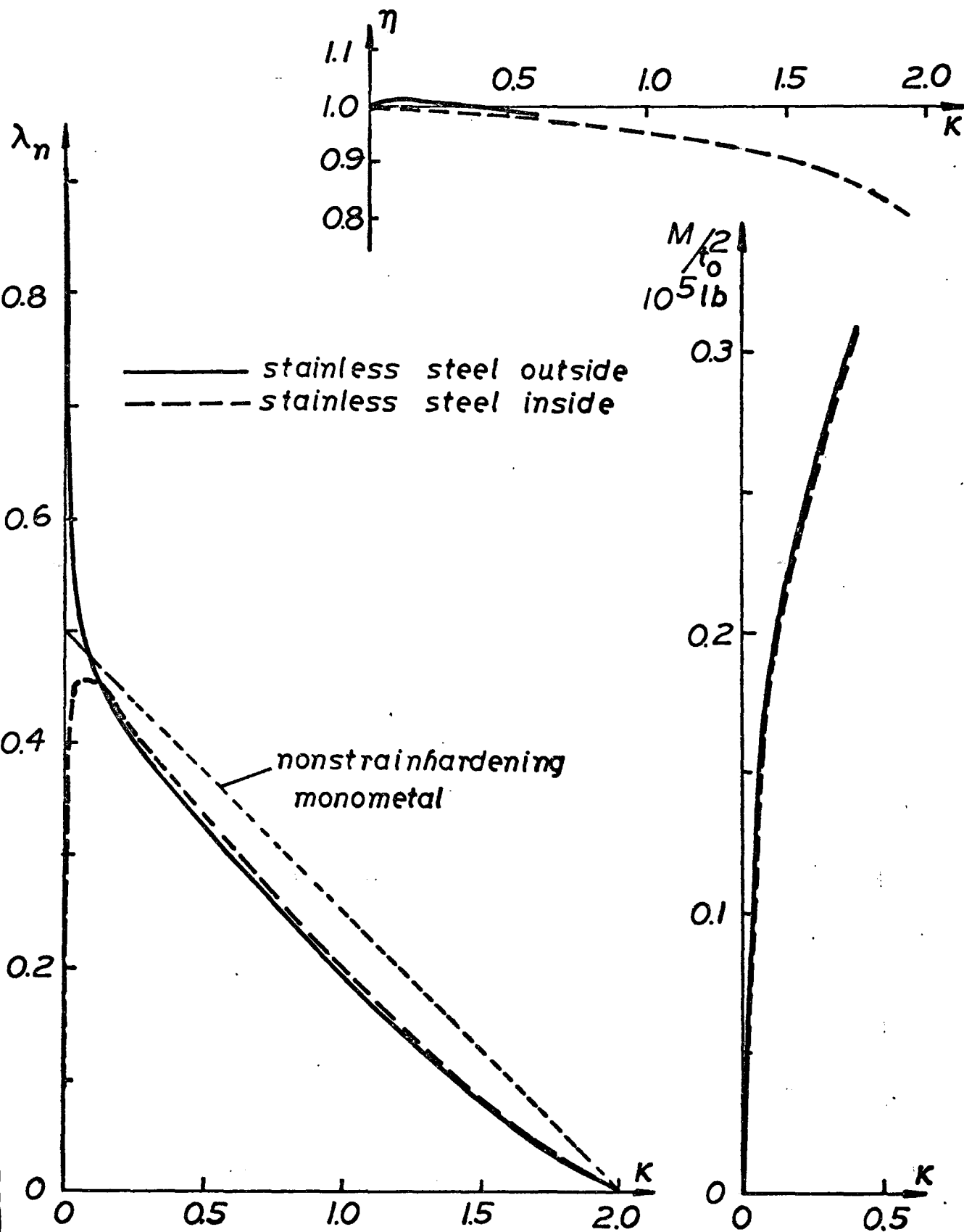


fig 6.2

NEUTRAL LAYER POSITION AND RELATIVE SHEET THICKNESS IN BENDING MATERIAL D (AL NON STRAIN HARDENING)

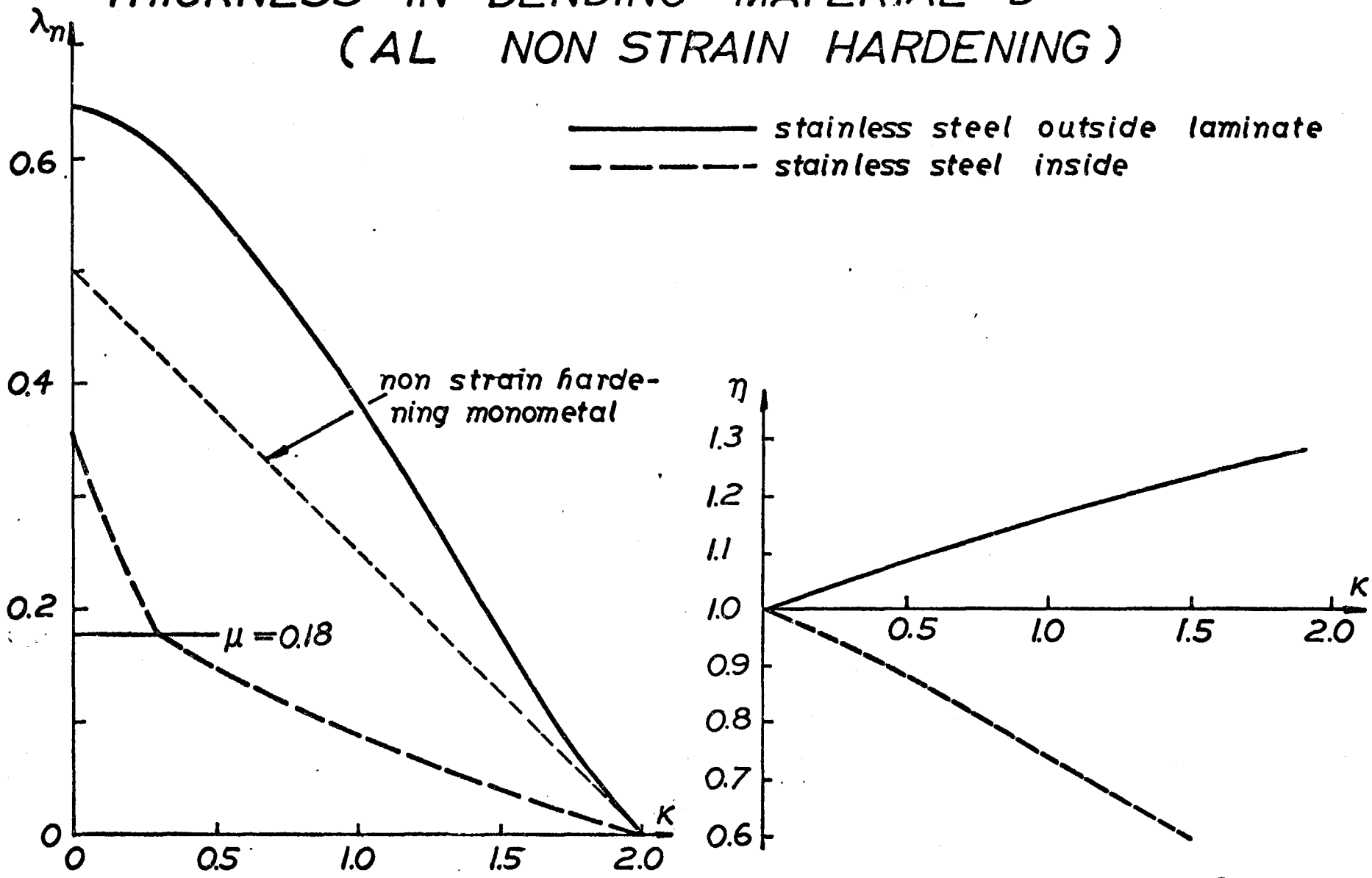


fig 6.3

BENDING MOMENT FOR BENDING MATERIAL D (AL NON STRAIN HARDENING)

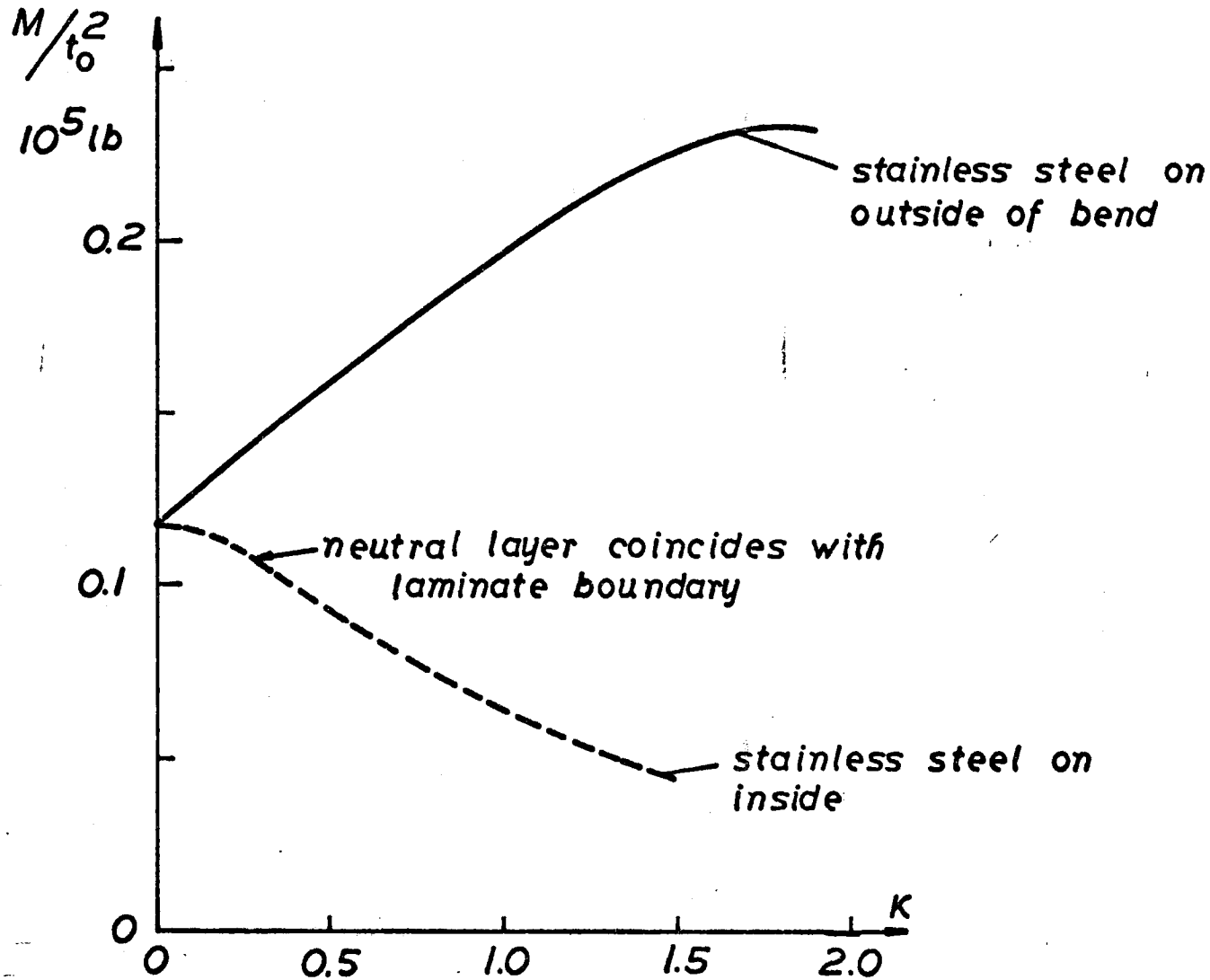
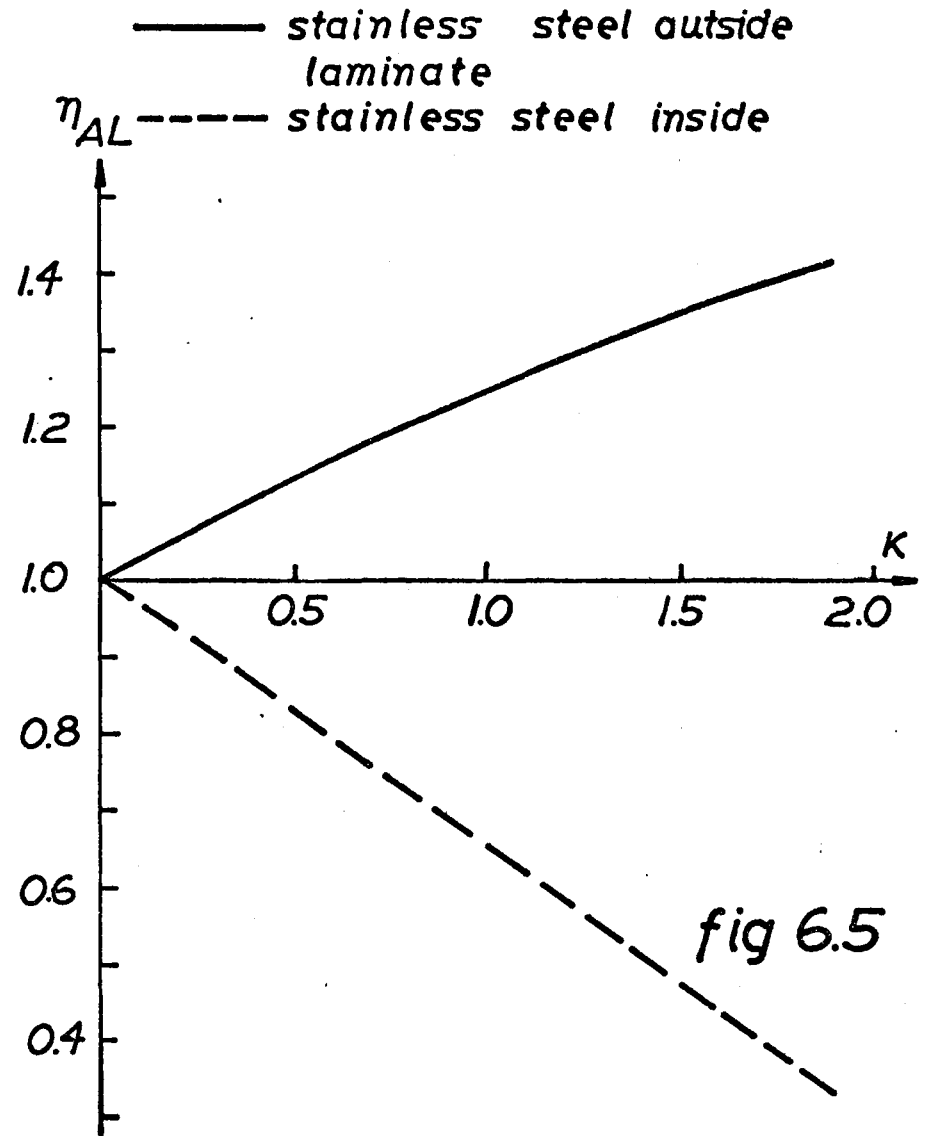
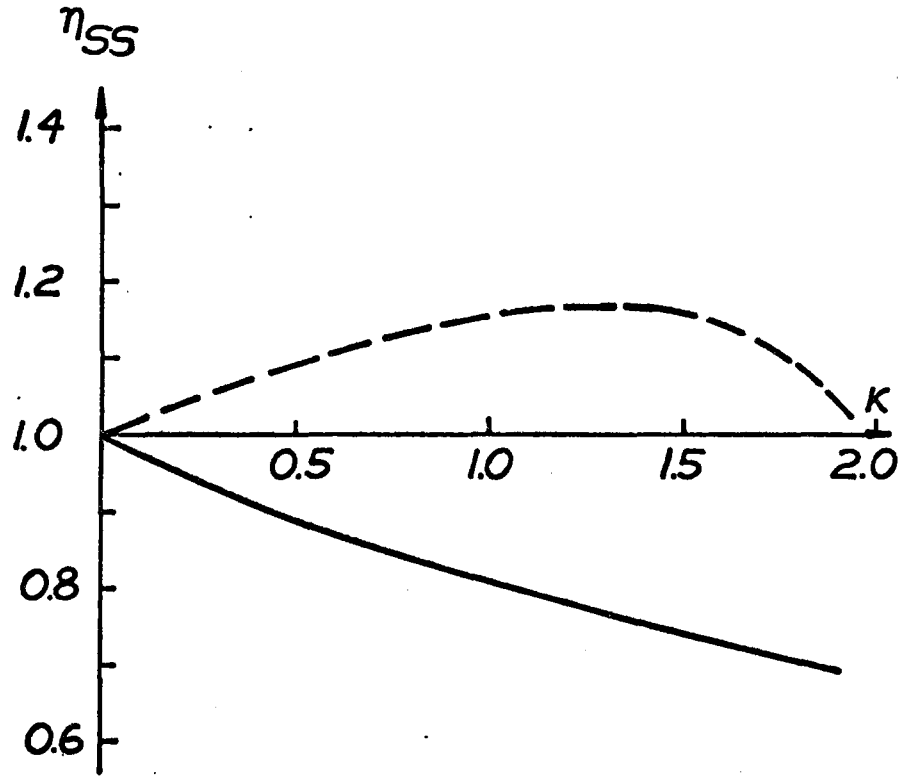


fig. 6.4

RELATIVE LAMINATE THICKNESSES IN BENDING MATERIAL D (AL NON STRAIN HARDENING)



BENDING EXPERIMENTS ON MATERIAL D

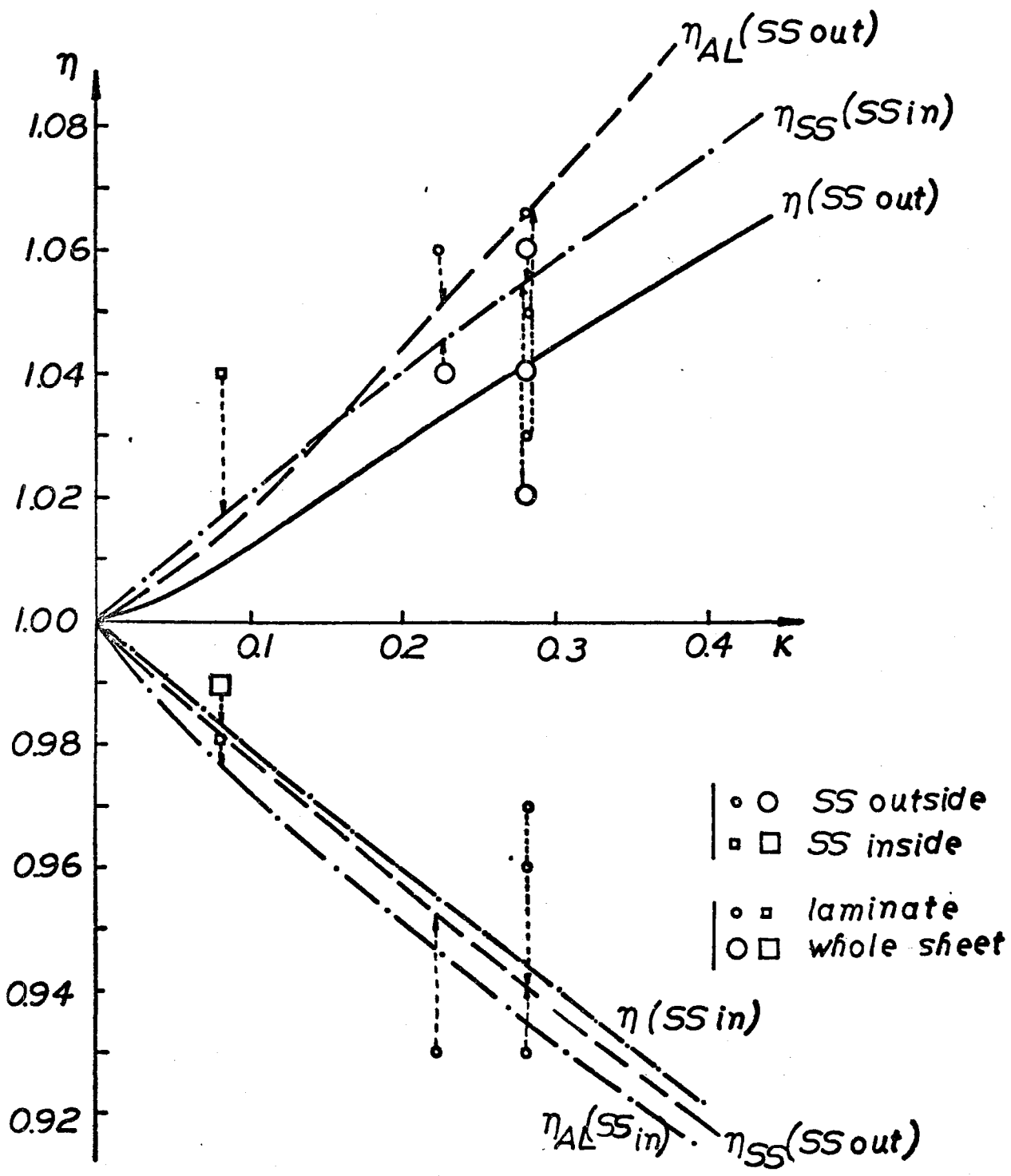


fig 6.6

GEOMETRY OF DEEP DRAWING TEST

Swift 50 mm

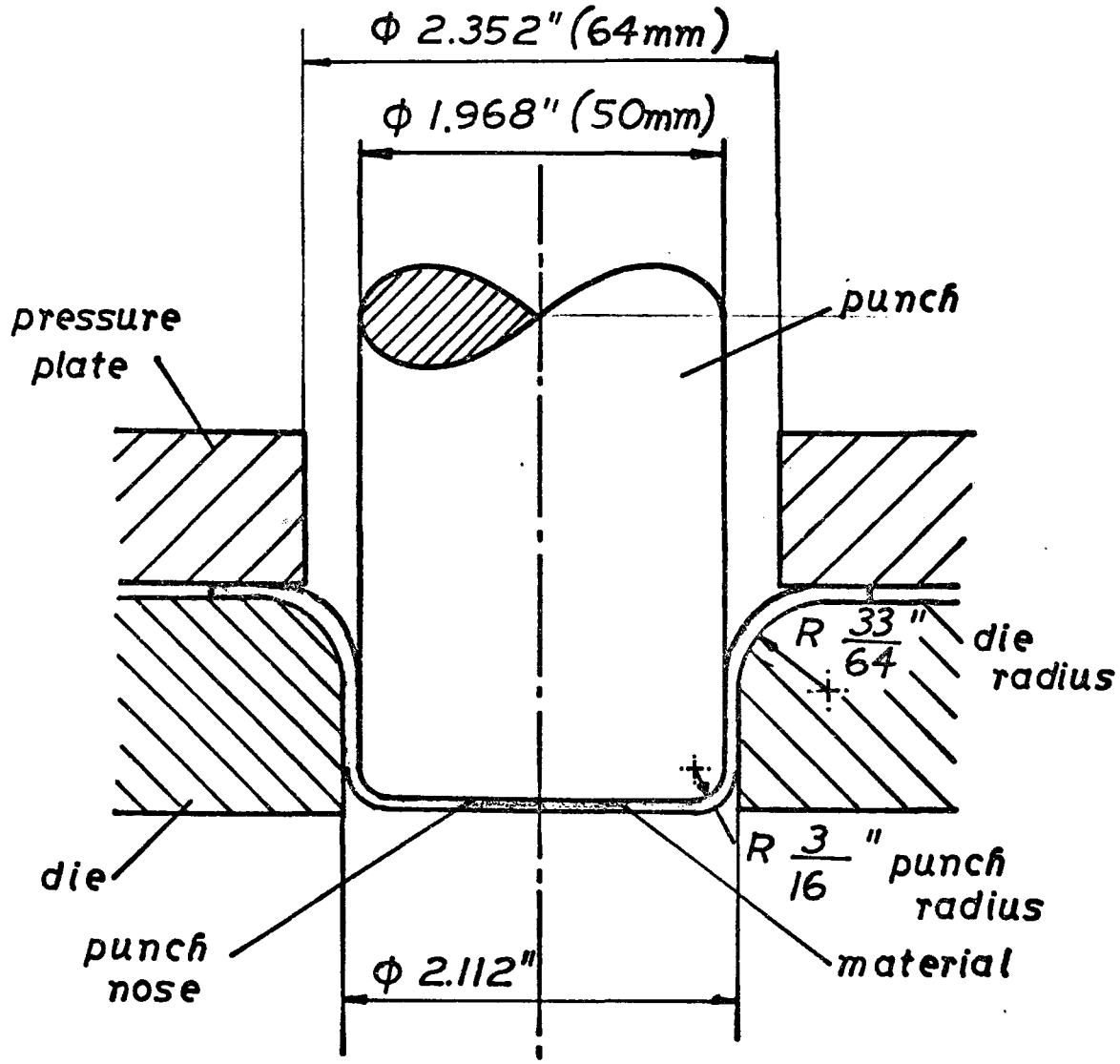


fig 6.7

INFLUENCE OF SHEET ORIENTATION ON THE RELATIVE THICKNESS OF DEEP DRAWN CUPS OF MATERIAL E BLANK DIAMETER 2.5 IN

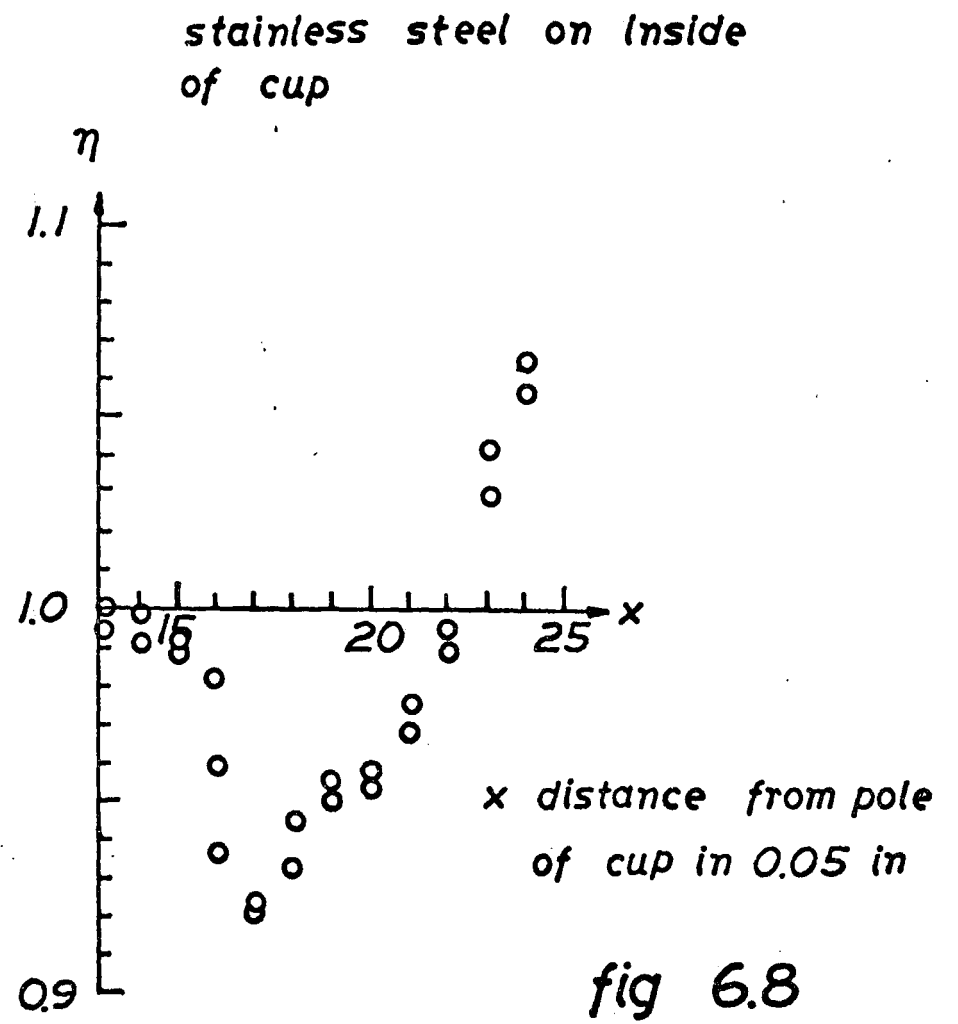
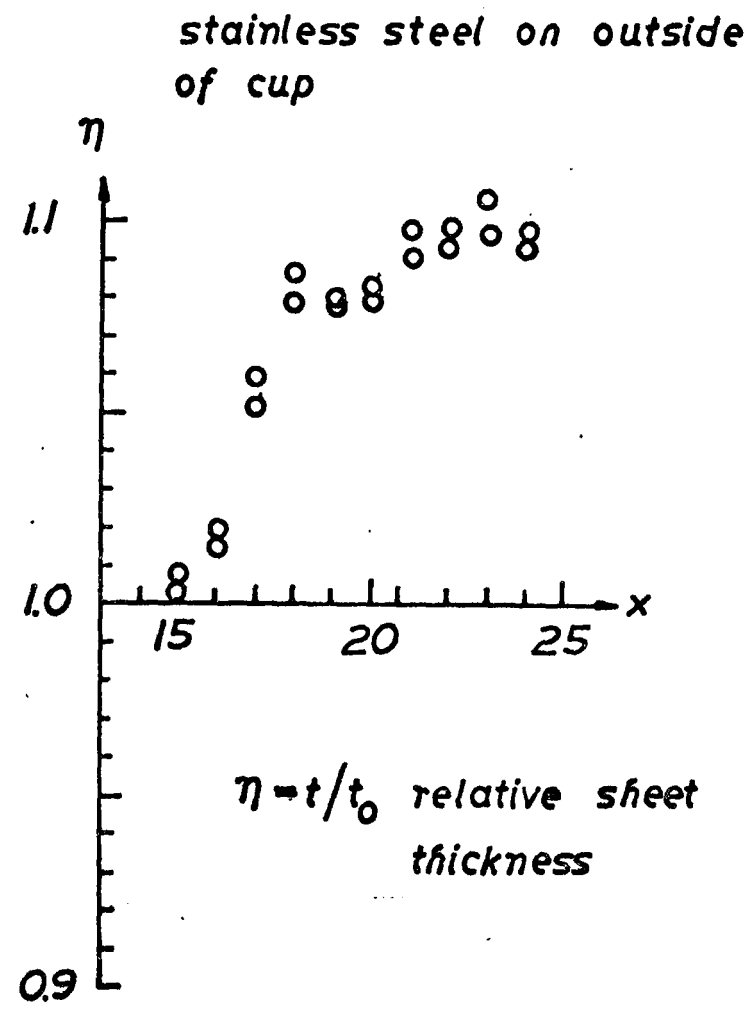


fig 6.8

INFLUENCE OF SHEET ORIENTATION ON MAXIMUM DEEP DRAWING LOAD FOR

MATERIAL D AND MATERIAL DD

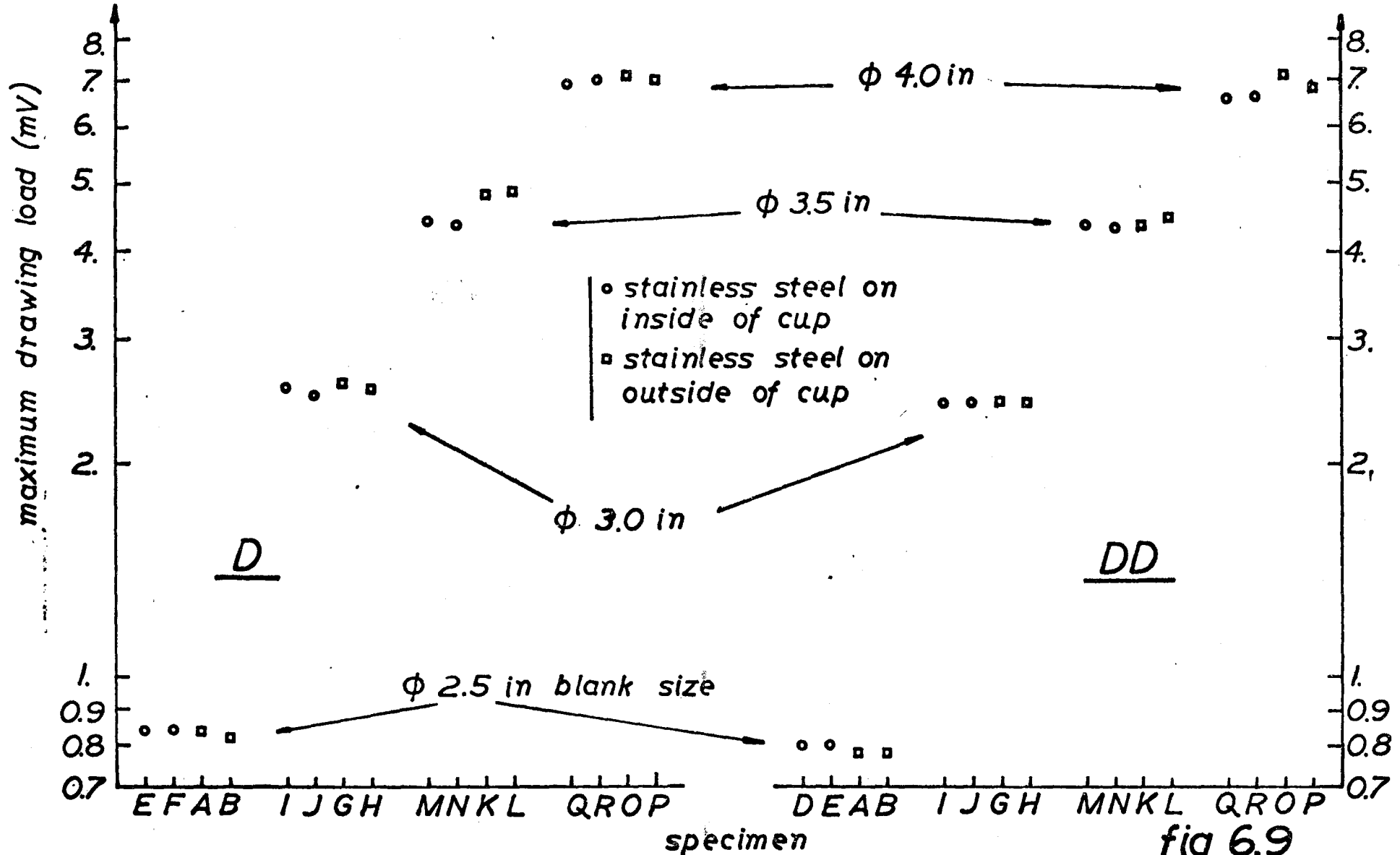


fig 6.9

INFLUENCE OF SHEET ORIENTATION ON THE PUNCH
LOAD WHEN DEEP DRAWING CUPS OF MATERIAL DD
BLANK DIAMETER 2.5 IN

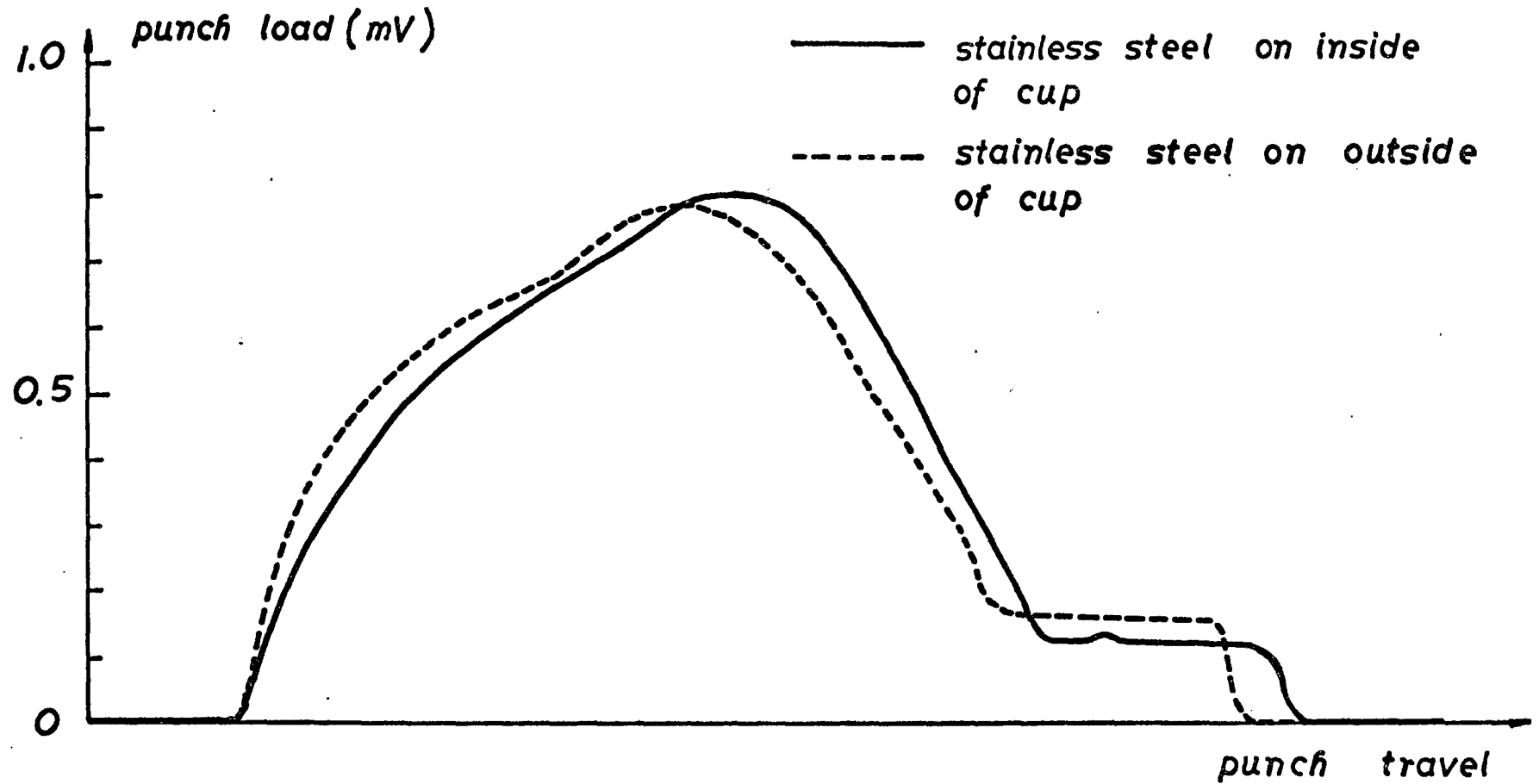


fig 6.10

INFLUENCE OF SHEET ORIENTATION ON THE PUNCH LOAD WHEN DEEP DRAWING CUPS OF MATERIAL D BLANK DIAMETER 3.5 IN

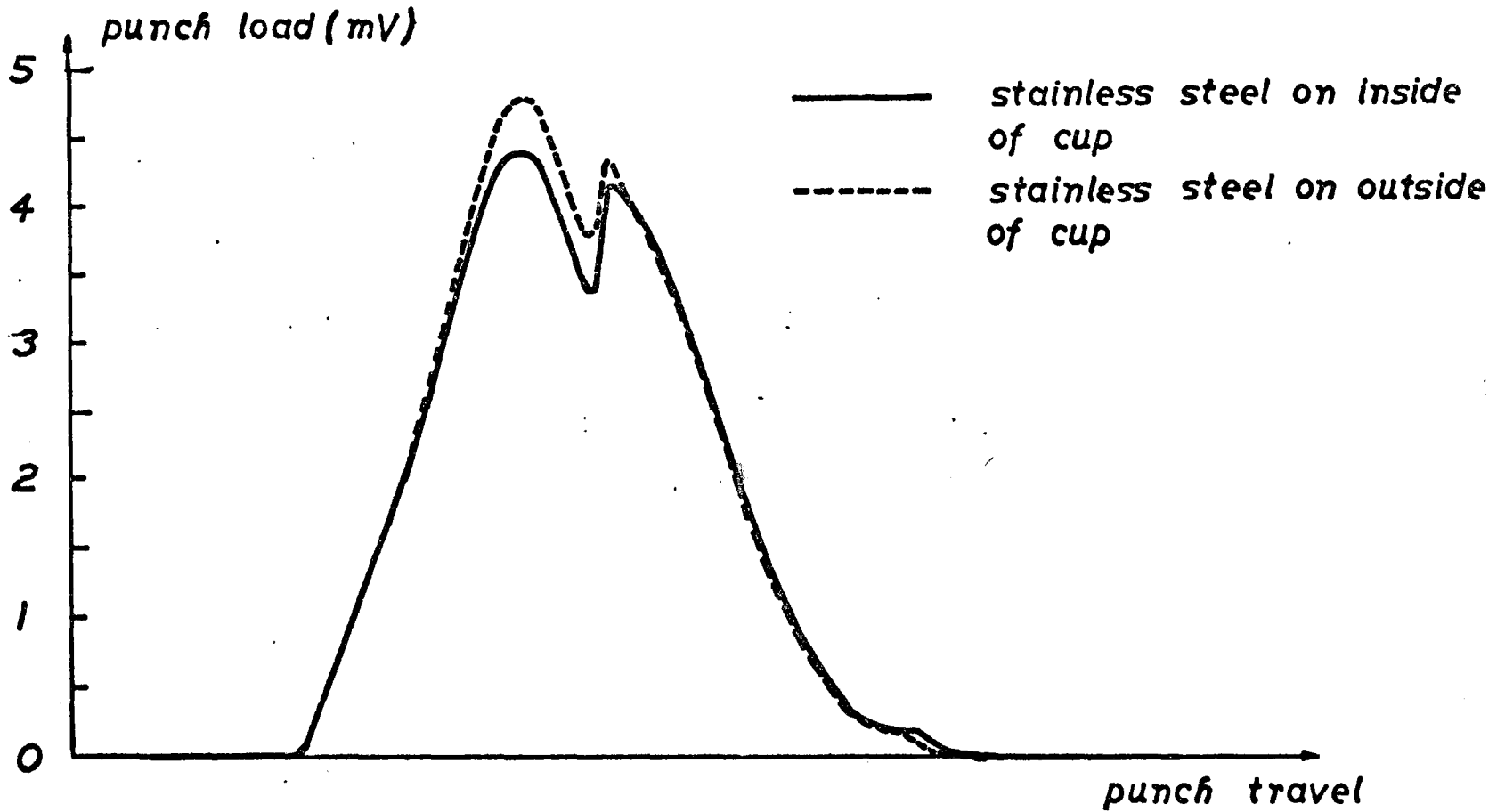
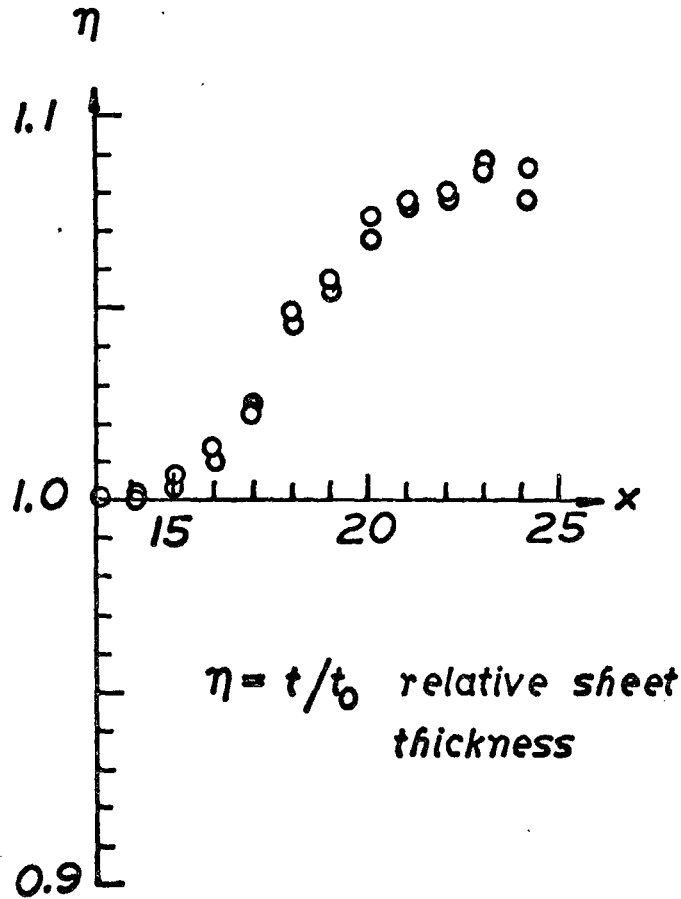


fig 6.11

INFLUENCE OF SHEET ORIENTATION ON THE RELATIVE THICKNESS OF DEEP DRAWN CUPS OF MATERIAL D BLANK DIAMETER 2.5 IN

stainless steel on outside
of cup



stainless steel on inside
of cup

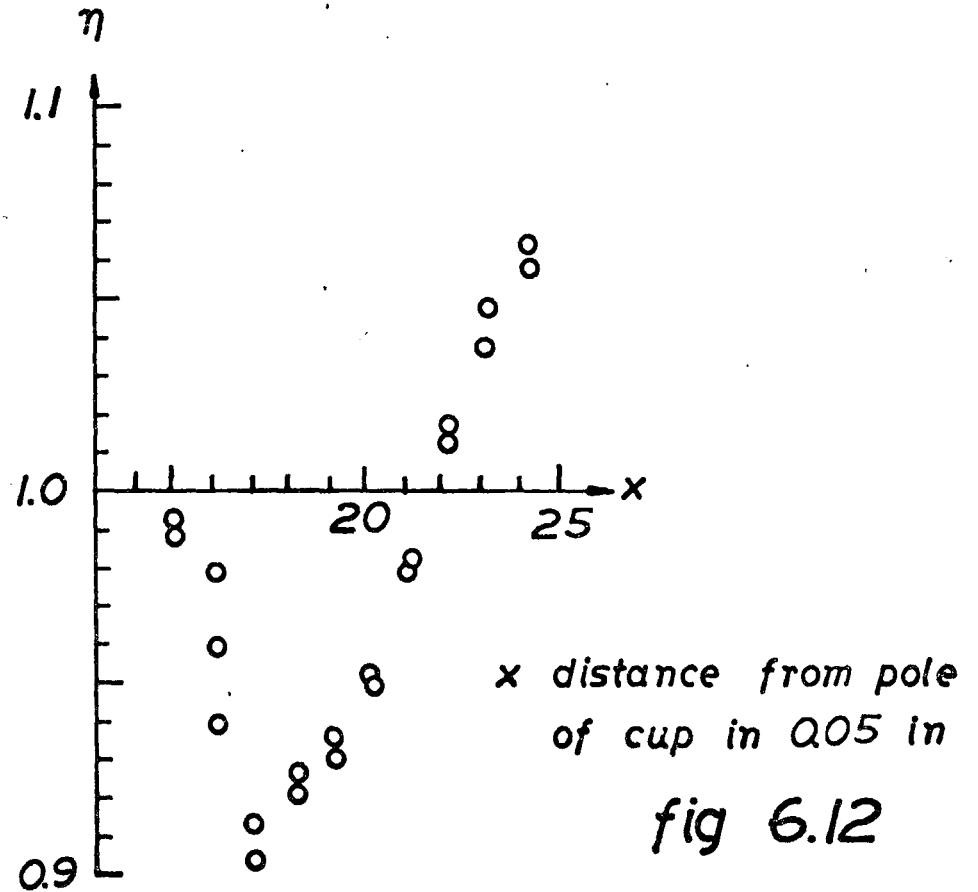


fig 6.12

INFLUENCE OF SHEET ORIENTATION ON THE RELATIVE THICKNESS OF DEEP DRAWN CUPS OF MATERIAL DD BLANK DIAMETER 2.5 IN

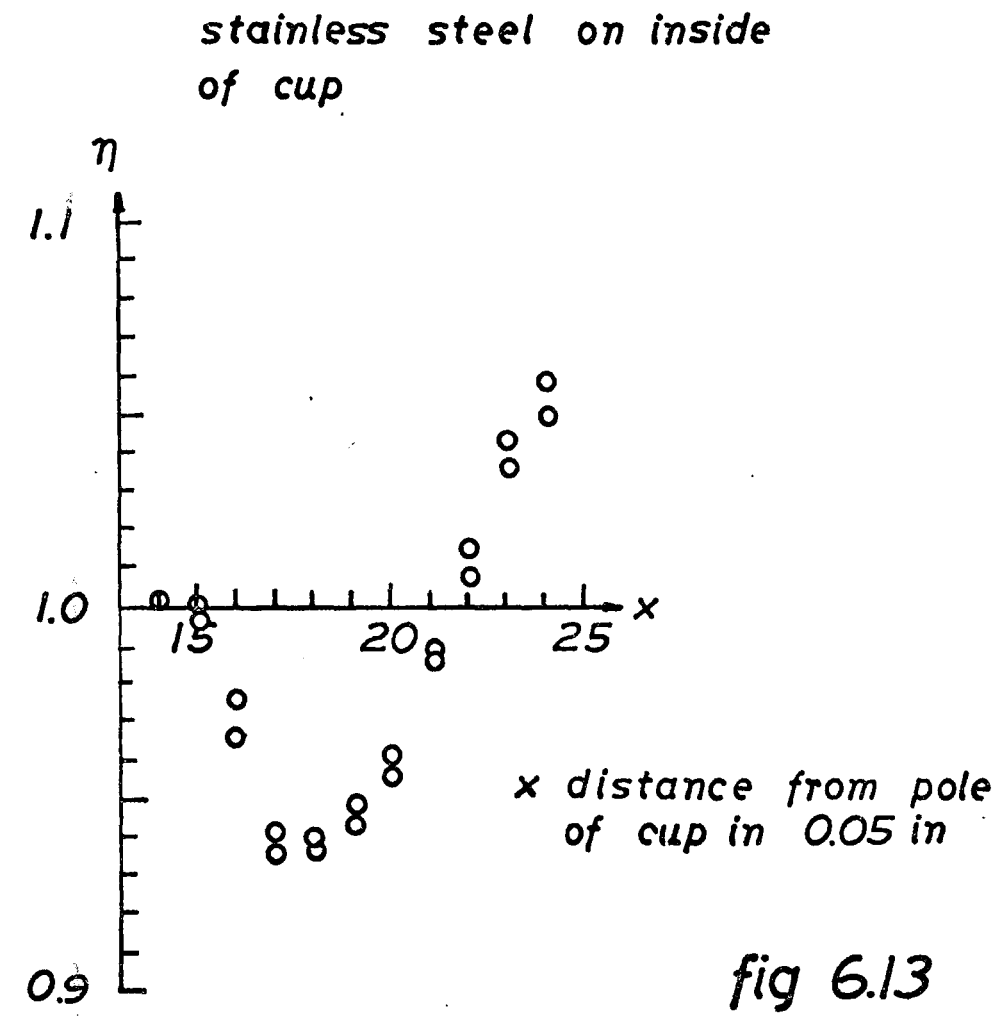
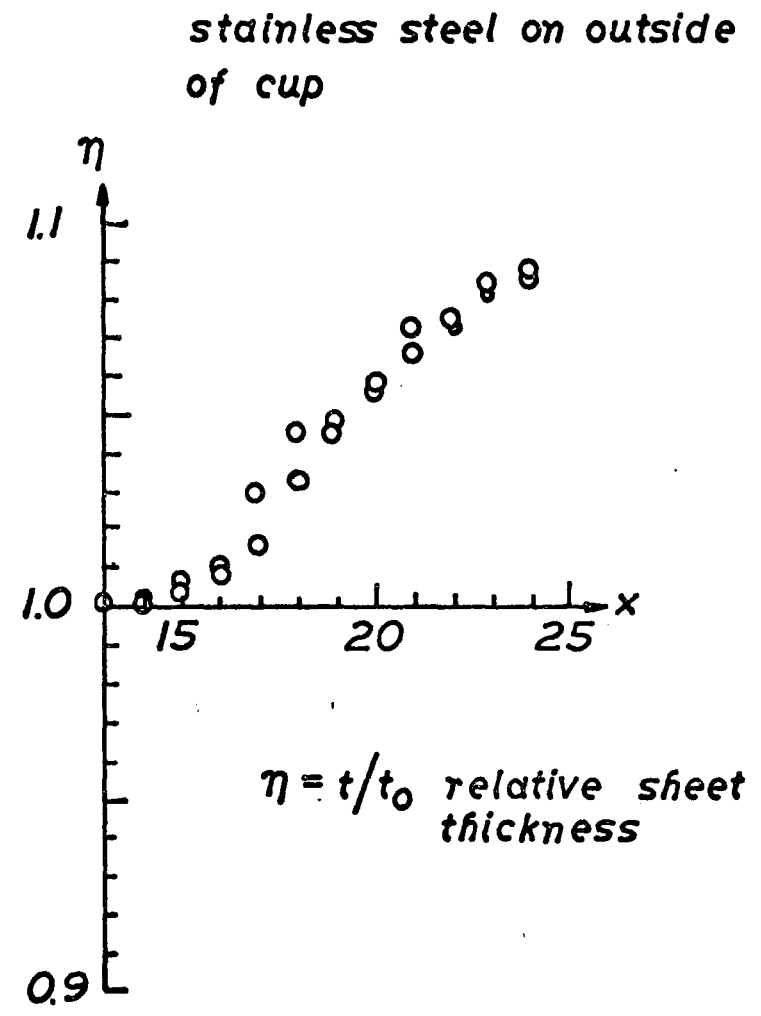


fig 6.13

INFLUENCE OF SHEET ORIENTATION ON THE RELATIVE THICKNESS OF DEEP DRAWN CUPS OF MATERIAL DD

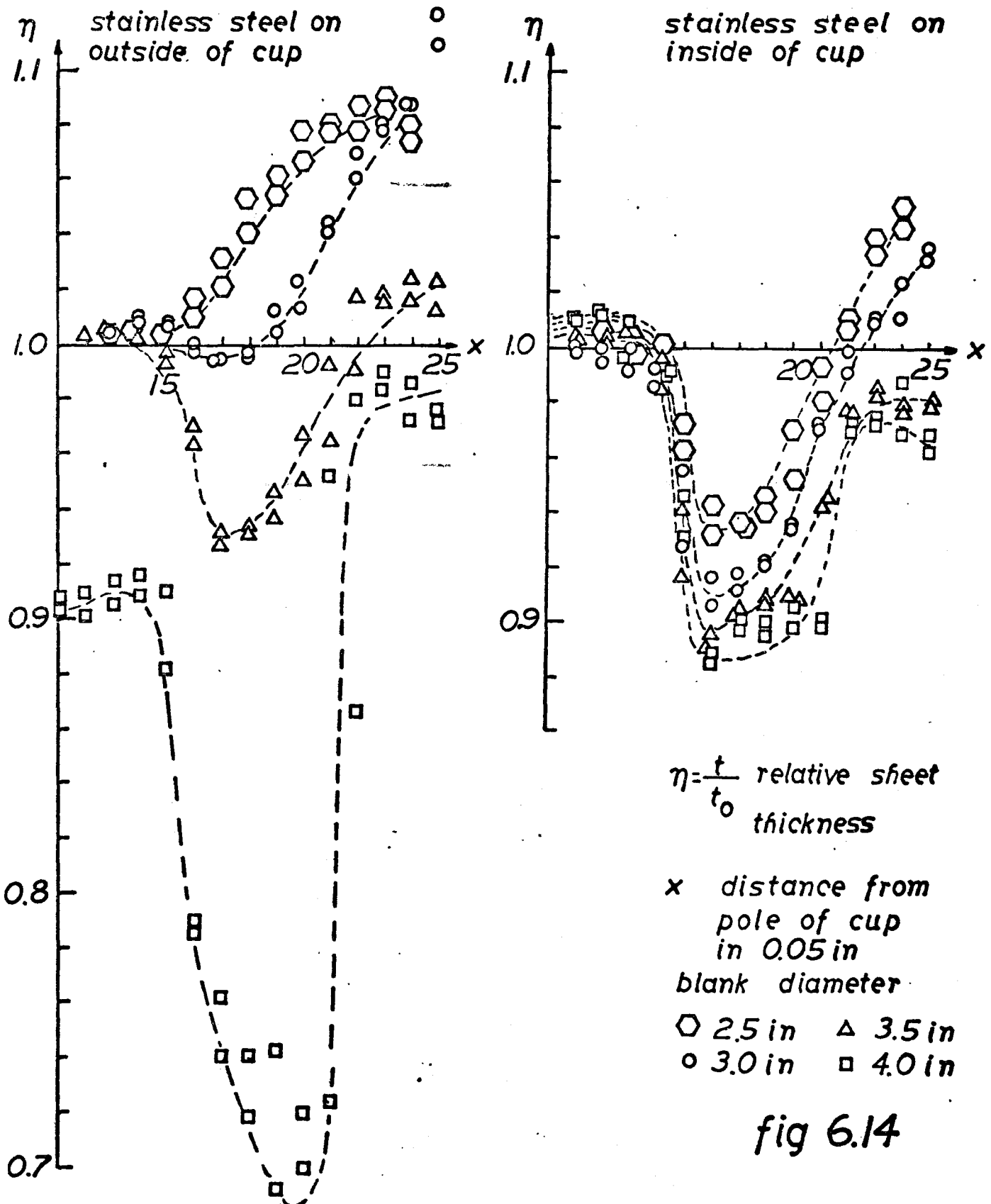


fig 6.14

RELATIVE LAMINATE THICKNESSES IN DEEP DRAWN CUPS OF MATERIAL DD WITH STAINLESS STEEL ON OUTSIDE OF CUPS

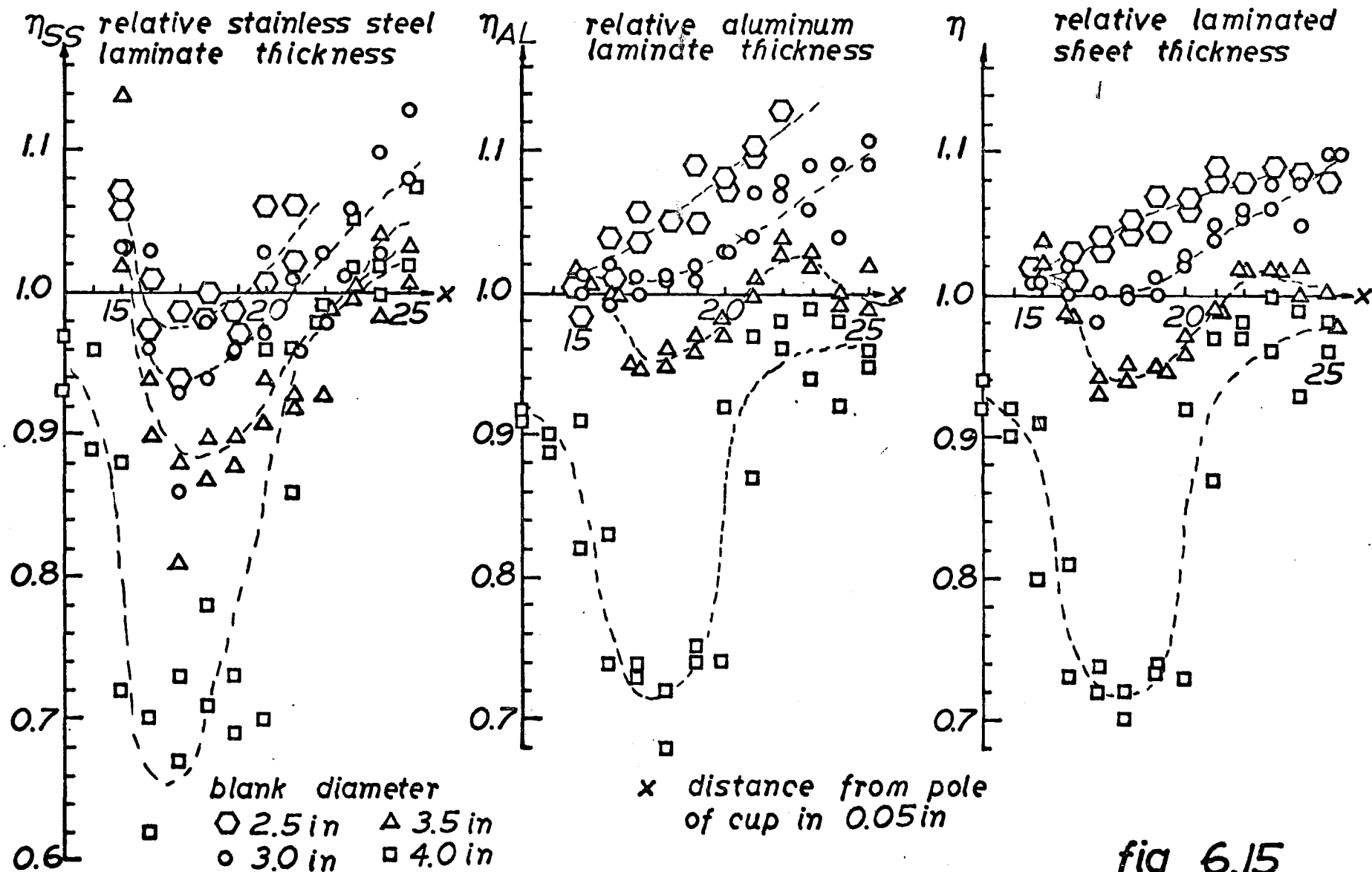
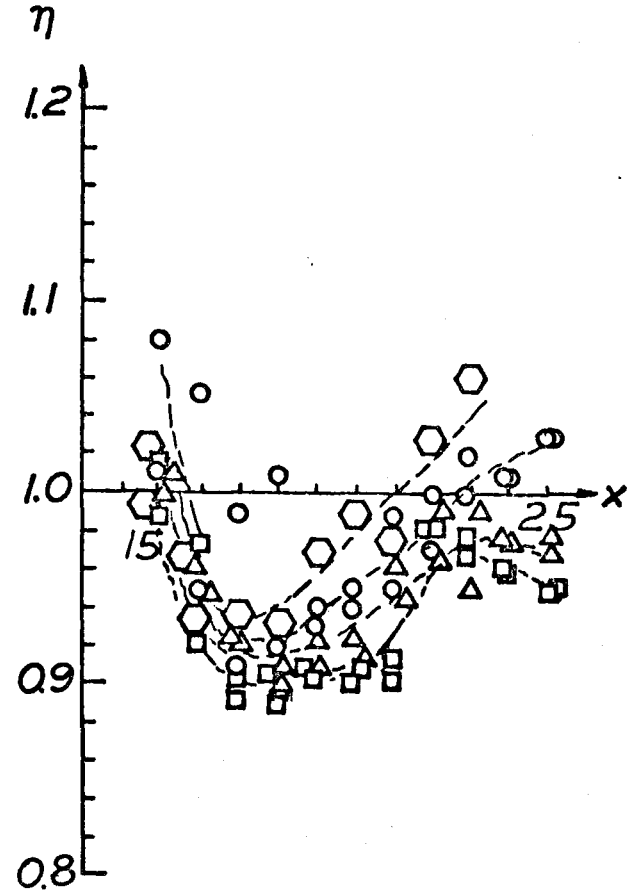
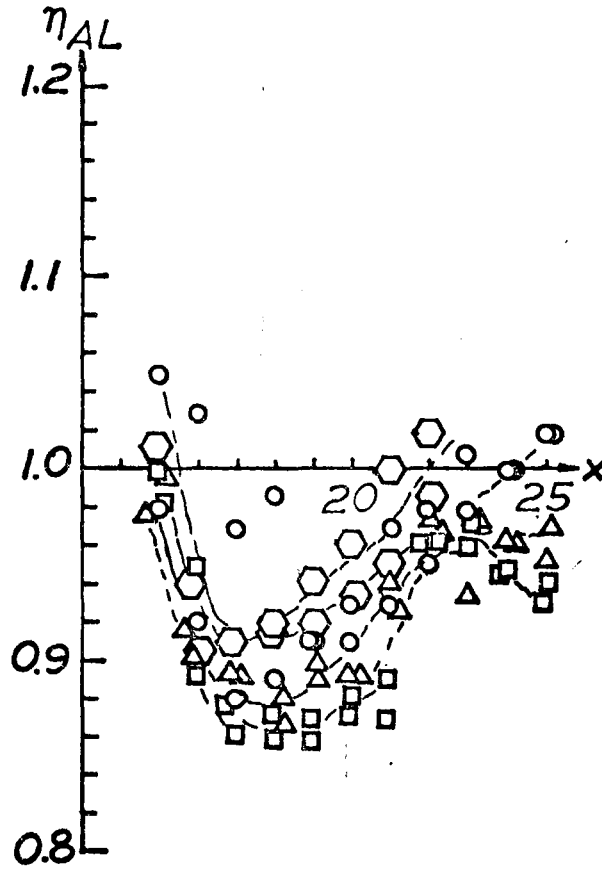
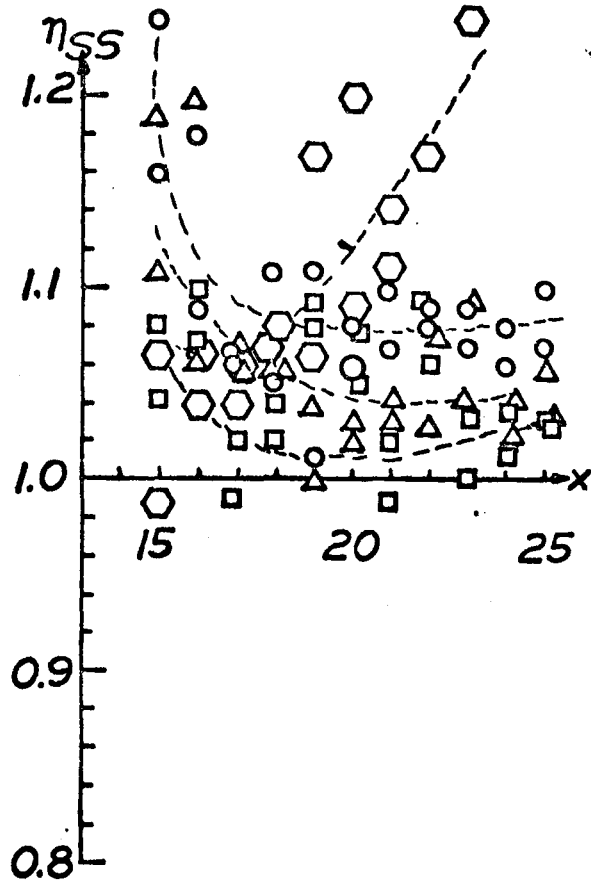


fig 6.15

RELATIVE LAMINATE THICKNESSES IN DEEP DRAWN CUPS OF MATERIAL DD WITH STAINLESS STEEL ON INSIDE OF CUPS



x distance from pole of cup in 0.05 in

blank diameter

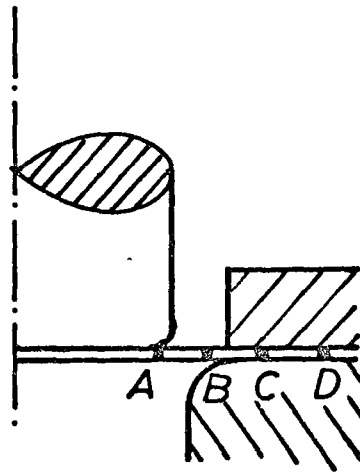
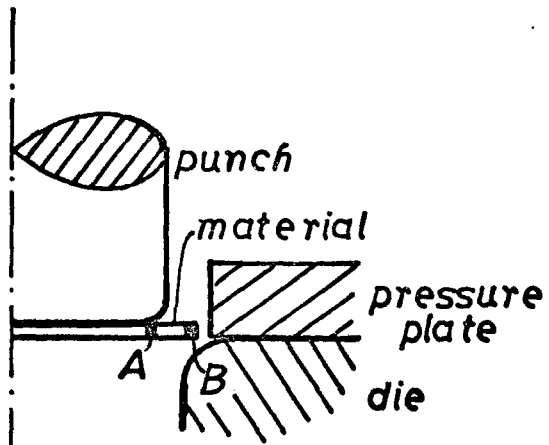
○ 2.5 in △ 3.5 in
 ○ 3.0 in □ 4.0 in

$\eta_{SS} = t_{SS}/t_{0SS}$ relative stainless steel laminate thickness

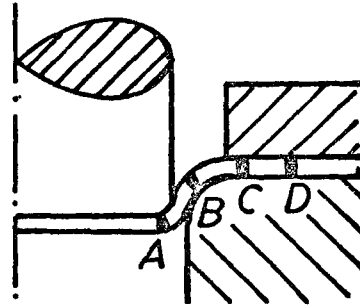
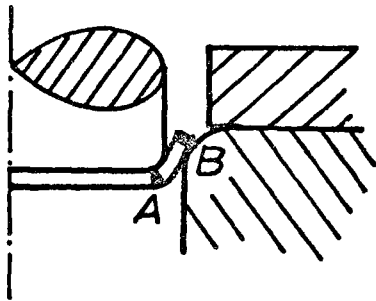
$\eta_{AL} = t_{AL}/t_{0AL}$ relative aluminum laminate thickness

$\eta = t/t_0$ relative laminated sheet thickness

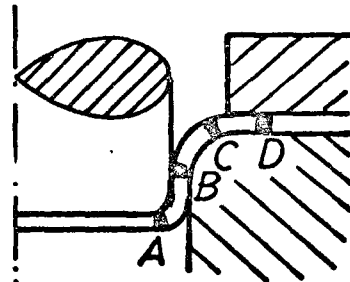
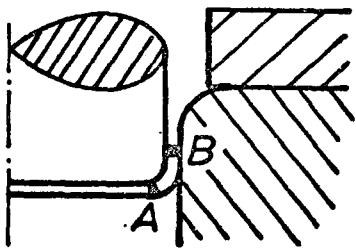
fig 6.16



I

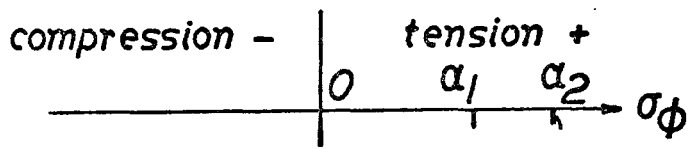


II



III

fig 6.17



$$\sigma_\phi^2 = \alpha_2$$

$$\sigma_\phi^1 = -\alpha_1$$

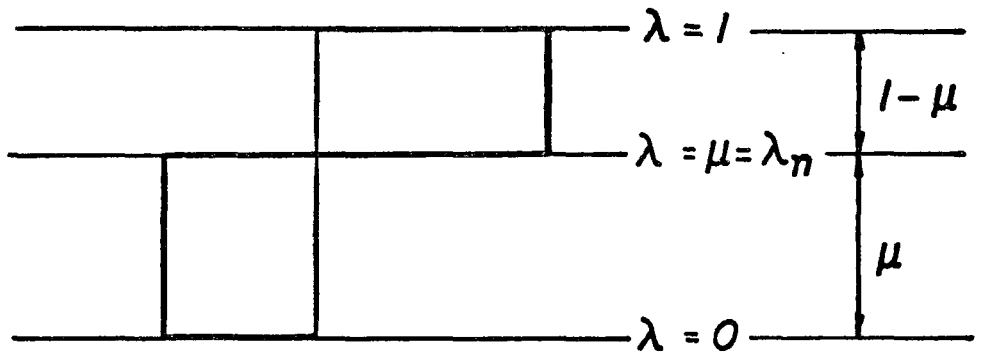


fig IV.1

$$\sigma_\phi^2 = \alpha_2$$

$$\sigma_\phi^1 = \alpha_1$$

$$\sigma_\phi^1 = -\alpha_1$$

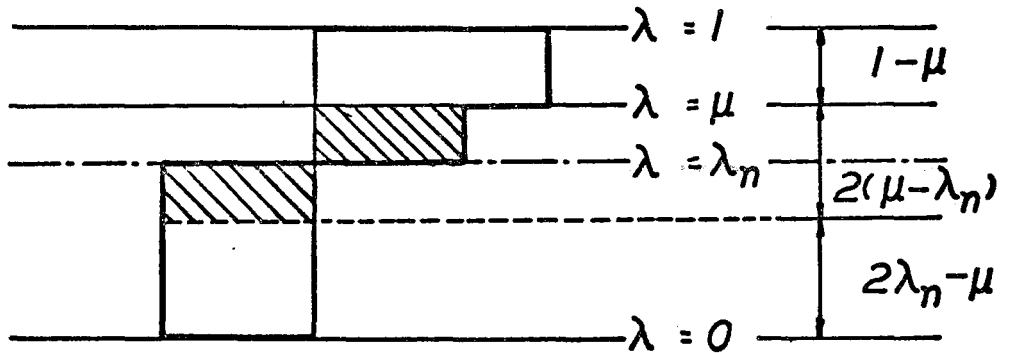


fig IV.2

$$\sigma_\phi^2 = \alpha_2$$

$$\sigma_\phi^2 = -\alpha_2$$

$$\sigma_\phi^1 = -\alpha_1$$

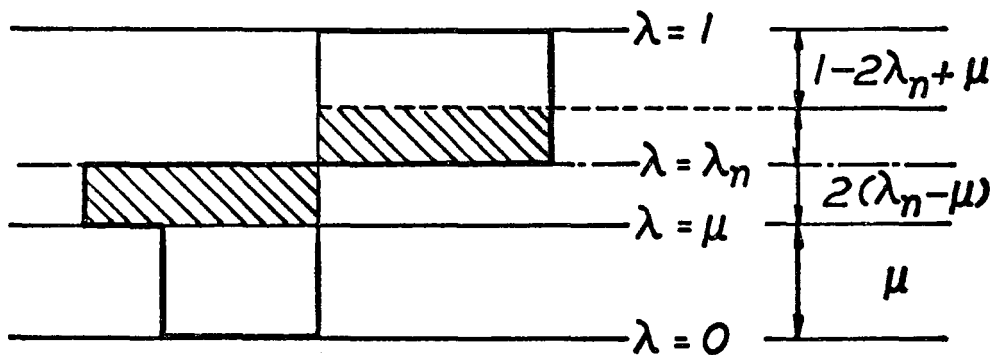


fig IV.3

ORIGINAL NEUTRAL LAYER POSITION λ_n^0 FOR BENDING OF A BIMETAL

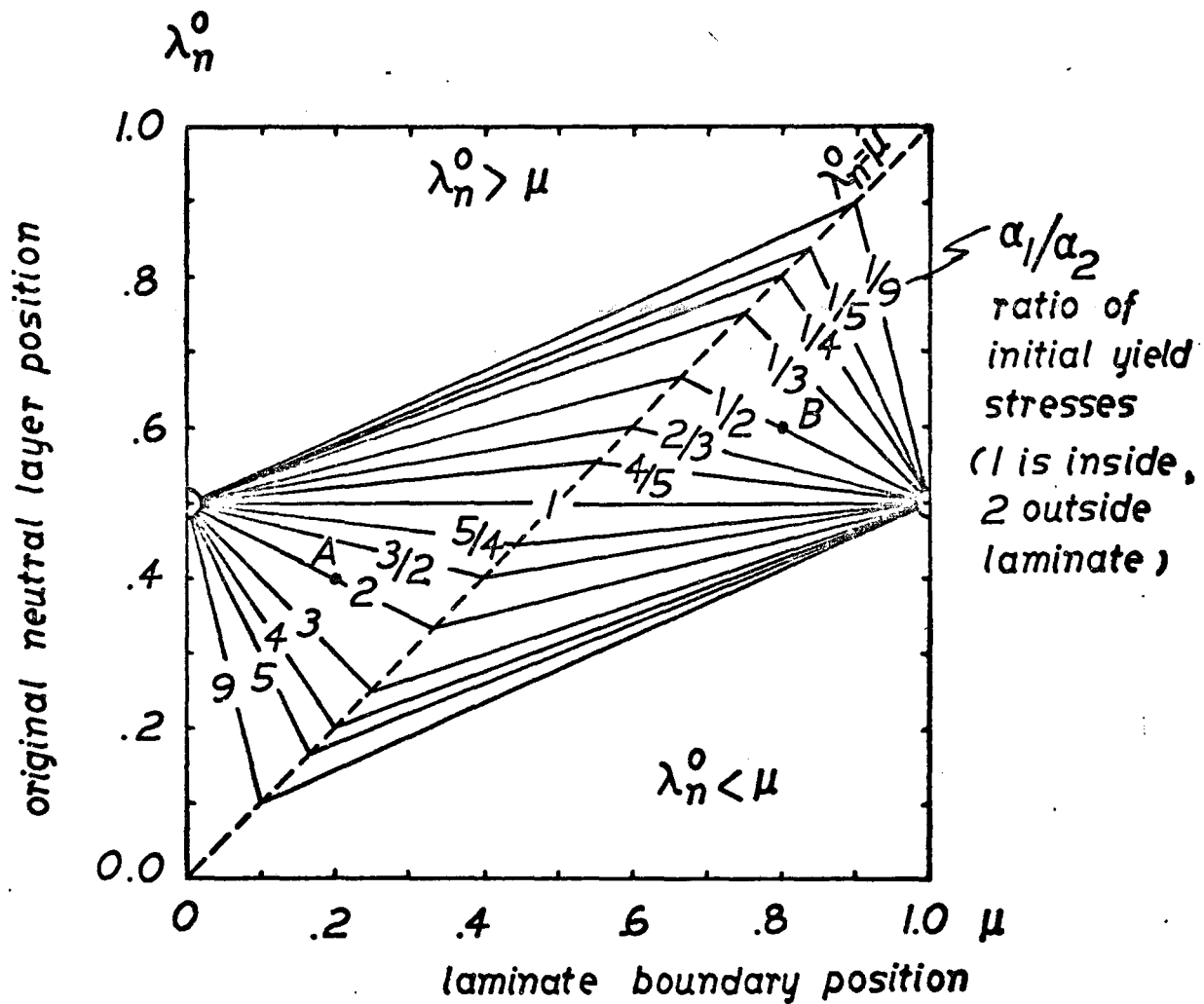


fig IV.4

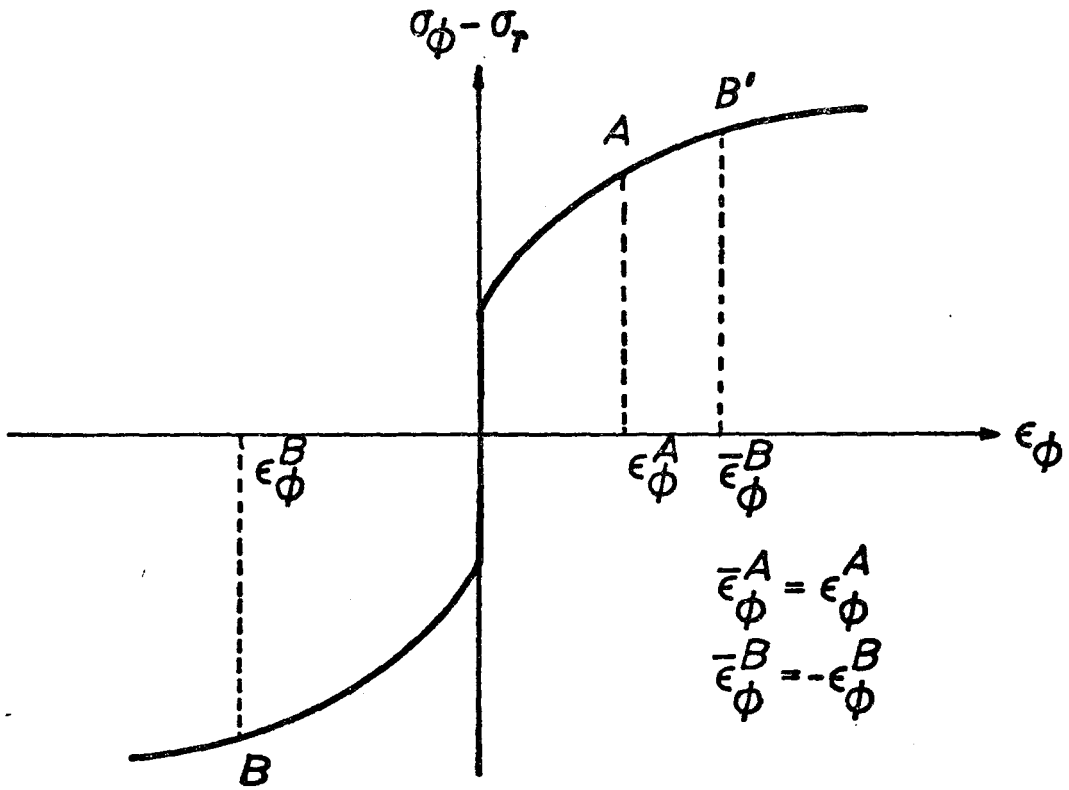


fig VII.1

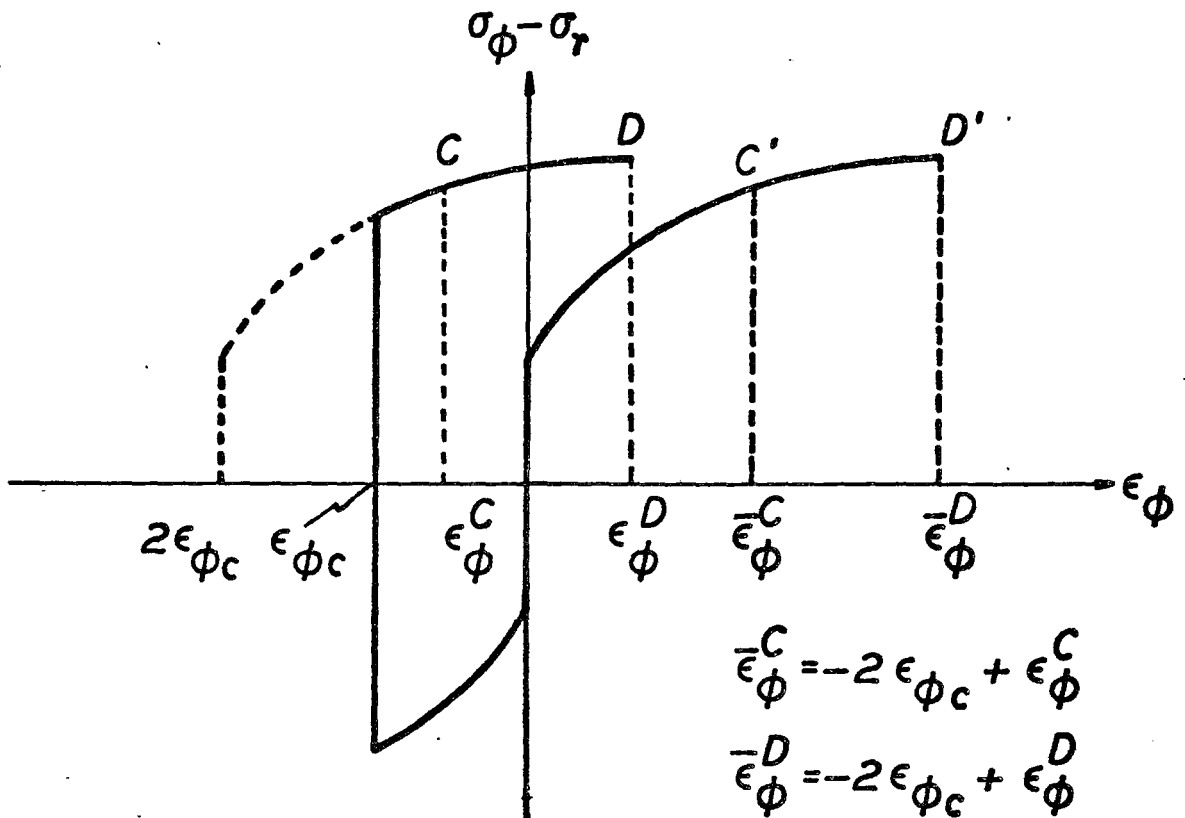
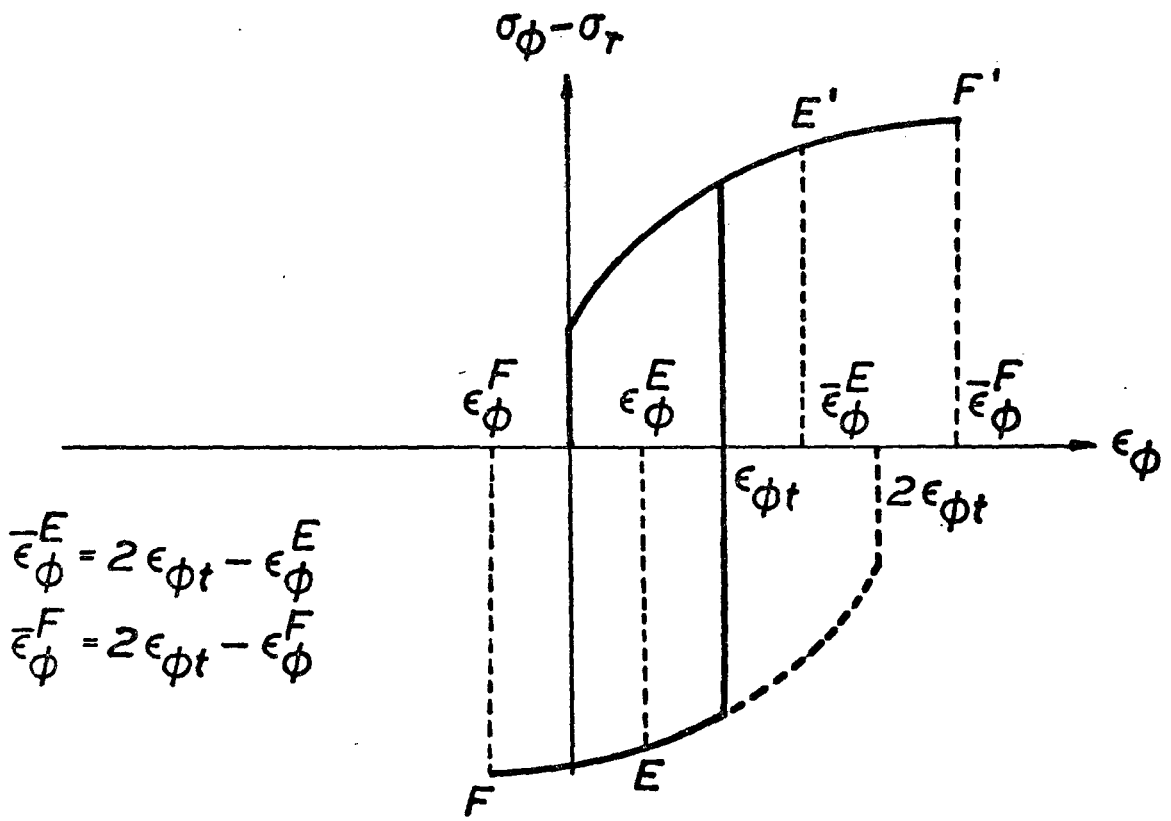


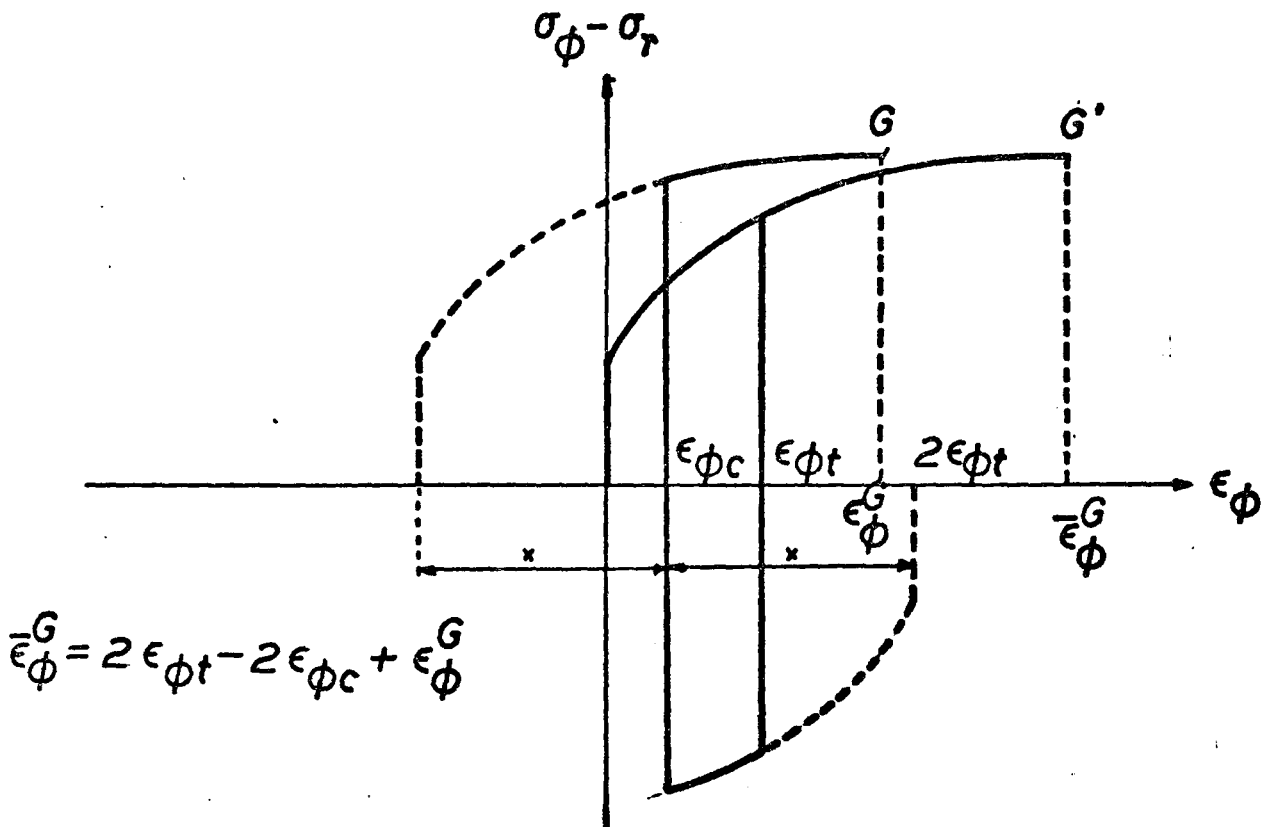
fig VII.2



$$\bar{\epsilon}_\phi^E = 2\epsilon_{\phi t} - \epsilon_\phi^E$$

$$\bar{\epsilon}_\phi^F = 2\epsilon_{\phi t} - \epsilon_\phi^F$$

fig VII.3



$$\bar{\epsilon}_\phi^G = 2\epsilon_{\phi t} - 2\epsilon_{\phi c} + \epsilon_\phi^G$$

fig VII.4

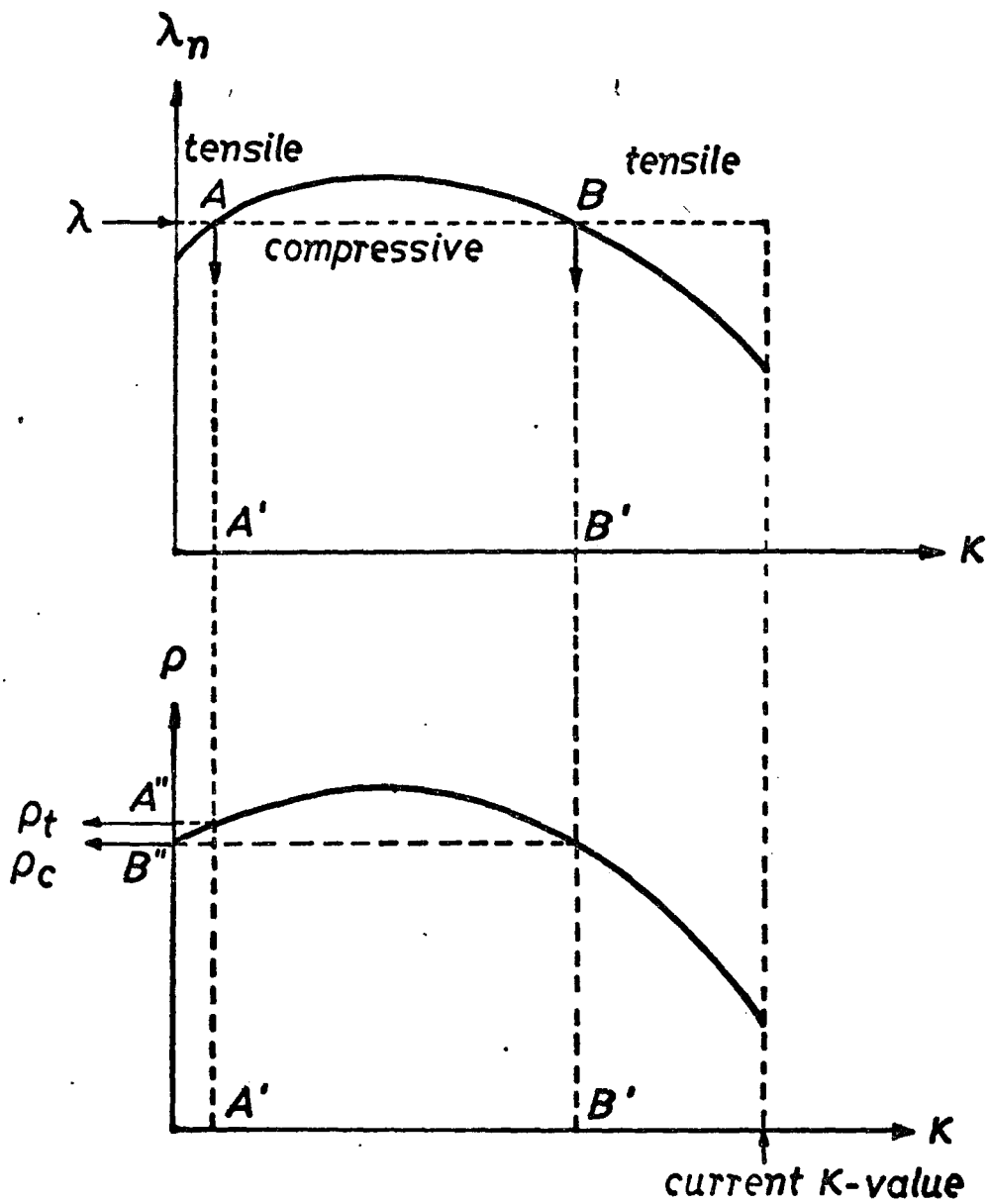


fig VII.5

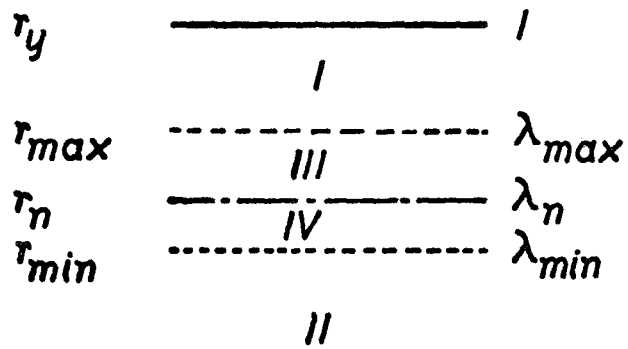


fig VII.6

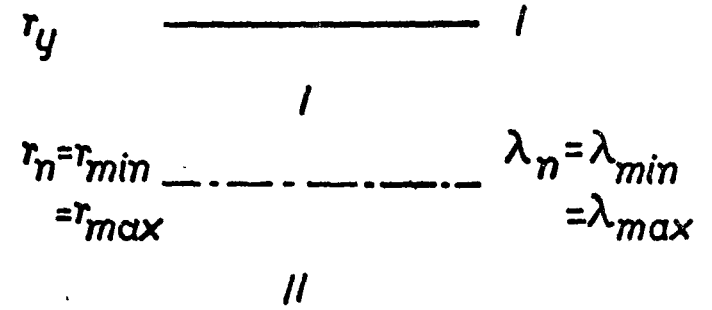


fig VII.7

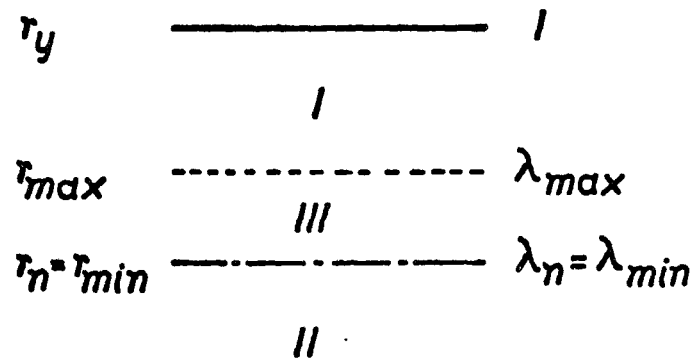


fig VII.8

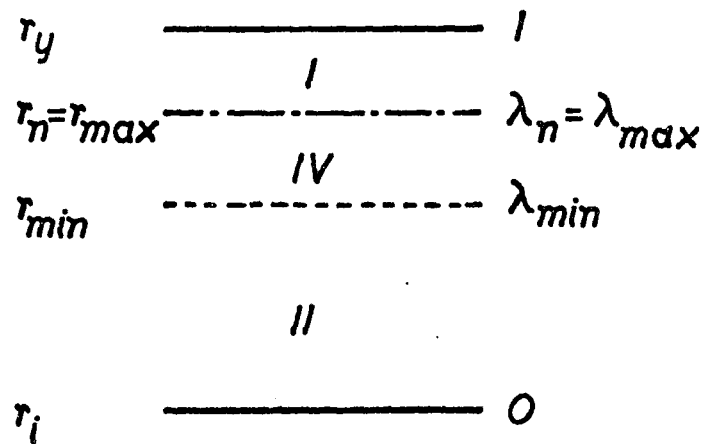


fig VII.9

	GAMMA=2./SQRT(3.)*C	A	51
C	STARTING POINT FOR THE INTEGRATION IS THE UNBEND CONDITION .	A	52
C		A	53
C	KAPPA=0.	A	54
	ETA=1.	A	55
	RHO=1.	A	56
C		A	57
C	CALCULATION OF THE ORIGINAL NEUTRAL LAYER .	A	58
C		A	59
	TEST=A*MU-C*(1.-MU)	A	60
	IF (TEST) 1,2,3	A	61
1	LN=.5+MU/2.-A*MU*.5/C	A	62
	GO TO 4	A	63
2	LN=MU	A	64
	GO TO 4	A	65
3	LN=MU/2.+C*(1.-MU)*.5/A	A	66
4	LO=LN	A	67
	IF (MU.LT.LN) ICASE=1	A	68
	IF (MU.GE.LO) ICASE=3	A	69
	WRITE (6,20)	A	70
	WRITE (6,21) A,C,MU,LO,ICASE	A	71
	GO TO (5,6,6), ICASE	A	72
5	KAPPAT=TRANS(ALFA,GAMMA,MU)	A	73
	WRITE (6,22) KAPPAT	A	74
6	WRITE (6,23)	A	75
	WRITE (6,24) KAPPA,ETA,RHO,ICASE,LO,LN	A	76
	N=2./DK-1.	A	77
C		A	78
C	INTEGRATION USING RUNGE-KUTTA METHOD .	A	79
C	STEPSIZE FOR KAPPA IS DK .	A	80
C		A	81
	DO 16 I=1,N	A	82
	IF (I.EQ.1) GO TO 7	A	83
	DE1=DK*DETA(KAPPA,ETA,ALFA,GAMMA,MU,ICASE)	A	84
	GO TO 8	A	85
7	DE1=0.	A	86
8	K1=KAPPA+DK/2.	A	87
	GO TO (9,10,10), ICASE	A	88
9	IF (K1.GT.KAPPAT) ICASE=2	A	89
10	E1=ETA+DE1/2.	A	90
	DE2=DK*DETA(K1,E1,ALFA,GAMMA,MU,ICASE)	A	91
	K2=K1	A	92
	E2=ETA+DE2/2.	A	93
	DE3=DK*DETA(K2,E2,ALFA,GAMMA,MU,ICASE)	A	94
	K3=KAPPA+DK	A	95
	GO TO (11,12,12), ICASE	A	96
11	IF (K3.GT.KAPPAT) ICASE=2	A	97
12	E3=ETA+DE3	A	98
	DE4=DK*DETA(K3,E3,ALFA,GAMMA,MU,ICASE)	A	99
		A	100

	DE=(DE1+DE4)/6.+(DE2+DE3)/3.	A	101
C	NEW VALUES FOR KAPPA,ETA,RHO .	A	102
C	KAPPA=KAPPA+DK	A	103
	ETA=ETA+DE	A	104
	RHO=RHO0(KAPPA,ETA,ALFA,GAMMA,MU,ICASE)	A	105
C		A	106
C	CALCULATION OF GEOMETRICAL SITUATION FOR THE CURRENT VALUE OF	A	107
C	KAPPA	A	108
	LO=(ETA**2-(1.-KAPPA*.5)**2)/(2.*KAPPA)	A	109
	GO TO (14,13,14), ICASE	A	110
13	IF (LO.LE.MU) ICASE=3	A	111
14	LN=(RHO**2*ETA**2-(1.-KAPPA*.5)**2)/(2.*KAPPA)	A	112
	RI=(1.-KAPPA*.5)*ETA*TO/KAPPA	A	113
	RY=(1.+KAPPA*.5)*ETA*TO/KAPPA	A	114
	RN=RHO*ETA**2*TO/KAPPA	A	115
	RM=ETA*TO/KAPPA	A	116
	RO=ETA**2*TO/KAPPA	A	117
	RB=ETA*TO/KAPPA*SQRT((1.-KAPPA*.5)**2+2.*MU*KAPPA)	A	118
	RATIO=(RB-RI)/(RY-RI)	A	119
	CALL MOM2 (XMOM)	A	120
	XMOM=XMOM/(TO**2)	A	121
	YMOM=XMOM/(ETA**2)	A	122
	XI=I	A	123
	X=XI/5.	A	124
	Y=XI/10.	A	125
	JX=X	A	126
	JY=Y	A	127
	J=JX*5	A	128
	JJ=JY*10	A	129
	IF (I.EQ.J) WRITE (6,21) A,G,MU	A	130
	IF (I.EQ.J) WRITE (6,23)	A	131
	WRITE (6,24) KAPPA,ETA,RHO,ICASE,LO,LN,RI,RY,RN,RO,RB,RATIO	A	132
	WRITE (6,25) XMOM,YMOM	A	133
C		A	134
C	WE DETERMINE THE STRESSDISTRIBUTION WHEN KAPPA IS .1 OR .2 OR .5	A	135
C	OR 1.	A	136
		A	137
	IF ((KAPPA.GT..0999).AND.(KAPPA.LT..1001)) CALL STRESS2 (SR1,ST1)	A	138
	IF ((KAPPA.GT..1999).AND.(KAPPA.LT..2001)) CALL STRESS2 (SR2,ST2)	A	139
	IF ((KAPPA.GT..4999).AND.(KAPPA.LT..5001)) CALL STRESS2 (SR5,ST5)	A	140
	IF ((KAPPA.GT..9999).AND.(KAPPA.LT.1.0001)) CALL STRESS2 (SR10,ST1	A	141
10)		A	142
		A	143
C		A	144
C	WE PLOT THE RELATIVE POSITIONS OF ORIGINALLY EQUIDISTANT LAYERS	A	145
C	WHEN KAPPA IS A MULTIPLE OF .1 .	A	146
		A	147
		A	148
	IF (I.EQ.JJ) GO TO 15	A	149
		A	150

	GO TO 16	A	151
15	TA(JY)=RB-RI	A	152
	TB(JY)=RY-RB	A	153
	XM(JY)=XMOM	A	154
	YM(JY)=YMOM	A	155
	PNUL=0.	A	156
	P1=RM*SQRT((1.-KAPPA*.5)**2+2.*.1*KAPPA)-RI	A	157
	P2=RM*SQRT((1.-KAPPA*.5)**2+2.*.2*KAPPA)-RI	A	158
	P3=RM*SQRT((1.-KAPPA*.5)**2+2.*.3*KAPPA)-RI	A	159
	P4=RM*SQRT((1.-KAPPA*.5)**2+2.*.4*KAPPA)-RI	A	160
	P5=RM*SQRT((1.-KAPPA*.5)**2+2.*.5*KAPPA)-RI	A	161
	P6=RM*SQRT((1.-KAPPA*.5)**2+2.*.6*KAPPA)-RI	A	162
	P7=RM*SQRT((1.-KAPPA*.5)**2+2.*.7*KAPPA)-RI	A	163
	P8=RM*SQRT((1.-KAPPA*.5)**2+2.*.8*KAPPA)-RI	A	164
	P9=RM*SQRT((1.-KAPPA*.5)**2+2.*.9*KAPPA)-RI	A	165
	P10=ETA*TO	A	166
	PO=RO-RI	A	167
	PN=RN-RI	A	168
	PB=RB-RI	A	169
	CALL PLOTPT (KAPPA,PNUL,10)	A	170
	CALL PLOTPT (KAPPA,P1,11)	A	171
	CALL PLOTPT (KAPPA,P2,12)	A	172
	CALL PLOTPT (KAPPA,P3,13)	A	173
	CALL PLOTPT (KAPPA,P4,14)	A	174
	CALL PLOTPT (KAPPA,P5,15)	A	175
	CALL PLOTPT (KAPPA,P6,16)	A	176
	CALL PLOTPT (KAPPA,P7,17)	A	177
	CALL PLOTPT (KAPPA,P8,18)	A	178
	CALL PLOTPT (KAPPA,P9,19)	A	179
	CALL PLOTPT (KAPPA,P10,20)	A	180
	CALL PLOTPT (KAPPA,PO,35)	A	181
	CALL PLOTPT (KAPPA,PN,34)	A	182
	CALL PLOTPT (KAPPA,PB,22)	A	183
16	CONTINUE	A	184
	CALL OUTPLT	A	185
	KAPPA=0.	A	186
	ETAA=1.	A	187
	ETAB=1.	A	188
	DK=.1	A	189
	TAO=MU*TO	A	190
	TBO=(1.-MU)*TO	A	191
	CALL PLOTPT (KAPPA,TAO,21)	A	192
	CALL PLOTPT (KAPPA,TBO,22)	A	193
	WRITE (6,27)	A	194
	WRITE (6,26) KAPPA,TAO,TBO,ETAA,ETAB	A	195
	DO 17 I=1,19	A	196
	KAPPA=KAPPA+DK	A	197
	ETAA=TA(I)/TAO	A	198
	ETAB=TB(I)/TBO	A	199
	WRITE (6,26) KAPPA,TA(I),TB(I),ETAA,ETAB	A	200

```
CALL PLOTPT (KAPPA,TA(I),21)
CALL PLOTPT (KAPPA,TB(I),22)
CALL PLOTPT (KAPPA,ETAA,21)
CALL PLOTPT (KAPPA,ETAB,22)
17 CALL PLOTPT (KAPPA,0.,10)
CONTINUE
CALL OUTPLT
C
C C PLOT THE STRESS DISTRIBUTION IN THE BEND SHEET .
C C STRESSES FOR KAPPA=.1 ARE PLOTTED WITH THE SYMBOL 1 .
C C STRESSES FOR KAPPA=.2 ARE PLOTTED WITH THE SYMBOL 2 .
C C STRESSES FOR KAPPA=.5 ARE PLOTTED WITH THE SYMBOL 5 .
C C STRESSES FOR KAPPA=1. ARE PLOTTED WITH THE SYMBOL $ .
C
DO 18 I=1,21
X=I-1
X=X/20.
CALL PLOTPT (X,SR1(I),11)
CALL PLOTPT (X,ST1(I),11)
CALL PLOTPT (X,SR2(I),12)
CALL PLOTPT (X,ST2(I),12)
CALL PLOTPT (X,SR5(I),15)
CALL PLOTPT (X,ST5(I),15)
CALL PLOTPT (X,SR10(I),20)
CALL PLOTPT (X,ST10(I),20)
18 CONTINUE
CALL OUTPLT
C
C C PLOT THE BENDING MOMENT .
C C XM=MOMENT PER UNIT WIDTH / SQUARE OF ORIGINAL SHEET THICKNESS .
C C XM IS PLOTTED WITH THE SYMBOL M .
C C YM = MOMENT PER UNIT WITH / SQUARE OF CURRENT SHEET THICKNESS .
C C YM IS PLOTTED WITH THE SYMBOL W .
C
KAPPA=0.
DK=.1
DO 19 I=1,19
KAPPA=KAPPA+DK
CALL PLOTPT (KAPPA,XM(I),33)
CALL PLOTPT (KAPPA,YM(I),43)
19 CONTINUE
CALL PLOTPT (0.,0.,10)
CALL PLOTPT (2.,0.,10)
CALL OUTPLT
STOP
C
20 FORMAT (1H1,*BINSH BINSH BINSH BINSH BINSH *,/
1)
21 FORMAT (1H ,*A=*,E13.5,/,1H ,*C=*,E13.5,/,1H ,*MU=*,E13.5,/,1H ,*L
10=*,E13.5,/,1H ,*ICASE=*,I2,/)
A 201
A 202
A 203
A 204
A 205
A 206
A 207
A 208
A 209
A 210
A 211
A 212
A 213
A 214
A 215
A 216
A 217
A 218
A 219
A 220
A 221
A 222
A 223
A 224
A 225
A 226
A 227
A 228
A 229
A 230
A 231
A 232
A 233
A 234
A 235
A 236
A 237
A 238
A 239
A 240
A 241
A 242
A 243
A 244
A 245
A 246
A 247
A 248
A 249
A 250
```



```

22 FORMAT (1H ,*KAPPAT=*,E13.5,/)
23 FORMAT (1H ,*KAPPA*,8X,*ETA*,10X,*RHO*,8X,*ICASE*,* LO*,7X,*LN*,9X
1,*RI*,9X,*RY*,9X,*RN*,9X,*RO*,9X,*RB*,9X,*RATIO*,/)
24 FORMAT (1H ,3F13.9,I2,8F11.7,/)
25 FORMAT (1H ,*XMOM=*,F13.7,5X,*YMOM=*,F13.7)
26 FORMAT (1H ,5E11.3)
27 FORMAT (1H ,*KAPPA*,6X,*TA*,9X,*TB*,9X,*ETAA*,7X,*ETAB*,/,)
END

```

```

FUNCTION ETARHO2 (KAPPA,ALFA,GAMMA,MU,ICASE)
REAL KAPPA,MU
C
C FUNCTION ETARHO2 CALCULATES (ETA*RHO)**2 FOR THE BENDING OF A
C BIMETAL
C STRIP COMPOSED OF NONSTRAINHARDENING LAMINAE .
C ETARHO2 IS TO BE USED WITH THE MAIN PROGRAM BINSH .
C
GO TO (1,2,2), ICASE
1 X=ALOG (1.+5*KAPPA)+ALFA/GAMMA*ALOG (1.-.5*KAPPA)+(1.-ALFA/GAMMA)*
15*ALOG ((1.-.5*KAPPA)**2+2.*MU*KAPPA)
GO TO 3
2 X=GAMMA/ALFA*ALOG (1.+5*KAPPA)+ALOG (1.-.5*KAPPA)+(1.-GAMMA/ALFA)*
15*ALOG ((1.-.5*KAPPA)**2+2.*MU*KAPPA)
GO TO 3
3 ETARHO2=EXP(X)
RETURN
END

```

```

FUNCTION TRANS (ALFA,GAMMA,MU)
REAL MU
C
C F(X)=(1.-X*.5)**(2.*ALFA/(ALFA+GAMMA))*(1.+X*.5)**(2.*GAMMA/(ALFA+
1GAMMA))- (1.-X*.5)**2-2.*MU*X
C D(X)=-ALFA/(ALFA+GAMMA)*(1.-X*.5)**((ALFA-GAMMA)/(ALFA+GAMMA))*(1.
1+X*.5)**(2.*GAMMA/(ALFA+GAMMA))+GAMMA/(ALFA+GAMMA)*(1.+5*X)**((GA
2MMA-ALFA)/(ALFA+GAMMA))*(1.-X*.5)**(2.*ALFA/(ALFA+GAMMA))+ (1.-X*.5
3)-2.*MU
C
C FUNCTION TRANS DETERMINES THE VALUE OF THE RELATIVE
C CURVATURE FOR WHICH THE NEUTRAL LAYER COINCIDES WITH THE
C LAMINATE BOUNDARY LAYER.
C TRANS IS USED BY BINSH
C
X=1.5
DO 1 I=1,50
X1=X-F(X)/D(X)
IF (X1.LT.0.) X1=1.
IF (X1.GE.2.) X1=1.9999
IF (X-X1.LT..000001) GO TO 2

```

	X=X1	C	21
1	CONTINUE	C	22
2	TRANS=X1	C	23
	RETURN	C	24
	END	C	25
	 SUBROUTINE SIGMAR2 (R,SR)	D	1
	REAL KAPPA,LO,LN,MU	D	2
	COMMON /STATE/ KAPPA,ETA,RHO,LO,LN,RI,RY,RN,RO,RM,RB,ICASE	D	3
	COMMON /SSCURV/ ALFA,GAMMA,MU	D	4
C		D	5
C	SUBROUTINE SIGMAR2 CALCULATES THE RADIAL STRESS FOR THE BENDING OF	D	6
C	A BIMETAL STRIP COMPOSED OF NONSTRAINHARDENING LAMINAE .	D	7
C	SIGMAR2 IS TO BE USED WITH THE MAIN PROGRAM BINSH .	D	8
		D	9
	IZONE=3	D	10
	GO TO (1,2,2), ICASE	D	11
1	IF (R.GE.RN) IZONE=1	D	12
	IF (R.LE.RB) IZONE=2	D	13
	GO TO (3,4,5), IZONE	D	14
2	IF (R.GE.RB) IZONE=1	D	15
	IF (R.LE.RN) IZONE=2	D	16
	GO TO (3,4,6), IZONE	D	17
3	SR=GAMMA*ALOG(R/RY)	D	18
	GO TO 7	D	19
4	SR=-ALFA*ALOG(R/RI)	D	20
	GO TO 7	D	21
5	SR=-ALFA*ALOG(RB/RI)-GAMMA*ALOG(R/RB)	D	22
	GO TO 7	D	23
6	SR=ALFA*ALOG(R/RB)+GAMMA*ALOG(RB/RY)	D	24
7	RETURN	D	25
	END	D	26
	 SUBROUTINE SIGMAT2 (R,SR,ST)	F	1
	REAL KAPPA,LO,LN,MU	F	2
	COMMON /STATE/ KAPPA,ETA,RHO,LO,LN,RI,RY,RN,RO,RM,RB,ICASE	F	3
	COMMON /SSCURV/ ALFA,GAMMA,MU	F	4
C		F	5
C	SUBROUTINE SIGMAT2 CALCULATES THE TANGENTIAL STRESS FOR THE	F	6
C	BENDING OF	F	7
C	A BIMETAL STRIP COMPOSED OF NONSTRAINHARDENING LAMINAE .	F	8
C	SIGMAT2 IS TO BE USED WITH THE MAIN PROGRAM BINSH .	F	9
		F	10
	CALL SIGMAR2 (R,SR)	F	11
	IZONE=3	F	12
	GO TO (1,2,2), ICASE	F	13
1	IF (R.GE.RN) IZONE=1	F	14
	IF (R.LE.RB) IZONE=2	F	15

	GO TO (3,4,5), IZONE	F	16
2	IF (R.GE.RB) IZONE=1	F	17
	IF (R.LE.RN) IZONE=2	F	18
	GO TO (3,4,6), IZONE	F	19
3	ST=SR+GAMMA	F	20
	GO TO 7	F	21
4	ST=SR-ALFA	F	22
	GO TO 7	F	23
5	ST=SR-GAMMA	F	24
	GO TO 7	F	25
6	ST=SR+ALFA	F	26
7	RETURN	F	27
	END	F	28

SUBROUTINE STRESS2 (SRN,STN)

REAL KAPPA,LO,LN,MU

DIMENSION SRN(21), STN(21)

COMMON /STATE/ KAPPA,ETA,RHO,LO,LN,RI,RY,RN,RO, RM, RB, ICASE

COMMON /SSCURV/ ALFA,GAMMA,MU

C
C
C
C
C

SUBROUTINE STRESS2 CALCULATES THE STRESSES FOR THE BENDING OF A
BIMETAL
STRIP COMPOSED OF NONSTRAINHARDENING LAMINAE .
STRESS2 IS TO BE USED WITH THE MAIN PROGRAM BINSH .

DR=(RY-RI)/20.

R=RI

DO 1 I=1,21

CALL SIGMAT2 (R,SRN(I),STN(I))

R=R+DR

1

CONTINUE

RETURN

END

SUBROUTINE MOM2 (XMOM)

REAL KAPPA,LO,LN,MU

COMMON /STATE/ KAPPA,ETA,RHO,LO,LN,RI,RY,RN,RO, RM, RB, ICASE

COMMON /SSCURV/ ALFA,GAMMA,MU

C
C
C
C

SUBROUTINE MOM2 CALCULATES THE BENDING MOMENT PER UNIT WIDTH FOR A
BIMETAL STRIP COMPOSED OF NONSTRAINHARDENING LAMINAE .
MOM2 IS TO BE USED WITH THE MAIN PROGRAM BINSH .

GO TO (1,2,2), ICASE

$$XMOM = GAMMA/4 * (RY**2 + RB**2) + ALFA/4 * (RI**2 - RB**2) - ALFA/2 * (RN**2) *$$

$$1 \text{ALOG}(RB/RI) - GAMMA/2 * (RN**2) * (1 + \text{ALOG}(RN/RY) + \text{ALOG}(RN/RB))$$

1

GO TO 3

2

$$XMOM = GAMMA/4 * (RY**2 - RB**2) + ALFA/4 * (RI**2 + RB**2) - GAMMA/2 * (RN**2)$$

F	1
F	2
F	3
F	4
F	5
F	6
F	7
F	8
F	9
F	10
F	11
F	12
F	13
F	14
F	15
F	16
F	17
F	18
F	19

G	1
G	2
G	3
G	4
G	5
G	6
G	7
G	8
G	9
G	10
G	11
G	12
G	13
G	14

3 1*ALOG(RB/RY)-ALFA/2.*(RN**2)*(1.+ALOG(RN/RI)+ALOG(RN/RB))
RETURN
END

G 15
G 16
G 17-

```

PROGRAM TRINSH(INPUT,OUTPUT,PUNCH,TAPE5=INPUT,TAPE6=OUTPUT,TAPE7=P
1UNCH)
INTEGER PROGRAM
REAL KAPPA,KAPPA1,KAPPA2,KAPPA3,LN,LO,LNNEW,MU,LETA
DIMENSION P(3)
DIMENSION BEPS(4)
DIMENSION A(3),T(3),TTO(3),LETA(3)
DIMENSION SIGMAL(4),TEST(4)
DIMENSION SR1(21),SR2(21),SR5(21),SR10(21)
DIMENSION ST1(21),ST2(21),ST5(21),ST10(21)
DIMENSION XM(20),YM(20)
COMMON /SSCURV/ NLT,ALFA(3),MU(3,2),TO
COMMON /STATE/ KAPPA,ETA,RHO,LN,RI,RN,RY,RB(4)

```

```

PROGRAM TRINSH ON 09/10/72 .
PROGRAM TRINSH DETERMINES THE BEHAVIOUR IN PURE PLAIN STRAIN
BENDING
OF A LAMINATED STRIP COMPOSED OF NLT NONSTRAINHARDENING LAMINAE .

```

```

TRINSH USES DETA,FINDLN,RADSTR,RSTRES,SIGMAT8,STRESS8,MOM8.

```

INPUT DATA

```

NLT      THE NUMBER OF LAYERS IN THE STRIP .
A(I)    IS THE EFFECTIVE YIELD STRESS FOR THE LAYER I .
        WE COUNT THE LAYERS FROM THE INSIDE OF THE BEND .
MU(I,1) IS THE INNERMOST LAMBDA VALUE FOR LAYER I .
MU(I,2) IS THE OUTERMOST LAMBDA VALUE FOR LAYER I .
TO      IS THE STRIP THICKNESS .
DK      IS THE STEPSIZE FOR THE NUMERICAL INTEGRATION OF
        THE SHEET THICKNESS DIFFERENTIAL EQUATION .

ETA      RELATIVE SHEET THICKNESS = RATIO OF CURRENT SHEET
THICKNES TO ORIGINAL SHEET THICKNESS
RHO      RATIO OF CURRENT NEUTRAL LAYER RADIUS TO CURRENT
        UNELONGATED LAYER RADIUS
LN       CURRENT VALUE OF LAMBDA OF THE NEUTRAL LAYER
LO       CURRENT VALUE OF LAMBDA OF THE UNELONGATED LAYER
RM       THE CURRENT AVERAGE RADIUS OF THE BEND STRIP
RI       THE CURRENT INSIDE RADIUS
RY       THE CURRENT OUTSIDE RADIUS
RB(I)    THE CURRENT RADIUS OF THE OUTSIDE SURFACE OF LAMINATE I
        (EVENTUALLY MINUS RI)
RN       CURRENT NEUTRAL LAYER RADIUS
RO       CURRENT UNELONGATED LAYER RADIUS
LETA(I)  CURRENT RELATIVE THICKNESS OF LAMINATE I , I.E. THE
        RATIO OF CURRENT LAMINATE THICKNESS TO ORIGINAL LAMINATE
        THICKNESS
XMOM     CURRENT BENDING MOMENT DIVIDED BY THE SQUARE OF THE
        ORIGINAL SHEET THICKNESS

```

CCCCCCCCCCCCCCCCCCCC

1
2
3
4
5
6
7
8
9
10
11
12
13
14
15
16
17
18
19
20
21
22
23
24
25
26
27
28
29
30
31
32
33
34
35
36
37
38
39
40
41
42
43
44
45
46
47
48
49
50

C	Y MOM	CURRENT BENDING MOMENT DIVIDED BY THE SQUARE OF THE	A	51
C		CURRENT SHEET THICKNESS	A	52
			A	53
	DATA PROGRAM/7HTRINSH /		A	54
	DATA TO,DK/1.,.01/		A	55
	DATA NLT,A(1),A(2),A(3)/3,4.,1.,4./		A	56
	DATA MU(2,1),MU(3,1)/.20,.60/		A	57
	MU(1,1)=0.		A	58
	DO 1 I=2,NLT		A	59
	MU(I-1,2)=MU(I,1)		A	60
1	CONTINUE		A	61
	MU(NLT,2)=1.		A	62
	DO 2 I=1,NLT		A	63
	LETA(I)=1.		A	64
	TTO(I)=(MU(I,2)-MU(I,1))*TO		A	65
	ALFA(I)=2./SQRT(3.)*A(I)		A	66
2	CONTINUE		A	67
C			A	68
C		STARTING POINT FOR INTEGRATION IS THE UNBEND CONDITION .	A	69
			A	70
	KAPPA=0.		A	71
	ETA=1.		A	72
	RHO=1.		A	73
C			A	74
C		CALCULATION OF THE ORIGINAL NEUTRAL LAYER .	A	75
			A	76
	SIGMAL(1)=0.		A	77
	DO 3 I=1,NLT		A	78
	J=I+1		A	79
3	SIGMAL(J)=SIGMAL(I)+ALFA(I)*(MU(I,2)-MU(I,1))		A	80
	CONTINUE		A	81
	TEST(1)=SIGMAL(NLT+1)		A	82
	DO 4 I=1,NLT		A	83
	J=I+1		A	84
	TEST(J)=TEST(1)-SIGMAL(J)*2.		A	85
	IF (TEST(J).EQ.0.) GO TO 5		A	86
	W=TEST(J)*TEST(J-1)		A	87
	IF (W.LT.0.) GO TO 6		A	88
4	CONTINUE		A	89
5	LN=MU(J,1)		A	90
	GO TO 7		A	91
6	LN=(TEST(J-1)*MU(J-1,2)-TEST(J)*MU(J-1,1))/(TEST(J-1)-TEST(J))		A	92
	GO TO 7		A	93
7	LO=LN		A	94
C			A	95
C		CALCULATION OF THE INITIAL BENDING MOMENT .	A	96
			A	97
	SIGN=-1.		A	98
	M=0		A	99
	XMOM=0.		A	100

```

DO 9 K=1,NLT
IF ((MU(K,2).GT.LN).AND.(M.EQ.0)) GO TO 8
XMOM=ALFA(K)/2.*SIGN*(MU(K,2)**2-MU(K,1)**2)+XMOM
GO TO 9
8 XMOM=ALFA(K)/2.*SIGN*(LN**2-MU(K,1)**2)+XMOM
SIGN=+1.
M=1
XMOM=ALFA(K)/2.*SIGN*(MU(K,2)**2-LN**2)+XMOM
9 CONTINUE
YMOM=XMOM
XM(1)=XMOM
YM(1)=YMOM
WRITE (6,24)
DO 10 I=1,NLT
J=0
C WRITE (7,701) J,PROGRAM,NLT,I,DK,A(I),MU(I,1),MU(I,2)
WRITE (6,25) I,A(I),MU(I,1),MU(I,2)
10 CONTINUE
WRITE (6,26) TO,DK
WRITE (6,27)
INDEX=1
WRITE (6,28) INDEX,NLT,KAPPA,ETA,RHO,LN,LO,XMOM,YMOM,(LETA(K),K=1,
1 NLT)
C WRITE (7,702) INDEX,NLT,KAPPA,ETA,LN,RHO,XMOM
XN=(1./DK)/10.
IF (XN.LT.1.) XN=1.
N=1999
IF (DK.GT..001) N=2./DK-1.
C
C C INTEGRATION USING RUNGE-KUTTA METHOD . STEPSIZE FOR KAPPA IS DK .
C
DO 16 I=1,N
IF (I.EQ.1) GO TO 11
DE1=DK*DETA(KAPPA,ETA,LN)
GO TO 12
11 DE1=0.
12 KAPPA1=KAPPA+DK/2.
ETA1=ETA+DE1/2.
CALL FINDLN (KAPPA1,ETA1,LN,LNNEW)
DE2=DK*DETA(KAPPA1,ETA1,LNNEW)
KAPPA2=KAPPA1
ETA2=ETA+DE2/2.
CALL FINDLN (KAPPA2,ETA2,LN,LNNEW)
DE3=DK*DETA(KAPPA2,ETA2,LNNEW)
KAPPA3=KAPPA2
ETA3=ETA+DE3
CALL FINDLN (KAPPA3,ETA3,LN,LNNEW)
DE4=DK*DETA(KAPPA3,ETA3,LNNEW)
DE=(DE1+DE4)/6.+(DE2+DE3)/3.
C

```

```

A 101
A 102
A 103
A 104
A 105
A 106
A 107
A 108
A 109
A 110
A 111
A 112
A 113
A 114
A 115
A 116
A 117
A 118
A 119
A 120
A 121
A 122
A 123
A 124
A 125
A 126
A 127
A 128
A 129
A 130
A 131
A 132
A 133
A 134
A 135
A 136
A 137
A 138
A 139
A 140
A 141
A 142
A 143
A 144
A 145
A 146
A 147
A 148
A 149
A 150

```


C	NEW VALUES FOR KAPPA,ETA LN,RHO	A	151
C	KAPPA=KAPPA+DK	A	152
	ETA=ETA+DE	A	153
	CALL FINDLN (KAPPA,ETA,LN,LNNEW)	A	154
	LN=LNNEW	A	155
	RHO=SQRT((1.-.5*KAPPA)**2+2.*KAPPA*LN)/ETA	A	156
C	GEOMETRICAL CONFIGURATION OF THE CURRENT BEND .	A	157
C	RM=ETA*TO/KAPPA	A	158
	RI=RM*(1.-KAPPA*.5)	A	159
	RY=RM*(1.+KAPPA*.5)	A	160
	RN=RM*RHO*ETA	A	161
	RO=RM*ETA	A	162
	LO=(ETA**2-(1.-KAPPA*.5)**2)/(2.*KAPPA)	A	163
	RB(1)=RI	A	164
	BEPS(1)=ALOG(RI/RO)	A	165
	DO 13 K=1,NLT	A	166
	M=K+1	A	167
	RB(M)=RM*SQRT((1.-KAPPA*.5)**2+2.*MU(K,2)*KAPPA)	A	168
	BEPS(M)=ALOG(RB(M)/RO)	A	169
	T(K)=RB(M)-RB(K)	A	170
	P(K)=RB(M)-RI	A	171
	LETA(K)=T(K)/TTO(K)	A	172
13	CONTINUE	A	173
	R1=RM*SQRT((1.-KAPPA*.5)**2+2.*.1*KAPPA)	A	174
	R2=RM*SQRT((1.-KAPPA*.5)**2+2.*.2*KAPPA)	A	175
	R3=RM*SQRT((1.-KAPPA*.5)**2+2.*.3*KAPPA)	A	176
	R4=RM*SQRT((1.-KAPPA*.5)**2+2.*.4*KAPPA)	A	177
	R5=RM*SQRT((1.-KAPPA*.5)**2+2.*.5*KAPPA)	A	178
	R6=RM*SQRT((1.-KAPPA*.5)**2+2.*.6*KAPPA)	A	179
	R7=RM*SQRT((1.-KAPPA*.5)**2+2.*.7*KAPPA)	A	180
	R8=RM*SQRT((1.-KAPPA*.5)**2+2.*.8*KAPPA)	A	181
	R9=RM*SQRT((1.-KAPPA*.5)**2+2.*.9*KAPPA)	A	182
	P1=R1-RI	A	183
	P2=R2-RI	A	184
	P3=R3-RI	A	185
	P4=R4-RI	A	186
	P5=R5-RI	A	187
	P6=R6-RI	A	188
	P7=R7-RI	A	189
	P8=R8-RI	A	190
	P9=R9-RI	A	191
	P0=R0-RI	A	192
	PN=RN-RI	A	193
	EI=ALOG(RI/RO)	A	194
	E1=ALOG(R1/RO)	A	195
	E2=ALOG(R2/RO)	A	196
	E3=ALOG(R3/RO)	A	197
		A	198
		A	199
		A	200

	E4=ALOG(R4/R0)	A	201
	E5=ALOG(R5/R0)	A	202
	E6=ALOG(R6/R0)	A	203
	E7=ALOG(R7/R0)	A	204
	E8=ALOG(R8/R0)	A	205
	E9=ALOG(R9/R0)	A	206
	EY=ALOG(RY/R0)	A	207
	EPSN=ALOG(RN/R0)	A	208
C		A	209
C	CALCULATION OF THE BENDING MOMENT .	A	210
C		A	211
	CALL MOM8 (XMCM)	A	212
	XMOM=XMOM/(TO**2)	A	213
	YMOM=XMOM/(ETA**2)	A	214
C		A	215
C	WE DETERMINE THE RADIAL AND TANGENTIAL STRESS DISTRIBUTION WHEN	A	216
C	KAPPA IS .1 OR .2 OR .5 OR 1. .	A	217
		A	218
	IF ((KAPPA.GT..0999).AND.(KAPPA.LT..1001)) CALL STRESS8 (SR1,ST1)	A	219
	IF ((KAPPA.GT..1999).AND.(KAPPA.LT..2001)) CALL STRESS8 (SR2,ST2)	A	220
	IF ((KAPPA.GT..4999).AND.(KAPPA.LT..5001)) CALL STRESS8 (SR5,ST5)	A	221
	IF ((KAPPA.GT..9999).AND.(KAPPA.LT.1.0001)) CALL STRESS8 (SR10,ST1	A	222
10)		A	223
	XI=I	A	224
	X=XI/5.	A	225
	Y=XI/XN	A	226
	JX=X	A	227
	JY=Y	A	228
	J=JX*5	A	229
	JJ=JY*10	A	230
	IF (I.EQ.J) WRITE (6,29)	A	231
	IF (I.EQ.J) WRITE (6,27)	A	232
	INDEX=I+1	A	233
	WRITE (6,28) INDEX,NLT,KAPPA,ETA,RHO,LN,LO,XMOM,YMOM,(LETA(K),K=1,	A	234
1	NLT)	A	235
	WRITE (6,19) P1,P2,P3,P4,P5,P6,P7,P8,P9,(P(K),K=1,NLT)	A	236
	WRITE (6,20) PN,PO	A	237
	WRITE (6,21) EI,E1,E2,E3,E4,E5,E6,E7,E8,E9,EY	A	238
	WRITE (6,22) (BEPS(K),K=1,NLT),EY	A	239
	WRITE (6,23) EPSN	A	240
C	WRITE(7,702)INDEX,NLT,KAPPA,ETA,LN,RHO,XMOM	A	241
	IF (I.EQ.JJ) GO TO 14	A	242
	GO TO 16	A	243
14	CONTINUE	A	244
	XM(JY+1)=XMOM	A	245
	YM(JY+1)=YMOM	A	246
	DO 15 K=1,NLT	A	247
	J=K+9	A	248
	RB(K)=RB(K)-RI	A	249
	CALL PLOTPT (KAPPA,RB(K),J)	A	250

15	CONTINUE	A	251
	CALL PLOTPT (KAPPA,ETA,25)	A	252
	RN=RN-RI	A	253
	CALL PLOTPT (KAPPA,RN,34)	A	254
	CALL PLOTPT (KAPPA,RHO,38)	A	255
16	CONTINUE	A	256
	CALL OUTPLT	A	257
C		A	258
C	PLOT THE STRESS DISTRIBUTION IN THE BEND SHEET .	A	259
C	STRESSES FOR KAPPA=.1 ARE PLOTTED WITH THE SYMBOL 1 .	A	260
C	STRESSES FOR KAPPA=.2 ARE PLOTTED WITH THE SYMBOL 2 .	A	261
C	STRESSES FOR KAPPA=.5 ARE PLOTTED WITH THE SYMBOL 5 .	A	262
C	STRESSES FOR KAPPA=1. ARE PLOTTED WITH THE SYMBOL \$.	A	263
C		A	264
	DO 17 I=1,21	A	265
	X=I-1	A	266
	X=X/20.	A	267
	CALL PLOTPT (X,SR1(I),11)	A	268
	CALL PLOTPT (X,ST1(I),11)	A	269
	CALL PLOTPT (X,SR2(I),12)	A	270
	CALL PLOTPT (X,ST2(I),12)	A	271
	CALL PLOTPT (X,SR5(I),15)	A	272
	CALL PLOTPT (X,ST5(I),15)	A	273
	CALL PLOTPT (X,SR10(I),20)	A	274
	CALL PLOTPT (X,ST10(I),20)	A	275
17	CONTINUE	A	276
	CALL OUTPLT	A	277
C		A	278
C	PLOT THE BENDING MOMENT .	A	279
C	XM=MOMENT PER UNIT WIDTH / SQUARE OF ORIGINAL SHEET THICKNESS .	A	280
C	XM IS PLOTTED WITH THE SYMBOL M .	A	281
C	YM = MOMENT PER UNIT WITH / SQUARE OF CURRENT SHEET THICKNESS .	A	282
C	YM IS PLOTTED WITH THE SYMBOL W .	A	283
C		A	284
	KAPPA=0.	A	285
	DK=.1	A	286
	DO 18 I=1,20	A	287
	CALL PLOTPT (KAPPA,XM(I),33)	A	288
	CALL PLOTPT (KAPPA,YM(I),43)	A	289
	KAPPA=KAPPA+DK	A	290
18	CONTINUE	A	291
	CALL PLOTPT (0.,0.,10)	A	292
	CALL OUTPLT	A	293
	STOP	A	294
C		A	295
19	FORMAT (1H ,* LAYER MOVEMENT *,9F10.7,/,1H ,* BOUNDARY MOVEMENT	A	296
	1 *,9F10.7,/,)	A	297
20	FORMAT (1H ,*NEUTRAL LAYER AND UNELONGATED LAYER MOVEMENT*,6X,2F10	A	298
	1.7,/,)	A	299
21	FORMAT (1H ,*LAYER HOOP STRAIN *,11F10.7)	A	300

	COMP=.FALSE.	C	26
	XO=LNOLD	C	27
	S0=RADSTR(KAPPA,ETA,X0,TENS)-RADSTR(KAPPA,ETA,X0,COMP)	C	28
	X1=XO-1.E-06	C	29
	S1=RADSTR(KAPPA,ETA,X1,TENS)-RADSTR(KAPPA,ETA,X1,COMP)	C	30
	DO 1 I=1,50	C	31
	IF (S1.EQ.S0) GO TO 3	C	32
	X2=X1-S1*(X1-XO)/(S1-S0)	C	33
	S2=RADSTR(KAPPA,ETA,X2,TENS)-RADSTR(KAPPA,ETA,X2,COMP)	C	34
	IF (S2.LT.1.E-10) GO TO 2	C	35
	XO=X1	C	36
	S0=S1	C	37
	X1=X2	C	38
	S1=S2	C	39
1	CONTINUE	C	40
2	LNNEW=X2	C	41
	GO TO 4	C	42
3	LNNEW=(X1+XO)/2.	C	43
4	CONTINUE	C	44
	RETURN	C	45
	END	C	46
	FUNCTION RADSTR (KAPPA,ETA,LAMDA,TENS)	D	1
	REAL KAPPA,LAMDA,MU	D	2
	LOGICAL TENS	D	3
	COMMON /SSCURV/ NLT,ALFA(3),MU(3,2),TO	D	4
C		D	5
C	FUNCTION RADSTR CALCULATES THE RADIAL STRESS FOR THE LAYER LAMDA	D	6
C	BY INTEGRATING THE EQUILIBRIUM EQUATION .	D	7
C	KAPPA AND ETA ARE GIVEN VALUES .	D	8
C	WHEN TENS=.TRUE. , THE TANGENTIAL STRESS IS TENSILE , AND THE	D	9
C	BOUNDARY CONDITION IS \$ RADIAL STRESS IS ZERO AT OUTERMOST LAYER	D	10
C	(LAMBDA=1.) .	D	11
C	WHEN TENS=.FALSE. , THE TANGENTIAL STRESS IS COMPRESSIVE , AND THE	D	12
C	BOUNDARY CONDITION IS \$ RADIAL STRESS IS ZERO AT INNERMOST LAYER	D	13
C	(LAMBDA=0.) .	D	14
C	THE INTEGRATION MOVES FROM ONE MATERIAL BOUNDARY TO THE NEXT AS	D	15
C	MANY TIMES ES NEEDED TO REACH LAMDA FROM THE BOUNDARY CONDITION .	D	16
C		D	17
C	RADSTR IS USED BY TRINSH	D	18
C		D	19
	BS=0.	D	20
	IF (TENS) GO TO 4	D	21
	BL=0.	D	22
	DO 2 I=1,NLT	D	23
	X=MU(I,2)	D	24
	IF (X.LT.LAMDA) GO TO 1	D	25
	GO TO 3	D	26
1	SMU=RSTRES (KAPPA,ETA,MU(I,2),I,TENS,BL,BS)	D	27

	BL=MU(I,2)	D	28
	BS=SMU	D	29
2	CONTINUE	D	30
3	RADSTR=RSTRES(KAPPA,ETA,LAMDA,I,TENS,BL,BS)	D	31
	GO TO 8	D	32
4	BL=1.	D	33
	DO 6 I=1,NLT	D	34
	J=NLT-I+1	D	35
	X=MU(J,1)	D	36
	IF (X.GT.LAMDA) GO TO 5	D	37
	GO TO 7	D	38
5	SMU=RSTRES(KAPPA,ETA,MU(J,1),J,TENS,BL,BS)	D	39
	BL=MU(J,1)	D	40
	BS=SMU	D	41
6	CONTINUE	D	42
7	RADSTR=RSTRES(KAPPA,ETA,LAMDA,J,TENS,BL,BS)	D	43
	GO TO 8	D	44
8	CONTINUE	D	45
	RETURN	D	46
	END	D	47-

	FUNCTION RSTRES (KAPPA,ETA,LAMDA,MAT,TENS,BL,BS)	F	1
	REAL KAPPA,LAMDA,MU	F	2
	LOGICAL TENS	F	3
	COMMON /SSCURV/ NLT,ALFA(3),MU(3,2),TO	F	4
C		F	5
C	FUNCTION RSTRES GIVES THE VALUE OF THE RADIAL STRESS FOR LAYER	F	6
C	LAMDA IN MATERIAL MAT, SUBJECT TO BOUNDARY CONDITIONS BL AND BS .	F	7
C	WHEN LAMBDA=BL, RADSTR=BS	F	8
C	KAPPA AND ETA ARE GIVEN VALUES .	F	9
C	WHEN TENS=.TRUE., THE TANGENTIAL STRESS IS TENSILE .	F	10
C	WHEN TENS=.FALSE., THE TANGENTIAL STRESS IS COMPRESSIVE .	F	11
C		F	12
C	RSTRES IS USED BY TRINSH	F	13
		F	14
	SIGN=-1.	F	15
	IF (TENS) SIGN=+1.	F	16
	CONST=BS-SIGN*ALFA(MAT)*ALOG(ETA*TO/KAPPA*SQRT((1.-.5*KAPPA)**2+2.	F	17
1	*BL*KAPPA))	F	18
	RSTRES=CONST+SIGN*ALFA(MAT)*ALOG(ETA*TO/KAPPA*SQRT((1.-.5*KAPPA)**	F	19
12	+2.*LAMDA*KAPPA))	F	20
	RETURN	F	21
	END	F	22-

	SUBROUTINE SIGMAT8 (R,SR,ST,MAT)	F	1
	REAL LAMDA,KAPPA,LN,MU	F	2
	LOGICAL TENS	F	3
	COMMON /STATE/ KAPPA,ETA,RHO,LN,RI,RN,RY,RB(4)	F	4

	R=R+DR	G	27
2	CONTINUE	G	28
	WRITE (6,5)	G	29
	RETURN	G	30
C		G	31
3	FORMAT (1H ,*R = *,F12.7,* (R-RI) = *,F10.7,* SR = *,E15.7,* ST =	G	32
	1*,E15.7,)	G	33
4	FORMAT (1H1,*RADIAL AND TANGENTIAL STRESS DISTRIBUTION FOR KAPPA =	G	34
	1*,F10.7,/,/;)	G	35
5	FORMAT (1H1,/,)	G	36
	END	G	37-
	SUBROUTINE MOM8 (XMOM)	H	1
	REAL KAPPA,MU,LN	H	2
	LOGICAL TENS,COMP	H	3
	COMMON /STATE/ KAPPA,ETA,RHO,LN,RI,RN,RY,RB(4)	H	4
	COMMON /SSCURV/ NLT,ALFA(3),MU(3,2),TO	H	5
C		H	6
C	SUBROUTINE MOM8 DETERMINES THE CURRENT MOMENT XMOM .	H	7
C	VERSION 09/10/72 .	H	8
C	MOM8 IS USED BY TRINSH	H	9
	TENS=.TRUE.	H	10
	COMP=.FALSE.	H	11
	XMOM=0.	H	12
	M=0	H	13
	DO 6 I=1,NLT	H	14
	X=MU(I,2)	H	15
	IF (X.GT.LN) GO TO 2	H	16
	R2=RB(I+1)	H	17
1	R1=RB(I)	H	18
	SR1=RADSTR(KAPPA,ETA,MU(I,1),COMP)	H	19
	XMOM=XMOM+ (R2**2-R1**2)/2.*(-ALFA(I)/2.+SR1)+ALFA(I)*R2**2/2.*ALOG	H	20
	1 (R1/R2)	H	21
	IF (M.EQ.1) GO TO 4	H	22
	GO TO 6	H	23
2	IF (M.EQ.0) GO TO 3	H	24
	R1=RB(I)	H	25
	GO TO 5	H	26
3	R2=RN	H	27
	M=1	H	28
	GO TO 1	H	29
4	R1=RN	H	30
5	R2=RB(I+1)	H	31
	SR2=RADSTR(KAPPA,ETA,MU(I,2),TENS)	H	32
	XMOM=XMOM+ (R2**2-R1**2)/2.*(ALFA(I)/2.+SR2)+ALFA(I)*R1**2/2.*ALOG(H	33
	1R2/R1)	H	34
	GO TO 6	H	35
6	CONTINUE	H	36
		H	37

RETURN
END

H 38
H 39-


```

DATA NPUNCH/0/
DATA DK/.01/
DATA NSS,A,B,EN/2,1.,.01,.5/
DATA TO/1./
GO TO (1,2),NSS
1 ALFA=2./SQRT(3.)*A
  BETA=(2./SQRT(3.))**(EN+1.)*B
  GO TO 3
2 ALFA=(2./SQRT(3.))**(EN+1.)*A
  BETA=SQRT(3.)/2.*B
  GO TO 3
3 CONTINUE

```

```

STARTING POINT FOR THE INTEGRATION IS THE UNBEND CONDITION .

```

```

KAPPA=0.
ETA=1.
RHO=1.
LO=.5
LN=.5
INDEX=0
IF (NPUNCH.NE.0) WRITE (7,10) INDEX,PROGRAM,NSS,DK,A,B,EN
WRITE (6,14) A,B,EN
WRITE (6,13)
WRITE (6,12) KAPPA,ETA,RHO,LO,LN
INDEX=1
IF (NPUNCH.NE.0) WRITE (7,11) INDEX,NSS,KAPPA,ETA,LN,RHO
XN=(1./DK)/10.
IF (XN.LT.1.) XN=1.
N=2./DK-1.

```

```

INTEGRATION USING RUNGE-KUTTA METHOD .
STEPSIZE FOR KAPPA IS DK .

```

```

DO 7 I=1,N
IF (I.EQ.1) GO TO 4
DE1=DK*DETA(KAPPA,ETA,RHO)
DR1=DK*DRHO(KAPPA,ETA,RHO)
GO TO 5
4 DE1=0.
  DR1=0.
5 K1=KAPPA+DK/2.
  E1=ETA+DE1/2.
  R1=RHO+DR1/2.
  IF (R1.GT.1.) R1=1.
  DE2=DK*DETA(K1,E1,R1)
  DR2=DK*DRHO(K1,E1,R1)
  K2=K1
  E2=ETA+DE2/2.
  R2=RHO+DR2/2.

```

```

A 51
A 52
A 53
A 54
A 55
A 56
A 57
A 58
A 59
A 60
A 61
A 62
A 63
A 64
A 65
A 66
A 67
A 68
A 69
A 70
A 71
A 72
A 73
A 74
A 75
A 76
A 77
A 78
A 79
A 80
A 81
A 82
A 83
A 84
A 85
A 86
A 87
A 88
A 89
A 90
A 91
A 92
A 93
A 94
A 95
A 96
A 97
A 98
A 99
A 100

```

```

IF (R2.GT.1.) R2=1.
DE3=DK*DETA(K2,E2,R2)
DR3=DK*DRHO(K2,E2,R2)
K3=KAPPA+DK
E3=ETA+DE3
R3=RHO+DR3
IF (R3.GT.1.) R3=1.
DE4=DK*DETA(K3,E3,R3)
DR4=DK*DRHO(K3,E3,R3)
DE=(DE1+2.*DE2+2.*DE3+DE4)/6.
DR=(DR1+2.*DR2+2.*DR3+DR4)/6.
C
C
NEW VALUES FOR KAPPA,ETA,RHO .
C
C
KAPPA=KAPPA+DK
ETA=ETA+DE
RHO=RHO+DR
IF (RHO.GT.1.) RHO=1.
C
C
CALCULATION OF GEOMETRICAL SITUATION FOR THE CURRENT VALUE OF
KAPPA
C
C
LO=(ETA**2-(1.-KAPPA*.5)**2)/(2.*KAPPA)
LN=(RHO**2*ETA**2-(1.-KAPPA*.5)**2)/(2.*KAPPA)
RI=(1.-KAPPA*.5)*ETA*TO/KAPPA
RY=(1.+KAPPA*.5)*ETA*TO/KAPPA
RN=RHO*ETA**2*TO/KAPPA
RM=ETA*TO/KAPPA
RO=ETA**2*TO/KAPPA
INDEX=I+1
IF (NPUNCH.NE.0) WRITE (7,11) INDEX,NSS,KAPPA,ETA,LN,RHO
XI=I
X=XI/5.
Y=XI/XN
JX=X
JY=Y
J=JX*5
JJ=JY*10
IF (I.EQ.J) WRITE (6,14) A,B,EN
IF (I.EQ.J) WRITE (6,13)
WRITE (6,12) KAPPA,ETA,RHO,LO,LN,RI,RN,RO,RY,RM
C
C
WE DETERMINE THE STRESSDISTRIBUTION WHEN KAPPA IS .1 OR .2 OR .5
OR
C
C
IF ((KAPPA.GT..0999).AND.(KAPPA.LT..1001)) CALL STRESS1 (SR1,ST1)
IF ((KAPPA.GT..1999).AND.(KAPPA.LT..2001)) CALL STRESS1 (SR2,ST2)
IF ((KAPPA.GT..4999).AND.(KAPPA.LT..5001)) CALL STRESS1 (SR5,ST5)
IF ((KAPPA.GT..9999).AND.(KAPPA.LT.1.0001)) CALL STRESS1 (SR10,ST1
10)

```

```

A 101
A 102
A 103
A 104
A 105
A 106
A 107
A 108
A 109
A 110
A 111
A 112
A 113
A 114
A 115
A 116
A 117
A 118
A 119
A 120
A 121
A 122
A 123
A 124
A 125
A 126
A 127
A 128
A 129
A 130
A 131
A 132
A 133
A 134
A 135
A 136
A 137
A 138
A 139
A 140
A 141
A 142
A 143
A 144
A 145
A 146
A 147
A 148
A 149
A 150

```


C
C
C
C

WE PLOT THE RELATIVE POSITIONS OF ORIGINALLY EQUIDISTANT LAYERS
WHEN KAPPA IS A MULTIPLE OF .1 .

6

```

IF (I.EQ.JJ) GO TO 6
GO TO 7
P0=RO-RI
PN=RN-RI
CALL MOM1 (XMOM)
XMOM=XMOM/(TO**2)
YMOM=XMOM/(ETA**2)
WRITE (6,15) XMOM,YMOM
XM(JY)=XMOM
YM(JY)=YMOM
P1=RM*SQRT((1.-KAPPA*.5)**2+2.*.1*KAPPA)-RI
P2=RM*SQRT((1.-KAPPA*.5)**2+2.*.2*KAPPA)-RI
P3=RM*SQRT((1.-KAPPA*.5)**2+2.*.3*KAPPA)-RI
P4=RM*SQRT((1.-KAPPA*.5)**2+2.*.4*KAPPA)-RI
P5=RM*SQRT((1.-KAPPA*.5)**2+2.*.5*KAPPA)-RI
P6=RM*SQRT((1.-KAPPA*.5)**2+2.*.6*KAPPA)-RI
P7=RM*SQRT((1.-KAPPA*.5)**2+2.*.7*KAPPA)-RI
P8=RM*SQRT((1.-KAPPA*.5)**2+2.*.8*KAPPA)-RI
P9=RM*SQRT((1.-KAPPA*.5)**2+2.*.9*KAPPA)-RI
CALL PLOTPT (KAPPA,0.,10)
CALL PLOTPT (KAPPA,P1,11)
CALL PLOTPT (KAPPA,P2,12)
CALL PLOTPT (KAPPA,P3,13)
CALL PLOTPT (KAPPA,P4,14)
CALL PLOTPT (KAPPA,P5,15)
CALL PLOTPT (KAPPA,P6,16)
CALL PLOTPT (KAPPA,P7,17)
CALL PLOTPT (KAPPA,P8,18)
CALL PLOTPT (KAPPA,P9,19)
CALL PLOTPT (KAPPA,ETA,25)
CALL PLOTPT (KAPPA,RHO,38)
CALL PLOTPT (KAPPA,P0,35)
CALL PLOTPT (KAPPA,PN,34)
CONTINUE
CALL PLOTPT (0.,0.,10)
CALL PLOTPT (0.,1.,25)
CALL PLOTPT (0.,1.,38)
CALL PLOTPT (0.,.5,34)
CALL OUTPLT

```

7

C
C
C
C
C

PLOT THE STRESS DISTRIBUTION IN THE BEND SHEET .
STRESSES FOR KAPPA=.1 ARE PLOTTED WITH THE SYMBOL 1 .
STRESSES FOR KAPPA=.2 ARE PLOTTED WITH THE SYMBOL 2 .
STRESSES FOR KAPPA=.5 ARE PLOTTED WITH THE SYMBOL 5 .
STRESSES FOR KAPPA=1. ARE PLOTTED WITH THE SYMBOL 8 .

A 151
A 152
A 153
A 154
A 155
A 156
A 157
A 158
A 159
A 160
A 161
A 162
A 163
A 164
A 165
A 166
A 167
A 168
A 169
A 170
A 171
A 172
A 173
A 174
A 175
A 176
A 177
A 178
A 179
A 180
A 181
A 182
A 183
A 184
A 185
A 186
A 187
A 188
A 189
A 190
A 191
A 192
A 193
A 194
A 195
A 196
A 197
A 198
A 199
A 200

	DO 8 I=1,21	A	201
	X=I-1	A	202
	X=X/20.	A	203
	CALL PLOTPT (X,SR1(I),11)	A	204
	CALL PLOTPT (X,ST1(I),11)	A	205
	CALL PLOTPT (X,SR2(I),12)	A	206
	CALL PLOTPT (X,ST2(I),12)	A	207
	CALL PLOTPT (X,SR5(I),15)	A	208
	CALL PLOTPT (X,ST5(I),15)	A	209
	CALL PLOTPT (X,SR10(I),20)	A	210
	CALL PLOTPT (X,ST10(I),20)	A	211
8	CONTINUE	A	212
	CALL OUTPLT	A	213
C		A	214
C	PLOT THE BENDING MOMENT .	A	215
C	XM=MOMENT PER UNIT WIDTH / SQUARE OF ORIGINAL SHEET THICKNESS .	A	216
C	XM IS PLOTTED WITH THE SYMBOL M .	A	217
C	YM = MOMENT PER UNIT WITH / SQUARE OF CURRENT SHEET THICKNESS .	A	218
C	YM IS PLOTTED WITH THE SYMBOL W .	A	219
	KAPPA=0.	A	220
	DK=.1	A	221
	DO 9 I=1,19	A	222
	KAPPA=KAPPA+DK	A	223
	CALL PLOTPT (KAPPA,XM(I),33)	A	224
	CALL PLOTPT (KAPPA,YM(I),43)	A	225
9	CONTINUE	A	226
	CALL PLOTPT (0.,0.,10)	A	227
	CALL PLOTPT (2.,0.,10)	A	228
	CALL OUTPLT	A	229
	STOP	A	230
C		A	231
10	FORMAT (I3,A7,I3,6X,F7.6,2E12.4,F10.7)	A	232
11	FORMAT (2I3,3X,F6.4,3E13.6)	A	233
12	FORMAT (1H ,10E13.5,/))	A	234
13	FORMAT (1H ,*KAPPA*,8X,*ETA*,10X,*RHO*,10X,*LO*,11X,*LN*,11X,*RI*,	A	235
	11X,*RN*,11X,*RO*,11X,*RY*,11X,*RM*,/)	A	236
14	FORMAT (1H ,*A =*,E13.5,/ ,1H ,*B =*,E13.5,/ ,1H ,*EN=*,E13.5,/)	A	237
15	FORMAT (1H ,*XMOM=*,E13.5,5X,*YMOM=*,E13.5)	A	238
	END	A	239
		A	240-
	FUNCTION DETA (KAPPA,ETA,RHO)	B	1
	REAL KAPPA	B	2
C		B	3
C	DETA DETERMINES THE DIFFERENTIAL OF ETA	B	4
C	DETA IS USED BY MONOSH	B	5
		B	6
	DETA=-.5*ETA/KAPPA*((1.-.25*KAPPA**2)/(ETA**2*RHO**2)-1.)	B	7
	RETURN	B	8

END

B 9

FUNCTION DRHO (KAPPA,ETA,RHO)

C 1

REAL KAPPA

C 2

COMMON /SSCURV/ NSS,ALFA,BETA,EN

C 3

DRHO CALCULATES THE DIFFERENTIAL OF RHO

C 4

DRHO IS USED BY MONOSH

C 5

GO TO (1,2), NSS

C 6

DRHO=-RHO/(2.*ALFA+BETA*(-ALOG(RHO))**EN)*(ALFA*KAPPA/(2.-KAPPA**2

C 7

1.*.5)+BETA*(-ALOG((1.-KAPPA*.5)/ETA))**EN/(2.-KAPPA)-BETA/(2.+KAPP

C 8

2A)*(ALOG((1.+5*KAPPA)/ETA))**EN+DETA(KAPPA,ETA,RHO)/ETA*(2.*ALFA+

C 9

3BETA*(-ALOG((1.-.5*KAPPA)/ETA))**EN+BETA*(ALOG((1.+5*KAPPA)/ETA))

C 10

4**EN))

C 11

GO TO 3

C 12

DE=DETA(KAPPA,ETA,RHO)

C 13

DRHO=RHO/(BETA**EN+(BETA-ALOG(RHO))**EN)*((BETA+ALOG(1.+5*KAPPA)-

C 14

1ALOG(ETA))**EN*(1./(2.+KAPPA)-DE/ETA)+(BETA-ALOG(1.-.5*KAPPA)+ALOG

C 15

2(ETA))**EN*(1./(KAPPA-2.))-DE/ETA))

C 16

GO TO 3

C 17

CONTINUE

C 18

RETURN

C 19

END

C 20

SUBROUTINE STRESS1 (SRN,STN)

D 1

REAL KAPPA,LO,LN

D 2

DIMENSION SRN(21), STN(21)

D 3

COMMON /STATE/ KAPPA,ETA,RHO,LO,LN,RI,RY,RN,RO,RM

D 4

COMMON /SSCURV/ NSS,ALFA,BETA,EN

D 5

SUBROUTINE STRESS1 CALCULATES THE STRESSES FOR THE BENDING OF A ST

D 6

HARDENING MONOMETAL (BAUSCHINGER EFFECT INCLUDED IN CRAFOORD#S

D 7

FASHI

D 8

STRESS1 IS TO BE USED WITH THE MAIN PROGRAM MONOSH .

D 9

DR=(RY-RI)/20.

D 10

R=RI

D 11

WRITE (6,2)

D 12

DO 1 I=1,21

D 13

CALL SIGMAT1 (R,SRN(I),STN(I))

D 14

Z=R-RI

D 15

STRAIN=ALOG(R/RO)

D 16

X=STN(I)-SRN(I)

D 17

X=ABS(X)

D 18

WRITE (6,3) Z,SRN(I),STN(I),STRAIN,X

D 19

R=R+DR

D 20

CONTINUE

D 21

D 22

D 23

C
C
C

1

2

3

C
C
C
C

1

```

C RETURN
C 2 FORMAT (1H1,* R-RI STRAIN *,* *,* SR EFFECTIVE YIELD STRESS*,/
1 2/,)
3 FORMAT (1H ,5E20.10)
END

```

```

D 24
D 25
D 26
D 27
D 28
D 29
D 30

```

```

C SUBROUTINE SIGMAR1 (R,SR)
C REAL KAPPA,LO,LN
C COMMON /STATE/ KAPPA,ETA,RHO,LO,LN,RI,RY,RN,RO,RM
C COMMON /SSCURV/ NSS,ALFA,BETA,EN
C PROGRAM TO CALCULATE THE RADIAL STRESS IN A STRAINHARDENING
C MONOMETA
C (BAUSCHINGER EFFECT INCLUDED IN CRAWFORD'S FASHION).
C SIGMAR1 IS TO BE USED WITH PROGRAM MONOSH .
C
C IZONE=3
C IF (R.GE.RO) IZONE=1
C IF (R.LE.RN) IZONE=2
C GO TO (1,5), NSS
C GO TO (2,3,4), IZONE
1 SR=ALFA*ALOG(R/RY)+BETA/(EN+1.)*((ALOG(R/RO))**(EN+1.)-(ALOG(RY/RO
2 1))**(EN+1.))
C GO TO 9
3 SR=-ALFA*ALOG(R/RI)+BETA/(EN+1.)*((-ALOG(R/RO))**(EN+1.)-(-ALOG(RI
4 1/RO))**(EN+1.))
C GO TO 9
5 SR=ALFA*ALOG(R/RY)-BETA/(EN+1.)*(ALOG(RY/RO))**(EN+1.)
C GO TO 9
6 SR=ALFA/(EN+1.)*((BETA+ALOG(R/RO))**(EN+1.)-(BETA+ALOG(RY/RO))**(E
7 1N+1.))
C GO TO 9
8 SR=ALFA/(EN+1.)*((BETA-ALOG(R/RO))**(EN+1.)-(BETA-ALOG(RI/RO))**(E
9 1N+1.))
C GO TO 9
1 SR=ALFA*BETA**EN*ALOG(R/RO)+ALFA/(EN+1.)*(BETA**EN-(BETA+ALOG
2 1(RY/RO))**(EN+1.))
C GO TO 9
3 CONTINUE
4 RETURN
5 END

```

```

F 1
F 2
F 3
F 4
F 5
F 6
F 7
F 8
F 9
F 10
F 11
F 12
F 13
F 14
F 15
F 16
F 17
F 18
F 19
F 20
F 21
F 22
F 23
F 24
F 25
F 26
F 27
F 28
F 29
F 30
F 31
F 32
F 33
F 34
F 35
F 36

```

```

SUBROUTINE SIGMAT1 (R,SR,ST)
REAL KAPPA,LO,LN
COMMON /STATE/ KAPPA,ETA,RHO,LO,LN,RI,RY,RN,RO,RM

```

```

F 1
F 2
F 3

```


	COMMON /SSCURV/ NSS,ALFA,BETA,EN	F	4
C	PROGRAM TO CALCULATE THE TANGENTIAL STRESS IN A STRAINHARDENING	F	5
C	MONO	F	6
C	(BAUSCHINGER EFFECT INCLUDED IN CRAFOORD'S FASHION).	F	7
C	SIGMAT1 IS TO BE USED WITH PROGRAM MONOSH .	F	8
	CALL SIGMAR1 (R,SR)	F	9
	IZONE=3	F	10
	IF (R.GE.RO) IZONE=1	F	11
	IF (R.LE.RN) IZONE=2	F	12
	GO TO (1,5), NSS	F	13
1	GO TO (2,3,4), IZONE	F	14
2	ST=SR+ALFA+BETA*(ALOG(R/RO))**EN	F	15
	GO TO 9	F	16
3	ST=SR-ALFA-BETA*(-ALOG(R/RO))**EN	F	17
	GO TO 9	F	18
4	ST=SR+ALFA	F	19
	GO TO 9	F	20
5	GO TO (6,7,8), IZONE	F	21
6	ST=SR+ALFA*(BETA+ALOG(R/RO))**EN	F	22
	GO TO 9	F	23
7	ST=SR-ALFA*(BETA-ALOG(R/RO))**EN	F	24
	GO TO 9	F	25
8	ST=SR+ALFA*BETA**EN	F	26
	GO TO 9	F	27
9	CONTINUE	F	28
	RETURN	F	29
	END	F	30
		F	31
		F	32
	SUBROUTINE MOM1 (XMOM)	G	1
	REAL KAPPA,LO,LN	G	2
	COMMON /STATE/ KAPPA,ETA,RHO,LO,LN,RI,RY,RN,RO,RM	G	3
	COMMON /SSCURV/ NSS,ALFA,BETA,EN	G	4
C	SUBROUTINE MOM1 CALCULATES THE BENDING MOMENT OF A STRAINHARDENING	G	5
C	MONOMETAL STRIP (BAUSCHINGER EFFECT INCLUDED IN CRAFOORD'S	G	6
C	FASHION).	G	7
C	MOM1 IS TO BE USED WITH PROGRAM MONOSH .	G	8
	XMOM=0.	G	9
	CALL INT1 (RI,RN, XMOM)	G	10
	CALL INT1 (RN,RO, XMOM)	G	11
	CALL INT1 (RO,RY, XMOM)	G	12
	RETURN	G	13
	END	G	14
		G	15
		G	16
	SUBROUTINE INT1 (R1,R2, XMOM)	H	1

```

REAL KAPPA,LO,LN
COMMON /STATE/ KAPPA,ETA,RHO,LO,LN,RI,RY,RN,RO,RM
COMMON /SSCURV/ NSS,ALFA,BETA,EN

```

```

H 2
H 3
H 4
H 5
H 6
H 7
H 8
H 9
H 10
H 11
H 12
H 13
H 14
H 15
H 16
H 17
H 18
H 19
H 20
H 21
H 22
H 23
H 24
H 25
H 26
H 27
H 28
H 29

```

```

SUBROUTINE INT1 CALCULATES THE MOMENT OF THE TANGENTIAL STRESS
BETWE
R1 AND R2 .
INT1 IS USED IN MOM1 .

```

```

D=(R2-R1)/(RY-RI)*100.

```

```

N=D

```

```

IF (N.LT.10) N=10

```

```

X=N

```

```

NN=N-1

```

```

DR=(R2-R1)/X

```

```

R=R1

```

```

CALL SIGMAT1 (R,SR,ST)

```

```

XMOM=XMOM+ST*R*DR/2.

```

```

DO 1 I=1,NN

```

```

R=R+DR

```

```

CALL SIGMAT1 (R,SR,ST)

```

```

XMOM=XMOM+ST*R*DR

```

```

CONTINUE

```

```

R=R2

```

```

CALL SIGMAT1 (R,SR,ST)

```

```

XMOM=XMOM+ST*R*DR/2.

```

```

RETURN

```

```

END

```

C
C
C
C
C
C

1

	DATA KZONE (5),KZONE (6),KZONE (7),KZONE (8)/.02,.01,.002,0./	A 101
	DATA DK/.01/	A 102
	DATA NSS,NLT,TO/2,2,1./	A 103
	DATA A (1),B (1),EN (1)/.29,1.,1.E-10/	A 104
	DATA A (2),B (2),EN (2)/2.12,.092,.430/	A 105
	DATA MU (2,1)/.82/	A 106
	MU (1,1)=0.	A 107
	DO 1 I=2,NLT	A 108
	MU (I-1,2)=MU (I,1)	A 109
1	CONTINUE	A 110
	MU (NLT,2)=1.	A 111
	DO 2 I=1,NLT	A 112
	LETA (I)=1.	A 113
	TTO (I)=(MU (I,2)-MU (I,1))*TO	A 114
2	CONTINUE	A 115
	GO TO (3,5), NSS	A 116
3	DO 4 I=1,NLT	A 117
	ALFA (I)=2./SQRT (3.)*A (I)	A 118
	BETA (I)=(2./SQRT (3.))* (EN (I)+1.)*B (I)	A 119
	SIGMAO (I)=ALFA (I)	A 120
4	CONTINUE	A 121
	GO TO 7	A 122
5	DO 6 I=1,NLT	A 123
	ALFA (I)=(2./SQRT (3.))* (EN (I)+1.)*A (I)	A 124
	BETA (I)=SQRT (3.)/2.*B (I)	A 125
	SIGMAO (I)=ALFA (I)*BETA (I)**EN (I)	A 126
6	CONTINUE	A 127
	GO TO 7	A 128
7	CONTINUE	A 129
C		A 130
C	STARTING POINT FOR INTEGRATION IS THE UNBEND CONDITION .	A 131
C		A 132
	KAPPA=0.	A 133
	ETA=1.	A 134
	RHO=1.	A 135
C		A 136
C	CALCULATION OF THE ORIGINAL NEUTRAL LAYER .	A 137
C		A 138
	SIGMAL (1)=0.	A 139
	DO 8 I=1,NLT	A 140
	J=I+1	A 141
	SIGMAL (J)=SIGMAL (I)+SIGMAO (I)*(MU (I,2)-MU (I,1))	A 142
8	CONTINUE	A 143
	TEST (1)=SIGMAL (NLT+1)	A 144
	DO 9 I=1,NLT	A 145
	J=I+1	A 146
	TEST (J)=TEST (1)-SIGMAL (J)*2.	A 147
	IF (TEST (J).EQ.0.) GO TO 10	A 148
	W=TEST (J)*TEST (J-1)	A 149
	IF (W.LT.0.) GO TO 11	A 150

9	CONTINUE	A 151
10	LN=MU(J,1) GO TO 12	A 152 A 153
11	LN=(TEST(J-1)*MU(J-1,2)-TEST(J)*MU(J-1,1))/(TEST(J-1)-TEST(J)) GO TO 12	A 154 A 155
12	LO=LN LMAX=LN+1.E-10 LMIN=LN-1.E-10 CALL STORE(LN,RHO,1)	A 156 A 157 A 158 A 159
C		A 160
C	CALCULATION OF THE INITIAL BENDING MOMENT .	A 161
C		A 162
	SIGN=-1. M=0 XMOM=0. DO 14 K=1,NLT IF ((MU(K,2).GT.LN).AND.(M.EQ.0)) GO TO 13 XMOM=SIGN*SIGMAO(K)/2.*(MU(K,2)**2-MU(K,1)**2)+XMOM GO TO 14	A 163 A 164 A 165 A 166 A 167 A 168 A 169
13	XMOM=SIGN*SIGMAO(K)/2.*(LN**2-MU(K,1)**2)+XMOM SIGN=+1. M=1	A 170 A 171 A 172
14	XMOM=SIGN*SIGMAO(K)/2.*(MU(K,2)**2-LN**2)+XMOM CONTINUE YMOM=XMOM XM(1)=XMOM YM(1)=YMOM WRITE(6,39) DO 16 I=1,NLT J=0 IF(NPUNCH.EQ.0) GO TO 15 WRITE(7,45) J,PROGRAM,NSS,NLT,I,DK,A(I),B(I),EN(I),MU(I,1),MU(I,2)	A 173 A 174 A 175 A 176 A 177 A 178 A 179 A 180 A 181 A 182
15	1) CONTINUE WRITE(6,44) WRITE(6,40) I,A(I),B(I),EN(I),MU(I,1),MU(I,2)	A 183 A 184 A 185 A 186
16	CONTINUE WRITE(6,44) WRITE(6,41) TO,DK WRITE(6,44) WRITE(6,42) WRITE(6,43) INDEX,NSS,NLT,KAPPA,ETA,RHO,LN,LO,LMIN,LMAX, XMOM, YMOM 1, (LETA(K), K=1,NLT) IF(NPUNCH.EQ.0) GO TO 17 WRITE(7,46) INDEX,NSS,NLT,KAPPA,ETA, LN, LMIN, LMAX, RHO	A 187 A 188 A 189 A 190 A 191 A 192 A 193 A 194 A 195
17	CONTINUE XN=(1./DK)/10. IF(XN.LT.1.) XN=1.	A 196 A 197 A 198 A 199 A 200
C		
C		

	N=1999	A	201
	IF (DK.GT..001) N=2./DK-1.	A	202
C		A	203
C	INTEGRATION USING RUNGE-KUTTA METHOD . STEPSIZE FOR KAPPA IS DK .	A	204
	DO 29 I=1,N	A	205
	IF (NCH.NE.0) GO TO 19	A	206
	DO 18 JK=1,8	A	207
	IK=9-JK	A	208
	IF (KAPPA.GE.KZONE(IK)) DK=DKZONE(IK)	A	209
18	CONTINUE	A	210
19	CONTINUE	A	211
	IF (I.EQ.1) GO TO 20	A	212
	CALL FINDLN (KAPPA,ETA,LN,XLN)	A	213
	DE1=DK*DETA(KAPPA,ETA,XLN)	A	214
	GO TO 21	A	215
20	DE1=0.	A	216
21	KAPPA1=KAPPA+DK/2.	A	217
	ETA1=ETA+DE1/2.	A	218
	CALL FINDLN (KAPPA1,ETA1,LN,XLN)	A	219
	DE2=DK*DETA(KAPPA1,ETA1,XLN)	A	220
	KAPPA2=KAPPA1	A	221
	ETA2=ETA+DE2/2.	A	222
	CALL FINDLN (KAPPA2,ETA2,LN,XLN)	A	223
	DE3=DK*DETA(KAPPA2,ETA2,XLN)	A	224
	KAPPA3=KAPPA+DK	A	225
	ETA3=ETA+DE3	A	226
	CALL FINDLN (KAPPA3,ETA3,LN,XLN)	A	227
	DE4=DK*DETA(KAPPA3,ETA3,XLN)	A	228
	DE=(DE1+DE4)/6.+(DE2+DE3)/3.	A	229
		A	230
C		A	231
C	NEW VALUES FOR KAPPA,ETA,RHO,LN .	A	232
C		A	233
	KAPPA=KAPPA+DK	A	234
	ETA=ETA+DE	A	235
	CALL FINDLN (KAPPA,ETA,LN,XLN)	A	236
	LN=XLN	A	237
	RHO=SQRT((1.-.5*KAPPA)**2+2.*KAPPA*LN)/ETA	A	238
	J=I+1	A	239
	CALL STORE (LN,RHO,J)	A	240
C		A	241
C	GEOMETRICAL CONFIGURATION OF THE CURRENT BEND .	A	242
C		A	243
	RM=ETA*TO/KAPPA	A	244
	RI=RM*(1.-KAPPA*.5)	A	245
	RY=RM*(1.+KAPPA*.5)	A	246
	RN=RM*ETA*RHO	A	247
	RO=RM*ETA	A	248
	LO=(ETA**2-(1.-KAPPA*.5)**2)/(2.*KAPPA)	A	249
	RB(1)=RI	A	250

	BEPS(1)=ALOG(RI/RO)	A	251
	DO 22 K=1,NLT	A	252
	M=K+1	A	253
	RB(M)=RM*SQRT((1.-KAPPA*.5)**2+2.*MU(K,2)*KAPPA)	A	254
	BEPS(M)=ALOG(RB(M)/RO)	A	255
	T(K)=RB(M)-RB(K)	A	256
	P(K)=RB(M)-RI	A	257
	LETA(K)=T(K)/TTO(K)	A	258
22	CONTINUE	A	259
	IF (NEXT1.EQ.0) GO TO 23	A	260
	R1=RM*SQRT((1.-KAPPA*.5)**2+2.*.1*KAPPA)	A	261
	R2=RM*SQRT((1.-KAPPA*.5)**2+2.*.2*KAPPA)	A	262
	R3=RM*SQRT((1.-KAPPA*.5)**2+2.*.3*KAPPA)	A	263
	R4=RM*SQRT((1.-KAPPA*.5)**2+2.*.4*KAPPA)	A	264
	R5=RM*SQRT((1.-KAPPA*.5)**2+2.*.5*KAPPA)	A	265
	R6=RM*SQRT((1.-KAPPA*.5)**2+2.*.6*KAPPA)	A	266
	R7=RM*SQRT((1.-KAPPA*.5)**2+2.*.7*KAPPA)	A	267
	R8=RM*SQRT((1.-KAPPA*.5)**2+2.*.8*KAPPA)	A	268
	R9=RM*SQRT((1.-KAPPA*.5)**2+2.*.9*KAPPA)	A	269
	P1=R1-RI	A	270
	P2=R2-RI	A	271
	P3=R3-RI	A	272
	P4=R4-RI	A	273
	P5=R5-RI	A	274
	P6=R6-RI	A	275
	P7=R7-RI	A	276
	P8=R8-RI	A	277
	P9=R9-RI	A	278
	P0=R0-RI	A	279
	PN=RN-RI	A	280
	E1=ALOG(R1/RO)	A	281
	E1=ALOG(R1/RO)	A	282
	E2=ALOG(R2/RO)	A	283
	E3=ALOG(R3/RO)	A	284
	E4=ALOG(R4/RO)	A	285
	E5=ALOG(R5/RO)	A	286
	E6=ALOG(R6/RO)	A	287
	E7=ALOG(R7/RO)	A	288
	E8=ALOG(R8/RO)	A	289
	E9=ALOG(R9/RO)	A	290
	EY=ALOG(RY/RO)	A	291
	EPSN=ALOG(RN/RO)	A	292
23	CONTINUE	A	293
C		A	294
C	CALCULATION OF THE BENDING MOMENT .	A	295
C		A	296
C	CALL BENMOM (KAPPA,ETA,LN,RM,RI,RY,XMOM)	A	297
C		A	298
C	XMOM=XMOM/(TO**2)	A	299
C		A	300
C	YMOM=XMOM/(ETA**2)	A	300
C		A	300

C	WE DETERMINE THE RADIAL AND TANGENTIAL STRESS DISTRIBUTION WHEN	A	301
C	KAPPA IS .1 OR .2 OR .5 OR 1. .	A	302
	IF (NEXT2.EQ.0) GO TO 24	A	303
	IF ((KAPPA.GT..0999).AND.(KAPPA.LT..1001)) CALL STRESS6 (R1,SR1,ST	A	304
	11,RI,KAPPA,ETA)	A	305
	IF ((KAPPA.GT..1999).AND.(KAPPA.LT..2001)) CALL STRESS6 (R2,SR2,ST	A	306
	12,RI,KAPPA,ETA)	A	307
	IF ((KAPPA.GT..4999).AND.(KAPPA.LT..5001)) CALL STRESS6 (R5,SR5,ST	A	308
	15,RI,KAPPA,ETA)	A	309
	IF ((KAPPA.GT..9999).AND.(KAPPA.LT.1.0001)) CALL STRESS6 (R10,SR10	A	310
	1,ST10,RI,KAPPA,ETA)	A	311
24	CONTINUE	A	312
	XI=I	A	313
	X=XI/5.	A	314
	JX=X	A	315
	J=JX*5	A	316
	JJ=0	A	317
	IF (I.EQ.J) WRITE (6,44)	A	318
	IF (I.EQ.J) WRITE (6,42)	A	319
	WRITE (6,43) INDEX,NSS,NLT,KAPPA,ETA,RHO,LN,LO,LMIN,LMAX,XMOM,YMOM	A	320
	1,{LETA(K),K=1,NLT)	A	321
	IF (NEXT1.EQ.0) GO TO 25	A	322
	WRITE (6,34) P1,P2,P3,P4,P5,P6,P7,P8,P9,(P(K),K=1,NLT)	A	323
	WRITE (6,35) PN,PO	A	324
	WRITE (6,36) EI,E1,E2,E3,E4,E5,E6,E7,E8,E9,EY	A	325
	WRITE (6,37) (BEP S(K),K=1,NLT),EY	A	326
	WRITE (6,38) EPSN	A	327
25	CONTINUE	A	328
	IF (NPUNCH.EQ.0) GO TO 26	A	329
26	WRITE (7,46) INDEX,NSS,NLT,KAPPA,ETA,LN,LMIN,LMAX,RHO	A	330
	CONTINUE	A	331
	IF (I.EQ.JJ) GO TO 27	A	332
	GO TO 29	A	333
27	CONTINUE	A	334
	XM(JY+1)=XMOM	A	335
	YM(JY+1)=YMOM	A	336
	DO 28 K=1,NLT	A	337
	J=K+9	A	338
	RB(K)=RB(K)-RI	A	339
	CALL PLOTPT (KAPPA,RB(K),J)	A	340
28	CONTINUE	A	341
	CALL PLOTPT (KAPPA,ETA,25)	A	342
	RN=RN-RI	A	343
	CALL PLOTPT (KAPPA,RN,34)	A	344
	CALL PLOTPT (KAPPA,RHO,38)	A	345
29	CONTINUE	A	346
	CALL OUTPLT	A	347
C		A	348
C	PLOT THE STRESS DISTRIBUTION IN THE BEND SHEET .	A	349
		A	350


```

C STRESSES FOR KAPPA=.1 ARE PLOTTED WITH THE SYMBOL 1 . A 351
C STRESSES FOR KAPPA=.2 ARE PLOTTED WITH THE SYMBOL 2 . A 352
C STRESSES FOR KAPPA=.5 ARE PLOTTED WITH THE SYMBOL 5 . A 353
C STRESSES FOR KAPPA=1. ARE PLOTTED WITH THE SYMBOL $ . A 354
C IF (NEXT2.EQ.0) GO TO 31 A 355
C DO 30 I=1,21 A 356
C X=I-1 A 357
C X=X/20. A 358
C CALL PLOTPT (X,SR1(I),11) A 359
C CALL PLOTPT (X,ST1(I),11) A 360
C CALL PLOTPT (X,SR2(I),12) A 361
C CALL PLOTPT (X,ST2(I),12) A 362
C CALL PLOTPT (X,SR5(I),15) A 363
C CALL PLOTPT (X,ST5(I),15) A 364
C CALL PLOTPT (X,SR10(I),20) A 365
C CALL PLOTPT (X,ST10(I),20) A 366
30 CONTINUE A 367
CALL OUTPLT A 368
31 CONTINUE A 369
C PLOT THE BENDING MOMENT . A 370
C XM=MOMENT PER UNIT WIDTH / SQUARE OF ORIGINAL SHEET THICKNESS . A 371
C XM IS PLOTTED WITH THE SYMBOL M . A 372
C YM = MOMENT PER UNIT WITH / SQUARE OF CURRENT SHEET THICKNESS . A 373
C YM IS PLOTTED WITH THE SYMBOL W . A 374
C IF (NEXT3.EQ.0) GO TO 33 A 375
C KAPPA=0. A 376
C DDK=.1 A 377
C DO 32 I=1,20 A 378
C CALL PLOTPT (KAPPA,XM(I),33) A 379
C CALL PLOTPT (KAPPA,YM(I),43) A 380
C KAPPA=KAPPA+DDK A 381
32 CONTINUE A 382
CALL PLOTPT (0.,0.,10) A 383
CALL OUTPLT A 384
33 CONTINUE A 385
C STOP A 386
C A 387
C A 388
C A 389
C A 390
C A 391
34 FORMAT (1H ,* LAYER MOVEMENT *,9F10.7,/,1H ,* BOUNDARY MOVEMENT A 392
1 *,9F10.7,/,) A 393
35 FORMAT (1H ,*NEUTRAL LAYER AND UNELONGATED LAYER MOVEMENT*,6X,2F10 A 394
1.7,/,) A 395
36 FORMAT (1H ,*LAYER HOOP STRAIN *,11F10.7) A 396
37 FORMAT (1H ,*BOUNDARY HOOP STRAIN*,11F10.7) A 397
38 FORMAT (1H ,*NEUTRAL LAYER HOOP STRAIN *,F10.7) A 398
39 FORMAT (1H1,* I *,*A(I)*,8X,*B(I)*,8X,*EN(I)*,7X,*MU(I,1)*,5X,*M A 399
1U(I,2)*,/) A 400

```


40	FORMAT (1H ,I5,5E12.5)	A	401
41	FORMAT (1H ,*T0=*,E12.4,5X,*DK=*,E12.4,/))	A	402
42	FORMAT (1H ,*IND NSS NLT KAPPA ETA RHO LN *,* 1 2T *,//,) LO LMIN LMAX XMOM YMOM LE TA(I),I=1, NL	A	403
43	FORMAT (1H ,3I3,9F10.7,4F8.5)	A	404
44	FORMAT (1H ,/)	A	405
45	FORMAT (I3, A7, 3I3, F7.6, 2E12.4, 3F10.7)	A	406
46	FORMAT (3I3, F6.4, 5E13.6)	A	407
	END	A	408
		A	409
		A	410-
	FUNCTION DETA (KAPPA,ETA,LN)	B	1
	REAL KAPPA,LN	B	2
C		B	3
C	FUNCTION DETA DETERMINES THE DERIVATIVE OF ETA TO KAPPA.	B	4
C	(SHEET-THICKNESS DIFFERENTIAL EQUATION)	B	5
C	DETA IS USED WITH BENDING	B	6
	DETA=-.5*ETA*(1.-2.*LN-.5*KAPPA)/((1.-.5*KAPPA)**2+2.*LN*KAPPA)	B	7
	RETURN	B	8
	END	B	9
		B	10-
	SUBROUTINE STORE (XLN,RHO,I)	C	1
	REAL LMIN,LMAX	C	2
	COMMON /REMEM/ INDEX,LMIN,LMAX,REMLN(200),REMRHO(200)	C	3
C		C	4
C	SUBROUTINE STORE STORES THE POSITION OF THE NEUTRAL LAYER IN	C	5
C	MEMORY	C	6
C	STORE IS USED WITH BENDING.	C	7
	REMLN(I)=XLN	C	8
	REMRHO(I)=RHO	C	9
	INDEX=I	C	10
	IF (XLN.LT.LMIN) LMIN=XLN	C	11
	IF (XLN.GT.LMAX) LMAX=XLN	C	12
	RETURN	C	13
	END	C	14
		C	15-
	SUBROUTINE SHIFT (LAM,REMSTR)	D	1
	REAL LAM,LMIN,LMAX	D	2
	LOGICAL TENS,COMP,STATE1,STATE2	D	3
	COMMON /REMEM/ INDEX,LMIN,LMAX,REMLN(200),REMRHO(200)	D	4
C		D	5
C	SUBROUTINE SHIFT DETERMINES HOW MUCH STRAIN A MATERIAL LAYER LAM	D	6
C	HAS UNDERGONE IN PREVIOUS DEFORMATION . THIS CAUSES A SHIFT IN THE	D	7
C	STRESS STRAIN CURVE RELATIVE TO THE CURRENT STRAIN .	D	8
C	THIS SHIFT IS NEEDED TO CALCULATE THE EFFECTIVE STRAIN .	D	9

C	SHIFT IS USED WITH BENDING	D	10
	REMSTR=0.	D	11
	IF (INDEX.LE.2) GO TO 5	D	12
	TENS=.TRUE.	D	13
	COMP=.FALSE.	D	14
	STATE1=TENS	D	15
	IF (LAM.LT.REMLN(1)) STATE1=COMP	D	16
	IF ((LAM.EQ.REMLN(1)).AND.(REMLN(2).LE.REMLN(1))) STATE1=COMP	D	17
	DO 4 I=3,INDEX	D	18
	STATE2=TENS	D	19
	IF (LAM.LT.REMLN(I)) STATE2=COMP	D	20
	IF (LAM.EQ.REMLN(I)) GO TO 1	D	21
	IF (STATE1.AND.STATE2) GO TO 3	D	22
	IF ((.NOT.STATE1).AND.(.NOT.STATE2)) GO TO 3	D	23
	RHO=POL2(LAM,REMLN(I),REMLN(I-1),REMLN(I-2),REMRHO(I),REMRHO(I-1),	D	24
1	REMRHO(I-2))	D	25
	GO TO 2	D	26
1	STATE2=.NOT.STATE1	D	27
	RHO=REMRHO(I)	D	28
	GO TO 2	D	29
2	CONTINUE	D	30
	SIGN=-1.	D	31
	IF (STATE1) SIGN=+1.	D	32
	REMSTR=REMSTR+SIGN*2.*ALOG(RHO)	D	33
	GO TO 3	D	34
3	STATE1=STATE2	D	35
4	CONTINUE	D	36
5	CONTINUE	D	37
	IF (REMSTR.LT.0.) REMSTR=0.	D	38
	RETURN	D	39
	END	D	40
		D	41-

	SUBROUTINE STRESS6 (R,SR,ST,RI,KAPPA,ETA)	F	1
	REAL KAPPA	F	2
	REAL MU	F	3
	REAL LMIN,LMAX,L	F	4
	DIMENSION R(1), SR(1), ST(1)	F	5
	COMMON /STRSTR/ RR(120),SRR(120),STT(120),NS	F	6
	COMMON /REMEM/ INDEX,LMIN,LMAX,REMLN(200),REMRHO(200)	F	7
	COMMON /SSCURV/ NSS,NLT,ALFA(4),BETA(4),EN(4),MU(4,2),TO	F	8
C		F	9
C	STRESS6 WRITES THE STRESSDISTRIBUTION FOR A GIVEN KAPPA .	F	10
C	STRESS6 IS USED WITH BENDING	F	11
		F	12
	N=(NS-1)/4	F	13
	WRITE (6,3) KAPPA	F	14
	RM=ETA*TO/KAPPA	F	15
	DO 1 I=1,N	F	16

	YEFF=STT(I)-SRR(I)	F	17
	SIGN=-1.	F	18
	IF (YEFF.GT.0.) SIGN=+1.	F	19
	X=RR(I)**2/(RM**2)	F	20
	L=(X-(1.-.5*KAPPA)**2)/(2.*KAPPA)	F	21
	REMSTR=0.	F	22
	IF ((L.GT.LMIN).AND.(L.LT.LMAX)) CALL SHIFT (L,REMSTR)	F	23
	EPSTOT=REMSTR+SIGN*(.5*ALOG(X)-ALOG(ETA))	F	24
	RR(I)=RR(I)-RI	F	25
1	WRITE (6,4) RR(I),SRR(I),STT(I),YEFF,EPSTOT	F	26
	CONTINUE	F	27
	NN=(N-1)/21	F	28
	IF ((NN*21).NE.(N-1)) NN=NN+1	F	29
	DO 2 I=1,N,NN	F	30
	J=I/NN	F	31
	SR(J)=SRR(I)	F	32
	ST(J)=STT(I)	F	33
2	R(J)=RR(I)	F	34
	CONTINUE	F	35
	RETURN	F	36
3	FORMAT (1H1,*RADIAL AND TANGENTIAL STRESSDISTRIBUTION FOR KAPPA =*	F	37
	1,F10.5,/,1H,* R - RI *,* SR *,* ST *,*EFFECTIVE*,*	F	38
	2 YIELD STRESS AND TOTAL STRAIN*,/,)	F	39
4	FORMAT (1H ,5F10.7)	F	40
	END	F	42-
C	FUNCTION POL2 (X,X1,X2,X3,Y1,Y2,Y3)	F	1
C	POL2 GIVES THE SECOND DEGREE POLYNOMIAL APPROXIMATION FOR A CURVE	F	2
C	GOING THROUGH 3 POINTS	F	3
C	POL2 IS USED WITH BENDING	F	4
	IF (X1-X2) 1,4,1	F	5
1	IF (X1-X3) 2,4,2	F	6
2	IF (X2-X3) 3,4,3	F	7
3	POL2=(X-X2)/(X1-X2)*(X-X3)/(X1-X3)*Y1+(X-X1)/(X2-X1)*(X-X3)/(X2-X3	F	8
	1)*Y2+(X-X1)/(X3-X1)*(X-X2)/(X3-X2)*Y3	F	9
	GO TO 5	F	10
4	WRITE (6,6) X,X1,X2,X3,Y1,Y2,Y3	F	11
5	RETURN	F	12
C	FORMAT (1H ,*ERROR IN POL2*,5X,*TWO POINTS IDENTICAL ABSCISSAE*,/,	F	13
6	11H ,*ARGUMENTS*,7(E12.5,3X),//,)	F	14
	END	F	15
		F	16
		F	17
		F	18-
	SUBROUTINE STR (L,SRR,STT,RM,KAPPA)	G	1
	REAL KAPPA,L	G	2

	COMMON /STRSTR/ R(120),SR(120),ST(120),NS	G	3
C	STR PLACES THE STRESSES IN MEMORY .	G	4
C	STR IS USED WITH BENDING	G	5
C		G	6
	NS=NS+1	G	7
	N=(NS-1)/4	G	8
	IF ((N*4).EQ.(NS-1)) GO TO 1	G	9
	GO TO 2	G	10
1	SR(N+1)=SRR	G	11
	ST(N+1)=STT	G	12
	R(N+1)=RM*SQRT((1.-.5*KAPPA)**2+2.*L*KAPPA)	G	13
2	CONTINUE	G	14
	RETURN	G	15
	END	G	16
		G	17
	FUNCTION STRAIN (KAPPA,ETA,L,SIGN)	H	1
	REAL KAPPA,L	H	2
	REAL LMIN,LMAX	H	3
	COMMON /REMEM/ INDEX,LMIN,LMAX,REMLN(200),REMRHO(200)	H	4
C	STRAIN CALCULATES THE EFFECTIVE STRAIN .	H	5
C	STRAIN IS USED WITH BENDING	H	6
C		H	7
	X=(1.-.5*KAPPA)**2+2.*L*KAPPA	H	8
	REMSTR=0.	H	9
	IF ((L.GT.LMIN).AND.(L.LT.LMAX)) CALL SHIFT (L,REMSTR)	H	10
	STRAIN=REMSTR+SIGN*(.5*ALOG(X)-ALOG(ETA))	H	11
	RETURN	H	12
	END	H	13
		H	14
	FUNCTION DZ (KAPPA,RN,RM,L,DL)	I	1
C	REAL KAPPA,L	I	2
	DZ IS USED WITH BENDING	I	3
	DZ=ABS(DL)*(1.-RN/(RM*SQRT((1.-KAPPA*.5)**2+2.*L*KAPPA)))	I	4
	RETURN	I	5
	END	I	6
	SUBROUTINE INTMOM (KAPPA,ETA,MAT,TENS,BL1,BS1,L1,L2,S2,XMOM,RN)	J	1
	LOGICAL MOM,TENS	J	2
	REAL KAPPA,L1,L2,L,MU	J	3
	COMMON /SSCURV/ NSS,NLT,ALFA(4),BETA(4),EN(4),MU(4,2),TO	J	4
C	SUBROUTINE INTMOM VERSION ... 24 SEPT 1972 ...	J	5
C		J	6
C		J	7
C		J	8
C	INTMOM CALCULATES THE BENDING MOMENT IN THE ZONES FOR WHICH THE	J	9

CCCCCCCC

1

2

3

4

5

6

7

COMMON /TAN/ BT

SUBROUTINE NUMINT VERSION ... 24 SEPT 1972 ...

NUMINT DETERMINES RADIAL AND TANGENTIAL STRESSES AND BENDING
MOMENT

IN ZONES WHERE THE RADIAL STRESS IS ONLY KNOWN BY ITS DERIVATIVE .

NUMINT IS USED WITH BENDING

SIGN=-1.

IF (TENS) SIGN=+1.

RM=ETA*TO/KAPPA

D=ABS(BL-L)*400.

N=D

IF (N.LT.1) N=1

XX=N

DLAM=(L-BL)/XX

DLAM2=DLAM/2.

W=DLAM*LSIGN

IF (W.LT.0.) WRITE (6,9) BL,L,DLAM,LSIGN

LAM=BL

SL=BSL

I=0

IF (MOM) GO TO 4

CALL DSIGMA (KAPPA,ETA,LAM,DLAM,MAT,TENS,DS1,SL)

DO 3 I=1,N

LAM2=LAM+DLAM2

CALL DSIGMA (KAPPA,ETA,LAM2,DLAM,MAT,TENS,DS2,SL)

DS3=DS2

LAM=LAM+DLAM

CALL DSIGMA (KAPPA,ETA,LAM,DLAM,MAT,TENS,DS4,SL)

DS=(DS1+DS4)/6.+(DS2+DS3)/3.

SL=SL+DS

DS1=DS4

T=DS/DLAM

BT=T

IF (MOM) GO TO 4

CONTINUE

CONTINUE

GO TO 8

GO TO (5,6), NSS

TS=SL+SIGN*ALFA(MAT)+SIGN*BETA(MAT)*ABS(STRAIN(KAPPA,ETA,LAM,SIGN)

1)**EN(MAT)

GO TO 7

TS=SL+SIGN*ALFA(MAT)*ABS(BETA(MAT)+STRAIN(KAPPA,ETA,LAM,SIGN))**EN

1(MAT)

DL=DLAM

IF ((I.EQ.0).OR.(I.EQ.N)) DL=DLAM2

D=DZ(KAPPA,RN,RM,LAM,DL)

K	7
K	8
K	9
K	10
K	11
K	12
K	13
K	14
K	15
K	16
K	17
K	18
K	19
K	20
K	21
K	22
K	23
K	24
K	25
K	26
K	27
K	28
K	29
K	30
K	31
K	32
K	33
K	34
K	35
K	36
K	37
K	38
K	39
K	40
K	41
K	42
K	43
K	44
K	45
K	46
K	47
K	48
K	49
K	50
K	51
K	52
K	53
K	54
K	55
K	56

	XMOM=XMOM+TS*D	K	57
	CALL STR (LAM,SL,TS,RM,KAPPA)	K	58
	IF (I.EQ.0) GO TO 1	K	59
	GO TO 2	K	60
8	CONTINUE	K	61
	RETURN	K	62
C		K	63
9	FORMAT (1H ,*ERROR IN INTEGRATION DIRECTION*,3E15.7,I3)	K	64
	END	K	65-
	SUBROUTINE ANAINT (KAPPA,ETA,MAT,TENS,MOM,L1,S1,L2,S2,T2,TS2,XMOM,	L	1
1	1RN)	L	2
	REAL KAPPA,L1,L2	L	3
	LOGICAL TENS,MOM	L	4
C		L	5
C	SUBROUTINE ANAINT VERSION ... 24 SEPT 1972 ...	L	6
C		L	7
C	ANAINT PERFORMS CALCULATIONS IN ZONES WHERE THE RADIAL STRESS IS	L	8
C	ANALYTICALLY KNOWN .	L	9
C	ANAINT IS USED WITH BENDING	L	10
		L	11
	IF (MOM) GO TO 1	L	12
	CALL STRESS (KAPPA,ETA,MAT,TENS,MOM,L1,S1,L2,S2,T2,TS2)	L	13
	GO TO 2	L	14
1	BL1=L1	L	15
2	CALL INTMOM (KAPPA,ETA,MAT,TENS,BL1,S1,L1,L2,S2,XMOM,RN)	L	16
	CONTINUE	L	17
	RETURN	L	18
	END	L	19-
	SUBROUTINE BENMOM (KAPPA,ETA,LN,RN,RI,RY,XMOM)	M	1
	REAL KAPPA,LN,MU	M	2
	LOGICAL MOM	M	3
	LOGICAL LLIMDO,LLIMUP	M	4
	COMMON /SSCURV/ NSS,NLT,ALFA(4),BETA(4),EN(4),MU(4,2),TO	M	5
	COMMON /STRSTR/ R(120),SR(120),ST(120),NS	M	6
	COMMON /LIMIT/ XLIMDO,SLIMDO,TLIMDO,MLIMDO,LLIMDO,XLIMUP,SLIMUP,TL	M	7
1	IMUP,MLIMUP,LLIMUP	M	8
	COMMON /TAN/ T	M	9
C		M	10
C	SUBROUTINE BENMOM VERSION ... 24 SEPT 1972 ...	M	11
C		M	12
C	BENMOM DETERMINES THE BENDINGMOMENT .	M	13
C	BENMOM IS USED WITH BENDING	M	14
		M	15
		M	16
	XLIMDO=0.	M	17
	SLIMDO=0.	M	18

	IF (MU(I,2)-BL2) 1,1,2	N	24
1	L2=MU(I,2)	N	25
	GO TO 3	N	26
2	L2=BL2	N	27
	NSTOP=1	N	28
	GO TO 3	N	29
3	IF (L2-LMIN) 4,4,5	N	30
4	CALL ANAINT (KAPPA,ETA,I,COMP,MOM,L1,S1,L2,S2,T2,TS2,XMOM,RN)	N	31
	T=T2	N	32
	MAT2=I	N	33
	L1=L2	N	34
	S1=S2	N	35
	GO TO 12	N	36
5	IF (L1-LMIN) 6,7,7	N	37
6	CALL ANAINT (KAPPA,ETA,I,COMP,MOM,L1,S1,LMIN,SLMIN,T2,TS2,XMOM,RN)	N	38
	T=T2	N	39
	MAT2=I	N	40
	L1=LMIN	N	41
	S1=SLMIN	N	42
	GO TO 7	N	43
7	IF (L2-LMAX) 8,8,9	N	44
8	CALL NUMINT (KAPPA,ETA,I,COMP,MOM,LSIGN,L1,S1,L2,S2,T2,TS2,XMOM,RN	N	45
	1)	N	46
	T=T2	N	47
	MAT2=I	N	48
	L1=L2	N	49
	S1=S2	N	50
	GO TO 12	N	51
9	IF (L1-LMAX) 10,11,11	N	52
10	CALL NUMINT (KAPPA,ETA,I,COMP,MOM,LSIGN,L1,S1,LMAX,SLMAX,T2,TS2,XM	N	53
	1OM,RN)	N	54
	T=T2	N	55
	MAT2=I	N	56
	L1=LMAX	N	57
	S1=SLMAX	N	58
11	CALL ANAINT (KAPPA,ETA,I,COMP,MOM,L1,S1,L2,S2,T2,TS2,XMOM,RN)	N	59
	T=T2	N	60
	MAT2=I	N	61
	L1=L2	N	62
	S1=S2	N	63
	GO TO 12	N	64
12	IF (NSTOP.EQ.1) GO TO 14	N	65
13	CONTINUE	N	66
14	BS2=S2	N	67
	RETURN	N	68
	END	N	69-

SUBROUTINE INTDO (KAPPA,ETA,MAT1,BL1,BS1,MAT2,BL2,BS2,T2,TS2,MOM,X	0	1
1MOM,RN)	0	2

	REAL KAPPA,LMIN,LMAX,MU,L1,L2	0	3
	LOGICAL MOM,TENS	0	4
	COMMON /SSCURV/ NSS,NLT,ALFA(4),BETA(4),EN(4),MU(4,2),TO	0	5
	COMMON /REMEM/ INDEX,LMIN,LMAX,REMLN(200),REMRHO(200)	0	6
	COMMON /TAN/ T	0	7
	SUBROUTINE INTDO VERSION ... 24 SEPT 1972 ...	0	8
		0	9
		0	10
	INTDO PERFORMS INTEGRATIONS IN THE DIRECTION \$ OUTSIDE TO INSIDE .	0	11
	INTDO IS USED WITH BENDING	0	12
		0	13
	TENS=.TRUE.	0	14
	LSIGN=-1	0	15
	NSTOP=0	0	16
	L1=BL1	0	17
	S1=BS1	0	18
	II=NLT+1-MAT1	0	19
	NN=NLT+1-MAT2	0	20
	IF (MAT2.EQ.0) NN=NLT	0	21
	IF (MAT2.EQ.0) MAT2=MAT1	0	22
	DO 13 I=II,NLT	0	23
	J=NLT-I+1	0	24
	IF (BL2-MU(J,1)) 1,1,2	0	25
1	L2=MU(J,1)	0	26
	GO TO 3	0	27
2	L2=BL2	0	28
	NSTOP=1	0	29
	GO TO 3	0	30
3	IF (L2-LMAX) 5,4,4	0	31
4	CALL ANAINT (KAPPA,ETA,J,TENS,MOM,L1,S1,L2,S2,T2,TS2,XMOM,RN)	0	32
	T=T2	0	33
	MAT2=J	0	34
	L1=L2	0	35
	S1=S2	0	36
	GO TO 12	0	37
5	IF (LMAX-L1) 6,7,7	0	38
6	CALL ANAINT (KAPPA,ETA,J,TENS,MOM,L1,S1,LMAX,SLMAX,T2,TS2,XMOM,RN)	0	39
	T=T2	0	40
	MAT2=J	0	41
	L1=LMAX	0	42
	S1=SLMAX	0	43
	GO TO 7	0	44
7	IF (L2-LMIN) 9,8,8	0	45
8	CALL NUMINT (KAPPA,ETA,J,TENS,MOM,LSIGN,L1,S1,L2,S2,T2,TS2,XMOM,RN	0	46
	1)	0	47
	T=T2	0	48
	MAT2=J	0	49
	L1=L2	0	50
	S1=S2	0	51
		0	52

C
C
C
C
C
C

	GO TO 12	0	53
9	IF (L1-LMIN) 11,11,10	0	54
10	CALL NUMINT (KAPPA,ETA,J,TENS,MOM,LSIGN,L1,S1,LMIN,SLMIN,T2,TS2,XMOM,RN)	0	55
	T=T2	0	56
	MAT2=J	0	57
	L1=LMIN	0	58
	S1=SLMIN	0	59
11	CALL ANAINT (KAPPA,ETA,J,TENS,MOM,L1,S1,L2,S2,T2,TS2,XMOM,RN)	0	60
	T=T2	0	61
	MAT2=J	0	62
	L1=L2	0	63
	S1=S2	0	64
	GO TO 12	0	65
12	IF (NSTOP.EQ.1) GO TO 14	0	66
13	CONTINUE	0	67
14	BS2=S2	0	68
	RETURN	0	69
	END	0	70

	SUBROUTINE FINDLN (KAPPA,ETA,LNOLD,LNNEW)	P	1
	REAL KAPPA, LNNEW, LNOLD, MU, LUP, LDO, L1UP, L1DO, L2UP, L2DO	P	2
	REAL LX, LY	P	3
	REAL LZ	P	4
	REAL L, L1, L2	P	5
	LOGICAL BUG	P	6
	LOGICAL MOM	P	7
	LOGICAL LLIMDC, LLIMUP	P	8
	DIMENSION L(26), S1(26), S2(26)	P	9
	DIMENSION T1(26), T2(26)	P	10
	DIMENSION MX(50), LX(50), SX(50), MY(50), LY(50), SY(50)	P	11
	DIMENSION TX(50), TY(50)	P	12
	DIMENSION LZ(50)	P	13
	COMMON /SSCURV/ NSS, NLT, ALFA(4), BETA(4), EN(4), MU(4,2), TO	P	14
	COMMON /REMEM/ INDEX, LMIN, LMAX, REMLN(200), REMRHO(200)	P	15
	COMMON /LIMIT/ XLIMDO, SLIMDO, TLIMDO, MLIMDO, LLIMDO, XLIMUP, SLIMUP, TL	P	16
	IMUP, MLIMUP, LLIMUP	P	17
	COMMON /DEBUG/ BUG	P	18
	COMMON /TAN/ T	P	19
	DATA LUP, SUP, LDO, SDO, MUP/0.,0.,1.,0.,1/	P	20
	DATA TUP, TDO/0.,0./	P	21
		P	22
	SUBROUTINE FINDLN VERSION ... 24 SEPT 1972 ...	P	23
		P	24
		P	25
	FINDLN .GIVEN KAPPA AND ETA, FINDS THE NEUTRAL LAYER POSITION	P	26
	BY USING THE CONTINUITY OF THE RADIAL STRESS IN THE NEUTRAL LAYER	P	27
		P	28
	FINDLN IS USED WITH BENDING	P	29

CCCCC
C

C		P	30
1	BUG=.FALSE.	P	31
	CONTINUE	P	32
	IF (BUG) WRITE (6,19)	P	33
	XLIMDO=0.	P	34
	SLIMDO=0.	P	35
	TLIMDO=0.	P	36
	MLIMDO=0	P	37
	LLIMDO=.FALSE.	P	38
	XLIMUP=1.	P	39
	SLIMUP=0.	P	40
	TLIMUP=0.	P	41
	MLIMUP=NL T	P	42
	LLIMUP=.FALSE.	P	43
	MDO=NL T	P	44
	MOM=.FALSE.	P	45
	T1UP=TUP	P	46
	T1DO=TDO	P	47
	L1UP=LUP	P	48
	S1UP=SUP	P	49
	L1DO=LDO	P	50
	S1DO=SDO	P	51
	MAT1UP=MUP	P	52
	MAT1DO=MDO	P	53
	L2UP=L1UP/3.+LNOLD*2./3.	P	54
	L2DO=L1DO/3.+LNOLD*2./3.	P	55
	I=1	P	56
	MX(I)=MAT1UP	P	57
	LX(I)=L1UP	P	58
	SX(I)=S1UP	P	59
	MY(I)=MAT1DO	P	60
	LY(I)=L1DO	P	61
	SY(I)=S1DO	P	62
	TX(I)=T1UP	P	63
	TY(I)=T1DO	P	64
2	MAT2UP=0	P	65
	MAT2DO=0	P	66
	T=T1UP	P	67
C		P	68
	CALL INTUP (KAPPA,ETA,MAT1UP,L1UP,S1UP,MAT2UP,L2UP,S2UP,T2UP,TS2,M	P	69
1	OM,XMOM,RN)	P	70
	IF (BUG) WRITE (6,20) MAT1UP,L1UP,S1UP,MAT2UP,L2UP,S2UP,T2UP	P	71
	T=T1DO	P	72
	CALL INTDO (KAPPA,ETA,MAT1DO,L1DO,S1DO,MAT2DO,L2DO,S2DO,T2DO,TS2,M	P	73
1	OM,XMOM,RN)	P	74
	IF (BUG) WRITE (6,20) MAT1DO,L1DO,S1DO,MAT2DO,L2DO,S2DO,T2DO	P	75
	Z=(S2UP-S2DO-T2UP*L2UP+T2DO*L2DO)/(T2DO-T2UP)	P	76
	IF (BUG) WRITE (6,20) I,Z	P	77
C		P	78
	LZ(I)=Z	P	79

	IF (ABS(L2UP-L2D0).LT.1.E-10) GO TO 15	P	80
3	IF (Z-L2UP) 4,4,3	P	81
	L1UP=L2UP	P	82
	S1UP=S2UP	P	83
	MAT1UP=MAT2UP	P	84
	T1UP=T2UP	P	85
	GO TO 8	P	86
4	IF (Z-L1UP) 5,5,8	P	87
5	L1UP=LUP	P	88
	KK=1	P	89
	DO 7 K=1,I	P	90
	IF ((LX(K).GT.L1UP).AND.(LX(K).LT.Z)) GO TO 6	P	91
	GO TO 7	P	92
6	L1UP=LX(K)	P	93
	KK=K	P	94
7	CONTINUE	P	95
	S1UP=SX(KK)	P	96
	MAT1UP=MX(KK)	P	97
	T1UP=TX(KK)	P	98
	IF (Z.LT.LUP) Z=LUP+1.E-10	P	99
	GO TO 8	P	100
8	L2UP=L1UP/3.+Z*2./3.	P	101
9	IF (Z-L2D0) 9,10,10	P	102
	L1D0=L2D0	P	103
	S1D0=S2D0	P	104
	MAT1D0=MAT2D0	P	105
	T1D0=T2D0	P	106
	GO TO 14	P	107
10	IF (Z-L1D0) 14,11,11	P	108
11	L1D0=L D0	P	109
	KK=1	P	110
	DO 13 K=1,I	P	111
	IF ((LY(K).LT.L1D0).AND.(LY(K).GT.Z)) GO TO 12	P	112
	GO TO 13	P	113
12	L1D0=LY(K)	P	114
	KK=K	P	115
13	CONTINUE	P	116
	S1D0=SY(KK)	P	117
	MAT1D0=MY(KK)	P	118
	T1D0=TY(KK)	P	119
	IF (Z.GT.LD0) Z=LD0-1.E-10	P	120
	GO TO 14	P	121
14	L2D0=L1D0/3.+Z*2./3.	P	122
	IF (I.GE.50) GO TO 15	P	123
	I=I+1	P	124
	MX(I)=MAT1UP	P	125
	LX(I)=L1UP	P	126
	SX(I)=S1UP	P	127
	MY(I)=MAT1D0	P	128
	LY(I)=L1D0	P	129

	SY(I)=S100	P	130
	TX(I)=T1UP	P	131
	TY(I)=T100	P	132
	GO TO 2	P	133
15	LNNEW=Z	P	134
	WRITE (6,21) I	P	135
	IF (I.LT.30) GO TO 18	P	136
	IF (BUG) GO TO 16	P	137
	BUG=.TRUE.	P	138
	GO TO 1	P	139
16	CONTINUE	P	140
	X1=LNOLD-.1	P	141
	X2=LNOLD+.1	P	142
	IF (X1.LT.0.) X1=0.	P	143
	IF (X2.GT.1.) X2=1.	P	144
	DO 17 K=1,I	P	145
	IF (LX(K).GT.X1) CALL PLOTPT (LX(K),SX(K),K)	P	146
	IF (LY(K).LT.X2) CALL PLOTPT (LY(K),SY(K),K)	P	147
	WRITE (6,22) K,LZ(K),LX(K),SX(K),LY(K),SY(K)	P	148
17	CONTINUE	P	149
	CALL OUTPLT	P	150
18	CONTINUE	P	151
	RETURN	P	152
C		P	153
19	FORMAT (1H ,*RETURN OF FINDLN*)	P	154
20	FORMAT (1H ,I3,2X,2E15.7,I3,2X,3E15.7)	P	155
21	FORMAT (1H ,*FINDLN*,* I=*,I2,* FINDLN*,)	P	156
22	FORMAT (1H ,I2,3X,10F10.7)	P	157
	END	P	158-
	SUBROUTINE DSIGMA (KAPPA,ETA,LAM,DLAM,MAT,TENS,DS,SL)	Q	1
	REAL KAPPA,MU,LAM	Q	2
	REAL LO	Q	3
	LOGICAL BUG	Q	4
	LOGICAL TENS	Q	5
	LOGICAL LLIMDO,LLIMUP	Q	6
	COMMON /SSCURV/ NSS,NLT,ALFA(4),BETA(4),EN(4),MU(4,2),TO	Q	7
	COMMON /REMEM/ INDEX,LMIN,LMAX,REMLN(200),REMRHO(200)	Q	8
	COMMON /LIMIT/ XLIMDO,SLIMDO,TLIMDO,MLIMDO,LLIMDO,XLIMUP,SLIMUP,TL	Q	9
1	IMUP,MLIMUP,LLIMUP	Q	10
	COMMON /DEBUG/ BUG	Q	11
	COMMON /TAN/ T	Q	12
C		Q	13
C	DSIGMA.....VERSION 27 OCT 1972	Q	14
C	DSIGMA IS USED WITH BENDING	Q	15
		Q	16
	SIGN=-1.	Q	17
	IF (TENS) SIGN=+1.	Q	18
	K=0	Q	19

	IF (BUG) WRITE (6,13) K,SIGN,LAM,DLAM,SL	0	20
	X=(1.-.5*KAPPA)**2+2.*LAM*KAPPA	0	21
	DS=DLAM*KAPPA*SIGN/X	0	22
	K=1	0	23
	IF (BUG) WRITE (6,13) K,X,DS	0	24
	IF (LLIMDO.AND.TENS) GO TO 11	0	25
1	IF (LLIMUP.AND.(.NOT.TENS)) GO TO 11	0	26
	CALL SHIFT (LAM,REMSTR)	0	27
	RLO=ETA	0	28
	IF (INDEX.EQ.1) RLO=SQRT((1.-.5*KAPPA)**2+2.*REMLN(1)*KAPPA)	0	29
	YY=SIGN*(.5*ALOG(X)-ALOG(RLO))	0	30
	STRAIN=REMSTR+YY	0	31
	K=90	0	32
	IF (BUG) WRITE (6,13) K,REMSTR,ETA,RLO,STRAIN,YY	0	33
	IF (STRAIN.LE.0.) GO TO 4	0	34
	GO TO (2,3), NSS	0	35
2	DS=DS*(ALFA(MAT)+BETA(MAT)*STRAIN**EN(MAT))	0	36
	K=10	0	37
	IF (BUG) WRITE (6,13) K,DS	0	38
	GO TO 12	0	39
3	DS=DS*ALFA(MAT)*(BETA(MAT)+STRAIN)**EN(MAT)	0	40
	K=20	0	41
	IF (BUG) WRITE (6,13) K,DS	0	42
	GO TO 12	0	43
4	LO=(RLO**2-(1.-KAPPA*.5)**2)/(2.*KAPPA)	0	44
	XO=(1.-.5*KAPPA)**2+(2.*LO*KAPPA)	0	45
	DLO=LO-LAM	0	46
	DSO=DLO*KAPPA*SIGN/XO	0	47
	K=40	0	48
	IF (BUG) WRITE (6,13) K,LO,XO,DLO,DSO	0	49
	GO TO (5,6), NSS	0	50
5	TLIM=KAPPA*SIGN/XO*ALFA(MAT)	0	51
	DSO=DSO*ALFA(MAT)	0	52
	SLIM=SL+DSO	0	53
	K=41	0	54
	IF (BUG) WRITE (6,13) K,TLIM,DSO,SLIM	0	55
	GO TO 7	0	56
6	TLIM=KAPPA*SIGN/XO*ALFA(MAT)*BETA(MAT)**EN(MAT)	0	57
	DSO=DSO*ALFA(MAT)*BETA(MAT)**EN(MAT)	0	58
	SLIM=SL+DSO	0	59
	K=42	0	60
	IF (BUG) WRITE (6,13) K,TLIM,DSO,SLIM	0	61
	GO TO 7	0	62
7	CONTINUE	0	63
	K=43	0	64
	IF (BUG) WRITE (6,13) K	0	65
	IF (TENS) GO TO 8	0	66
	LLIMUP=.TRUE.	0	67
	XLIMUP=LO	0	68
	MLIMUP=MAT	0	69

	TLIMUP=TLIM	Q	70
	SLIMUP=SLIM	Q	71
	IF (BUG) WRITE (6,13) K,XLIMUP,TLIMUP,SLIMUP	Q	72
	GO TO 9	Q	73
8	LLIMDO=.TRUE.	Q	74
	XLIMDO=LO	Q	75
	MLIMDO=MAT	Q	76
	TLIMDO=TLIM	Q	77
	SLIMDO=SLIM	Q	78
	IF (BUG) WRITE (6,13) K,XLIMDO,TLIMDO,SLIMDO	Q	79
	GO TO 10	Q	80
9	DS=DLAM*TLIMUP*X0/X	Q	81
	K=60	Q	82
	IF (BUG) WRITE (6,13) K,DS	Q	83
	GO TO 12	Q	84
10	DS=DLAM*TLIMDO*X0/X	Q	85
	K=70	Q	86
	IF (BUG) WRITE (6,13) K,DS	Q	87
	GO TO 12	Q	88
11	CONTINUE	Q	89
	K=80	Q	90
	IF (BUG) WRITE (6,13) K	Q	91
	IF (TENS.AND.(LAM.GT.XLIMDO)) GO TO 1	Q	92
	IF ((.NOT.TENS).AND.(LAM.LT.XLIMUP)) GO TO 1	Q	93
	LO=(RLO**2-(1.-KAPPA*.5)**2)/(2.*KAPPA)	Q	94
	XO=(1.-.5*KAPPA)**2+(2.*LO*KAPPA)	Q	95
	IF (BUG) WRITE (6,13) K,LO,XO	Q	96
	IF (TENS) GO TO 10	Q	97
	GO TO 9	Q	98
12	RETURN	Q	99
C		Q	100
13	FORMAT (1H ,*RETURN OF DSIGMA*,I3,2X,8E10.3)	Q	101
	END	Q	102
	SUBROUTINE STRESS (KAPPA,ETA,MAT,TENS,MOM,BL,BS,L,SL,T,TS)	R	1
	REAL KAPPA,MU,L	R	2
	REAL LO	R	3
	LOGICAL BUG	R	4
	LOGICAL MOM	R	5
	LOGICAL TENS	R	6
	LOGICAL LLIMDO,LLIMUP	R	7
	COMMON /SSCURV/ NSS,NLT,ALFA(4),BETA(4),EN(4),MU(4,2),TO	R	8
	COMMON /REMEM/ INDEX,LMIN,LMAX,REMLN(200),REMRHO(200)	R	9
	COMMON /LIMIT/ XLIMDO,SLIMDO,TLIMDO,MLIMDO,LLIMDO,XLIMUP,SLIMUP,TL	R	10
	IMUP,MLIMUP,LLIMUP	R	11
	COMMON /DEBUG/ BUG	R	12
	COMMON /TAN/ BT	R	13
	R(A,B)=SQRT((1.-.5*A)**2+2.*B*A)	R	14
C		R	15

0	STRESS.....VERSION 27 OCT 1972	R	16
C		R	17
C		R	18
C	STRESS DETERMINES THE RADIAL AND TANGENTIAL STRESS IN ZONES WHERE	R	19
C	THEY ARE ANALYTICALLY KNOWN .	R	20
C	STRESS IS USED WITH BENDING	R	21
	GO TO (1,2), NSS	R	22
1	X=ALFA (MAT)	R	23
	Z=EN (MAT)+1.	R	24
	Y=BETA (MAT)/Z	R	25
	GO TO 3	R	26
2	Y=BETA (MAT)	R	27
	Z=EN (MAT)+1.	R	28
	X=ALFA (MAT)/Z	R	29
	GO TO 3	R	30
3	CONTINUE	R	31
	SIGN=-1.	R	32
	IF (TENS) SIGN=+1.	R	33
	K=30	R	34
	IF (BUG) WRITE (6,19) K,SIGN	R	35
	RL=R(KAPPA,L)	R	36
	IF (LLIMDO.AND.TENS) GO TO 14	R	37
	IF (LLIMUP.AND.(.NOT.TENS)) GO TO 12	R	38
4	RM=ETA*TO/KAPPA	R	39
	RBL=R(KAPPA,BL)	R	40
	RLO=ETA	R	41
	IF (INDEX.EQ.1) RLO=R(KAPPA,REMLN(1))	R	42
	YY=SIGN*ALOG(RL/RLO)	R	43
	IF (BUG) WRITE (6,19) K,RL,RM,RBL,YY	R	44
	IF (YY.LT.0.) GO TO 7	R	45
	GO TO (5,6), NSS	R	46
5	CONST=BS-SIGN*X*ALOG(RM*RBL)-Y*(ABS(ALOG(RBL/RLO)))**Z	R	47
	SL=CONST+SIGN*X*ALOG(RM*RL)+Y*YY**Z	R	48
	XX=SIGN*(X+BETA(MAT)*YY**EN(MAT))	R	49
	T=KAPPA*XX/(RL**2)	R	50
	K=40	R	51
	IF (BUG) WRITE (6,19) K,CONST,SL,XX,T	R	52
	IF (MOM) TS=SL+XX	R	53
	GO TO 18	R	54
6	CONST=BS-X*(ABS(Y+SIGN*ALOG(RBL/RLO)))**Z	R	55
	SL=CONST+X*(Y+YY)**Z	R	56
	XX=SIGN*ALFA(MAT)*(Y+YY)**EN(MAT)	R	57
	T=KAPPA*XX/(RL**2)	R	58
	K=50	R	59
	IF (BUG) WRITE (6,19) K,CONST,SL,XX,T	R	60
	IF (MOM) TS=SL+XX	R	61
	GO TO 18	R	62
7	LO=(RLO**2-(1.-KAPPA*.5)**2)/(2.*KAPPA)	R	63
	IF (TENS.AND.(LO.GT.BL)) GO TO 16	R	64
		R	65

	IF ((.NOT.TENS).AND.(LO.LT.BL)) GO TO 17	R	66
	RO=R(KAPPA,LO)	R	67
	K=60	R	68
	IF (BUG) WRITE (6,19) K,LO,RO	R	69
	GO TO (8,9),NSS	R	70
8	CONST=BS-SIGN*X*ALOG(RM*RBL)-Y*(ABS(ALOG(RBL/RL0)))**Z	R	71
	SL=CONST+SIGN*X*ALOG(RM*RO)	R	72
	XX=SIGN*X	R	73
	K=64	R	74
	IF (BUG) WRITE (6,19) K,CONST,SL,XX	R	75
	GO TO 10	R	76
9	CONST=BS-X*(ABS(Y+SIGN*ALOG(RBL/RL0)))**Z	R	77
	SL=CONST+X*Y**Z	R	78
	XX=SIGN*ALFA(MAT)*Y**EN(MAT)	R	79
	K=65	R	80
	IF (BUG) WRITE (6,19) K,CONST,SL,XX	R	81
	GO TO 10	R	82
10	T=KAPPA*XX/(RL**2)	R	83
	K=66	R	84
	IF (BUG) WRITE (6,19) K,T	R	85
	IF (TENS) GO TO 11	R	86
	XLIMUP=LO	R	87
	SLIMUP=SL	R	88
	TLIMUP=T	R	89
	MLIMUP=MAT	R	90
	LLIMUP=.TRUE.	R	91
	GO TO 13	R	92
11	XLIMDO=LO	R	93
	SLIMDO=SL	R	94
	TLIMDO=T	R	95
	MLIMDO=MAT	R	96
	LLIMDO=.TRUE.	R	97
	GO TO 15	R	98
12	IF (L.LT.XLIMUP) GO TO 4	R	99
13	DL=L-XLIMUP	R	100
	DS=TLIMUP*DL	R	101
	SL=SLIMUP+DS	R	102
	T=TLIMUP	R	103
	K=80	R	104
	IF (BUG) WRITE (6,19) K,DL,DS,SL,T	R	105
	IF (MOM) TS=SL+T*RL**2/KAPPA	R	106
	GO TO 18	R	107
14	IF (L.GT.XLIMDO) GO TO 4	R	108
15	DL=L-XLIMDO	R	109
	DS=TLIMDO*DL	R	110
	SL=SLIMDO+DS	R	111
	T=TLIMDO	R	112
	K=90	R	113
	IF (BUG) WRITE (6,19) K,DL,DS,SL,T	R	114
	IF (MOM) TS=SL+T*RL**2/KAPPA	R	115

	GO TO 18	R	116
16	XLIMDO=BL	R	117
	SLIMDO=SL	R	118
	MLIMDO=MAT	R	119
	LLIMDO=.TRUE.	R	120
	TLIMDO=BT	R	121
	K=120	R	122
	IF (BUG) WRITE (6,19) K,XLIMDO,SLIMDO,TLIMDO	R	123
	GO TO 14	R	124
17	XLIMUP=BL	R	125
	SLIMUP=SL	R	126
	MLIMUP=MAT	R	127
	LLIMUP=.TRUE.	R	128
	TLIMUP=BT	R	129
	K=130	R	130
	IF (BUG) WRITE (6,19) K,XLIMUP,SLIMUP,TLIMUP	R	131
	GO TO 12	R	132
18	CONTINUE	R	133
	RETURN	R	134
C		R	135
19	FORMAT (1H ,*RETURN OF STRESS*,I3,2X,8E10.3)	R	136
	END	R	137-